ISSN: 2408-2384 (Online)
ISSN: 1686-5456 (Print)

Environment and Natural Resources Journal

Volume 18, Number 3, July - September 2020

Environment and Natural Resources Journal (EnNRJ)

Volume 18, Number 3, July-September 2020 ISSN: 1686-5456 (Print)
ISSN: 2408-2384 (Online)

AIMS AND SCOPE

The Environment and Natural Resources Journal is a peer-reviewed journal, which provides insight scientific knowledge into the diverse dimensions of integrated environmental and natural resource management. The journal aims to provide a platform for exchange and distribution of the knowledge and cutting-edge research in the fields of environmental science and natural resource management to academicians, scientists and researchers. The journal accepts a varied array of manuscripts on all aspects of environmental science and natural resource management. The journal scope covers the integration of multidisciplinary sciences for prevention, control, treatment, environmental clean-up and restoration. The study of the existing or emerging problems of environment and natural resources in the region of Southeast Asia and the creation of novel knowledge and/or recommendations of mitigation measures for sustainable development policies are emphasized.

The subject areas are diverse, but specific topics of interest include:

- Biodiversity
- Climate change
- Detection and monitoring of polluted sources e.g., industry, mining
- Disaster e.g., forest fire, flooding, earthquake, tsunami, or tidal wave
- Ecological/Environmental modelling
- Emerging contaminants/hazardous wastes investigation and remediation
- Environmental dynamics e.g., coastal erosion, sea level rise
- Environmental assessment tools, policy and management e.g., GIS, remote sensing, Environmental Management System (EMS)
- Environmental pollution and other novel solutions to pollution
- Remediation technology of contaminated environments
- Transboundary pollution
- Waste and wastewater treatments and disposal technology

Schedule

Environment and Natural Resources Journal (EnNRJ) is a quarterly published journal in January-March, April-June, July-September and October-December.

Publication Fees

There is no cost of the article-processing and publication.

Ethics in publishing

EnNRJ follows closely a set of guidelines and recommendations published by Committee on Publication Ethics (COPE) (http://publicationethics.org/).

Environment and Natural Resources Journal (EnNRJ)
Volume 18, Number 3, July-September 2020
ISSN: 1686-5456 (Print)
ISSN: 2408-2384 (Online)

Editorial Office Address
Research and Academic Services Section,
Faculty of Environment and Resource Studies, Mahidol University
999, Phutthamonthon Sai 4 Road, Salaya, Phutthamonthon, Nakhon Pathom, Thailand, 73170
Phone +662 441 5000 ext. 2108 Fax. +662 441 9509-10
Website: https://ph02.tci-thaijo.org/index.php/ennrj/index
E-mail: ennrjournal@gmail.com

Environment and Natural Resources Journal (EnNRJ)

Volume 18, Number 3, July-September 2020 ISSN: 1686-5456 (Print)
ISSN: 2408-2384 (Online)

CONTENT

Environment and Natural Resources Journal 2020; 18(3): 224-233

Indicator Based Vulnerability Assessment of Chhayanath-Rara Municipality, Western Nepal

Padam Bahadur Budha[1*], Kabiraj Paudyal[2], and Motilal Ghimire[3]

[1]*Central Department of Environmental Science, Tribhuvan University, Kathmandu, Nepal*
[2]*Central Department of Geology, Tribhuvan University, Kathmandu, Nepal*
[3]*Central Department of Geography, Tribhuvan University, Kathmandu, Nepal*

ARTICLE INFO

Received: 29 Aug 2019
Received in revised: 11 Feb 2020
Accepted: 13 Feb 2020
Published online: 16 Mar 2020
DOI: 10.32526/ennrj.18.3.2020.21

Keywords:
Landslides risk/ Vulnerability assessment/ Vulnerability indices/ Socio-economic indicators

*** Corresponding author:**
E-mail: padambudha88@gmail.com

ABSTRACT

The dense settlements at the eastern hills of Rara Lake are at higher risk of existing landslides. Seepage of water from the lake has increased erosion rates, exaggerating the threats to villages. People are worried due to the potential of inadvertent disaster, therefore it became necessary to estimate the vulnerability of the communities and inform concerned authorities. Setting this requirement as an objective, underlying influencing indicators were assessed. The vulnerability assessment was based on the scoring of the responses emanated from indicator-based household's survey. These scores were summed up to generate indices and also mapped with their true locations. Vulnerability scores ranged from 16.50 to 21.75 and were categorized into five classes after standardization. A moderate vulnerability was exhibited by 33.08% of households sampled. High and very high categories of vulnerability occupied 18.80% and 4.51% of households, respectively. Field observation showed solitary households built away from village clusters were highly vulnerable. Most households showed moderate vulnerability and characteristics like stones/mud-built houses, firewood as a primary fuel, decreasing forests and grasslands, increasing temperatures, and decreasing rainfall were major influencing indicators for higher vulnerability in the research area.

1. INTRODUCTION

Vulnerability is conceptualized as complex-multidimensional, dynamic, time and space-specific (Joseph, 2013). According to the definition provided by United Nations International Strategy for Disaster Reduction (UNISDR) the characteristics and circumstances of a community, system or asset that make it susceptible to the damaging effects of a hazard (UNISDR, 2009) give rise to vulnerability condition. This definition encompasses the two sides of vulnerability. First, the external side of risk, shock or stress to which individuals or households are subject to; and other is the internal side which is defenselessness, means lack of coping without damaging loss (Haki et al., 2004). Therefore it is vital to incorporate both the components in vulnerability assessments and consider the social system along with environmental changes. Vulnerability depends on economic, social, geographic, demographic, cultural, institutional, governance, and environmental factors (Cardona et al., 2012). The strengths of the communities as well as the external factors that are crucial in shaping the capabilities of those communities. The vulnerability can be related to the susceptibility of the system in question to adverse consequences following hazard impact and the value placed on the system by society (Tapsell et al., 2010). Considering this definition the inclusion of the economic status of the individuals or communities is a must in vulnerability estimation. Vulnerability to environmental hazards means the potential for loss (Cutter et al., 2003). In the disaster risk management discourse, the need for a paradigm shift from quantification and analysis of hazard to identification, assessment, and ranking of vulnerability has taken center-stage (Joseph, 2013). Thus, at present times it is a must to assess the vulnerability to quantify the risk of a particular hazard. Such assessments in

Citation: Budha PB, Paudyal K, Ghimire M. Indicator based vulnerability assessment of Chhayanath-Rara Municipality, Western Nepal. Environ. Nat. Resour. J. 2020;18(3):224-233. DOI: 10.32526/ennrj.18.3.2020.21

mountainous countries like Nepal, where multi-hazards are prevalent, would be crucial for disaster management.

Nepal is prone to disasters due to the number of factors, both natural and human-induced, including adverse geo-climatic conditions, topographic features, environmental degradation, population growth, development practices that are not sustainable, etc. When the database of the Ministry of Home Affairs (MoHA) of Government of Nepal (GoN) from 1971 till 2016 was reviewed, it revealed landslides and floods among the top five hazards and are annual in nature unlike earthquakes (MoHA, 2018). The database of landslides (August 1993 to May 2002) of different countries for casualties and damage, by (Alexander, 2004), ranked Nepal as 12th considering only 4 events causing 203 deaths.

The report prepared by the Ministry of Environment (MoE) regarding vulnerability of climate change identified the Mugu District, where the study area is located, among very high vulnerable districts in Nepal (MoE, 2010). Also, the same study found that the district Mugu is very low in socio-economic and technologic adaptation capability, and in infrastructure adaptation capability. This means the district has the least adaptive capacity in Nepal which has an inverse relation with vulnerability. Mugu District was ranked 66th out of 75 districts in the human development index with the score of 0.397 and 5th district in the human poverty index with a score of 45.22 (Sharma et al., 2014). These figures from government and non-governmental institutions made it clear that there is a requirement of research at the grassroots level. Similarly, a social vulnerability analysis done by Aksha et al. (2019) showed that the district having moderate to high vulnerability contrasting to high vulnerability estimated by Gautam (2017). These two scientific pieces of research were carried out at the national scale so there is a need to find out what is the actual scenario at a local scale. Further, Aksha et al. (2019) insist that the drivers of vulnerability may vary at component and local scale which made the necessity to produce the local level vulnerability estimates and for particular hazards. The local level vulnerability assessment could find what would be the level of vulnerability for each household and/or individual peoples. Besides, such local-level analysis can find the major driving factors behind the high vulnerability of each household. Thus, this research was carried out in the headquarter of the Mugu District where landslide hazard is one of a major problem (Budha et al., 2016). Also, the district is one of the remote areas of Nepal. The major objective to assess the vulnerability status of households and find the extent of influence by particular causative factors as household or individual is distinguished as the first level of social vulnerability (Dwyer et al., 2004) in the spatial scale of analysis. The inference drawn will provide the differences in results of national and local scale vulnerability assessment.

2. METHODOLOGY

2.1 Study area

The study area for this research is located in the Mugu District of western Nepal at the longitude of 82°6’E to 82°12’E and latitude of 29°30’N to 29°35’N. It included households from 10 villages of Chhayanath-Rara Municipality as shown in Figure 1. Most part of the experimental site makes the buffer zone of the Rara National Park. The study area comprised of uneven terrain and steep east-facing slopes with gradient ranged from 0° to 72°. It had an elevation difference from 1,622 m to 3,460 m.

Mugu Karnali River formed the border of the study area at the Northern edge as shown in Figure 1. The River is snow-fed and a major tributary of the Karnali River. Gumgadh River flowed in the Eastern part. Rara Lake is situated on the Western border. Here most water bodies, even small streams, were perennial. Minor gullies and streams become highly destructive in monsoon periods, due to steep gradients, making landslides a recurrent phenomenon (Budha et al., 2016).

2.2 Indicator selection

The flow chart shown in Figure 2 represents the different stages in the vulnerability assessment of this research. The first stage was to select indicators based on works of literature available. As vulnerability cannot be determined by a single factor, combinations of many indicators were considered for study (Dwyer et al., 2004). Indicators of social vulnerability for individual/household level were selected based on a literature review (Armas and Gavris, 2013; Cutter et al., 2003; Devkota et al., 2013; Dwyer et al., 2004; Ebert and Kerle, 2008; Tesso et al., 2012) and acknowledging the local conditions. 36 indicators selected for this study are listed into four major indicators as Social, Economic, Environmental and Institutional as shown in Table 2. This selection of indicators was based on the list of generally accepted

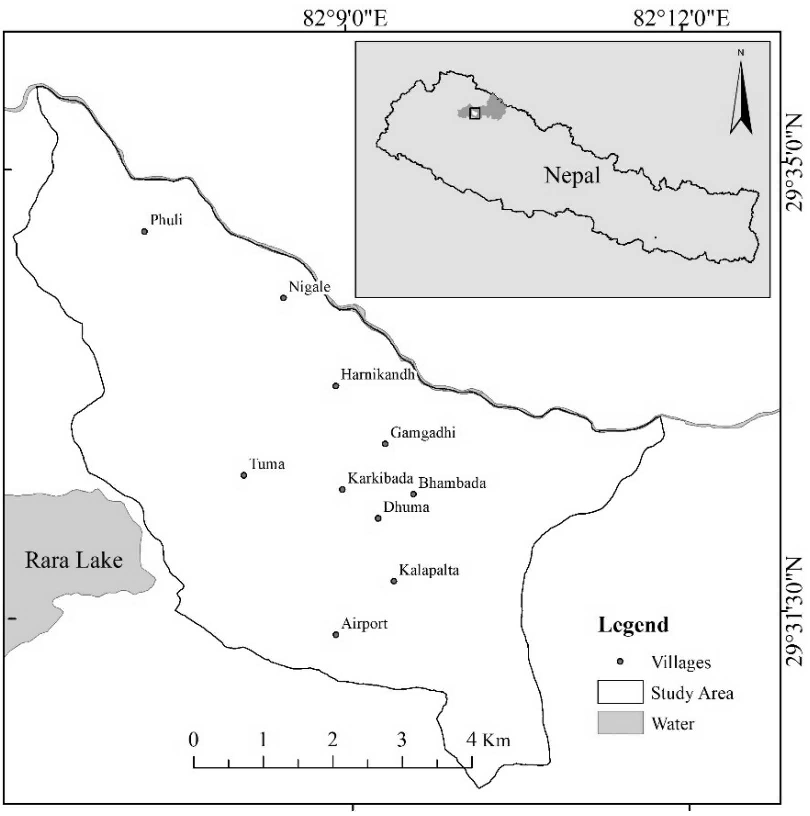

Figure 1. Location of the study area

criteria with considerations of data availability and quality, simplicity, quantitative, sensitivity (Dwyer et al., 2004) and response.

Household-level questionnaire development, a second step of the process (Figure 2), was based on the selected indicators. It was made sure that the response from the questionnaire would be as quantitative as possible so that expert judgment can be applied for scoring purposes. In the process of questionnaire formation, past works of literature on hazard assessments were referred. The questionnaire was then scheduled for the household interview and data was accumulated. Data collected from each household were focused on the collection of specific information about each household (Rajesh et al., 2018). The information obtained includes their social status and economic conditions as well as the influences from the changing environmental conditions and level of support provided by nearby organizations.

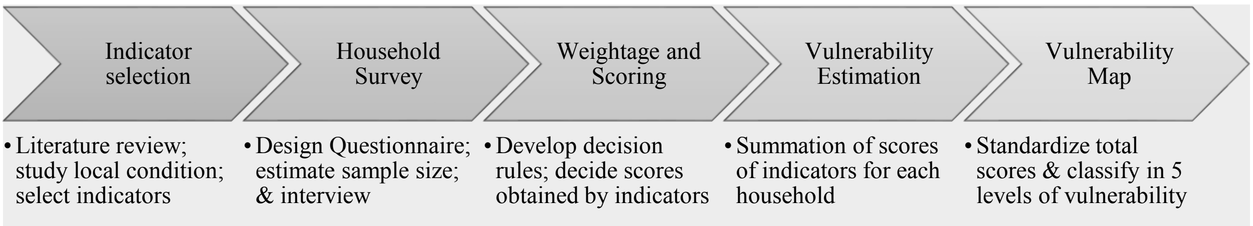

Figure 2. Flow chart for vulnerability assessment

2.3 Sample size for household survey

To estimate the sample size of the household formula by Arkin and Colton (1963) was used. The statistical relation for sample size (n) calculation is given in Equation 1.

$$n = \frac{N*Z^2*P(1-P)}{N*d^2+Z^2*P(1-P)} \quad (1)$$

Where; n=sample size, N=total number of household, Z=value of standard variate at 95% confidence level (1.96), P=estimated population proportion (0.05), and d=error limit of 5% (0.05).

The population database repository can be found at Central Bureau of Statistics (CBS) who conducts the national census for GoN. Total number of households in the experimental area was 1434 (CBS, 2011). Using Equation 1 sample size was calculated to be 133. Therefore, a household survey was carried out in 133 houses as a random stratified manner, considering the distribution in all villages.

2.4 Calculation and scoring of vulnerability

A vulnerability score (V^s) was obtained by adding the weighted values or individual scores assigned for each indicator. Calculation of V^s was done through Equation 2 (Ebert et al., 2009; Haki et al., 2004). V^s is based on the scores obtained by indicators which in turn was reliant on the response of the survey done. The approach was based on indicators' revealed vulnerabilities at ground level. After conducting the interview, their response for each indicator was classified into three options indicating low, moderate or high vulnerability. The scores were assigned, accordingly for each response, ranging from 0 to 1. Here 0 represents low vulnerability and 1 represents a high vulnerability. These scores were summed to obtain total scores which indicated the overall vulnerability of the households. Here, higher V^s resembled high vulnerability and vice-versa.

$$V^s = \sum_i^m v_i q_i \quad (2)$$

Where; m is the number of factors, v_i is a weighted score (values ranging from 0-1), and q_i is the relative frequency or the amount of factor i.

The V^s for all houses was then standardized from 0 to 1. For standardization, the min-max standardization method (Briguglio et al., 2009) was used. Equation 3 transforms the values of the vulnerability score of individual households in a particular variable array so that they take a range of values from zero to unity.

$$SVI = \frac{V - V_{min}}{V_{max} - V_{min}} \quad (3)$$

Where; SVI is a social vulnerability index, V is the total score for a study unit derived from Equation 2, V_{max} is maximum score value, and V_{min} is minimum score value.

The standard scores obtained by each household were then categorized into five levels of vulnerability with 0.2 as a class interval as shown in Table 1. The vulnerability levels were very low, low, moderate, high, and very high, as shown in Table 1, with their score ranges as 0-0.2, 0.2-0.4, 0.4-0.6, 0.6-0.8, and 0.8-1.0 respectively.

Table 1. Vulnerability classes for standardized scores

Range	Vulnerability Classes	Symbols
0.0-0.2	Very Low Vulnerable	VLV
0.2-0.4	Low Vulnerable	LV
0.4-0.6	Moderate Vulnerable	MV
0.6-0.8	High Vulnerable	HV
0.8-1.0	Very High Vulnerable	VHV

The standardized results can be compared with other similar vulnerability researches either of the same areas or different places, but it should be kept in mind the variety of indicators used in respective researches.

3. RESULTS AND DISCUSSION

3.1 Household vulnerability

The vulnerability score values ranged from a minimum of 16.5 to a maximum of 21.75 with the average score as 18.77. Figure 3 showed the number of households at different vulnerability levels based on standardized vulnerability scores. Most households' total score lies around average such that it would reflect moderate vulnerability while considering the overall area. 133 households were surveyed for vulnerability assessment where a maximum number of houses showed moderate vulnerability. As depicted in Figure 3, the numbers of households were 21, 37, 44, 25, and 6 as we move from very low, low, moderate, high, to very high vulnerability respectively. Therefore, 33.08% of houses showed moderate vulnerability with the average standard score of 0.43215. Data collected from the survey included household characteristics, landholding, crops and livestock variety, disaster occurrence, perception level, and different coping strategies pursued changing environmental conditions.

Households clustered as a large village illustrated household's vulnerability range from very low to high. These villages with clustered form include 500 families or above. Some of the clustered settlements were Gamgadhi, Bhambada, and Karkibada as shown in Figure 4. Very high vulnerable houses were found scattered and away from the clusters of the village and having a solitary status. Such families were generally minority casts and don't have enough resources to build houses in the main village. Those individual households were devoid of most facilities while those in clustered villages were taking benefits of common services. The unequal distribution of resources and services can be attributed to their solitary nature of living and negligence from the government's side as more time and costs should be considered to make infrastructures accessible to those individual households.

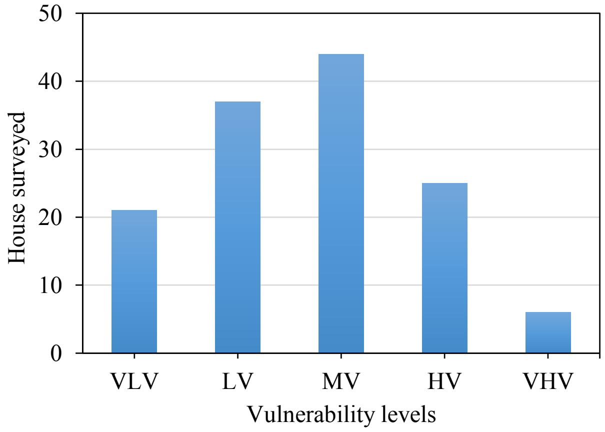

Figure 3. Vulnerability levels of household surveyed after standardization

In Figure 4 the scores of the individual household were interpolated so as to represent the spatial coverage of vulnerability. This further reflected that clustered villages and areas with high economic activities like Gamgadhi (subset image 1 of Figure 4) and Airport have a lower vulnerability. On the other side, a higher vulnerability was distributed where the villages are small and are away (subset image 2 of Figure 4) from headquarter Gamgadhi.

Moreover, the moderate vulnerability in a higher number of households showed similar results as concluded by Aksha et al. (2019) but causative factors for higher vulnerability can be different. As the higher vulnerability being the outcome of solitary nature some families, considerations by government authorities to bring them in the mainstream so that they can get enough supply of all the services that are provided in other clustered villages. Here, further researches needed to be carried out about the ways to make those individual households inclusive.

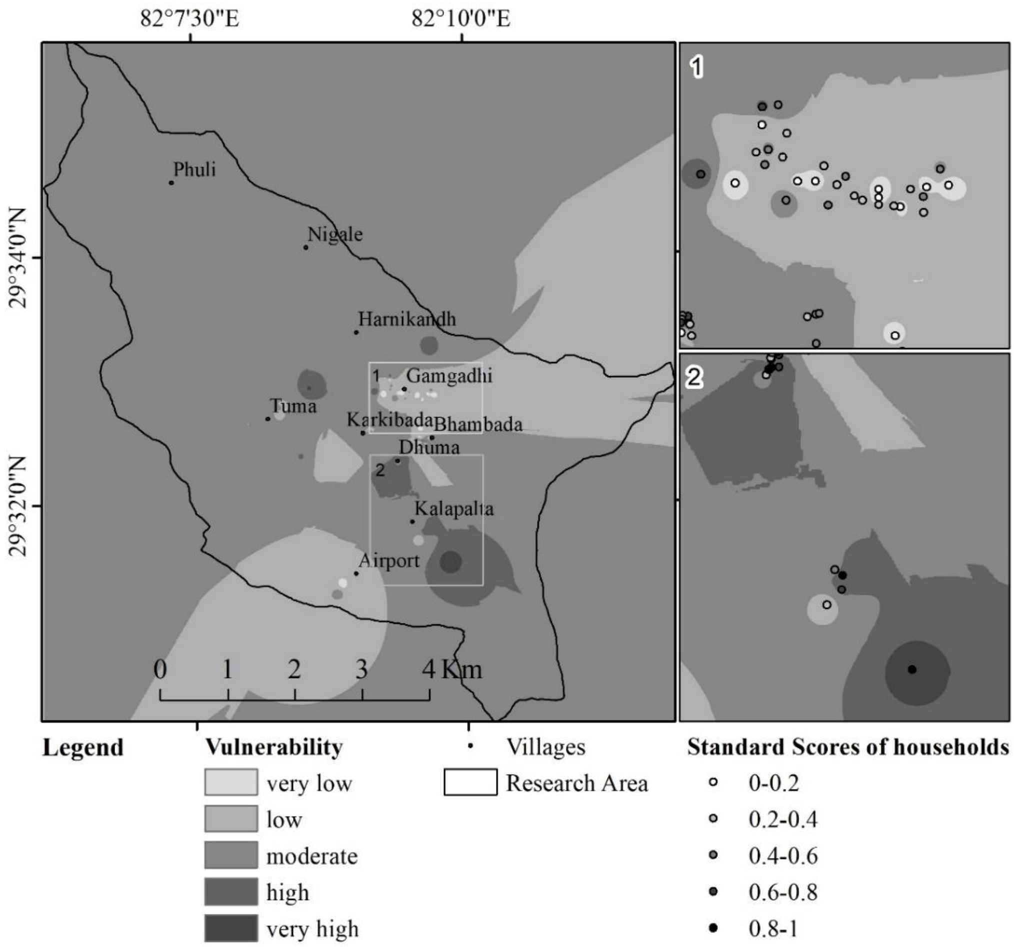

Figure 4. Spatial distribution of the vulnerability in the research site with representations: 1 as low vulnerable area, and 2 as a highly vulnerable area

3.2 Indicators producing high vulnerability

The responses that influence higher vulnerability for each indicator are shown inside parenthesis for each indicator in Table 2. The percentages indicate the number of responses out of 133 households for each indicator that indicated high vulnerability. The higher the percentage the higher was its contribution in very high vulnerability.

For example, indicator 1 in Table 2 shows 12.78% of respondents had females as heads of the family indicating lower influence in high vulnerability. In the case of economic vulnerability variables in Table 2, indicator 23 is producing high vulnerability as most of the peoples are generating income from a single profession and they don't tend to change higher income-generating businesses. This indicates lesser diversity in occupation and in case of catastrophic events they may not have alternatives for their livelihood. Lack of perennial cash crops like fruits and less diversity in livestock also inflicts high vulnerability. Decreasing grasslands and decreased agricultural productivity were indicators among environmental vulnerability variables that were perpetrating the high vulnerability of peoples. Lack of institutional or governmental support, as well as insignificant community-level activities for hazard control, were also contributing to increased vulnerability of the locality.

Table 2. Share in the higher vulnerability of each indicator

Ind.	Vulnerability Indicators	%	Ind.	Vulnerability Indicators	%
Social Vulnerability Variables			*Economic Vulnerability Variables*		
1	Head of the Household (female)	12.8	19	Income (less than average)	53.4
2	Occupation (depending on only one occupation)	73.7	20	cash reserve (no)	24.8
3	Family size (small than the average size of six)	35.3	21	access to credit (no)	41.4
4	Dependent population (age group: infant, 6-12, & above 60)	34.9	22	access to information (no)	3.01
5	Education (illiterate and less than grade 2)	11.3	23	changed profession (no)	95.5
6	No of relatives (less than three)	45.9	*Environmental Vulnerability Variables*		
7	Involvement in social activities (no)	53.4	24	Forest (decreasing)	100
8	non-working people in family	68.0	25	Grassland (decreasing)	97.0
9	House type (stone/mud and wood)	94.7	26	Agriculture (decreasing)	91.7
10	roof type (wood)	68.4	27	Productivity (decreasing)	97.0
11	Cooking (firewood only)	92.5	28	Settlement (increasing)	87.2
12	Standard (low)	48.9	29	Hazards (increasing)	42.9
Economic Vulnerability Variables			30	Temperature (increasing)	96.2
13	Land holding (only one plot or no)	37.6	31	Rainfall (decreasing)	91.7
14	Land availability (lower than average of 5.48 no. of plots)	57.1	32	Landslide occurrences (observed in their surroundings)	89.5
15	cultivation (less than 2 crops or non-cultivating)	27.1	33	Landslide damage (two or more items)	62.4
16	perennial crops (nil)	72.2	*Institutional vulnerability variables*		
17	having 1 or less variety of livestock	56.4	34	Landslide control practices (nothing had done)	53.4
18	Food Sufficiency (only up to six months)	31.6	35	Control practices at household and community level (no)	80.5
			36	Institutional support (no support GoN and organisations)	62.8

The following sections present the discussion of each indicator's influence on vulnerability.

3.2.1 Social indicators

Indicators like occupation, non-working population, house type, and cooking fuel (shown as in 2, 8, 10, and 11 in Table 2) showed very high vulnerability among social indicators. Average working to non-working ratio was found to be 1:2 in the study area but most jobs done were to sustain the daily life requirements. Almost all houses had access to electricity but almost 92.5% of houses surveyed use firewood as a primary fuel for cooking. This indicated a lack of petroleum fuels in the area and the pressures on existing forests are greater. 125 houses were made from stone and mud with 91 having wooden roofs. KC (2013) found that; with the increase in 1% of permanent housing in Hills and Mountains of Nepal there was a 1% decrease in deaths due to landslides had flood hazards. In the research all houses were permanent. Some researchers consider large families as more vulnerable than smaller ones (Dwyer et al., 2004). In contrast, there are fewer human resources to work in crop fields in families with 4 or 5 members which in turn will decrease productivity making them more vulnerable. As mentioned by Sujakhu et al. (2019) households headed by females increased vulnerability but in this research area, the share of household head was only 12.78% by females showing less influence of the indicator. From the field survey, it was found that 118 respondents were literate but most of them didn't have higher education. This will reduce the coping capacities of people towards hazardous conditions. 46.6 percent of respondents showed involvement in social activities which seems they like to work in cooperation with one another. This is obligatory when adverse condition prevails.

3.2.2 Economic indicators

Indicators like land availability, perennial crops, less livestock diversity, and less diversity in the profession showed inflicting high vulnerability. Here, properties, income, and assets were noted during the survey. 18 people in the study area didn't possess any land and 16 of which were from headquarter of the municipality. On the other side, 83 peoples have land properties in two or more areas where food crops and cash crops can be grown depending upon the existing land conditions. This increased the diversity of crops which helps in sustaining livelihoods throughout the year. All families who depend on agriculture had cultivated manually, and used animal manure as primary fertilizers, depended upon rain and nearest stream for irrigation and had their own seed stocks. This reflects the lack of modern technologies, the use of which could increase productivity and hence reduce vulnerability which is also found by Sujakhu et al. (2018) that access to information and education can reduce vulnerability.

As the study area is located in district headquarter the income level from the questionnaire interview was found to be higher with an average monthly income of Nepalese Rupees (NRs) 21,676.7 (~200$). Likewise, the average expenditure per month was revealed as NRs 13,804.5 (~125$). There were banking facilities in headquarter so that people can do savings. 42.1% of people had the cash reserve, 58.6% of people had access to credit and 97% had access to information. The facilities of headquarter can be reached from every part of the study area within one day. Thus, the access banking facilities and savings of people can be useful in hazardous conditions. These indicators have less contribution to the higher vulnerability of the area.

3.2.3 Environmental indicator

Most of the indicators of environmental vulnerability variables indicate high vulnerability. Most of the respondents said that the forests and grasslands were decreasing whereas settlements had the opposite trend. The main reasons behind these were depicted by the respondent as population growth, need of the wood for building construction and fuel, road access to district, lack of awareness, lack of proper management and so on. Many trees in Mugu district have fire scars deep within their cones, an indication that forest fires have been periodic over at least the past 70 years (Nightingale, 2010) which can be one reason for a decrease in forest stands. The farming trend was also found to be decreasing as many youngsters were attracted to other employments making higher food deficit in houses. Lower-income from agriculture became a push factor towards other jobs.

It was reported by 128 respondents the temperatures were increasing in the last 10 years while 122 respondents felt decreasing precipitation at the same time period. These climatic conditions were thought to be a playing role in climatic hazards like drought, hailstorm or climate-induced hazards like landslides. Climate change had increased the vulnerability by increasing disaster risk, adding stress on natural protectors of hazards, and undermining livelihoods that provide resilience against disaster (MoHA, 2013). Mugu District is prone to multi-hazards; of which major are earthquakes of 500 year return period, rainfall-induced landslides, and disease/outbreaks (Nepal Hazard Risk Assessment, 2010). Also, the district falls into the very high category for drought risk/exposures with indices ranging from 0.563 to 1; where decreasing precipitation and increasing temperatures were proxy indicators (MoE, 2010). Also, climate change and variability are expected to affect the frequency of heavy rainfall and wildfires that enhance the potential for landslide occurrence (Alcantara-Ayala et al., 2017). Thus, it can be concluded that adverse environmental changes were imposing adverse conditions on the livelihoods of people and hence inflicting high vulnerability.

3.2.4 Institutional indicators

Though the study area was located in the district headquarter institutional support was negligible in different phases of the disaster cycle. Inadequate institutional support was noted from this survey as 62.78% responded to this. Post-disaster remedies were major activities of some institutions like the Red Cross and Natural Calamity Relief Fund at District Administrative Office (DAO). While, one village named Bhambada; was involved in the construction of gabion walls, tree plantation, and awareness as pre-disaster measures to reduce vulnerability. People were found not reporting the disaster loss as the compensation from DAO was relative to a smaller amount. 80.45% of respondents said they do nothing to control landslides at the household/community level. As there exist lengthy processes to acquire financial and logistic support, it was difficult for communities to conduct hazard mitigation practices at the community level. The National Adaptation Programme of Action (NAPA) prepared by GoN lists out the factors that exacerbate vulnerability to climate-related disasters. The factors include inadequate institutional guidance and land-use regulation, failure to implement building codes, inadequate public awareness, and limited access to early warning systems (NAPA, 2010). As the installation of early warning systems and skill development for disaster risk management reduces the vulnerability of households (Bista, 2019), this can be an important step to lowering vulnerability.

Thus, it is recommended to diversify livelihood options, increasing crop productivity by using modern technology, intensify the governmental services and work for environment protection in order to lower the vulnerability. Exploring mitigation measures can be further research steps in order to find suitable options to reduce vulnerability.

3.3 Vulnerability from different sectors

It can be observed in Table 2 that for social, economic, environmental, and institutional indicators the average percentages of scores causing high vulnerability becomes 53.31, 45.45, 85.56, and 65.54, respectively. This revealed that social and economic indicators in the study area were illustrating vulnerability in a moderate way whereas environmental and institutional sectors had a greater share in causing higher vulnerability which is also clarified in Figure 5. Results in this research were contrasting to that of Aksha et al. (2019) where social and economic sectors contributed to higher vulnerability. Here, the findings show that changing environmental conditions and the accessibility/distribution of facilities as prime causative factors of high vulnerability which is contrasting to that of Gautam (2017).

Figure 5, represents the share of a single sector in low, moderate or high vulnerability. Social and economic sectors show that their contribution to high vulnerability is minimal as compared to economic and institutional vulnerability. Among environmental and institutional sectors high vulnerability is depicted as 72.63 and 64.66% respectively (Figure 5). In social sectors percentages of moderate vulnerability were found higher whereas in economic sectors percentages of low vulnerability were greater.

Thus, when a single sector was considered it was found the environmental and institutional having their greater share leading to higher vulnerability. Measures to strengthen the institutional capacity and assurance of their presence in each village can be a topic to research in this case.

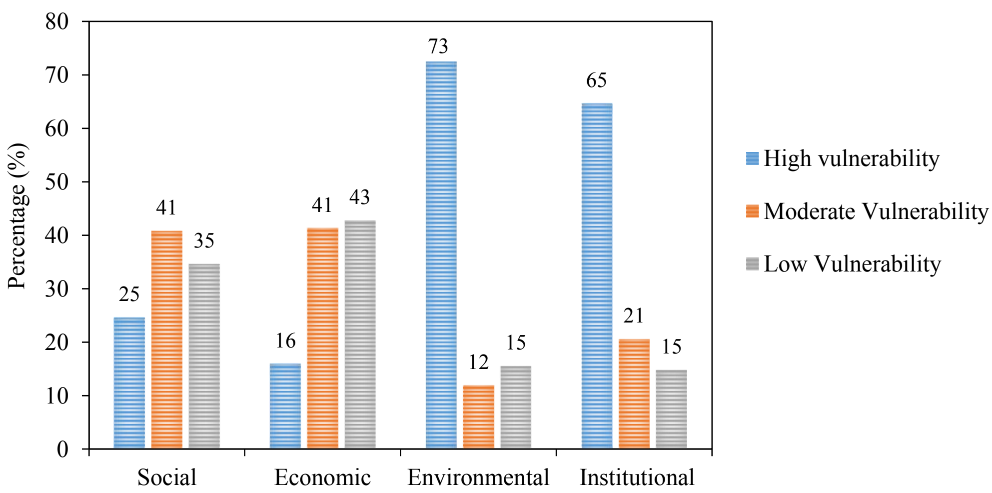

Figure 5. Contribution of a sector to vulnerability (three levels of vulnerability)

4. CONCLUSION

As the research was conducted at a local scale and use revealed circumstances for each indicator, directly from households, the vulnerability status of the people residing in headquarter of Mugu District was presented in a more accurate way. Most households reflected the moderate vulnerability and the results are quite contrasting to that of national-level assessments done by other researchers. Other vulnerability assessments showed the Mugu District as high to very high vulnerable districts. The findings showed that changing environmental conditions and the accessibility/distribution of facilities as prime causative factors. The common findings are that the isolation of an individual from the core community makes it more vulnerable such that it would be difficult and costly to provide services to people located in remote areas. Based on the inferences of this research, the reduction of vulnerability can be possible when access to infrastructures and the services are provided to all households. The isolated households should be provided with opportunities for integration in the core community to increase their capacities. Further researches in other parts of the Mugu District can provide a state of vulnerability whole district.

Besides, vulnerability is a critical issue needed to be addressed during the disaster cycle and vague inferences can lead to faulty management practices. The findings showed that results done at a local scale can be different from that of national-level studies and thus there is the necessity of local-level vulnerability assessment for precise results and fair disaster risk management. Further researches should be carried out to explore livelihood opportunities, mitigation options, and ways to effectively link governmental services to isolated areas.

ACKNOWLEDGEMENTS

We would like to acknowledge Strengthening Disaster Risk Management in Academia (Tribhuvan University-Central Department of Environmental Science) for their financial support in this research.

REFERENCES

Aksha SK, Juran L, Resler LM, Zhang Y. An analysis of social vulnerability to natural hazards in Nepal using a modified social vulnerability index. International Journal of Disaster Risk Science 2019;10(1):103-16.

Alcantara-Ayala I, Sassa K, Mikoš M, Han Q, Rhyner J, Takara K, Nishikawa S, Rouhban B, Briceño S. The 4th World Landslide Forum: Landslide research and risk reduction for advancing the culture of living with natural hazards. International Journal of Disaster Risk Science 2017;8(4):498-502.

Alexander D. Vulnerability to landslides. In: Glade T, Anderson M, Crozier MJ, editors. Landslide Hazard and Risk. Chichester, England: John Wiley and Sons; 2004. p. 175-90.

Arkin H, Colton RR. Tables for Statisticians. New York: Barnes and Noble Books; 1963.

Armas I, Gavris A. Social vulnerability assessment using spatial multi-criteria analysis (SEVI model) and the social vulnerability index (SOVI model): A case study for Bucharest, Romania. Natural Hazards and Earth System Sciences 2013;13(6):1481-99.

Bista RB. Determinants of flood disaster households' vulnerability in Nepal. Economic Journal of Development Issues 2019;25(1):47-59.

Briguglio L, Cordina G, Farrugia N, Vella S. Economic vulnerability and resilience: Concepts and measurements. Oxford Development Studies 2009;37(3):229-47.

Budha PB, Paudyal K, Ghimire M. Landslide susceptibility mapping in eastern hills of Rara Lake, western Nepal. Journal of Nepal Geological Society 2016;50(1):125-31.

Cardona OD, van Aalst MK, Birkmann J, Fordham M, McGregor G, Perez R, Pulwarty RS, Schipper ELF, Sinh BT. Determinants of risk : Exposure and vulnerability. In: Field CB, Barros V, Stocker TF, Qin D, Dokken DJ, Ebi KL, et al. editors. Managing the Risks of Extreme Events and Disasters to Advance Climate Change Adaptation: A Special Report of Working Groups I and II of the Intergovernmental Panel on Climate Change (IPCC). Cambridge, UK, and New York, USA: Cambridge University Press; 2012. p. 65-108.

Central Bureau of Statistics (CBS). National Population and Housing Census 2011. Volume 1. Kathmandu, Nepal: National Planning Commission Secretariat; 2011.

Cutter SL, Boruff BJ, Shirley WL. Social vulnerability to environmental hazards. Social Science Quarterly 2003;84(2):242-61.

Devkota RP, Marseni TN, Cockfield G, Devkota LP. Flood vulnerability through the eyes of vulnerable people in Mid-western terai of Nepal. Journal of Earth Science and Climatic Change 2013;4(1):1-7.

Dwyer A, Zoppou C, Nielsen O, Day S, Roberts S. Quantifying social vulnerability: A methodology for identifying those at risk to natural hazards. Geoscience Australia Record 2004/14. Commonwealth of Australia; 2004.

Ebert A, Kerle N. Urban Social vulnerability assessment using object-oriented analysis of remote sensing and GIS data: A case study for Tegucigalpa, Honduras. International Archives of the Photogrammetry, Remote Sensing and Spatial Information Sciences 2008;37:1307-12.

Ebert A, Kerle N, Stein A. Urban social vulnerability assessment with physical proxies and spatial metrics derived from air and spaceborne imagery and GIS data. Natural Hazards 2009;48(2):275-94.

Gautam D. Assessment of social vulnerability to natural hazards in Nepal. Natural Hazards and Earth System Sciences 2017;12:2313-20.

Haki Z, Akyürek Z, Düzgün Ş. Assessment of social vulnerability using geographic information systems, Pendik Istanbul case study. Proceedings of the 7th AGILE Conference on Geographic Information Science; 2004 Apr 29-May 1; Heraklion, Greece Parallel; 2004.

Joseph J. Measuring vulnerability to natural hazards: A macro framework. Disasters 2013;37(2):185-200.

KC S. Community vulnerability to floods and landslides in Nepal. Ecology and Society 2013;18(1):art8.

Ministry of Environment (MoE). Climate Change and Vulnerability Mapping for Nepal. Kathmandu, Nepal: Government of Nepal; 2010.

Ministry of Home Affairs (MoHA). Nepal Disaster Report 2017: The Road to Sendai. Kathmandu, Nepal: Government of Nepal; 2018.

Ministry of Home Affairs (MoHA). Nepal Disaster Report 2013; Focus on Participation and Inclusion. Kathmandu, Nepal: Government of Nepal and Disaster Preparedness Network-Nepal (DPNet-Nepal); 2013.

National Adaptation Programme of Action (NAPA). National Adaptation Programme of Action (NAPA) to Climate Change. Kathmandu, Nepal: Ministry of Environment, Government of Nepal; 2010.

Nepal Hazard Risk Assessment. Part 3: Hazard Assessment. Kathmandu, Nepal: Government of Nepal, Asian Disaster Preparedness Centre (ADPC), Norwegian Geotechnical Institute (NGI), and Centre for International Studies and Cooperation (CECI); 2010. p. 27-76.

Nightingale A. Research synopsis: Land management in Mugu District of western Nepal: power, cultural practices and ecological conditions. Journal of the Association for Nepal and Himalayan Studies 2010;21(1):41-4.

Rajesh S, Jain S, Sharma P. Inherent vulnerability assessment of rural households based on socio-economic indicators using categorical principal component analysis: A case study of Kimsar region, Uttarakhand. Ecological Indicators 2018; 85:93-104.

Sharma P, Guha-Khasnobis B, Khanal DR. Nepal Human Development Report 2014; Beyond Geography, Unlocking Human Potential. Kathmandu, Nepal: National Planning Commission-Government of Nepal, and United Nations Development Programme; 2014.

Sujakhu NM, Ranjitkar S, He J, Schmidt-Vogt D, Su Y, Xu J. Assessing the livelihood vulnerability of rural indigenous households to climate changes in central Nepal, Himalaya. Sustainability 2019;11(10):2977.

Sujakhu NM, Ranjitkar S, Niraula RR, Salim MA, Nizami A, Schmidt-Vogt D, Xu J. Determinants of livelihood vulnerability in farming communities in two sites in the Asian Highlands. Water International 2018;43(2):165-82.

Tapsell S, McCarthy S, Faulkner H, Alexander M, Steinführer A, Kuhlicke C, et al. Social Vulnerability to Natural Hazards. CapHaz-Net WP4 Report. Middlesex University, London: Flood Hazard Research Centre - FHRC; 2010.

Tesso G, Emana B, Ketema M. Analysis of vulnerability and resilience to climate change induced shocks in North Shewa, Ethiopia. Agricultural Sciences 2012;03(06):871-88.

United Nations International Strategy for Disaster Reduction (UNISDR). UNISDR Terminology on Disaster Risk Reduction. Geneva, Switzerland: United Nations International Strategy for Disaster Reduction; 2009.

Effects of Climate Variability on the Annual and Intra-annual Ring Formation of *Pinus merkusii* Growing in Central Thailand

Nathsuda Pumijumnong[1] and Kritsadapan Palakit[2*]

[1]*Faculty of Environment and Resource Studies, Mahidol University, Thailand*
[2]*Laboratory of Tropical Dendrochronology, Department of Forest Management, Faculty of Forestry, Kasetsart University, Thailand*

ARTICLE INFO

Received: 5 Aug 2019
Received in revised: 3 Feb 2020
Accepted: 19 Feb 2020
Published online: 26 May 2020
DOI: 10.32526/ennrj.18.3.2020.22

Keywords:
Climate reconstruction/ Dendrochronology/ False ring/ Merkus pine/ *Pinus latteri*

***Corresponding author:**
E-mail: fforkpp@ku.ac.th

ABSTRACT

The research clarifies which climatic factors induce annual and intra-annual ring formation in merkus pine (*Pinus merkusii*) growing in the low lying plains of central Thailand and reconstructs the past climate by using climate modelling derived from climate-growth response. Not only are climate variations longer than a century in central Thailand explained, but the study also explores for the first time the variability in climate using the formation of intra-annual rings in Thai merkus pines. The tree-ring analysis of wood core samples indicated that the pine stand was more than 150 years old with the oldest tree being 191 years old. The annual variation in tree growth significantly correlated with local climate variables, the number of rainy days in each year ($r=0.520$, $p<0.01$) and the extreme maximum temperature in April ($r=-0.377$, $p<0.01$). The regional climate of the Equatorial Southern Oscillation in March (EQ_SOI_{March}) also highly correlated with the pine growth ($r=0.360$, $p<0.01$). The climate reconstruction indicated a declining trend in the number of rainy days during the 20th century and a decline in the number of rainy days was observed during the first and second decades of the 21st century, respectively, while the past climate reconstruction of maximum temperature in April and EQ SOI_{March} indicated a decline during the previous century and an increase in this century. A multiple regression analysis indicated that the extreme maximum temperature, which declined at the beginning of the wet season and increased around the transitional period of the late rainy and the cold seasons, influenced the formation of intra-annual rings ($r^2=40.5\%$, $p<0.05$). It can be summarized that the number of rainy days increasing in each year associated with the declining temperature at the beginning of the wet season indicated a rapid growth in *P. merkusii*, while the anomalous temperature declining at the beginning and increasing at the end of the wet season was the main factor inducing the intra-annual ring formation. Therefore the activity of forest and planation management, especially in the watering at the beginning of the wet season when anomalous increased temperature occurred, shall be specified in the forest management plan in order to increase annual pine growth and wood formation.

1. INTRODUCTION

Climate change has recently impacted human life and natural systems worldwide. Natural disasters related to climate systems have continuously increased since 1950 with a trend of warmer temperatures. IPCC (2014) suggested that during the period from 1880 to 2012, the global temperature rose by 0.85 °C (0.65 to 1.06 °C) and the sea level since the mid-19th century rose by 0.19 m (0.17 to 0.21 m.) and has been higher than the mean rate during the previous two millennia. In general, climate trends based on short records do not reflect precise long-term fluctuations (IPCC, 2014). As an example, consider the warmer period of 1998-2012, during which the rise in temperature was 0.05 °C (-0.05 to 0.15 °C per decade), which is smaller than the rise of 0.12 °C (0.08 to 0.14 °C per decade) calculated since

Citation: Pumijumnong N, Palakit K. Effects of climate variability on the annual and intra-annual ring formation of *Pinus merkusii* growing in Central Thailand. Environ. Nat. Resour. J. 2020;18(3):234-248. DOI: 10.32526/ennrj.18.3.2020.22

1951. It could be assumed that the recorded meteorological data is not enough to accurately predict the climatic trend in the future. Therefore, the understanding of the past climate system is necessitated and can be combined with the recorded meteorological data to construct a climate model in order to forecast the precise climate trend in the future.

Several climate proxies such as ice cores, sub-fossil pollen, boreholes, corals, sediments, and carbonate speleothems are used to reconstruct the past climate conditions. Tree-rings are another climate proxy generally used to reconstruct climatic patterns in many regions of temperate and tropical zones. In Southeast Asia, teak (*Tectona grandis* L.f.) in Java was first used for tree-ring analysis to investigate the climate related growth by Berlage (1931) and other dendrochronologists (e.g., DeBoer, 1951; Jacoby and D'Arrigo, 1990; D'Arrigo et al., 1994; D'Arrigo et al., 2006; Bijaksana et al., 2007). Apart from the initial studies in Indonesia, other countries in this region such as Myanmar, Laos PDR and Thailand also undertook teak ring analysis to investigate climate-growth response and past climate reconstruction (Pumijumnong et al., 1995a; Pumijumnong et al., 1995b; Pumijumnong and Park, 1999; Pumijumnong and Park, 2001; Buckley et al., 2007b; D'Arrigo et al., 2011; Lumyai et al., 2017).

The possibility of tropical tree-ring analysis in this region is not only limited to teak trees. Studies in Laos PDR and Thailand found the feasibility of using *Pinus kesiya* and *P. merkusii*, especially growing in the highlands and on the slopes in the north and northeastern regions, for investigating the climate-growth response and the past climate reconstruction (Pumijumnong and Eckstein, 2011; Pumijumnong and Wanyaphet, 2006; Buckley et al., 1995; Buckley et al., 2007a; Duangsathaporn and Palakit, 2013). Once the relationships between climate and tree-ring formation were understood, the past climate was also reconstructed. Climate not only induces annual ring width variations, but it also induces the formation of intra-annual rings in several tree species in both tropical and temperate zones (Palakit et al., 2012; Vieira et al., 2010; De Luis et al., 2011; Olivar et al., 2012). Although it is clear that the formation of intra-annual rings can be directly induced by climate factors, especially precipitation and temperature (De Micco et al., 2016), the patterns or periods of climate response varies for each tree species. Therefore, in this study, the climate inducing annual and intra-annual ring occurrences in Thai mountain pine was studied in order to understand the climate-growth relationship and its adaptation to the changing climate.

This research (i) identifies the relationship between climate and annual ring widths of *P. merkusii* located in the Suphan Buri province, central Thailand; (ii) reconstructs the past climate by using climate modelling derived from climate-growth response; and (iii) clarifies which factors induce the formation of intra-annual rings. A pine stand, near the margin of the natural range, was selected following the principle of the ecological amplitude for dendrochronology which states that the growth of marginal trees is highly limited by climate and reflects the climate-growth responses greater than trees growing near the center of its geographical distribution (Fritts, 1976).

2. METHODOLOGY

2.1 Study area and climate data

The study area is a natural pine (*Pinus merkusii*) stand located at the Phu Toei National Park in Suphan Buri province, central Thailand (Figure 1). *P. merkusii* can be found alongside other dry dipterocarp trees such as *Dipterocarpus obtusifolius*, *Shorea obtuse* and *S. siamensis*, at an elevation of 500-800 m above mean sea level. These dipterocarp trees and *P. merkusii* are the dominant species accounting for 41.92% and 31.68% of crown cover, respectively. The climate data in A.D. 1953-2016, measured by the Suphan Buri Meteorological Station included temperature, rainfall, and relative humidity and was divided into 2 seasons as dry (Nov-Apr) and wet (May-Oct). The dry season, when the mean monthly temperature and rainfall were 27.68 ºC and 29.13 mm, respectively, could be further divided into cold (Nov-Feb: The mean temperature was 26.36 ºC) and hot (Mar-Apr: The mean temperature was 30.33 ºC) periods. The wet season, when the mean monthly temperature and rainfall were 25.50 ºC and 156.31 mm, respectively, could be further divided into 3 periods of early (May-Jun), mid (July-Aug), and late (Sep-Oct) rainy seasons with the mean monthly rainfall for 119, 120 and 230 mm, respectively. The amount of rainfall decreased during the mid-rainy season and rapidly increased during the late rainy season (Figure 1).

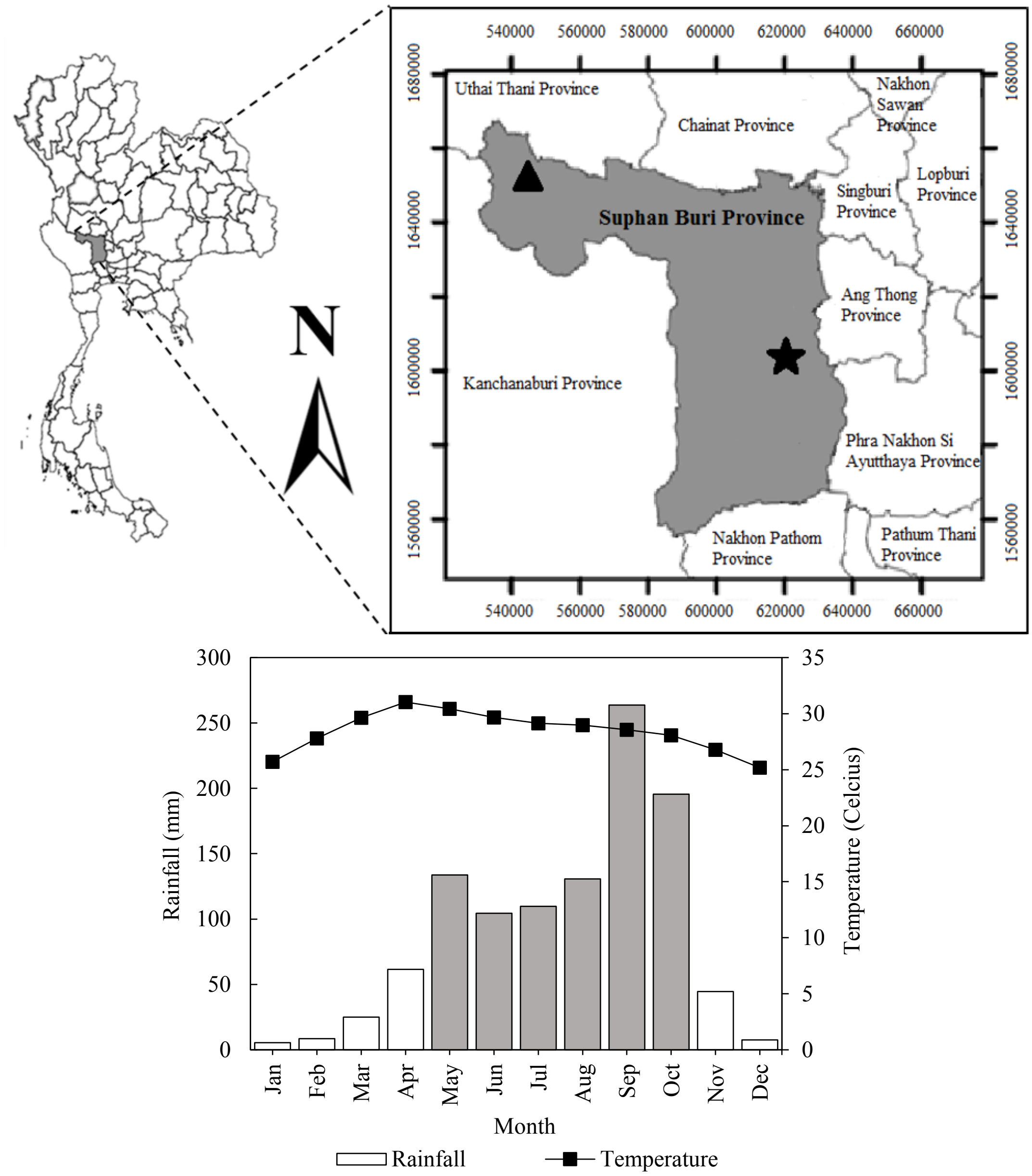

Figure 1. Location of the study site (triangle and star symbols indicate the study site and the Suphan Buri Meteorological station, respectively) and the average monthly climate data obtained from the Suphan Buri Meteorological Station in A.D. 1953-2016 (Gray columns indicate the wet season).

2.2 Wood core collection and annual ring measurement

At a breast height of 1.3 m, a total of 24 wood cores were collected from healthy pine trees using an incremental borer with a 40 cm long and 0.5 cm diameter drill bit, in order to avoid the effect of buttress and injury to the tree base. Following the standard method of dendrochronology (Stokes and Smiley, 1996), after drying at room temperature, all the wood cores were fixed on wood support using a soluble glue and adhesive tape and carefully polished by using several grades of sandpapers to obtain clean and smooth wood surfaces to expose the ring boundaries.

The patterns of variations in annual ring width and the calendar year, during which each annual ring was formed, were examined and matched with sample cores using the technique of cross-matching by observing under a stereo microscope with a magnification of 10x-40x. During cross-matching, intra-annual rings were identified and their frequencies during each year were marked. The annual ring width was measured by using the Velmex Tree-Ring Measurement System (Velmex Inc., New York, USA), consisting of 3 components of a unislide linear stage, 0.001 mm resolution linear encoder, and an encoder readout.

2.3 Data analysis

The accuracy of the annual ring measurement and cross-matching was then verified using the software COFECHA (Holmes, 1983). The software used the technique of segmented time series correlation to assess the quality of the measurement (Grissino-Mayer, 2001). The statistical value of annual ring width series including the intercorrelation, autocorrelation and mean sensitivity coefficients derived from the software COFECHA were then informed. All the annual ring-width series were transformed to annual ring width indices as a ratio of the measured annual ring width and the expected growth in order to eliminate the age effect and maximize the climatic signal using the double detrending technique. By using the ARSTAN software with autoregressive modelling (Cook and Peters, 1981), the first detrending was done using a negative exponential curve or straight line with a negative slope, followed by a second detrending using a 66 years spline curve, which was fitted to each ring-width series. All the indices were averaged to obtain a master chronology by using the arithmetic mean with a mean value of 1. The index with the lowest autocorrelation coefficient and the highest mean sensitivity was selected. To indicate an acceptable sample size and common variance, the expressed population signal (EPS) was also calculated (Borgaonkar et al., 2010; Cook et al., 1990; Wigley et al., 1984).

In order to investigate the significant climate-growth relationship, the correlation coefficient (r) and the coefficient of determination (r^2) were calculated by using the statistics of simple correlation and regression analysis, respectively. The local climate data of monthly rainfall (total rainfall, number of rainy day and maximum rainfall), monthly temperature (extreme maximum temperature, extreme minimum temperature, mean maximum temperature, mean minimum temperature and mean temperature) and relative humidity were defined as the predictors (independent variables) and the constructed ring width index was defined as the predictand (dependent variable). The regional climate data of the Equatorial Southern Oscillation Index (EQ_SOI) and the Equatorial Sea Surface Temperature (EQ_SST), obtained from https://www.esrl.noaa.gov/psd/data/climateindices/, were other important predictors selected for investigating the relationship with the ring width index.

2.4 Climate reconstruction

The past climate reconstruction was performed by using the patterns of climate-growth response derived from the above statistical analysis. The resemblance between instrumental and reconstructed climate was compared to indicate the efficiency of the past climate modeling using several statistics such as Pearson product-moment correlation (Rp), sign-product test (ST), reduction of error test (RE), T-value, means, and standard deviation (SD). The Verify Calibration Model (VFY) software, under the Dendrochronology Program Library (DPL), was used for calculating these statistics.

2.5 Climate factors affecting intra-annual ring formation

The frequencies of intra-annual rings, which were marked during each calendar year, were converted into a percentage and termed as false ring frequency (Fn). Osborn et al. (1997) proposed an equation to stabilize the intra-annual ring frequencies and eliminate bias by changing the sample depth (n) as:

$$f = Fn^{0.5}$$

Where, f is the stabilized intra-annual ring frequency and Fn is the percentage of intra-annual ring frequency. The stabilized intra-annual ring frequency was then related to the local and regional climatic data by using the statistical analysis of linear correlation and multiple regression in order to determine climate factors inducing the intra-annual ring formation.

3. RESULTS AND DISCUSSION

3.1 Annual ring width data

A total of 16 samples were successfully cross-dated from 24 samples of collected wood cores while the anomalous growth patterns of 8 samples could not be cross-matched and cross-dated with other samples. The oldest sampled tree had been growing for longer than 191 years, as indicated by the annual ring samples collected at a height of 1.3 m. These illustrated a growing period during A.D. 1825-2015, while the growing period of the youngest tree was 147 years during A.D. 1869-2015. Although the average ring width was only 1.67 mm/year, Pumijumnong and Eckstein (2011) reported that the mean growth rate of merkus pine (*Pinus merkusii*) distributed in Thailand grew at 1.28 mm/year indicating that their growth was faster than merkus pines in other sites of Thailand, while the average growth of khasi pine (2.15 mm/year) was higher than that of merkus pine.

The statistical values of annual ring width series intercorrelation, autocorrelation, and mean sensitivity were 0.633, 0.603, and 0.266, respectively. These values indicated the similarity of pine growing pattern suitable for studying climate-growth relationship, although the autocorrelation was quite high (Fritts, 1976). The annual growth pattern and growth rate of the merkus pine indicated an average growth of 1.61 mm in the first 46 years in A.D. 1825-1870 followed by an increasing trend of 2.19 mm during the next 50 years in A.D. 1871-1920. Tree growth declined to 1.37 mm for 30 years in A.D. 1921-1950 and declined to 1.01 mm for the next 40 years in A.D. 1951-1990. Pine growth rate was re-stimulated to 1.44 mm from A.D. 1991 to the present time as shown in Figure 2(a) and (b).

Using an autoregressive modeling, the constructed annual ring width index (Figure 2(c)) indicated that the autocorrelation reduced from 0.603 to -0.120, while the mean sensitivity increased from 0.266 to 0.293. EPS indicated that the acceptable sample sizes in all the segments ranged between 0.85-0.97, which was higher than the critical value of 0.85 (Figure 2(d)). The mean sensitivity of these merkus pines was higher than that reported by Pumijumnong and Eckstein (2011), who stated that the mean sensitivity of this species in Thailand was about 0.26 and varied between 0.22-0.33, while the mean sensitivity of khasi pine in Thailand was 0.32 and varying within a range of 0.28-0.37. The reduced growth during A.D. 1951-1990 (Figure 2(a)) was induced by environmental factors and was similar to other studies in several sites of Thailand and Lao PDR followed by an increased growth trend until the current period (Buckley et al., 2007a; Duangsathaporn and Palakit, 2013).

(a)

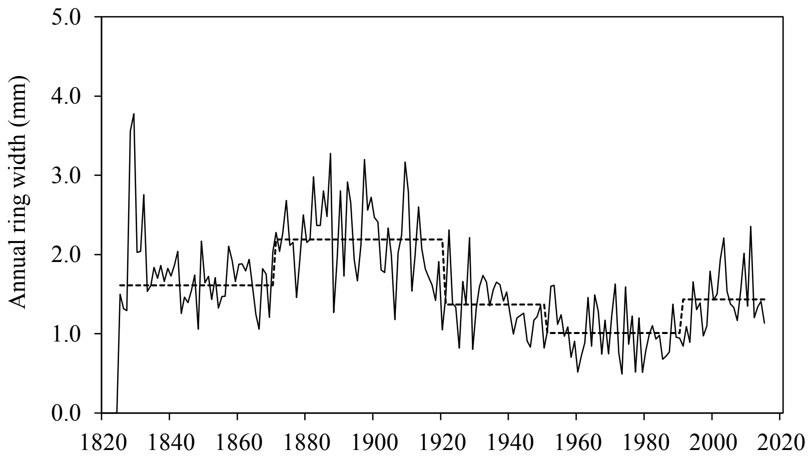

(b)

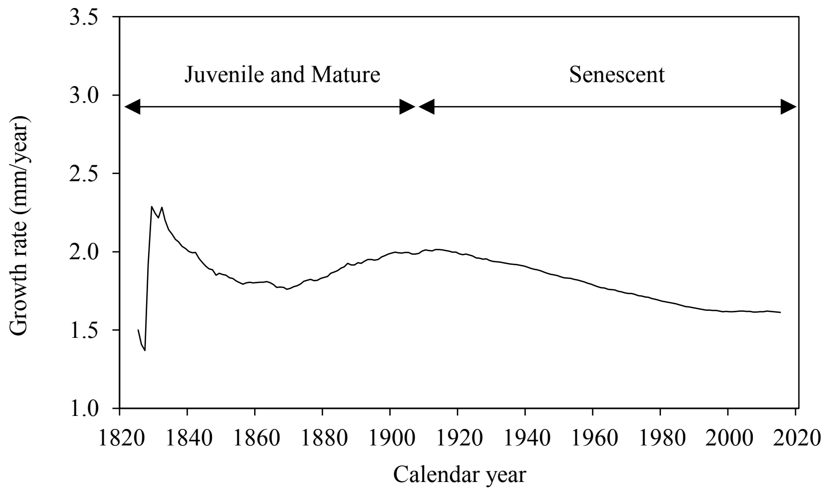

Figure 2. Annual ring width data of merkus pines at the Phu Toei National Park: a) average annual ring widths with mean (dash line) in each segments; b) growth rates; c) annual ring width index (dash line) with a 5 year moving average (thick line); and d) Expressed Population Signal (EPS: thick line) with the critical value of 0.85 (dash line).

(c)

(d)

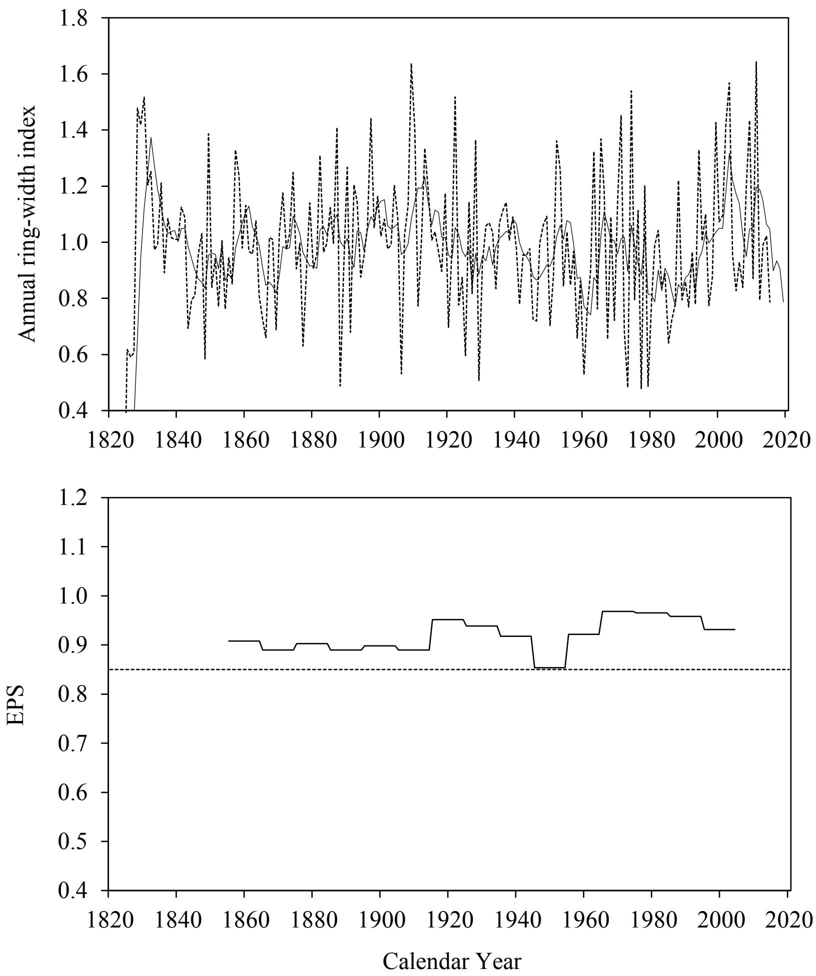

Figure 2. Annual ring width data of merkus pines at the Phu Toei National Park: a) average annual ring widths with mean (dash line) in each segments; b) growth rates; c) annual ring width index (dash line) with a 5 year moving average (thick line); and d) Expressed Population Signal (EPS: thick line) with the critical value of 0.85 (dash line) (cont.).

3.2 The Relationship between climate and annual ring width index

By using the simple correlation analysis, rainfall data and relative humidity were significantly related to the variations in the annual ring width index (Figure 3), suggesting they are factors inducing tree growth. Monthly rainfall in February, March, and April were significantly correlated with the index as indicated by a correlation coefficient (r)=0.255, 0.298, and 0.262, respectively ($p<0.05$). The number of rainy days in February, May, July and annual rainy days were significantly related with the annual ring width index as indicated by r=0.344, 0.341, 0.366 and 0.520, respectively ($p<0.01$). The number of rainy days in March, April, and October were also significantly related to the annual ring width index as indicated by r=0.319, 0.321, and 0.283, respectively ($p<0.05$). The maximum rainfall in July and the relative humidity in May and August were significantly related to the annual ring width index as indicated by r=-0.288, 0.254, and 0.256, respectively ($p<0.05$).

The variation of temperature was also illustrated the significant correlation with the pine index (Figure 4). The extreme maximum temperature in April was significantly correlated with the index as indicated by r=-0.377 ($p<0.01$). At $p<0.05$, the extreme maximum temperature in February and June was significantly correlated with the index for r=-0.305, and -0.266, respectively, while the extreme minimum temperature and mean minimum temperature were not significantly correlated with the growth. The pine index was significantly correlated with the mean maximum temperature in January (r=-0.300; $p<0.05$), February (r=-0.268; $p<0.05$), March (r=-0.325; $p<0.01$), May (r=-0.258; $p<0.05$) and June (-0.282; $p<0.05$). The mean temperature was another local climate variable which was significantly correlated with the index, with the mean temperature in May being significantly correlated with the index as indicated by r=0.323 (p<0.01). The index was also significantly related to the monthly temperature in March, April and June (r=-0.278, -0.257, -0.276, respectively; p<0.05).

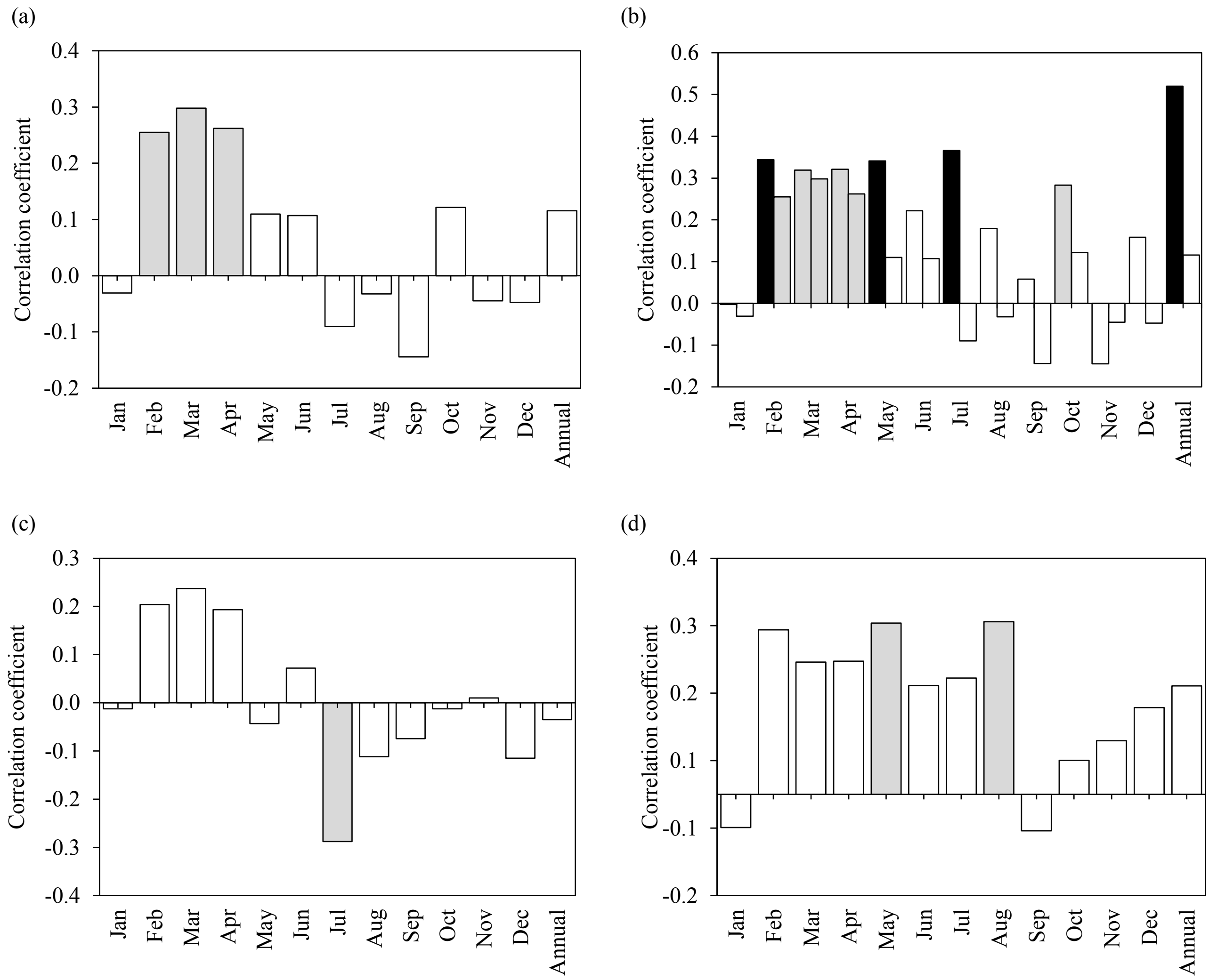

Figure 3. Correlation coefficient between annual ring width index and climate data of rainfall (a), number of rainy days (b), maximum rainfall (c) and relative humidity (d). Gray and black bars indicate the significant (p<0.05) and highly significant (p<0.01) correlation between variables.

Although merkus pines growing at Phu Toei National Park were significantly related to several local climate data, rainfall and temperature at the transition period of the hot (Mar-Apr) and the beginning of the wet (May-Jun) seasons were the main factors inducing pine growth. This observation is similar to the study of Pumijumnong and Eckstein (2011), who found a significant correlation of rainfall and temperature during pre-monsoon (Mar-May) with the merkus pine growing in northern Thailand, while Buckley et al. (2007a) reported a significant correlation of monsoon climate with merkus pine growth in Lao PDR. Lumyai et al. (2008) also indicated the post-monsoon temperature in October as being a key factor affecting the growth of merkus pine in central Thailand. Not only the responses to merkus pine growth, but the pre-monsoon climate was also significantly correlated with the growth of khasi pines in Thailand and India (Chaudhary and Bhattacharyya, 2002; Pumijumnong and Eckstein, 2011), indicating the importance of the pre-monsoon climate on tree growth in Thailand and other countries.

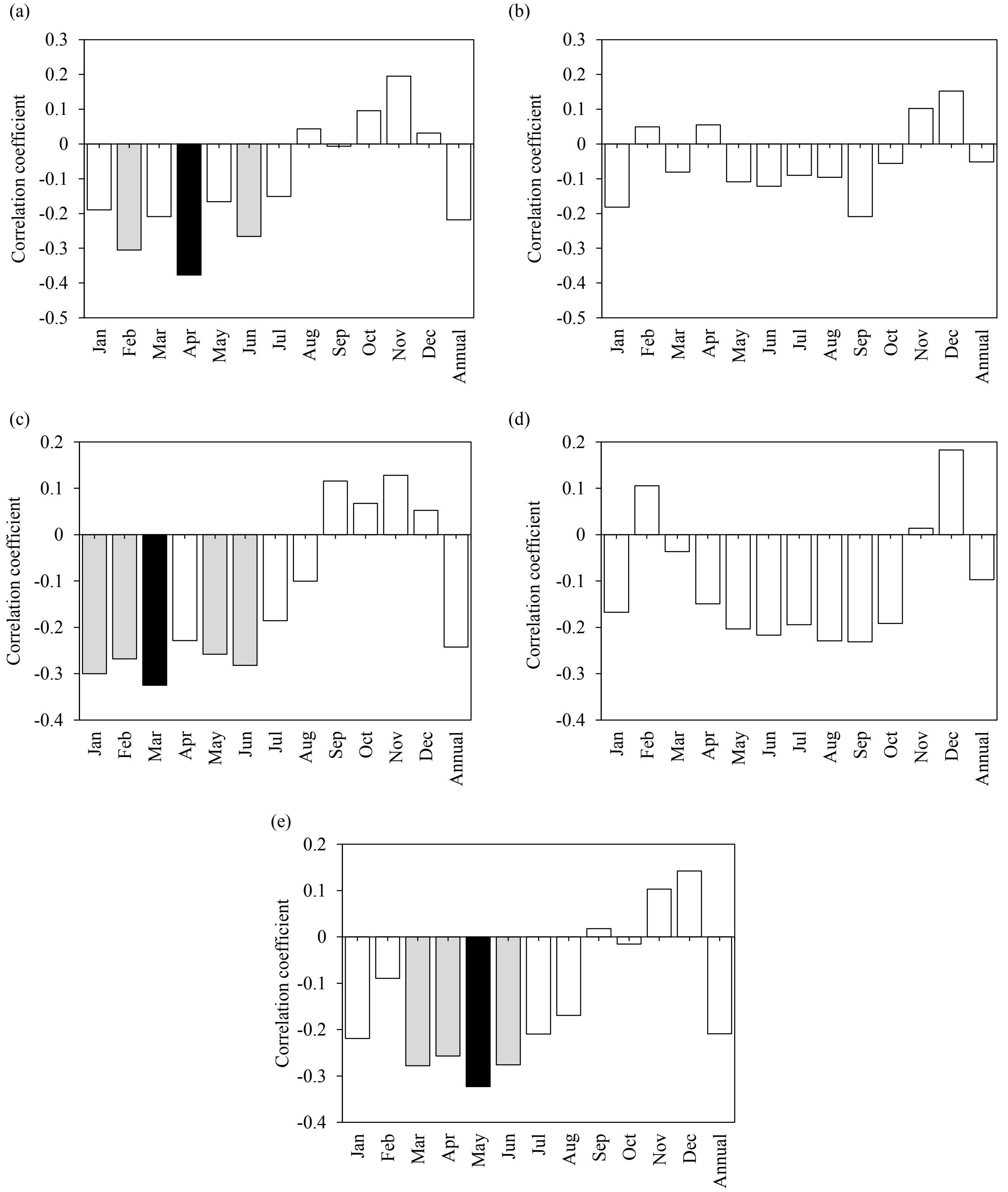

Figure 4. Correlation coefficient between annual ring width index and climate data of extreme maximum temperature (a), extreme minimum temperature (b), mean maximum temperature (c), mean minimum temperature (d), and mean temperature (e). Gray and black bars indicate the significant ($p<0.05$) and highly significant ($p<0.01$) correlation between variables.

The regional climate data of Equatorial Southern Oscillation Index (EQ_SOI) and Equatorial Sea Surface Temperature (EQ_SST) were significantly correlated with the annual ring index (Figure 5). It was found that the EQ_SOI in January, March and April were significantly related to the merkus pine index as indicated by r=0.270 ($p<0.05$), 0.360 ($p<0.01$) and 0.282 ($p<0.05$), respectively, while the EQ_SST was not significantly correlated with the pine growth.

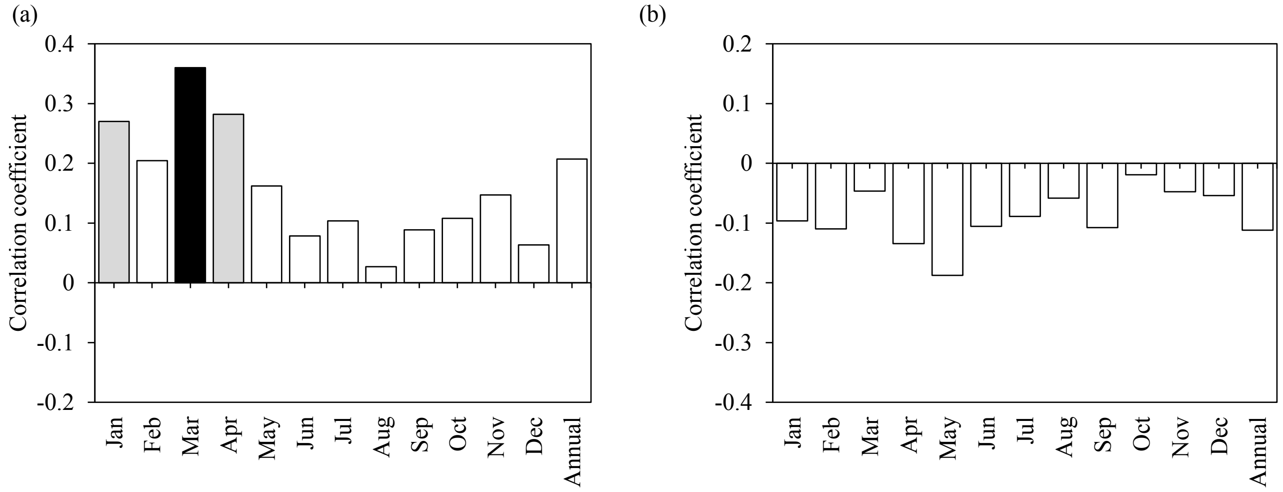

Figure 5. Correlation coefficient between annual ring width index and the regional climate data of Equatorial Southern Oscillation Index (a) and Equatorial Sea Surface Temperature (b). Gray and black bars indicate the significant ($p<0.05$) and highly significant ($p<0.01$) correlation between variables.

The regional climate, as measured by EQ_SOI during the hot season (Mar-Apr) was highly significantly related with the growth of merkus pines, while their growth in the easternmost part Thailand was significantly correlated with EQ_SOI and EQ_SST during the dry season of the current year and the monsoon season of the previous year (Duangsathaporn and Palakit, 2013). In Lao PDR, Buckley et al. (2007a) found a direct growth response of merkus pines to gridded SST over the central and eastern tropical Pacific and was strongest during Mar-May. It could be suggested that the pine growth in Thailand and other countries in Southeast Asia was mainly forced by local and regional climate variations which are then appropriate to study climate variability in the past and future.

3.3 The Past climate reconstruction

The top three highest correlation coefficients between annual ring width index and climate included the number of rainy days during each year, the extreme maximum temperature in April, and the EQ_SOI in March and were selected to reconstruct the past climate up until AD 1825. The number of rainy days ($Rainday_{annual}$) during 1986-2015 was used to construct mathematical equations to describe the fluctuations of the index as indicated by Equation (1) and (2).

$$Index = 0.0015 + 0.0103\ (Rainday_{annual}) \quad (1)$$

$$Rainday_{annual} = 74.559 + 24.388\ (Index) \quad (2)$$

The annual number of rainy days reconstructed using Equation (2) during the years A.D. 1986-2015 and A.D. 1953-1985 were compared with the recorded meteorological data to verify the reliability of the climate model, using the statistics of Pearson correlation, sign product test, reduction of error (RE), and T-test, also known as the standard procedure of model calibration and verification (Table 1). The actual and reconstructed $Rainday_{annual}$ with its trend line are shown in Figure 6. It can be seen that the average number of rainy days during each year in Suphan Buri province was around 98.7 days. The trend of $Rainday_{annual}$ gradually increased from 97.7 days in the 1840s to be 100.9 days in the 1910s and gradually declined to 95.8 days during the 1980s. $Rainday_{annual}$ rapidly increased to 102.2 days during the 2000s and declined to 99.4 days in the current decade.

The extreme maximum temperature in April (Ext_MaxT_{April}) was negatively related with the variations in annual ring-width index. The related pattern of these 2 factors durig A.D. 1995-2015 was used to construct mathematical equations as shown in Equation (3) and (4).

$$Index = 7.4213 - 0.1607\ (Ext\_MaxT_{April}) \quad (3)$$

$$Ext\_MaxT_{April} = 41.362 - 1.7414\ (Index) \quad (4)$$

Table 1. Statistics of climate reconstructed with the number of rainy days ($Rainday_{annual}$), extreme maximum temperature (Ext_MaxT_{April}), and Equatorial Southern Oscillation Index (EQ_SOI_{March})

Statistic	$Rainday_{annual}$		Ext_MaxT_{April}		EQ_SOI_{March}	
	Calibration	Verification	Calibration	Verification	Calibration	Verification
Pearson Correlation	0.49*>= 0.31	0.63*>= 0.29	0.55*>= 0.35	0.29*>= 0.26	0.41*>= 0.32	0.26*>= 0.26
Sign product test	9*<= 10	13<= 11	7*<= 7	18<= 14	7*<= 8	16<= 14
Reduction of error (RE)	0.24*>= 0.09	0.19*>= 0.09	0.30*>= 0.12	0.10*>= 0.06	0.17*>= 0.10	0.14*>= 0.07
T-test	2.11*>= 1.70	2.36*>= 1.70	1.72*>= 1.72	2.06*>= 1.68	0.60>= 1.71	2.69*>= 1.68
Degree of freedom	28	31	21	38	25	38

Remark*: Indicates a significant correlation at $p<0.05$

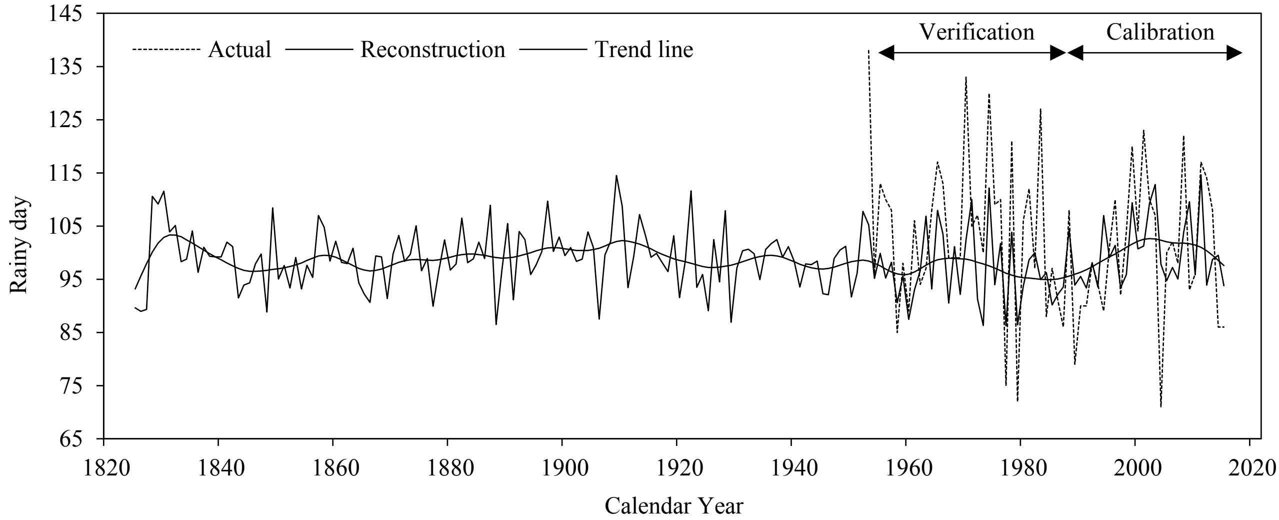

Figure 6. Actual and reconstructed values of the number of rainy days in Suphan Buri province.

The reconstructed values of extreme maximum temperature in April during the two phases of A.D. 1953-1994 and A.D. 1995-2015 were compared with the recorded data derived from the meteorological station to verify the reliability of the model (Table 1). The reconstructed and actual Ext_MaxT_{April} are shown in Figure 7. The fluctuation in the trend line indicated that the extreme maximum temperature decreased from 39.7 °C in the 1840s to 39.5 °C in the 1900s. Later, the temperature gradually increased for 80 years with the highest maximum temperature during the 1980s at 39.8 °C and rapidly declined to 39.4 °C during the 1990s. In this decade, the temperature in April increased to 39.6 °C, while the average of the extreme maximum temperature in April was 39.6 °C.

The regional climate as measured by the Equatorial Southern Oscillation Index increased in March (EQ_SOI_{March}) and also stimulated the growth in merkus pine at this site. The relationship between EQ_SOI_{March} and the index during A.D. 1989-2015 was used to construct mathematical equations as shown in Equation (5) and (6).

$$Index = 1.0251+0.1088\ (EQ\_SOI_{March}) \quad (5)$$

$$EQ\_SOI_{March} = 1.5702\ (Index)–1.4836 \quad (6)$$

The reconstruction of EQ_SOI_{March} during A.D. 1949-1988 and A.D. 1989-2015 was compared with the measured EQ_SOI_{March} to verify the reliability of the model as shown in Table 1 and Figure 8. It was found that EQ_SOI_{March} gradually declined from 0.14 in the 1820s to 0.03 in the 1850s and increased to 0.18 during the 1900s. Seventy years later, it decreased to -0.02 during the 1980s before rapidly increasing to 0.022 during the current decade.

The reconstructed climate indicated a declining trend in the number of rainy days in each year and increasing trends in the extreme maximum temperature and EQ_SOI in the twenty-first century which led to a reduced annual rainfall, while the temperature in April increased with a mild rainfall.

Using tree-ring analysis of *P. sylvestris* in northern Scandinavia, Esper et al. (2012) also found a rapidly increased temperature of 0.5 °C during the twentieth-century which was higher than that found this study of 2 °C. Using tree-ring analysis of merkus pines in central Vietnam, Viet et al. (2018) found a warming trend with the temperature increasing by 0.18 °C per decade. The observation of mild wet conditions during the month of April was consistent with the tree-ring study of northern Thai teak indicating an increased rainfall in April, which was higher than the average (Lumyai and Duangsathaporn, 2017).

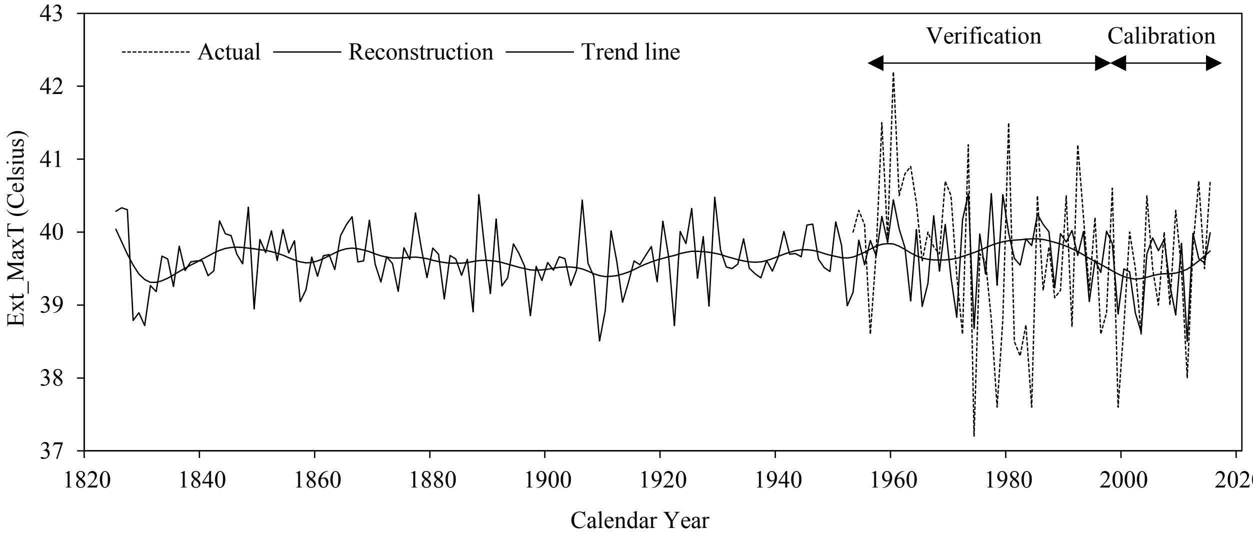

Figure 7. Actual and reconstructed values of the extreme maximum temperature in April.

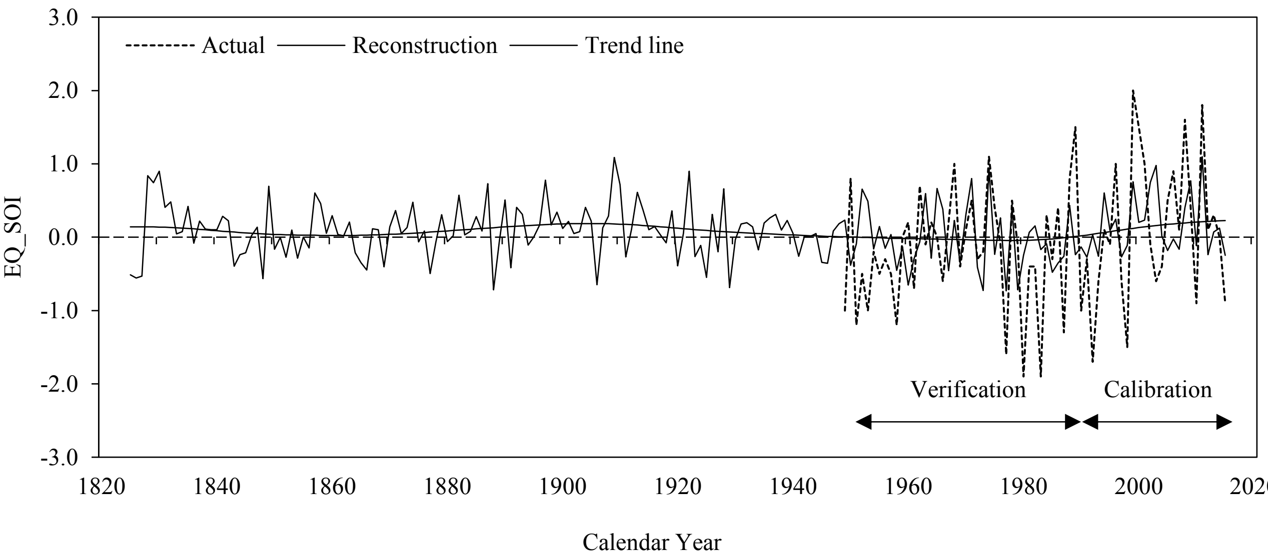

Figure 8. Actual and reconstructed values of Equatorial Southern Oscillation Index in March

3.4 Climate inducing intra-annual ring formation

Intra-annual rings, which were marked during the cross-matching and cross-dating steps, were abundantly found in A.D. 2001 in 15 cores sampled out of the total 16 cores. It was also frequently found in A.D. 1883, 1907, 1919 and 2009 in 14 sample cores (Figure 9(a)). To eliminate the effect of sample size variation in each year, the intra-annual ring frequencies were transformed to stabilize intra-annual density fluctuations (IADFs), as illustrated in Figure 9(b). By using a stepwise regression analysis, a relationship between the stabilized IADFs and climatic data at local and regional scales indicated that the occurrences of intra-annual ring formation could be explained by the fluctuations in the extreme rainfall (r^2=16.8%, $p<0.05$), monthly total rainfall (r^2=29.1%, $p<0.05$), relative humidity (r^2=32.7%, $p<0.05$), extreme maximum temperature (r^2=40.5%,

$p<0.05$), extreme minimum temperature (r^2=15.3%, $p<0.05$), mean maximum temperature (r^2=34.5%, $p<0.05$), mean minimum temperature (r^2=15.7%, $p<0.05$), mean temperature (r^2=29.7%, $p<0.05$), EQ_SOI (r^2=16.3%, $p<0.05$), and EQ_SST (r^2=11.9%, $p<0.05$). The mathematic model described a causation of intra-annual ring formation by using the highest significant relationship among the intra-annual ring occurrences and the extreme maximum temperature in February, June, September and November as shown in Equation (7).

$$\text{Stabilized IADF (\%)} = 18.147 - 5.684(\text{Ext\_MaxT}_{Feb}) - 8.916(\text{Ext\_MaxT}_{Jun}) + 7.995(\text{Ext\_MaxT}_{Sep}) + 7.904(\text{Ext\_MaxT}_{Nov}) \quad (7)$$

In central Thailand, intra-annual ring occurrences in merkus pines were related to several climatic factors, especially the extreme maximum temperature (40.5% variance explained), which declined at the beginning of the wet season and increased during the transitional period of the late rainy and cold seasons. Due to anomalous fluctuations in temperature, water stress was a possible cause of the intra-annual ring formation, which reduced the photosynthesis and cambial cell division (Cherubini et al., 2003; Copenheaver et al., 2006; De Micco et al., 2016).

Not only was the formation of intra-annual rings in merkus pines influenced by anomalous climate, but this was also the case with khasi pines at the beginning and during the late growing season. Singh et al. (2016) reported a causation of intra-annual ring formation in khasi pines growing in the northeastern part of India, which was caused by a reduction in precipitation during the growing season (Apr-Jul) and increased precipitation in the late growing season (Aug-Sep). Effect of water stress on the intra-annual ring formation was also confirmed by Vieira et al. (2010), who found the occurrence of intra-annual ring associated with the amount of rainfall during the transition period of summer and rainy seasons.

Intra-annual rings of Austrian pines (*P. nigra*) were frequently found in the years in which water stress during the wet season was recorded (Wimmer et al., 2000). This observation was similar to the occurrence of intra-annual rings in *P. halepensis*, with an increased water stress from increased rainfall during the dry period and increased temperature at the beginning of the rainy season, respectively (de Luis et al., 2011). A relatively higher frequency of intra-annual rings was found in younger trees, with narrow annual ring widths (Bogino and Bravo, 2009). It was shown that changes in the current and past climates at local and regional scales could be detected by using annual and intra-annual ring widths of pine trees as a valuable proxy in Thailand and other countries.

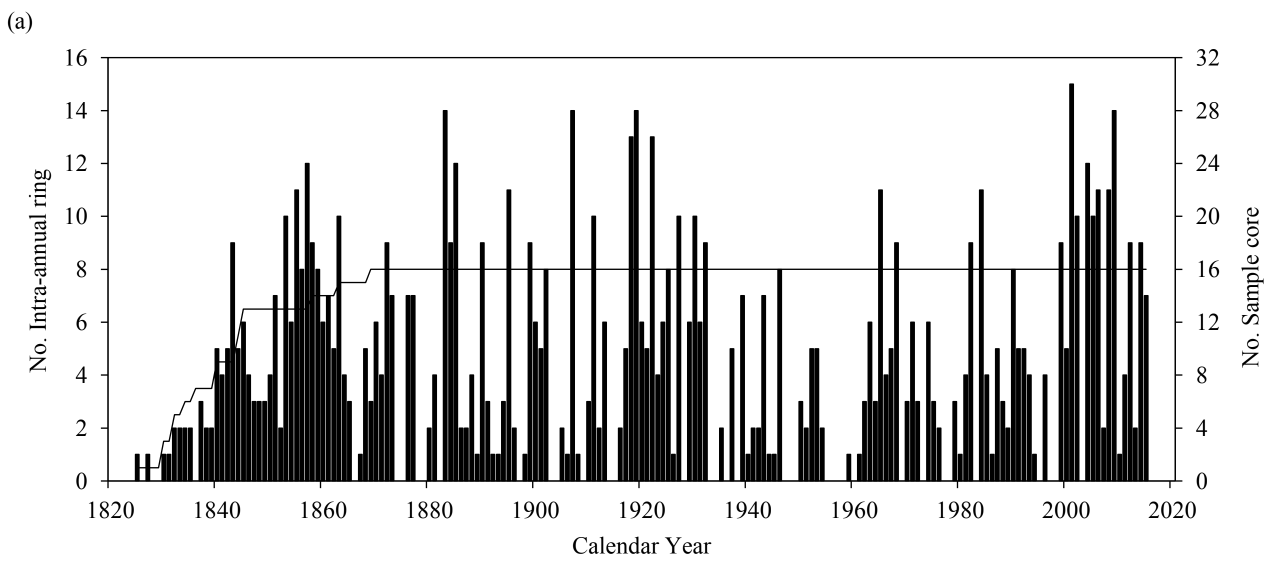

Figure 9. Intra-annual ring frequencies: a) number of intra-annual ring in each year; b) stabilized intra-annual ring in each year. The horizontal line indicated number of sample core in each year.

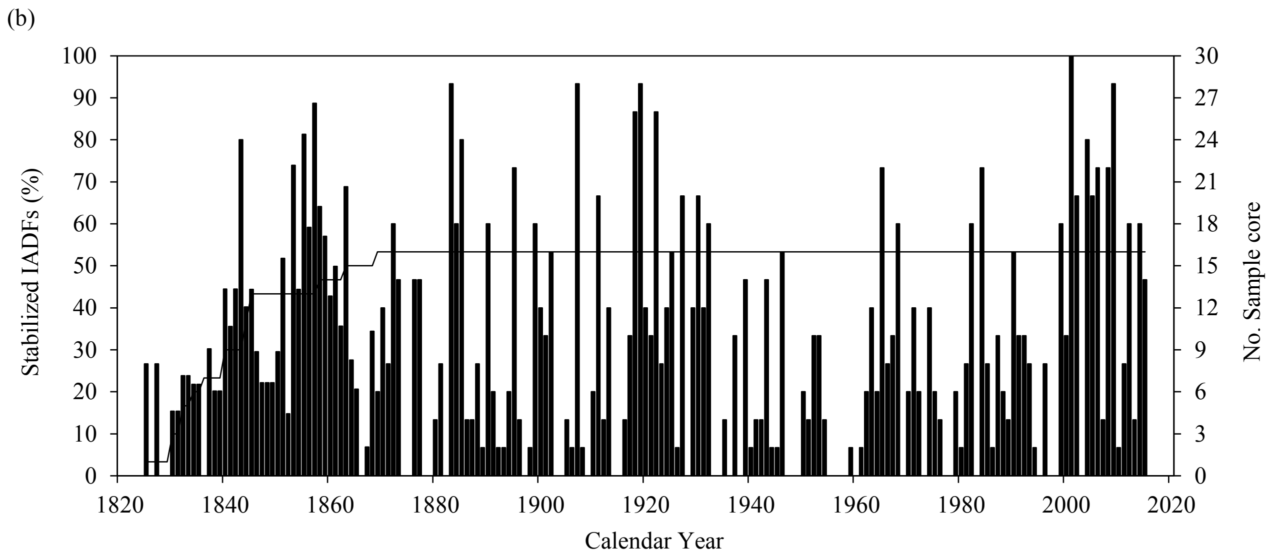

Figure 9. Intra-annual ring frequencies: a) number of intra-annual ring in each year; b) stabilized intra-annual ring in each year. The horizontal line indicated number of sample core in each year.

4. CONCLUSIONS

In this study, we found that the formation of annual and intra-annual rings in the merkus pine (*Pinus merkusii*) of central Thailand could be explained by the fluctuations in local and regional climates. The local and regional climate variables most strongly related to the variations in annual ring index included the number of rainy days in each year, the extreme maximum temperature in April, and the Equatorial Southern Oscillation Index in March (EQ_SOI_{March}), and were chosen for the past climate reconstruction. Since AD 1825, the number of rainy days during each year gradually increased until the beginning of the twentieth century and declined towards the end of the century. It shortly increased during the first decade of the twenty-first century followed by a declining trend in this decade. This was in contrast with the extreme maximum temperature in April which declined at the beginning of the nineteenth century and increased during the twentieth century with a short period of decline in temperature observed towards the end of the century followed by an increase during the current period. Reconstruction of EQ_SOI_{March} indicated mild fluctuations during the 19th century, reduction in the twentieth century and increase in the last century. Not only could the model explain the climate variations longer than 150 years in central Thailand but the study explored, for the first time, the variability in climate using the formation of intra-annual rings in Thai merkus pine. The occurrence of these anomalous annual rings could refer to and explain the climate abnormalities compared to normal years when the extreme maximum temperate decreased at the beginning of the wet season and increased at the transitional period of the late rainy and cold seasons. Additionally, to support the forest and plantation management, the activity of watering, especially at the beginning of the wet season when anomalous increased temperature occurred, shall be contained in the forest management plan in order to increase annual pine growth and wood formation. To confirm this observation of homogenous factors inducing annual and intra-annual ring formation, merkus pines growing in other regions of Thailand shall be analysed and compared with this study in the near future.

ACKNOWLEDGEMENTS

This research project was supported by the Thailand Research Fund: TRF (Grant No. MRG5980167). We also thank the Laboratory of Tropical Dendrochronology (LTD) at the Faculty of Forestry, Kasetsart University and the Tree-ring Laboratory at the Faculty of Environment and Resource Studies, Mahidol University for the equipment to collect, prepare and measure wood core samples.

REFERENCES

Berlage HP. On the relationships between thickness of tree-rings of Djati (teak) trees and rainfall on Java. Tectona 1931;24:939-53.

Bijaksana S, Ngkoimani LO, D'Arrigo R, Krusic P, Palmer J, Sakulich J, Zulaikah S. Status of tree-ring research from teak (*Tectona grandis*) for climate studies. Geofisika 2007;2:1-7.

Bogino S, Bravo F. Climate and intraannual density fluctuations in *Pinus pinaster* subsp. mesogeensis in Spanish woodlands. Canadian Journal of Forest Research 2009;39:1557-65.

Borgaonkar HP, Sikder AB, Ram S, Pant GB. El Niño and related monsoon drought signals in 523-year-long ring width records of teak (*Tectona grandis* L.F.) trees from south India. Palaeogeography, Palaeoclimatology, Palaeoecology 2010; 210:74-84.

Buckley BM, Barbetti M, Watanasak M, D'Arrigo RD, Boonchirdchoo S, Sarutanon S. Dendrochronological investigations in Thailand. International Association of Wood Anatomists Journal 1995;16(4):393-409.

Buckley, BM, Duangsathaporn K, Palakit K, Butler S, Syhapanya V, Xaybouangeun N. Analyses of growth rings of *Pinus merkusii* from Lao P.D.R. Forest Ecology and Management 2007a;253:120-7.

Buckley BM, Palakit K, Duangsathaporn K, Sanguantham P, Prasomsin P. Decadal scale droughts over northwestern Thailand over the past 448 years: Links to the tropical Pacific and Indian Ocean sectors. Climate Dynamics 2007b;29(1):63-71.

Chaudhary V, Bhattacharyya A. Suitability of *Pinus kesiya* in Shillong, Meghalaya for tree-ring analyses. Current Science 2002;83(8):1010-5.

Cherubini P, Garther BL, Tognetti R, Braker OU, Schoch W, Innes JL. Identification, measurement and interpretation of tree rings in woody species from Mediterranean climates. Biological Reviews 2003;78:119-48.

Cook ER, Briffa KR, Shiyatov S, Mazepa V. Tree-ring standardization and growth-trend estimation. In: Cook ER, Kairiukstis LA, editors. Method of Dendrochronology. Dordrecht: Kluwer Academic Publishers: 1990. p. 104-23.

Cook ER, Peters K. The smoothing spline: A new approach to standardizing forest interior tree-ring width series for dendroclimatic studies. Tree-Ring Bulletin 1981;41:45-53.

Copenheaver CA, Pokorski EA, Currie JE, Abrams MD. Causation of false ring formation in *Pinus banksiana*: A comparison of age, canopy class, climate and growth rate. Forest Ecology and Management 2006;236:348-55.

D'Arrigo RD, Jacoby GC, Krusic PJ. Progress in dendroclimatic studies in Indonesia. Terrestrial, Atmospheric and Oceanic Sciences 1994;5(3):349-63.

D'Arrigo R, Palmer J, Ummenhofer CC, Kyaw NN, Krusic P. Three centuries of Myanmar monsoon climate variability inferred from teak tree rings. Geophysical Research Letters 2011;38:1-5.

D'Arrigo RD, Wilson R, Palmer J, Krusic PJ, Curtis A, Sakulich J, et al. Monsoon drought over Java, Indonesia, during the past two centuries. Geophysical Research Letters 2006;33(4):1-4.

DeBoer HJ. Tree-ring measurement and weather fluctuations in Java from AD 1514. Proceedings of the Koninklijke Nederlandse Akademie van Wetenschappen 1951;5(3):431-42.

De Luis M, Novak K, Raventós J, Gričar J, Prislan P, Čufar K. Climate factors promoting intra-annual density fluctuations in Aleppo pine (*Pinus halepensis*) from semiarid sites. Dendrochronologia 2011;29(3):163-9.

De Micco V, Campelo F, De Luis M, Bräuning A, Grabner M, Battipaglia G, Cherubini P. Intra-annual density fluctuations in tree rings: How, when, where, and why? International Association of Wood Anatomists Journal 2016;37(2):232-59.

Duangsathaporn K, Palakit K. Climatic signals derived from the growth variation and cycles of *Pinus merkusii* in easternmost Thailand. Thai Journal of Forestry 2013;32(1):9-23.

Esper J, Frank DC, Timonen M, Zorita E, Wilson R, Luterbacher J, et al. Orbital forcing of tree-ring data. Nature Climate Change 2012;2:862-6.

Fritts HC. Tree Rings and Climate. New York, USA: Academic Press; 1976.

Grissino-Mayer H. Evaluating crossdating accuracy: A manual and tutorial for the computer program COFECHA. Tree-Ring Research 2001;57(2):205-21.

Holmes RL. Computer-assisted quality control in tree-ring dating and measurement. Tree-Ring Bulletin 1983;43:69-78.

Intergovernmental Panel on Climate Change (IPCC). Climate Change 2014: Synthesis Report Summary for Policy Makers. Geneva, Switzerland: IPCC; 2014.

Jacoby GC, D'Arrigo RD. Teak (*Tectona grandis* L.F.), a tropical species of large-scale dendroclimatic potential. Dendrochronologia 1990;8:83-98.

Lumyai P, Duangsathaporn K. Climate reconstruction on the growth of teak in Umphang Wildlife Sanctuary, Thailand. Environment and Natural Resources Journal 2017;16(1):21-30.

Lumyai P, Duangsathaporn K, Diloksumpun S, Palakit K, Srinoppawan K. Pine growth variation and its climate response: The challenges for climatic reconstruction in central Thailand. FORTROP II International Conference Tropical Forestry Change in a Changing World; 2008 Nov 17-20; Kasetsart University, Bangkok: Thailand; 2008.

Olivar J, Bogino S, Spiecker H, Bravo F. Climate impact on growth dynamic and intra-annual density fluctuations in Aleppo pine (*Pinus halepensis*) trees of different crown classes. Dendrochronologia 2012;30(1):35-47.

Osborn TJ, Briffa KR, Jones PD. Adjusting variance for sample size in tree-ring chronologies and other regional mean time series. Dendrochronologia 1997;15:89-99.

Palakit K, Siripattanadilok S, Duangsathaporn K. False ring occurrences and their identification in teak (*Tectona grandis*) in Northeastern Thailand. Journal of Tropical Forest Science 2012;24(4):387-98.

Pumijumnong N, Eckstein D. Reconstruction of pre-monsoon weather conditions in northwest Thailand from the tree-ring widths of *Pinus merkusii* and *Pinus kesiya*. Trees 2011;25:125-32.

Pumijumnong N, Eckstein D, Sass U. Tree-Ring research on *Tectona grandis* in Northern Thailand. International Association of Wood Anatomists Journal 1995a;16(4):385-92.

Pumijumnong N, Eckstein D, Sass U. Reconstruction of rainfall in northern Thailand from tree-ring series of teak. Proceedings of the IGBPPAGES/PEP-II Symposium on Paleoclimate and Environment Variability in Austral-Asian Transect During the Past 2000 Years; 1995 Nov 28-Dec 1; Nagoya: Japan; 1995b.

Pumijumnong N, Park WK. Vessel chronologies from teak in northern Thailand and their climatic signal. International Association of Wood Anatomists Journal 1999;20:285-94.

Pumijumnong N, Park WK. Teak vessel chronologies as an indicator of Southeast Asian pre-monsoon temperature. Palaobotanist 2001;50:21-6.

Pumijumnong N, Wanyaphet T. Seasonal cambial activity and tree-ring formation of *Pinus merkusii* and *Pinus kesiya* in

Northern Thailand in dependence on climate. Forest Ecology and Management 2006;226:279-89.

Singh ND, Yadav RR, Venugopal N, Singh V, Yadava AK, Misra KG, et al. Climate control on ring width and intra-annual density fluctuations in *Pinus kesiya* growing in a sub-tropical forest of Manipur, Northeast India. Trees 2016;30(5):1711-21.

Stokes MA, Smiley TL. An Introduction to Tree-Ring Dating. Arizona, USA: The University of Arizona Press; 1996.

Vieira J, Campelo F, Nabais C. Intra-annual density fluctuations of *Pinus pinaster* are a record of climatic changes in the Western Mediterranean region. Canadian Journal of Forest Research 2010;40(8):1567-75.

Viet HD, Tu KN, Kwak JH, Choi WJ. Warming increased nitrogen availability and tree growth during the last five decades as revealed by annual ring data of *Pinus merkusii* in central Vietnam. Communications in Soil Science and Plant Analysis 2018;49:416-25.

Wigley TML, Briffa KR, Jones PD. On the average value of correlated time series, with applications in dendroclimatology and hydrometeorology. Journal of Climate and Applied Meteorology 1984;23:201-13.

Wimmer R, Strumia G, Holawe F. Use of false rings in Austrian pine to reconstruct early growing season precipitation. Canadian Journal of Forest Research 2000;30:1691-7.

Antagonistic Activity against Plant Pathogenic Fungus by Various Indigenous Microorganisms from Different Cropping Systems in Soc Trang Province, Vietnam

Le Thi Xa[1] and Nguyen Khoi Nghia[2*]

[1]*Biotechnology Research and Development Institute, Can Tho University, Can Tho City, Vietnam*
[2]*Department of Soil Science, College of Agriculture and Applied Biology, Can Tho University, Can Tho City, Vietnam*

ARTICLE INFO

Received: 23 Oct 2019
Received in revised: 9 Feb 2020
Accepted: 27 Feb 2020
Published online: 19 Mar 2020
DOI: 10.32526/ennrj.18.3.2020.23

Keywords:
Antagonism/ Fungal plant pathogens/ *Fusarium oxysporum*/ Indigenous microorganism/ *Rhizoctonia solani*

*** Corresponding author:**
E-mail: nknghia@ctu.edu.vn

ABSTRACT

This study assessed antagonistic capacity of various indigenous microorganisms (IMO) collected from different cropping systems within Soc Trang province against plant pathogenic fungus including *Fusarium oxysporum* and *Rhizoctonia solani*. Biocontrol activity of fifteen collected IMOs was investigated on PDA agar media for 5-7 days under laboratory conditions with three different scenarios. IMO and pathogenic fungus were incubated at the same time and IMO was introduced before and after inoculation of plant pathogenic fungus. The results illustrated that all surveyed IMOs were found to have highly potential biocontrol against two plant pathogenic fungi to different extents and IMOs which were introduced before the inoculation of pathogenic fungi showed the highest efficiency in biocontrol of plant pathogen. Particularly, four out of fifteen IMOs which were collected from bamboo, shallot, grapefruit and guava farms showed their highest antagonistic efficacy on *Fusarium oxysporum* biocontrol by completely decaying fungal hyphae of this fungal strain after seven incubation days. For *Rhizoctonia solani,* all IMOs displayed highly antagonistic ability with inhibitory percentages varying between 52.96% and 92.59% after two days. The antagonistic functions of all collected IMOs could be exploited for plant protection from plant-pathogenic fungus.

1. INTRODUCTION

The concept of indigenous microorganisms (IMO) was developed by Kyu in the 1960s at the Janong Farming Institute, South Korea. IMO-based technology is a great technology applied in the eastern part of the world. IMO cultures contain consortia of beneficial microorganisms comprising of fungi and bacteria that are deliberately collected and cultured from soils to enhance plant growth promotion (Reddy, 2011). Indigenous micro-organisms are a group of innate microbial consortium that inhabit the soil and the surfaces of all living things. It has a potential in biodegradation, bioleaching, bio-composting, nitrogen fixation, phosphate solubilization, soil fertility improvement and in the production of plant growth hormones as well as biocontrol (Kumar and Gopal, 2015). In fact, according to Chiemela et al. (2013b), many studies indicated that application of IMO in agriculture has been a friendly environmental method and helped to enhance organic matter decomposition, plant nutrition, soil fertility, crop yields and resistance to plant diseases. Application of IMO is effective in compost production since it promotes the rapid degradation of agricultural and plant residues, producing large amounts of micronutrients in the soluble form that are very easy to be taken up by plants (Chiemela et al., 2013a). Another research study was conducted in Hawaii to evaluate the biocontrol function of IMOs against *Ceratocystis* sp. fungus causing a deadly plant disease for Ohia trees. The result showed that IMOs had a very good function in recovery of Ohia trees's health from plant disease (Board of Land and Natural Resources State of Hawaii, 2018). Moreover, we know that different cropping system and management practices play an important role in soil physico-chemical properties and microbiome composition and diversity (Fierer et al., 2012; Zhang et al., 2016). Thus, in this study we sampled many different locations corresponding to different cropping systems and

Citation: Xa LT, Nghia NK. Antagonistic activity against plant pathogenic fungus by various indigenous microorganisms from different cropping systems in Soc Trang Province, Vietnam. Environ. Nat. Resour. J. 2020;18(3):249-256. DOI: 10.32526/ennrj.18.3.2020.23

management practices with an aim of having more choices in finding the very best microbial community in biocontrol for some very common plant pathogens, *Fusarium oxysporum* and *Rhizoctonia solani*. These pathogens cause many diseases for many kinds of economic crop plants in the Mekong Delta Region of Vietnam where agriculture is very important. However, deep and scientific knowledge about the abilities of IMO for biocontrol of plant pathogens are still lacking and should be scientifically elucidated. Therefore, the aim of this study was to assess antagonistic activity against plant pathogenic fungus of various indigenous microorganism communities from different agro-ecosystems.

2. METHODOLOGY

2.1 IMO sample collection

Fourteen different IMOs were collected from different crop models in Soc Trang Province, Vietnam including bamboo, crop rotation (corn, watermelon, courgette), banana, shallot, vegetables, rice, water-melon, grassland, maize, lettuce, oranges, grapefruit, guava, and sugarcane by following the method described by Kyu and Koyama (1997) (Figure 1).

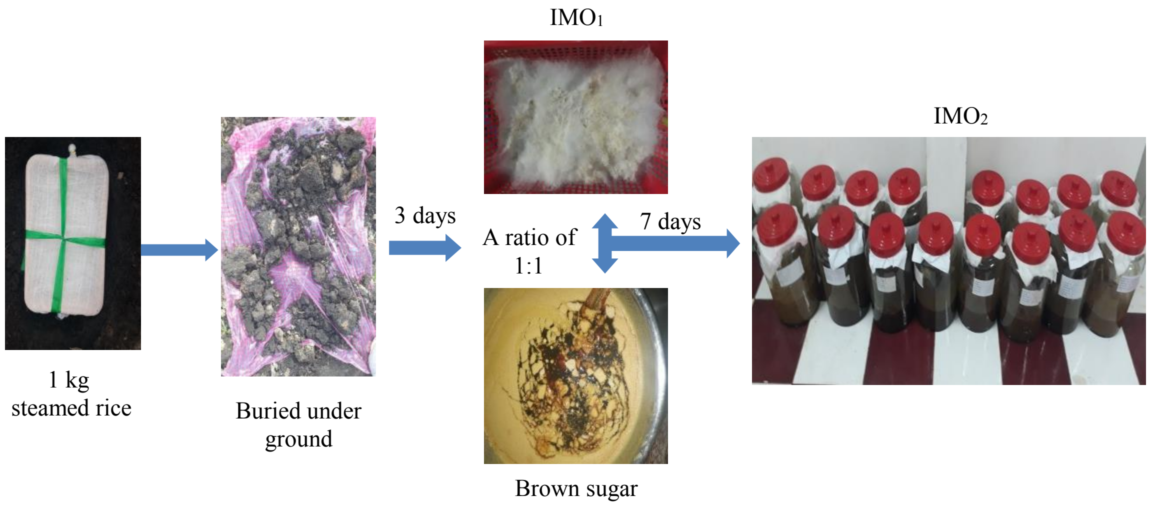

Figure 1. Procedure of IMO collection

Sites of sample collection are presented in Table 1. At each sampling site, three plastic baskets (25 × 15 × 8 cm) were used, corresponding to 3 replicates. Each basket was filled with 1 kg of steamed rice and covered using cloth and a waist belt. The baskets were buried under ground at a depth of 20-30 cm at each sampling site and covered with leaf litter for three days. After four days of incubation, the fermented rice samples colonized by indigenous microorganisms were harvested. The microorganism-infected rice were put into a glass jar and carried to the laboratory. This source of microorganisms was called IMO_1. Mix IMO_1 was prepared by combining an equal amount of 150 g of each IMO_1 together. All collected IMO_1 were mixed well with brown sugar with a ratio of 1:1 (w/w) until the mixed material became gooey. These mixed materials were stored in ceramic pots in a cool area and away from direct sunlight for seven days for another fermentation time. After seven days of fermentation, these sources of microorganisms were called IMO_2. The IMO_2 were kept in the refrigerator at 4 ^{o}C for further studies.

Table 1. The location of fourteen IMO samples in Soc Trang Province

Code	Origin of IMO	Located in Soc Trang Province
IMO1	Bamboo	Phu Tam Commune, Chau Thanh District
IMO2	Crop rotation	5 Ward, Soc Trang City
IMO3	Banana	7 Ward , Soc Trang City
IMO4	Shallot	Vinh Phuoc Commune, Vinh Chau District
IMO5	Lettuce	3 Ward, Soc Trang City
IMO6	Rice	My Xuyen Town, My Xuyen District

Table 1. The location of fourteen IMO samples in Soc Trang Province (cont.)

Code	Origin of IMO	Located in Soc Trang Province
IMO7	Watermelon	Truong Khanh Commune, Long Phu District
IMO8	Grassland	Truong Khanh Commune, Long Phu District
IMO9	Maize	Thanh Tri Commune, Thanh Tri District
IMO10	Vegetables	Thanh Quoi Commune, My Xuyen District
IMO11	Oranges	Xuan Hoa Commune, Ke Sach District
IMO12	Grapefruit	Xuan Hoa Commune, Ke Sach District
IMO13	Guava	Xuan Hoa Commune, Ke Sach District
IMO14	Sugarcane	Dai An II Commune, Cu Lao Dung District

2.2 Plant pathogenic fungal sources

The two fungal pathogens used in this study were *Fusarium oxysporum* and *Rhizoctonia solani*. The first one causes wilt disease on sesame and the latter causes a root rot disease on vegetables. These fungal sources were provided from the plant pathogen laboratory, Plant Protection Department, College of Agriculture, Can Tho University.

2.3 Evaluation of IMO with antagonistic potentials

An aliquot of 10 g of each IMO was transferred into 250 mL glass bottles containing 90 mL sterilized distilled water. The bottles were put on a horizontal shaker at a speed of 150 rpm for 60 min, and then left to stand for 10 min. This microbial IMO suspension was used as a microbial source for antagonistic experiments.

For the fungus, *Fusarium oxysporum*, biological control activity of fifteen collected IMO was investigated on PDA agar media with three different scenarios: (1) IMO and *Fusarium oxysporum* were incubated on PDA agar media at the same time and with a 4 cm interval space between the two colonies; (2) IMO were introduced two days before *Fusarium oxysporum* inoculation; and (3) IMO were introduced two days after *Fusarium oxysporum* inoculation.

Unlike *Fusarium oxysporum*, the growth of fungus *Rhizoctonia solani* was very fast and after just two days of incubation, the fungal hyphae of *Rhizoctonia solani* was spread fully on the PDA medium. Therefore, for the case of *Rhizoctonia solani* only two scenarios were applied: (1) IMO and *Rhizoctonia solani* were introduced on PDA agar media at the same time and with a 4 cm interval space between two colonies; and (2) IMO was introduce two days before *Rhizoctonia solani* inoculation.

Antagonistic activity of IMOs against fungi *Fusarium oxysporum* and *Rhizoctonia solani* was assessed by bilateral symmetrical implantation technique adopted by Vincent (1947). A brief description is described as follows: A five millimeter diameter core of PDA agar containing five days old culture of targeted fungi was taken and inoculated into the center of the right half of a Petri dish in complete aseptic condition. Then a 20 µL aliquot of IMO suspension was transferred into the center of the left half of the left Petri dish in complete aseptic condition and left for 30 min to dry completely. The PDA media containing Petri dish without IMO inoculation served as a negative control. Each IMO was tested in three replicates. All the Petri dishes were incubated at room temperature and dark condition during the incubation period. Radical growth of colonies was measured after seven days of incubation for *Fusarium oxysporum* and after five days of incubation for *Rhizoctinia solani*. The result of mycelia growth was expressed as the mean of the triplicates. Percent inhibition of mycelia growth over control was calculated by the formula given by Vincent (1947).

$$H\ (\%) = [(Dc - Dt)/Dc] \times 100$$

Where; H: inhibition efficacy (%)
Dc: diameter of mycelia growth in control
Dt: diameter of mycelia in treated

2.4 Data analysis

The data were analyzed by ANOVA and compared by DUNCAN test with MINITAB software with 16.2 version.

3. RESULTS AND DISCUSSION

3.1 Antagonistic potentials of IMOs with *Fusarium oxysporum*

The results of the study of the antagonistic activity of 14 different IMOs from different cropping systems and mixed IMO against fungus *F. oxysporum*, presented in Table 2 and Figure 2, indicated that all 15 tested IMOs had a highly antagonistic effect against *F. oxysporum* with significantly different extents. Among three scenarios, it can be seen clearly from Table 2 that the percentage of mycelia inhibition were recorded as follows: IMO were introduced on PDA containing Petri dish two days before fungus *F. oxysporum* > IMO and fungus *F. oxysporum* were introduced on PDA containing Petri dish at the same time > IMO were introduced on PDA containing Petri dish two days after fungus *F. oxysporum*.

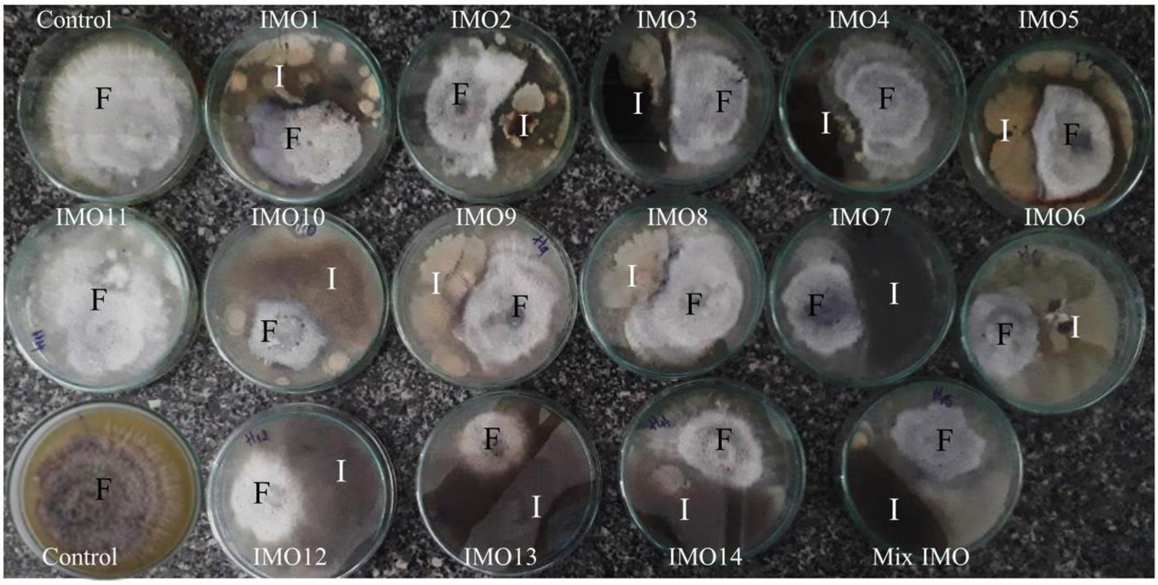

Figure 2. Antagonistic activities of 15 IMOs against fungus *F. oxysporum* after 7 days of incubation in the case IMOs introduced 2 days after *F. oxysporum; "*F": *F. oxysporum* and "I": IMO

Table 2. Mycelia inhibitory capacity of 15 IMOs for fungus *Fusarium oxysporum* after 7 days of incubation

Code	Origin of samples	Inhibition efficacy (%)			
		IMO>Fungus	IMO=Fungus	IMO<Fungus	Average
IMO1	Bamboo	100.0^{a}	100.0^{a}	25.25^{cd}	75.08
IMO2	Crop rotation	80.14^{b}	54.08^{cd}	25.57^{cd}	52.26
IMO3	Banana	81.19^{b}	44.90^{ef}	22.95^{cd}	49.68
IMO4	Shallot	100.0^{a}	47.48^{c}	23.78^{cd}	57.08
IMO5	Lettuce	68.99^{bcd}	49.66^{de}	24.26^{cd}	47.64
IMO6	Rice	66.20^{cde}	67.01^{b}	40.98^{bc}	58.06
IMO7	Watermelon	44.98^{g}	45.24^{ef}	22.30^{cd}	37.50
IMO8	Grassland	51.97^{fg}	38.79^{f}	13.12^{d}	34.63
IMO9	Maize	60.98^{def}	51.70^{cde}	26.56^{c}	46.41
IMO10	Vegetables	70.73^{bcd}	52.04^{cde}	48.53^{ab}	57.10
IMO11	Oranges	58.54^{def}	38.10^{f}	26.56^{c}	40.07
IMO12	Grapefruit	100.0^{a}	100.0^{a}	46.89^{ab}	82.30
IMO13	Guava	100.0^{a}	100.0^{a}	56.39^{a}	85.46
IMO14	Sugarcane	53.31^{efg}	46.60^{e}	26.23^{c}	42.05
Mix IMO	Mixed	76.31^{bc}	54.42^{cd}	26.87^{c}	52.53

Note: Values in the same column with the same letters are not significant difference ($p<0.05$), "=" means IMO and *F. oxysporum* were incubated at the same time, ">" means IMO was introduced 2 days before *F. oxysporum* and "<" means IMO was introduced 2 days after *F. oxysporum*.

For the case that IMOs were incubated two days before fungus *F. oxysporum* inoculated, the mycelia inhibition of all 15 tested IMOs were recorded to be very high with the amount varying between 44.98% and 100%. The highest antagonistic effects of IMO against fungus *F. oxysporum* were determined for four

IMOs from bamboo, shallot, grapefruit, and guava farms with the mycelia inhibition of up to 100% and also significantly higher than those of the remaining IMOs ($p<0.05$), since these four IMOs decayed completely fungal hyphae of fungus *F. oxysporum*. In addition, two IMOs collected originally from crop rotation and banana cultivation fields had the ability to stop the growth of *F. oxysporum* mycelia of up to 80% even when IMOs were incubated on PDA agar containing Petri dish two days before fungus *F. oxysporum*. Also in this scenario, the remaining IMOs showed good resistance against *F. oxysporum*, with antagonistic efficacy ranged from 51.97% to 73.31%, except for IMO of grassland which had an antagonistic efficacy of 44.98%.

Regarding the scenarios that both IMO and fungus *F. oxysporum* introduced on PDA containing Petri dish at the same time, there was a slight decrease in inhibition efficacy of some IMOs when compared to the case of IMO was incubated two days before fungus. However, the mycelia inhibition of three tested IMOs from bamboo, grapefruit, and guava were still very high with the stable amount at 100%, while the inhibition of mycelia dropped to 47.38% for IMO from shallot farm. In addition, the IMOs collected from rice, watermelon resisted stably against *F. oxysporum* in both cases and with the mycelia inhibition of around 66% and 45%, respectively. Particularly, IMOs collected from grassland and orange farms had the lowest antagonistic effect against *F. oxysporum* and with the inhibition efficacy was just over 38% whilst the seven remaining tested IMOs including crop rotation, banana, maize, lettuce, vegetables, sugarcane and mixture had a slight drop of inhibition efficacy and this value varied between 44.90% and 54.42%.

For the case that IMOs were incubated two days after fungus *F. oxysporum* incubation. It was found that the inhibitory effect of all fifteen IMO were lowest. The mycelia inhibition of all 15 tested IMOs showed a significant inhibition with a rate varied between 13.12% and 56.39% and also had a slight decrease in inhibition efficacy of some IMOs as compared with two other scenarios. The highest antagonistic effects of IMO against fungus *F. oxysporum* were determined for IMOs collected from guava farm and significantly higher than others. In addition, three IMOs collected from rice, vegetables and grapefruit farms had a high inhibitory effect on the growth of *F. oxysporum* mycelia with the inhibition efficacy was found at 40.98%, 48.53%, and 46.98%, respectively. Meanwhile, the mycelia inhibition of the IMOs from bamboo, crop rotation, banana, shallot, watermelon, maize, lettuce, oranges, sugarcane, and mixture varied between 22.3% and 26.87%. Particularly, IMO collected from grassland had the lowest antagonistic effect against *F. oxysporum* (13.12%). It means that this IMO had less antagonistic effect against fungus *F. oxysporum* than other IMOs under the condition of *F. oxysporum* introduced two days before.

From the results it can be seen that all surveyed IMOs were found to have great potential in biocontrol against *F. oxysporum*, and IMOs collected from guava and grapefruit cultivation fields showed the highest efficiency as compared to others. They were possible to prevent the growth of *F. oxysporum* up to around 50% even when incubated two days after pathogen fungus and decayed completely fungal hyphae of fungus when introduced two days before fungus (average efficiency was over 80%). Other remaining IMOs had an average efficiency for fungus *F. oxysporum* ranged from 34.63 to 75.08%. This could be explained that microbial community in IMO including fungi, bacteria and actinomycetes could excrete some antimicrobial-like compounds and enzymes to inhibit the growth of mycelium *F. oxysporum* (Xa and Nghia, 2019).

Stanojkovic-Sebic et al. (2017) indicated that it is very hard to completely control the soil-borne diseases caused by *Fusarium* species in soil by means of chemical approaches. Inconsistencies of inhibition effect in biocontrol of soil-borne pathogens under varying environmental conditions were identified as a common limiting factor. However, research focusing on the efficacy of indigenous microbial communities against these soil-borne pathogens is still limited. Huy et al. (2017) recommended that treating seeds with *Trichoderma asperrellum* in a combination with bio-fertilizer about 2-3 days before planting would help plants to develop well, prevent plant diseases and give high biological control efficiency for plant pathogen. The reason for this result was that microorganisms could excrete many enzymes that could destroy the walls of mycelium of fungi and they may also directly kill fungal pathogens.

In general, application of IMOs as a source of beneficial microbes for crops and plants was found to have great inhibitory capacity to *F. oxysporum* with fungal hyphae suppression rates ranged between 34.63% and 85.46%. Additionally, Yuliar et al. (2013) indicated that when 100 μL endophytic bacteria were used to biocontrol *F. oxysporum,* the mycelia growth inhibition effect was recorded to be up to of 35% after 5 days of incubation. Besides, Dar et al. (2013) investigated the antagonistic potential of some beneficial fungi to *F. oxysporum*, suggesting that they could excrete anti-fungal compounds which may suppress the growth of *F. oxysporum* from 54.4% to 92.5%. A study of Stanojkovic-Sebic et al. (2017) indicated that *Pseudomonas* strains from star anise plantation soil had a great ability to inhibit *F. oxysporum* up to of 77.8%. Similarly, Toppo and Naik (2015) determined the biocontrol activity of nine bacterial strains against *Fusarium* spp. The results showed that these strains had high mycelia growth inhibition capacity and the inhibiting values varied between 33% and 73%.

3.2 Antagonistic potentials of IMOs with *Rhizoctonia solani*

The results of antagonistic potentials of 14 different IMOs from different cropping systems and mixed IMO with fungus *Rhizoctonia solani* are presented in Figure 3 and Figure 4. In the case of which both IMOs and fungus were incubated at the same time, IMOs showed less effect in inhibiting of fungus *R. solani* than the case of which IMOs were introduced two days before fungus *R. solani* inoculated and it could be due to the fungal hyphae developed very rapid and it took only two days for fungal hyphae to grow fully on the surface of the containing PDA medium Petri dish dishes (Figure 3). Nevertheless, fungal hyphae of *R. solani* could not touch the growing zones of IMOs, except for the case of IMOs collected from grassland and oranges. This means that these two IMOs did not have an ability to resist fungus *R. solani*. This result was similar to the study of Ghai et al. (2007) who examined the biocompatibility of isolated strains and showed that bacterial isolates strongly resisted against *F. sclerotium,* but did not inhibit effectively fungus *R. solani*.

A

B

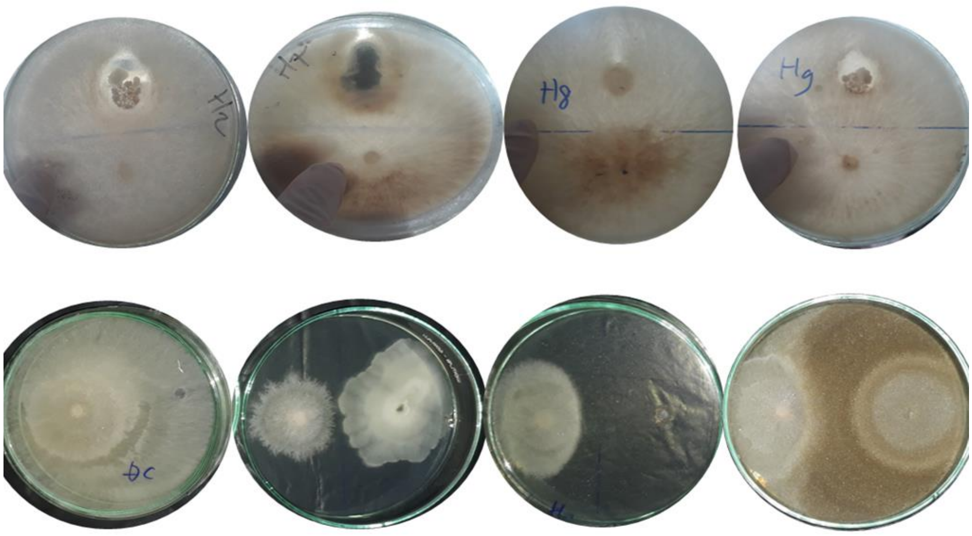

Figure 3. Antagonistic activities of some representative IMOs against fungus *Rhizoctonia solani* after 2 days of incubation (Note: A: IMO and *R. solani* were incubated at the same time; B: IMO was incubated 2 days before *R. solani*; "R"means Rhizoctonia solani; "I" means IMO)

When IMOs were placed on PDA agar medium two days before fungus inoculation, the high anti-fungal capacities of IMOs were recorded with a large variation. The mycelial growth of fungus *R. solani* was inhibited by IOMs with a range varying between 52.96% and 92.59%. It can be seen that maximum inhibition capacity was observed for IMO collected from guava cultivation farm with the rate of efficiency over 90%, closely followed by IMO from grapefruit farm (88.19%).The lowest inhibition efficacy to fungus *R. solani* were found between 52.96% and 54.26% for grassland and maize IMOs while others showed inhibition rates between 59.26% and 71.11%.

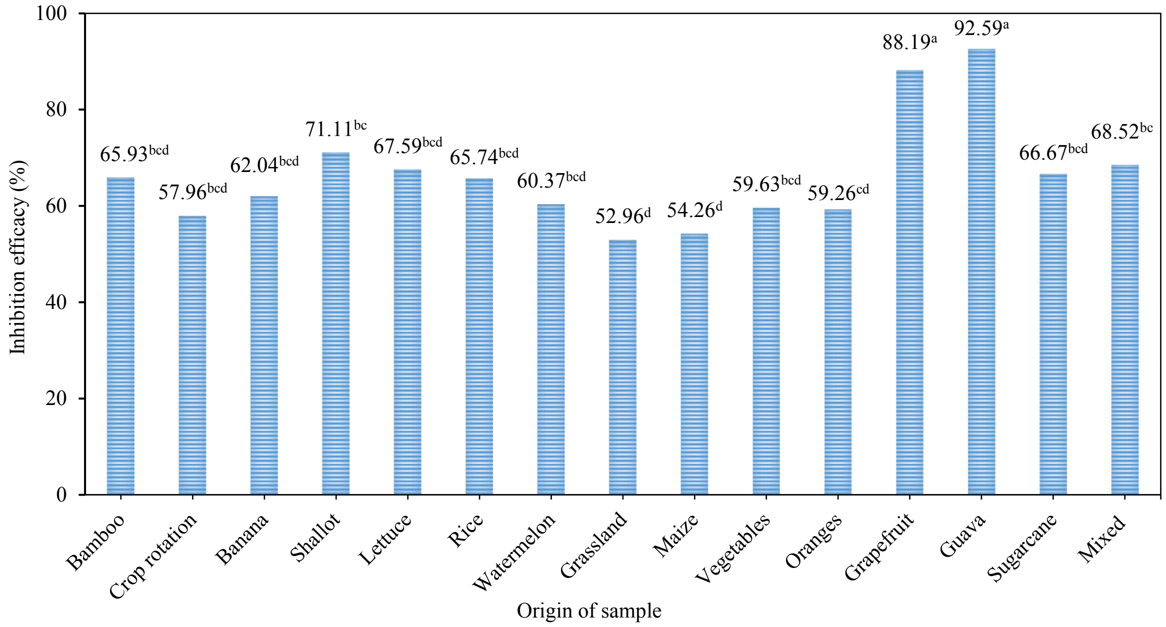

Figure 4. Mycelia inhibitory capacity of 15 IMOs after 2 days of incubation in the case of IMOs were incubated 2 days before fungus *Rhizoctonia solani* (Note: Values with the same letters are not significant difference (p<0.05), "=" means IMO and *F. oxysporum* were incubated at the same time, ">" means IMO was introduced 2 days before *F. oxysporum.*)

From this result, it can be seen that all 15 tested IMOs had very good function in antagonisms against fungal pathogen *F. oxysporum* better than against fungus *Rhizoctonia*, the inhibitory effect of IMOs for both two fungi was shown to be more effective when IMOs were placed before fungi (from 50% to 93% of inhibitory efficacy). This implies that IMO can be used to prevent the soil born diseases like *Fusarium oxysporum* and *Rhizoctonia solani*. The result of this study was consistent with study of Ghai et al. (2007) and Robles-Yerena et al. (2010). Their results showed that when *Ascomycete* and plant pathogenic fungus *P. capsici* were introduced at the same time, about 53.1% of *P. capsici*'s milleial growth was inhibited. When *Ascomycete* was incubated 3 days before fungus *P. capsici*, the inhibition capacity toward the growth of micellia was improved up to of 73%. However, *Ascomycete* did not have any effect on fungus *Rhizoctonia solani.* Similarly, Ramzan et al. (2014) obtained 15 indigenous bacteria and 44 fungi and tested for their inhibition effect on soil-borne pathogens such as *Fusarium solani, Macrophomina phaseolina, Pythium aphanidermatum, Rhizoctonia solani,* and *Sclerotium rolfsii* under in vitro conditions. The result indicated that a total of 20 fungal and 7 bacterial strains showed their high biocontrol efficiency in dual culture plate assay against these soil-borne pathogens. Furthermore, Koche et al. (2013) found that the antifungal compounds extracted from culture solution were found to be very effective in inhibiting the growth of fungus up to of 42.79% and 20.45% for *Rhizoctonia solani* and *Fusarium solani*, respectively.

Moreover, according to Duffy and Weller (1995) and Hervas et al. (1998), a mixture of compatible biocontrol agents was an ecologically sound approach to biocontrol of soil borne diseases, especially when used in combination with limited or partial resistance. Mixtures of different species of microorganisms may result in better plant colonization, may be better adapted to environmental changes, may present a large number of pathogen suppressive mechanisms, and/or may protect against a broad range of pathogens. In short, all achieved results of this study and some other previous studies' results supported our finding about the biocontrol function of indigenous microorganisms against plant pathogenic fungi such as *F. oxysporum* and *R. solani*. However, the mechanisms in biocontrol function of IMOs should be intensively investigated more in further studies.

4. CONCLUSION

Biological control of phytopathogenic fungi is an ecological approach of plant protection. This investigation confirmed highly pronounced antifungal activity of all tested IMOs collected from different farming system habitats within Soc Trang Province, Vietnam. With IMO, there is no need to isolate single strains of microorganisms for application purposes, while still having good function in anti-fungal capacity to a high extent beside other functions like plant growth promotion which has been proven via previous studies. Two IMOs collected from guava and grapefruit farms showed their most pronounced activity in biological control of two plant pathogenic fungi *Fusarium oxysporum* and *Rhizoctonia solani*. The results of this study imply that the indigenous microorganism communities have a great potential in biological control of phytopathogen fungi in soil and can be exploited in plant protection.

REFERENCES

Board of Land and Natural Resources State of Hawaii. Project Issuance of Right-of-Entry Permit to Big Island Resource Conservation and Development Council for the Purpose of Conducting Research on the Efficacy of li~digenous Microorganisms to Confer Resistance to Ohia against Rapid Ohia Death on State Lands. Puna, Hawaii; 2018.

Chiemela FA, Serafin LN, Ricardo LI, Joseph LN. Isolation and characterization of indigenous microorganism (IMO) from fugao bamboo (*Phyllostachys Aurea*) forest. International Journal of Science and Research 2013a;4(2):1319-24.

Chiemela FA, Serafin LN, Ricardo LI, Joseph LN. Application of indigenous microorganisms (IMO) for bio-conversion of agricultural waste. International Journal of Science and Research 2013b;4(5):778-84.

Dar WA, Beig MA, Ganie SA, Bhat JA, Shabir-u-Rehman, Razvi SM. In vitro study of fungicides and biocontrol agents against *Fusarium oxysporum* f.sp. pini causing root rot of Western Himalayan fir (*Abies pindrow*). Academin Journal: Scientific Research and Essays 2013;8(30):1407-12.

Duffy BK, Weller DM. Use of *Gaeumannomyces graminis* var. graminis alone and in combination with fluorescent *Pseudomonas* spp. to suppress take-all of wheat. Plant Disease 1995;79:907-11.

Fierer N, Lauber CL, Ramirez KS, Zaneveld J, Bradford MA, Knight R. Comparative metagenomic, phylogenetic and physiological analyses of soil microbial communities across nitrogen gradients. International Society for Microbial Ecology Journal 2012;6:1007-17.

Ghai S, Sood SS, Jain RK. Antagonistic and antimicrobial activities of some bacterial isolates collected from soil samples. Indian Journal of Microbiology 2007;47:77-80.

Hervas A, Landa B, Datnoff LEm, Jime´nez-Dı´az RM. Effects of commercial and indigenous microorganisms on *Fusarium* wilt development in chickpea. Biological Control 1998;13(3):166-76.

Huy ND, Nguyen PQ, Hong NTT, Giang H, Vien NV, Canh NT. Isolation and evaluation of antagonistic ability of *Trichoderma asperellum* against soil borne plant pathogen. Vietnam Journal of Agricultural Sciences 2017;15(12):1593-640.

Koche D, Gade RM, Deshmukh AG. Antifungal activity of secondary metabolites produced by *Pseudomonas fluorescens*. The Bioscan 2013;8(2):723-6.

Kumar BL, Gopal DVR. Effective role of indigenous microorganism for sustainable environment. 3 Biotech 2015; 5(6):867-76.

Kyu CH, Koyama A. Korean Natural Farming: Indigenous Microorganisms and Vital Power of Crop/Livestock. Republic of Korea: Korean Nature Farming Association Publisher: 1997. p. 39-48.

Ramzan N, Noreen N, Shahzad S. Inhibition of in vitro growth of soil-borne pathogens by compost-inhabiting indigenous bacteria and fungi. Pakistan Journal of Botany 2014; 46(3):1093-9.

Reddy R. Cho’s Global Natural Farming. Bengaluru, India: South Asia Rural Reconstruction Association; 2011.

Robles-Yerena L, Rodríguez-Villarreal RA, Ortega-Amaro MA, Fraire-elázquez S, Simpson J, Rodríguez-Guerra R, Jiménez-Bremont JF. Characterization of a new fungal antagonist of *Phytophthora capsici*. Scientia Horticulturae 2010; 125(3):248-55.

Stanojković-Sebić A, Pavlović S, Starović M, Pivić R, Dinić1 Z, Lepšanović Z, Jošić D. Antagonistic activity of indigenous *Pseudomonas* isolates against *Fusarium* species isolated from anise. Scientific Papers. Series B. Horticulture 2017;61:413-6.

Toppo SR, Naik UC. Isolation and characterization of bacterial antagonist to plant pathogenic fungi (*Fusarium* spp.) from agro based area of Bilaspur. International Journal of Research Studies in Biosciences 2015:6-14.

Vincent JM. Distortion of fungal hyphae in the presence of certain inhibitors. Nature 1947;159(4051):850.

Xa LT, Nghia NK. Microbial diversity of indigenous microorganism communities from different agri-ecosystems in Soc Trang province, Vietnam. Proceeding of the International Conference on Biotechnology of Ho Chi Minh City Open University 2019: Research and Application in Biotechnology; 2019 July 26; Ho Chi Minh City Open University, Vietnam; 2019.

Yuliar S, Supriyati D, Rahmansyah M. Biodiversity of endophytic bacteria and their antagonistic activity to rhizoctonia solaniand *Fusarium oxysporum*. Global Journal of Biology, Agriculture and Health Sciences 2013;2(4):111-8.

Zhang C, Liu G, Xue S, Wang G. Soil bacterial community dynamics reflect changes in plant community and soil properties during the secondary succession of abandoned farmland in the Loess Plateau. Soil Biology and Biochemistry 2016;97:40-9.

Effect of *Hyphomicrobium* sp. in Biogas Formation from Organic Waste Treated by Batch Mode Anaerobic Digestion

Etih Hartati[1*], Nurul Aiman Musodiqoh[1], Elin Nurlina[2], and Didin Agustian Permadi[1]

[1]Environmental Engineering, Institut Teknologi Nasional Bandung, Indonesia
[2]Electrical Engineering, Universitas Jendral Ahmad Yani, Cimahi, Indonesia

ARTICLE INFO

Received: 25 Jul 2019
Received in revised: 27 Feb 2020
Accepted: 2 Mar 2020
Published online: 8 Apr 2020
DOI: 10.32526/ennrj.18.3.2020.24

Keywords:
Renewable energy/ Anaerobic digestion/ *Hyphomicrobium* sp./ Methane biogas/ Methanogenesis

*** Corresponding author:**
E-mail: etih@itenas.ac.id

ABSTRACT

Huge consumption of fossil fuel energy creates environmental problems, while the amount of organic solid waste is in an increasing trend especially in developing countries. Biogas is known as a renewable energy that can be used as an alternative fuel which is promising to reduce dependency on fossil fuels. This study identified the concentration of methane gas that can be produced from organic waste treated in an anaerobic digestion with the addition of *Hyphomicrobium* sp. Two-stage batch anaerobic digestion was used with an operational volume of 6 L. Four different starting concentrations of bacteria *Hyphomicrobium* sp. added to the reactors: 0.29×10^9 cells/L in reactor A, 0.87×10^9 cells/L in reactor B, 1.75×10^9 cells/L in reactor C, and no *Hyphomicrobium* sp. in the control reactor. The results showed that the concentration of methane gas produced was 38.4% in the reactor A while in reactor B and C were 35.6% and 33%, respectively. In reactor K with no addition of bacteria, the amount of methane produced was 52%. In contrary to the hypothesis, the addition of *Hyphomicrobium* sp. to the anaerobic process was contra-productive to the yield of methane. Further research is required to investigate the role of *Hyphomicrobium* sp. on the methane gas formation in the reactor.

1. INTRODUCTION

Energy has an important and indispensable role in human life, especially nowadays since almost all human activities are highly dependent on fossil fuel energy. Therefore, using renewable energy is a potential option to reduce both greenhouse gas and air pollutant emissions. In Indonesia, the fourth most populous country in the world, the pressure on energy demand is high and the amount of organic waste has been increasing. Indonesia was ranked 2nd in the world as the major contributor to the total generated food waste and the amount reached 113 Tg annually (EIU, 2017). Therefore, it is an opportunity to utilize the huge amount of generated waste to produce an alternative energy such as biogas. Biogas is a combustible mix of gases produced by anaerobic digestion process to degrade biodegradable materials (Ilaboya et al., 2010). Biogas is produced with methanogen bacteria which exist naturally in organic waste and is able to produce methane and other gases under anaerobic condition (Utami, 2010).

Several factors that may affect the biogas yield from the anaerobic digestion process have been well studied such as temperature, pH, organic loading rate and retention time in the reactor (Noraini et al., 2017). In an anaerobic digestion process, due to the symbiotic effects of various anaerobic and relatively anaerobic bacteria, organic substances are decomposed into simple, chemically stabilized compounds of methane and CO_2 (Naik et al., 2010). A two-stage thermophilic fermentation process has been reported to effectively enhance biomethane production and at the same time reduce the amount of organic waste (Wongthanate and Mongkarothai, 2018). One of the common bacteria used for methane formation is *Hyphomicrobium* sp. which can be isolated from mixed bacteria (Wilkinson and Hamer, 1972). Its habitat is widespread in soil and water and

Citation: Hartati E, Musodiqoh NA, Nurlina E, Permadi DA. Effect of *Hyphomicrobium* sp. in biogas formation from organic waste treated by batch mode anaerobic digestion. Environ. Nat. Resour. J. 2020;18(3):257-267. DOI: 10.32526/ennrj.18.3.2020.24

it is considered as a facultative anaerobic bacterium with a gram-negative genus that uses various carbon compounds as a source of energy. It also acts as helper to increase the methane oxidation rate in the methanotrophic process (Jeong and Kim, 2019). However, its effect in the anaerobic digestion process to treat organic waste has not been widely investigated.

This research examined the amount of methane gas concentration resulting from the utilization of organic waste from food waste as substrate with variations of *Hyphomicrobium* sp. bacteria concentrations. We used *Hyphomicrobium* sp. as the inoculum source for methane production based on previous research and we found *Hyphomicrobium* sp. as a dominant microorganism existing locally in the collected food waste. The effects on methane gas production are particularly of most concern, especially its synergistic effect to increase biogas yield using a two-stage fermentation process. The results can serve as science-based evidence to promote a feasible and workable system to produce renewable energy.

2. METHODOLOGY

2.1 Source of substrates

Organic solid waste was sampled from a restaurant with a consideration of having high organic content. Grab sampling was done in the morning time at 08.00 AM in a working day to collect of about 5 kg with the average measured density of 0.798 kg/L. Characteristics of organic waste such as density, water content, volatile level, C-organic, Total Kjehdahl Nitrogen (TKN), and C/N ratio were measured once a day (duplicate) as presented in Table 1. Hard materials such as animal bones and shells in food waste were removed before chopping the waste into more homogenous sizes to increase the surface area. Further it was mixed with tap water to obtain the substrate.

The purpose of addition of water is to resolute organic matter in the waste. Tap water from the Environmental Engineering Research Laboratory, Environmental Engineering Department, National Institute of Technology Bandung (ITENAS), Indonesia was used for the purpose. Several water characteristics such as pH, temperature and COD were measured once a day (duplicate) as presented in Table 1.

Table 1. Measurement methods

Parameter	Method	Reference	Measurement frequency			
			Waste and water characteristics	Acid formation	Substrate characteristics	Methane formation
pH	Potentiometry	SNI 06-6989.11:2004	1× /day	1× / 2 day	1× /day	1×/ 3 day
Temperature	Potentiometry	SNI 06-6989.11:2004	1× /day	1× / 2 day	1× /day	1×/ 3 day
Density	Gravimetry	-	1× /day	-	-	-
Water content	Gravimetry	SNI 03-197-1990	1× /day	-	-	-
Volatile levels	Gravimetry	SMEWW 5220,2012	1× /day	-	-	-
TVA	Distillation, titrimetric	SMEWW 5570,2012	-	1× / 2 day	1× /day	1×/ 3 day
COD	Reflux	SNI 6989.72:2009	1× /day	1×/ 2 day	1× /day	1×/ 3 day
BOD	Winkler Titration	SNI 6989.72:2009	-	-	1× /day	1× /day
Alkalinity	Acid-base Titration	SNI 06-2422-1991	-	-	1× /day	1×/ 3 day
C-Organic	Reflux	SMEWW 5220,2012	1× /day	-	-	-
TKN	Kjeldahl Analyzer	SNI 2081:2010	1× /day	-	1× /day	-
Phosphate	Spektrophotometry	SNI 6246-2010	1× /day	-	1× /day	-
Biogas	Orsat Analyzer	SNI 0029:2008	-	-	-	1× /2 day

Note: 1× /day: samples were taken once per day (duplicate), 1× /2 day: samples were taken once in two days (duplicate), 1× /3 day: samples were taken once in three days (duplicate). SNI–National Standard of Indonesia, SMEWW: Standard Methods for the Examination of Water and Wastewater.

2.2 Type of reactor

This research used a two stage anaerobic digestion system using two types of reactor: a hydrolysis reactor and a methanogenesis reactor. This system was chosen because the pH adjustment in the hydrolysis reactor caused the methanogen bacteria to digest organic matter quickly and accelerated methane formation (Hayes et al., 1988).

The hydrolysis reactor used in this study has a capacity of 180 L, made of a plastic drum equipped with lids and taps with a working volume of 5 L. The methanogenesis reactor consists of four tubular reactors with a height of 35 cm and 16 cm in diameter with an operating volume of 6 L each. The methanogenesis reactor was made of glass fiber and was equipped with a thermometer, stirrer, influent and effluent ports, pressure regulator, sample point, and gas holder. Schematic illustrations of the reactors are presented in Figure 1(a) (hydrolysis) and Figure 1(b) (methanogenesis). Hydraulic retention time (HRT) for this batch mode reactor was set to 111 days. The value was actually based on the observation during the reactor operation.

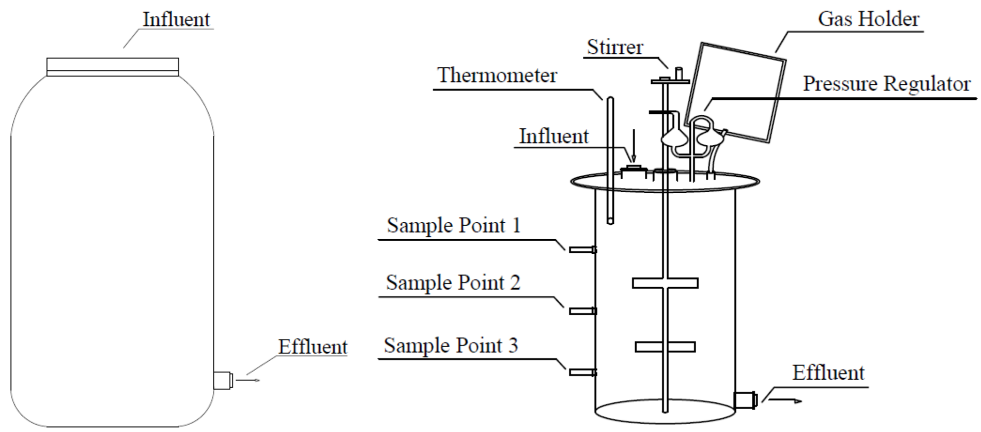

Figure 1. Scheme of hydrolysis (a); and methanogenesis (b) reactor

2.3 Research stages

2.3.1 Stages of acid formation

The ratio of organic waste and water used in this study was set to 1:1. This is because of the optimal C:N:P ratio of 400:5:1 in an anaerobic process was generally achieved using that ratio (Liberty and Prayatni, 2008). The density of organic waste in the hydrolysis reactor was 0.789 kg/L, while the amount of organic waste and water put in the hydrolysis reactor was set in the ratio of 25:20 (weight-based ratio). Parameters measured in this stage were pH, temperature, total volatile acid (TVA) and chemical oxygen demand (COD). The ratio of 1:1 was a volumetric ratio. Then, the density of organic waste and water were used to calculate the mass-based ratio of 1 kg/L: 0.789 kg/L. It yielded an actual weight ratio of 1.25 (25:20).

The measurement of substrate characteristics was performed to determine the initial conditions of the substrate used for methane formation. The substrate used was organic waste and water that have passed the stage of acid formation.

2.3.2 Stages of methane formation

This stage was done at the methanogenesis reactor with four variations of *Hyphomicrobium* sp. concentration (measured in cells per liter) bacteria added to the substrate. Different variations were done for different reactors (namely A, B, C, and K) with the different concentrations of bacteria as shown in Figure 2. *Hyphomicrobium* sp. bacteria was obtained from the identification of mixed bacteria used in methane formation and the concentration was calculated using the counting chamber method with a hemocytometer (Marin et al., 2014).

The concentrations of bacteria added to each reactor are as follows:

- Reactor A = substrate + 0.29 × 10^9 cells/L
- Reactor B = substrate + 0.87 × 10^9 cells/L
- Reactor C = substrate + 1.75 × 10^9 cells/L
- Reactor K = substrate without *Hyphomicrobium* sp.

Substrate amount was 5 L for each reactor.

3. RESULTS AND DISCUSSION

3.1 Characteristics of organic waste and water

Characteristics of organic waste and water used as substrates in methane formation are presented in Table 2. The parameters measured for organic waste characteristics were density, water content, volatile levels, C-organic and TKN while for water were pH, temperature, and COD.

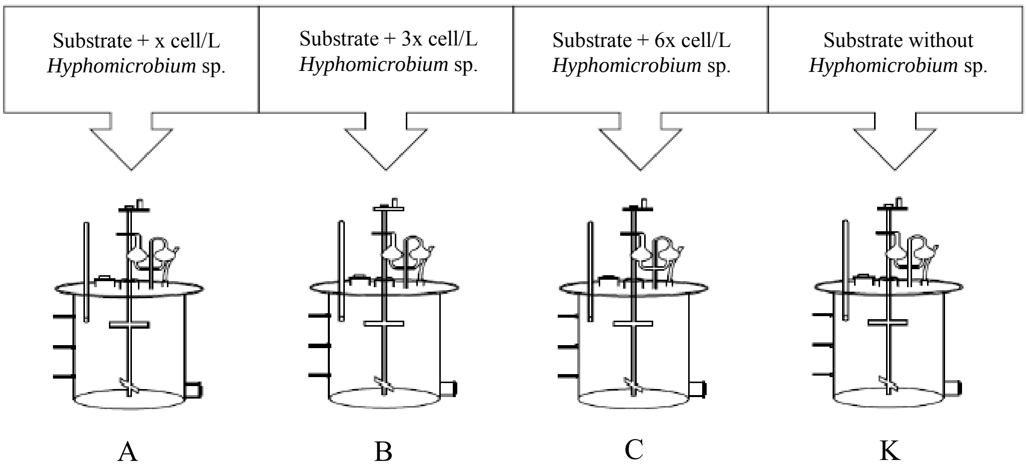

Figure 2. Variation of *Hyphomicrobium* sp. concentrations added to the reactors

Table 2. Characteristics of organic waste and water

No	Characteristics of organic waste			Water characteristics		
	Parameter	Results	Unit	Parameter	Results	Unit
1	Density	0.798	kg/L	pH	7.56	-
2	Water content	74.95	%	Temperature	29.25	°C
3	Volatile levels	86.92	%	COD	48	mg/L
4	C-Organic	50.04	%	-	-	-
5	TKN	2.24	%	-	-	-
6	C/N	22.33	-	-	-	-

Density is considered as one important factor that affects the rate of an organic waste decomposition process (Ramadanthi, 2008). The density on the organic waste used for this experiment was 0.798 kg/L while the water content was 74.9%. We considered analysis of the latter because water content would dissolve organic content and would act as a nutrient solvent for microorganisms (Rees, 1980). Note that the general value for water content in waste is about 50-80% (Tchobanoglous, 2004), hence the measured value was still within the range.

The volatile content of organic waste used was 86.92% which was lower than the values commonly reported for waste of about 95% (Tchobanoglous, 2004). Volatile level is important to determine the amount of organic matter contained in the waste. High volatile levels showed that organic waste was rich in organic materials which were easily degraded by bacteria (Ramadanthi, 2008). Carbon acts as a source of energy and nitrogen acts as a cell-builder for microorganisms. Therefore, the ratio of both is important for the anaerobic process (C/N ratio). The initial value of C/N ratio that is sufficient for starting the anaerobic processes should be within the range of 20-35 (Gotaas, 1956). In this research, organic waste used had a C/N ratio of 22.33% which showed sufficient amount of organic materials required to support the anaerobic process.

Temperature and pH are factors that greatly affect the growth of microorganisms in the process of anaerobic degradation of organic matter (Utami, 2010). According to Eckenfelder (1988), methanogenic bacteria worked well at pH 6.6-7.6. The pH of tap water used to dilute the organic waste was 7.56 so it was presumably suitable for growth and activity of the bacteria. The temperature of rinse water was 29.25 °C which was considered to be in an acceptable value to undergo the anaerobic process (Tchobanoglous, 2004). This indicated that the rinse water temperature may not potentially disturb the anaerobic process. The measured COD represents the organic content of the rinse water and the measured value was 48 mg/L which is an acceptable value for the process in the reactor.

3.2 Stages of acid formation

Acid formation was observed in this study as seen from the pH results from the 21 days run (Figure 3). It was clearly observed that pH values decreased up to the 6th day and continuously increased afterwards. To prevent the formation of methane in the hydrolysis reactor, on the 21st day the substrate was transferred to the reactor for the methane generation stage. This is because we observed that the increasing concentration of TVA during the period of 10th - 21st day, the pH of the substrate slightly decreased from 5.1 to 5.0, thus methane formation may soon follow.

The pH value showed the activity of anaerobic bacteria in each process at its stage. As shown in Figure 3, during the period between the 2nd - 6th days, the pH on the substrate decreased from 6.1 to 4.4. The decrease in pH indicated that there has been an onset of the acidogenesis stage. During the period of the 6th - 10th days, the pH increased from 4.4 to 5.1 indicating the onset of the acetogenesis stage. While during the period of the 10th - 21st days, the concentration of TVA increased and the pH of the substrate slightly decreased from 5.1 to 5.0. The pH in the range of 5.5-6.5 is often reported as the optimal range for the acidogenesis stage (Mao et al., 2015), while acetogenesis has been reported to occur within a range of 6.0-6.2 (Ramos-Suárez et al., 2015).

Increased concentrations of TVA indicated the process of acid formation. It is shown in Figure 3 that the TVA concentration continued to increase. In the beginning, the TVA concentration was 1,463 mg/L and then increased to 11,552 mg/L after 21 days. The high TVA concentration could inhibit methane gas formation. According to Wilkie (2008), the concentration of the TVA of more than 10,000 mg/L could be toxic and act as an inhibitor in the anaerobic process. The increase of TVA over a given range did not cause a decrease in pH. This could be due to the buffering capacity in which the substrate could neutralize the formed acid. Therefore, it is necessary to measure the alkalinity to know the buffering capacity of the substrate.

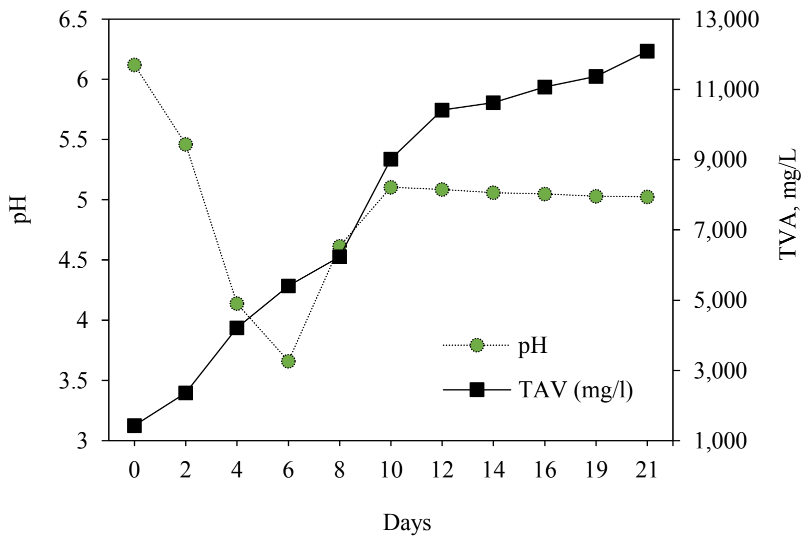

Figure 3. pH and TVA at hydrolysis reactor

Figure 4 shows that the temperature at the acid formation process ranged from 26.4 to 26.6 °C. According to Tchobanoglous (2004), the optimal temperature to support anaerobic degradation should be within the range of 25-35 °C. Temperature affects the growth of microorganisms and the rate of reaction in the formation of biogas. This is because microorganisms do not have temperature control systems in their cells (Widjajanti 2008). It can be said that the temperature range of the process carried out could support the anaerobic degradation.

Figure 5 showed that the decrease in COD concentration occurred during acid formation. Organic content from day 0 to day 21 decreased by 24.9% which was due to the degradation of organic compounds by the microbial activity (Ramadanthi, 2008).

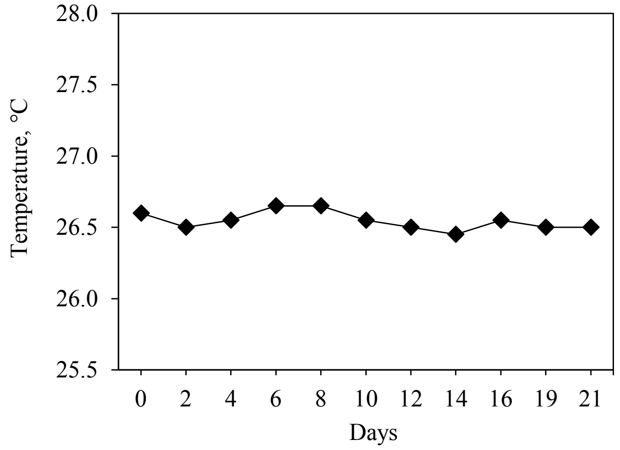

Figure 4. Temperature in the hydrolysis reactor

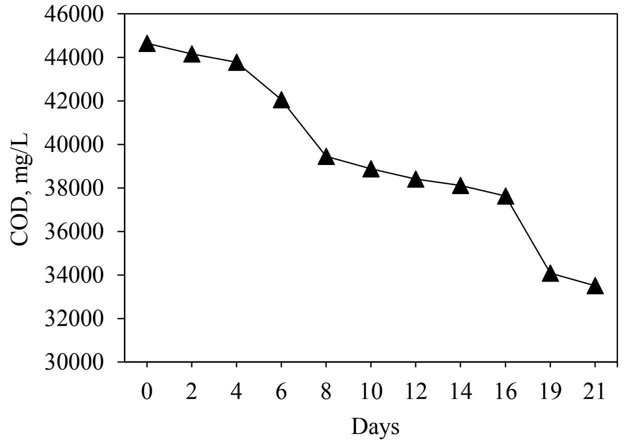

Figure 5. Concentration of COD in hydrolysis reactor

According to Malina et al. (1992), the suitable COD concentrations for anaerobic processing should range from 2,000 to 20,000 mg/L. The initial concentration of COD in the hydrolysis reactor was 44,640 mg/L. According to Syafila and Djajadiningrat (2003), this high concentration of organics would lead to more production of volatile acids from the acidogenesis process. Volatile acids formed in the acid formation process reached 11,552 mg/L. The amount of TVA content would interfere the process of methanogenesis, because acid is toxic to the methanogenesis bacteria.

On the 21st day, the liquid part of hydrolysis reactor, known as the substrate, was separated and transferred into the methanogen reactor. The initial characteristics of the starting substrate were measured and the results are presented in Table 3. The pH of substrate was 5.03 showing a typical acidic output from the acidogenesis stage. Substrate removal under these conditions was accomplished to prevent the occurrence of methane formation in the hydrolysis reactor. The temperature of the substrate was 25.6 °C, hence it can be said that the temperature of the substrate supports the anaerobic degradation. The concentration of the TVA in the substrate that was separated from the hydrolysis reactor was 13,253 mg/L. Under these conditions, the volatile acids contained in the substrate can be toxic to methanogenic bacteria, which would inhibit methane formation and growth of methanogenic bacteria (Grady and Lim, 1990).

Table 3. Substrate characteristics before entering methanogen reactor

No	Parameter	Concentration	Unit
1	pH	5.03	-
2	Temperature	25.60	°C
3	TVA	13,253	mg/L
4	COD	37,440	mg/L
5	BOD	31,049	mg/L
6	TKN	104	mg/L
7	Phosphate	2,319	mg/L
8	BOD/COD	0.83	-
9	COD/N	357	-
10	COD/P	16	-

The concentration of COD in the substrate that was separated from the hydrolysis reactor was 37,440 mg/L. High COD concentrations would result in high TVA concentrations, which are known to inhibit methane formation. The BOD/COD ratio was used as an early indication of the biodegradability of a material. The BOD/COD ratio of the substrate is 0.83 and this showed that the substrate could be used for methane formation through the biological process. Substrate characteristics in this study had COD/N 357 and COD/P ratio of 16. According to Veenstra and Lubberding (1993), the COD/N ratio should be 200 and COD/P of 1000. This indicated that the nutrient content was balanced with the existing organic content, so it is able to inhibit the growth of methanogen bacteria.

3.3 Stages of methane formation

Methanogenic process was identified clearly after 111 days of reactor run. We measured the parameters of temperature, pH, total volatile acid, alkalinity, COD and concentrations of methane gas. Figure 6(a) showed the time series of temperature and pH at four different methanogenesis reactors. There was little difference in temperature between reactor A, B, C and K. The temperature at the four methanogenesis reactors ranged from 24 to 26.5 °C which was classified under mesophilic conditions (20-45 °C). Mesophilic bacteria had stability against the rapid changes in environmental temperature, so it was often used in anaerobic processing (Tchobanoglous, 2004). *Hyphomicrobium* sp. is a mesophilic bacteria (25-40 °C). The temperature in the methane formation process in this study supported the growth of *Hyphomicrobium* sp.

Figure 6(b) showed that the pH of the four methanogenesis reactors increased, but not significantly, after two days by only 0.01-0.02. On the second day, all four reactors had a similar pH of 5, while after 111 days the pH ranged from 5.4 to 5.5. The increase of pH at reactors A, B and C was relatively the same while the increase in pH of reactor K occurred slower. This can be because the concentrations of TVA at the reactor A, B, and C were lower than reactor K. However, after 47 days the pH at reactor K increased faster than reactors A, B and C. According Rahayu (2011), if the environmental conditions for the growth of methanogen bacteria are not suitable, then the bacteria will not consume acids anymore hence it further causes the increase in the TVA concentration.

Figure 7(a) showed that the concentration of the TVA in the four reactors tends to increase until the 44th day and the turn-over was seen after the 47th. The concentration of TVA at reactor K was higher than that measured in reactors A, B, and C that was due to the methanol content which was produced from the acid formation and was further utilized by *Hyphomicrobium* sp. bacteria for its growth (Wilkinson and Harrison, 1973).

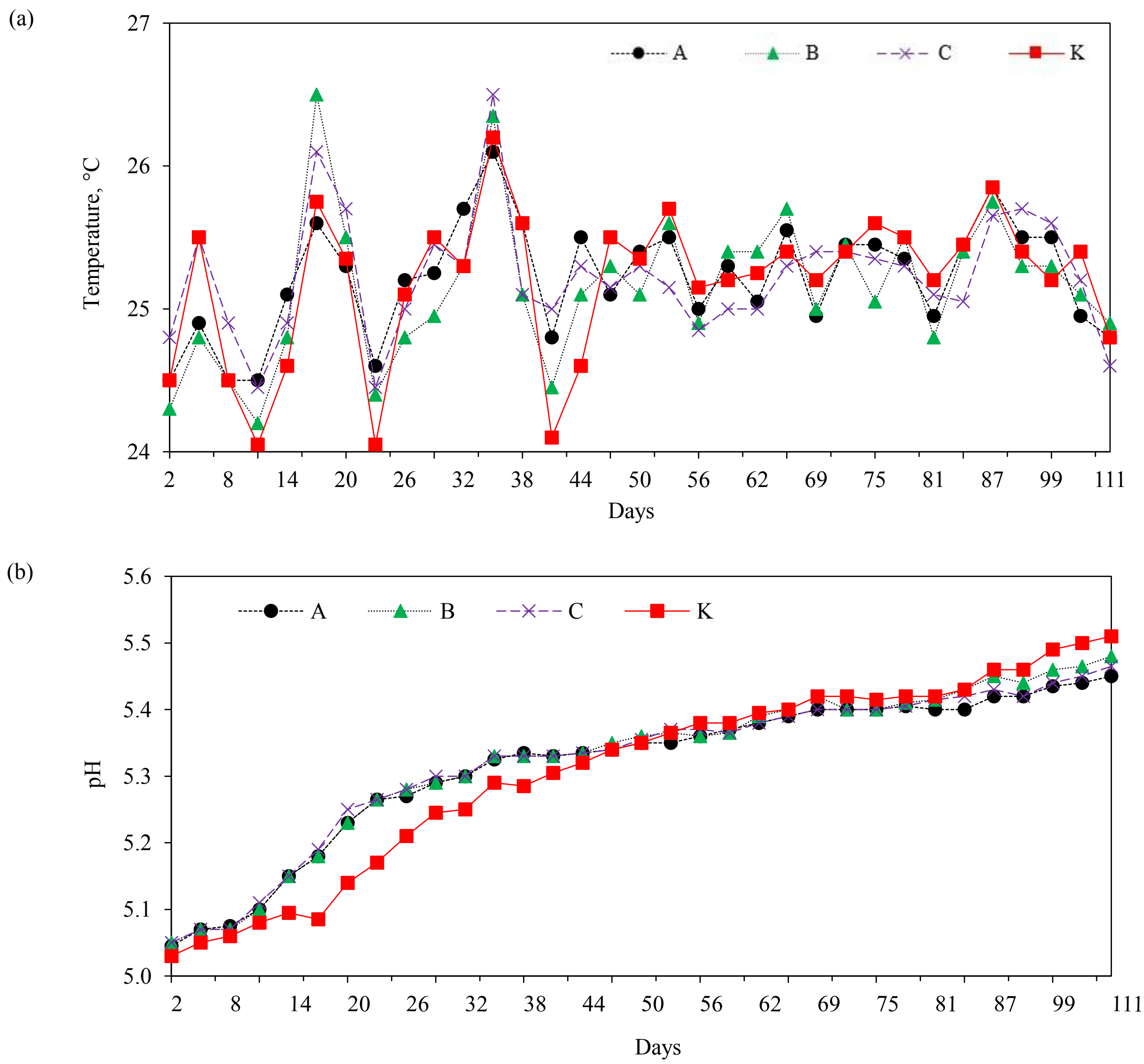

Figure 6. Measured parameters at the methanogen reactors: (a) temperature; and (b) pH

Alkalinity indicated buffer capacity in the anaerobic process, therefore high concentration of volatile acids would lead to the formation of acids, which in turn caused the pH to decrease. This showed that the buffer was not able to neutralize volatile acids. As a result, there was accumulation of volatile acids that could make the acidic environment of the microorganisms (Rahayu, 2011). The TVA/alkalinity ratio value of below 0.4 was a favorable condition for methanogen bacteria to grow so that methane gas production could be maintained (Grady and Lim, 1990).

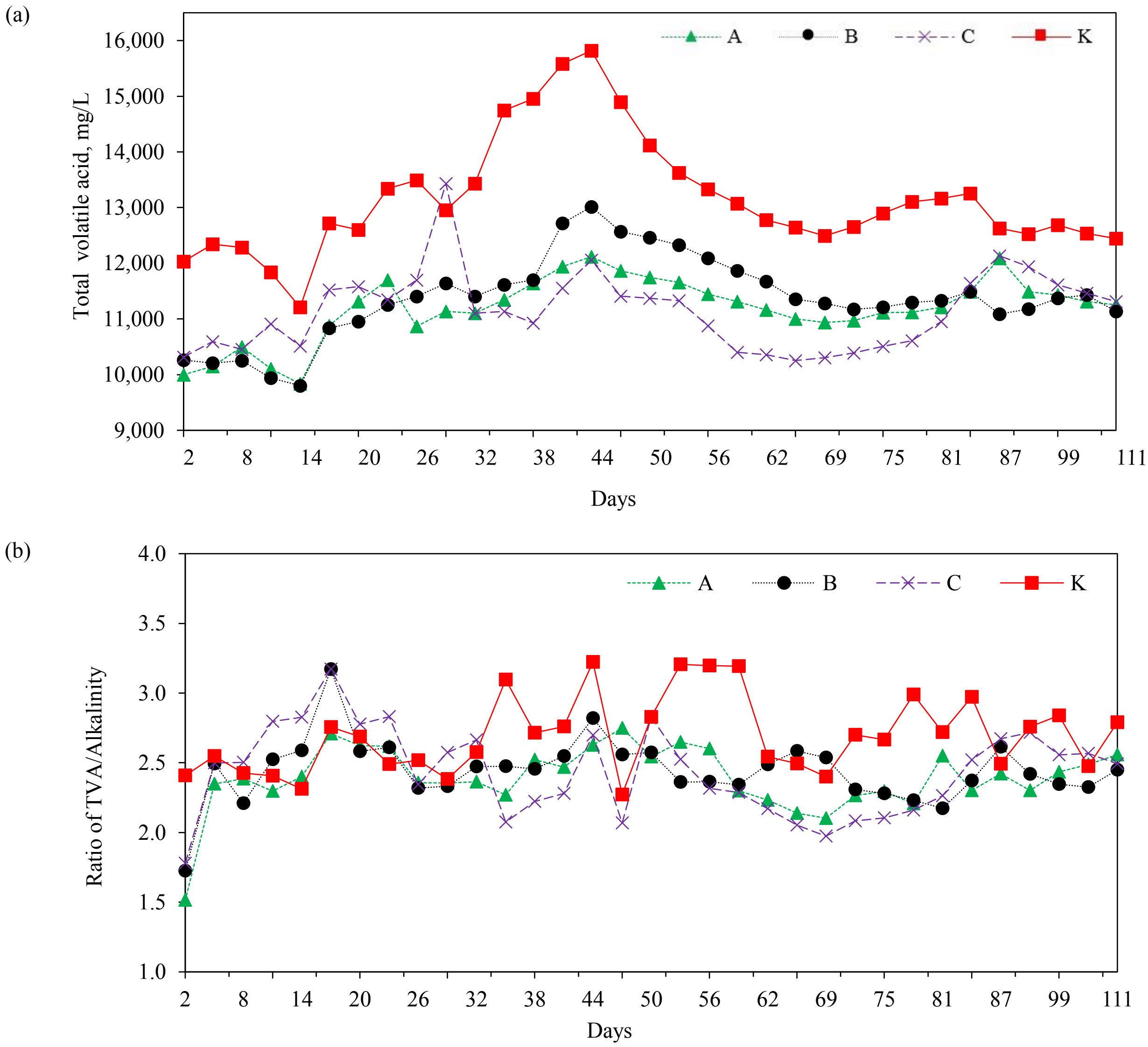

Figure 7. Measured parameters at the methanogen reactor: (a) TVA concentration; and (b) the ratio of TVA/alkalinity

Figure 7(b) presented the TVA/Alkalinity ratios of reactors A, B, C and K which ranged from 1.51 to 3.21. This indicated that the buffer could not neutralize excessive volatile acids. Figure 8(a) showed the concentration of bicarbonate alkalinity in reactor A was in the range of 3,064-5,530 mg/L, while in reactor B ranged from 2,167 to 5,066 mg/L. The associated concentrations in reactor C and K were 2,391-5,096 mg/L and 2,840-5,530 mg/L, respectively. According to Eckenfelder et al. (1988), the optimum bicarbonate alkalinity concentration for anaerobic treatment ranged from 2,500 to 5,000 mg/L. The average concentrations of bicarbonate alkalinity in all four reactors in the process are suitable for anaerobic treatment. The high ratio of TVA/Alkalinity was due to the high concentration of volatile acids formed in the process. Too high TVA or TVA/alkalinity ratio may suppress methane gas production because it will not provide suitable condition for the methanogen bacteria to grow in such environment.

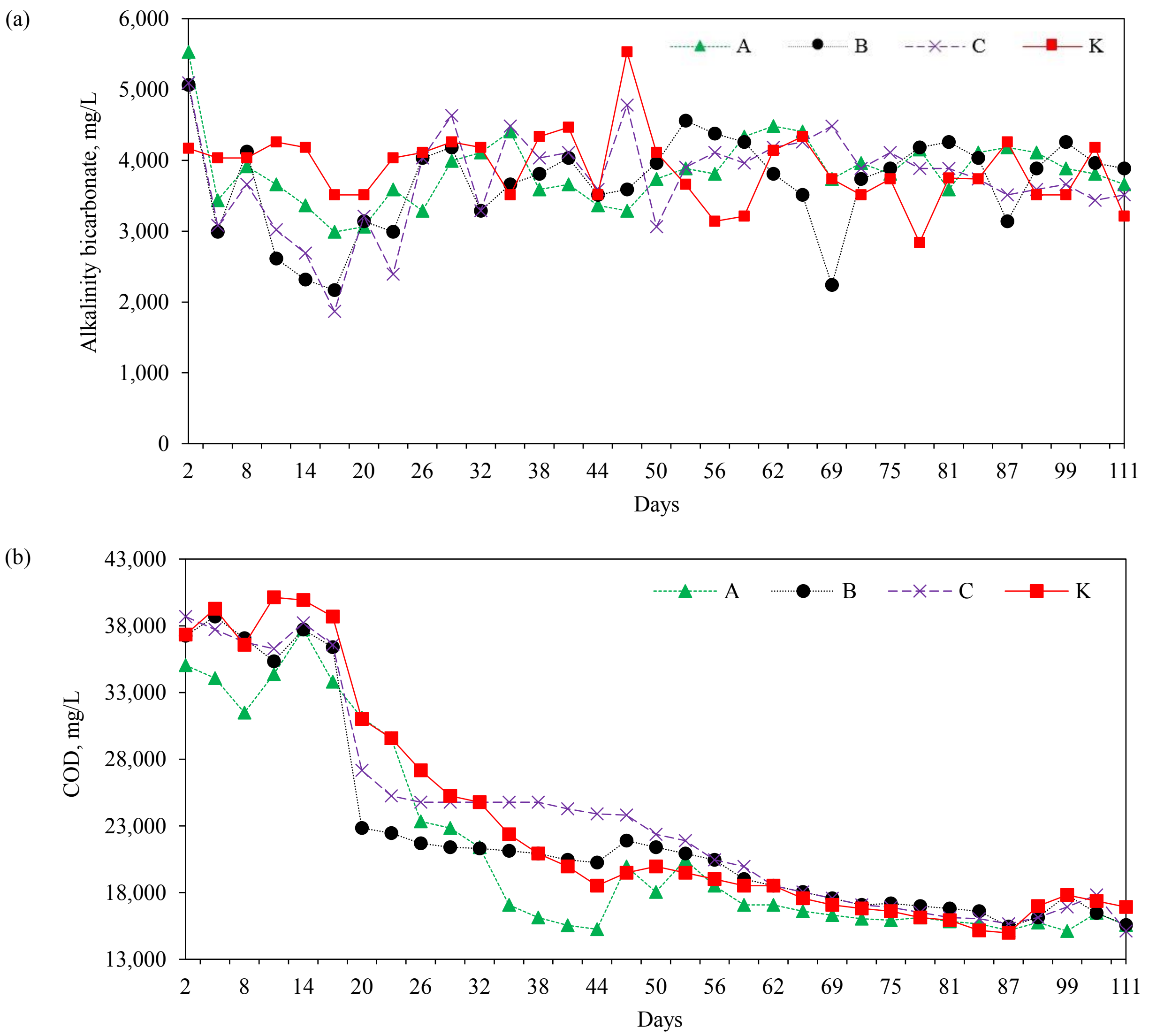

Figure 8. Concentrations of alkalinity bicarbonate: (a); and COD (b)

Figure 8(b) showed variations of COD concentration during the methane formation. The concentration of COD on the methanogenesis reactor tends to decrease. In reactor A, COD decreased by 49%, while in rectors B, C, and K were 52%, 53% and 54%, respectively. Decrease in COD concentration can be caused by the process of organic degradation by bacteria. Organic content is also used as a food source for bacteria present in the process (Ramadanthi, 2008).

3.4 Methane gas concentration

Methane gas is the final product of anaerobic processing. The methane gas formation is the result of the degradation of organic compounds, thus during the end of the operation (days 93rd -111th) we highlighted the changes of CH_4, TVA and COD concentrations in each reactor. The results are presented in Figure 9. There was a substantial decrease in methane gas concentration from day 93rd to day 111th. As shown in Figure 9(a), the concentration of methane gas at reactor K is higher than that of reactors A, B, and C. This is due to the absence of *Hyphomicrobium* sp. bacteria in reactor K as compared to others in which *Hyphomicrobium* sp. was added with different concentrations. *Hyphomicrobium* sp. is generally known as a methanol-beneficial bacterium where high methanol production can inhibit methane oxidation (Wilkinson and Harrison, 1973). As found in this study, the higher of the *Hyphomicrobium* sp. bacteria, the lower of methane gas would be produced.

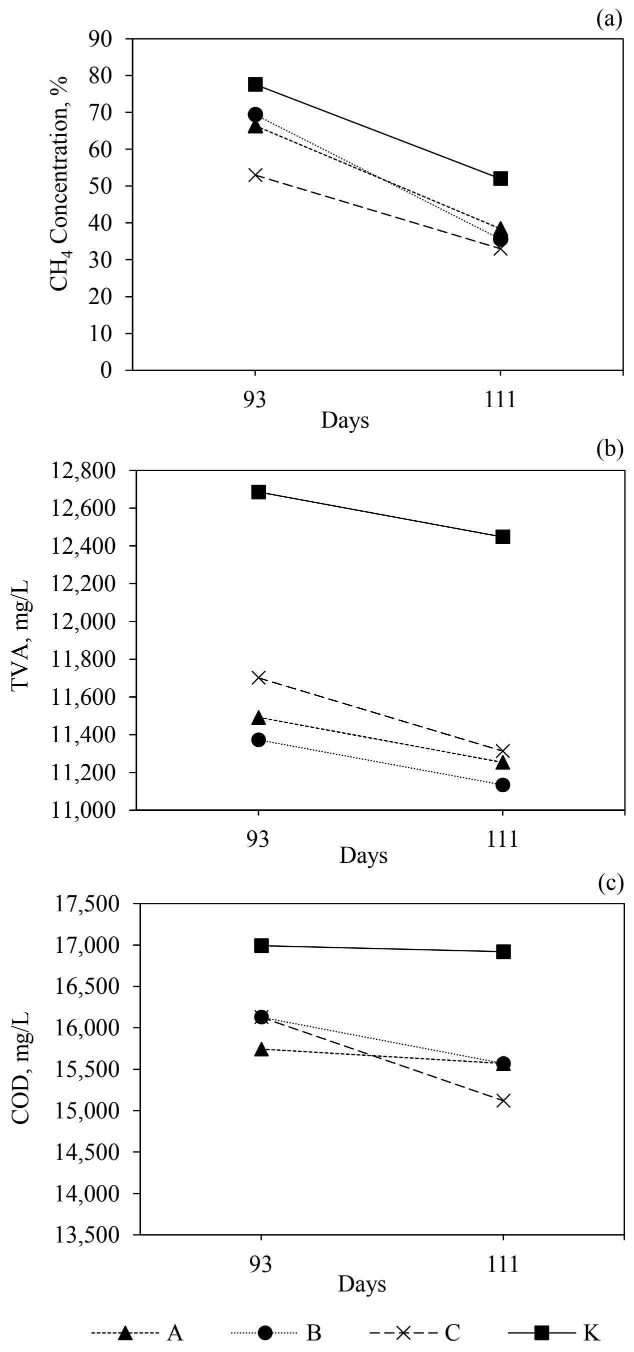

Figure 9. Concentrations of methane gas (a); TVA concentration (b); and COD (c)

Figure 9(b) showed a comparison between methane formation from the four variations of *Hyphomicrobium* sp. concentration in correlation with the TVA. The concentration of TVA in the K reactor was higher than that of reactors A, B, and C, and the methane gas concentration generated at the reactor K was greater than that of reactors A, B and C. According to Syafila and Djajadiningrat (2003) the amount of TVA would decrease as a result of the methanogenesis process which would convert the product from the process of acidogenesis into methane gas. In this study the decrease in TVA concentration was not accompanied by an increase in methane gas concentration which was caused by the addition of *Hyphomicrobium* sp. This would influence the formation of TVA because the *Hyphomicrobium* sp. bacteria utilized methanol for its growth (Wilkinson and Harrisons, 1973).

Methanol is one of the intermediate products of the acididogenesis stage in the formation of methane formation. The accumulation methanol production would inhibit the oxidation of methane, so that the methane concentration would be higher (Wilkinson and Harrisons, 1973). When methanol was utilized by *Hyphomicrobium* sp. bacteria, its concentration would decrease hence the methane formation would be limited. When a higher amount of the *Hyphomicrobium* sp. bacteria was added, the TVA concentration would be higher as well as the methane.

Concentration of COD in the four reactors (Figure 9(c)) tended to decrease along with the decrease of methane gas concentration in Figure 9(a). Reactors were operated in a batch system hence this affected the organic degradation to be slow which further bring in the lower production of methane. The concentration of methane gas would decrease along with the decrease in COD concentration. Under the condition of high concentration of *Hyphomicrobium* sp., the concentration of COD tended to be lower. Ramadanthi (2008) confirmed the situation that the decrease in COD concentration could be caused by the organic degradation process by bacteria.

In contrary to our previous hypothesis, the addition of *Hyphomicrobium* sp. seemed to be contra-productive to the methane production. The inoculum also consumed the organic hence reduced the TVA as compared to reactor K. Therefore, methane production in the reactor without inoculum was higher than those with the bacteria. *Hyphomicrobium* sp. was reported to use many carbon compounds (including methanol carbon as an intermediate compound for CH_4 production) as growth substrates (Wilkinson and Hamer, 1972). These explained our findings that higher concentration of *Hyphomicrobium* sp. did not yield higher concentration of CH_4, thus *Hyphomicrobium* sp. rich containing organic source should be avoided.

4. CONCLUSION

Maximum concentrations of methane gas produced from organic waste treated in the reactor were 66.4% (A), 69.4% (B), 53% (C) and 77.6 % (K).

It can be concluded that the concentration of *Hyphomicrobium* sp. has an effect on the formation of methane gas in the reactor however the production of methane was higher if it was not added. Inverse correlation was found between both parameters meaning that the higher concentration of *Hyphomicrobium* sp. would lead to lower concentration of the methane gas. This can be explained due to the formation of methanol as an intermediate product of the methane formation process which was further utilized by *Hyphomicrobium* sp. It also uses many carbon compounds such as methanol carbon as growth substrates. However, further research is required to investigate solely the role of *Hyphomicrobium* sp. on the methane gas formation in the reactor without contribution from the microbial activity from the substrate. Control experiment of tap water "+" inoculum and tap water only should be conducted in the future to isolate the impact of inoculum to the bio methane production.

REFERENCES

Eckenfelder WW, Patoczka JB, Pulliam GW. Anaerobic versus aerobic treatment in the USA. Proceedings of the 5th International Symposium on Anaerobic Digestion; 1988 May; Bologna, Italy. Oxford, UK: Pergamon Press; 1988.

Economist Intelligence Unit (EIU). Fixing Food: Towards a More Sustainable Food System [Internet]. 2017 [cited 2020 Jan 30]. Available from: https://foodsustainability.eiu.com/wp-content /uploads/sites/34/2017/03/FIXING-FOOD-TOWARDS-A-MORE-SUSTAINABLE-FOOD-SYSTEM.pdf.

Gotaas HB. Composting, Sanitary Disposal and Reclamation of Organic Wastes. Geneva: WHO Nanograph Series No 31; 1956.

Grady Jr. CPL, Lim HC. Biological Wastewater Treatment. New York, USA: Marcel Dekker Inc.; 1990. p. 29.

Hayes D, Thomas IH, Ronald R, Frank RJ. Production of High Methane Content Product by Two Phase Anaerobic Digestion. USA: Gas Research Institute; 1988.

Ilaboya IR, Asekhame FF, Ezugwu MO, Erameh AA, Omofuma FE. Studies on Biogas Generation from Agricultural Waste; Analysis of the Effects of Alkaline on Gas Generation. World Applied Sciences Journal 2010;9(5):537-45.

Jeong SY, Kim TG. Development of a novel methanothropic process with the helper microorganism *Hyphomicrobium* sp. NM3. Journal of Applied Microbiology 2019;126(2):534-44.

Liberty L, Prayatni S. The Effect of Adding Water to the CNP Ratio of Biowaste in a Mechanical Biological Treatment [dissertation]. Bandung: Bandung Institute of Technology; 2008.

Mao C, Feng Y, Wang X, Ren G. Review on research achievements of biogas from anaerobic digestion. Renewable and Sustainable Energy Reviews 2015;45:540-55.

Malina Jr., Joseph F, dan Pohland GF. Design of Anaerobic Processes For The Treatment Of Industrial and Municipal Wastes. USA: Technomic Publishing Co, Inc; 1992. p. 153.

Marin A, Denimal E, Guyot S, Journaux L, Molin P. A robust generic method for grid detection in White Light Microscopy Malassez Blade Images in the context of cell counting. Microscopy and Microanalysis 2014;21(1):239-48.

Naik SN, Goud VV, Rout PK, Dalai AK. Production of first and second generation biofuels: A comprehensive review. Renewable and Sustainable Energy Reviews 2010;14(2):578-97.

Noraini M, Sanusi SMA, Elham OSJ. Factors affecting production of biogas from organic solid waste via anaerobic digestion process: A review. Solid State Science and Technology 2017;25(1):29-39.

Rahayu NS. The Performance of Upflow Anaerobic Fixed Bed (UAFB) Reactor for Organic Removal in Solid Waste under Liquid Phase without pH Adjustment [dissertation]. Bandung: Bandung Institute of Technology; 2011.

Ramadanthi GP. Degradation of Liquid Phase Organic Waste Using Batch Mode Anaerobic Digestion [dissertation]. Bandung: Bandung Institute of Technology; 2008.

Ramos-Suárez J, Arroyo NC, González-Fernández C. The role of anaerobic digestion in algal biorefineries: Clean energy production, organic waste treatment, and nutrient loop closure. In: Singh B, Kuldeep B, Faizal B, editors. Algae and Environmental Sustainability. India: Springer; 2015. p. 53-76.

Rees JF. The fate of carbon compounds in the landfill disposal of Organik Matter. Journal of Chemical Technology and Biotechnology 1980;30:25-36.

Syafila M, Djajadiningrat A. Performance of hybrid anaerobic digestion with rock stone to treat molase contained waste water. Proceedings of ITB Science and Technology: 2003; Bandung, Indonesia: ITB Publisher; 2003.

Tchobanoglous GB. Wastewater Engineering: Treatment, Disposal, and Reuse. New York, USA: McGraw-Hill, Inc.; 2004.

Utami A. Organic Waste Removal in Slurry Phase Treated in an Anaerobic Digestion Reactor [dissertation]. Bandung: Bandung Institute of Technology; 2010.

Veenstra S, Lubberding HJ. Anaerobic Wastewater Treatment. Delf, Netherland: International Institute for Infrastructural Hydraulic and Environmental Engineering (IHE); 1993.

Widjajanti S. Treatment of Waste Water from Security Printing Using Anaerobic Biological Process of Circulating Bed Reactor (CBR) with Sequencing Batch Reactor (SBR) System [dissertation]. Bandung: Bandung Institute of Technology; 2008.

Wilkie AC. Biomethane from biomass, biowaste, and biofuels. In: Wall J, Harwood C, Demain A, editors. Bioenergy. Washington DC, USA: ASM Press; 2008. p. 195-205.

Wilkinson TG, Hamer G. Some growth characteristics of a *Hyphomicrobium* sp. in batch culture. Journal of Applied Bacteriology 1972;35:577-88.

Wilkinson TG, Harrison DEF. The affinity methane and methanol of mixed cultures grown on methane in continuous culture. Journal of Applied Microbiology 1973;36:309-13.

Wongthanate J, Mongkarothai K. Enhanced thermophilic bioenergy production from food waste by a two-stage fermentation process. International Journal of Recycling of Organic Waste in Agriculture 2018;7:109-16.

Characterization of Pb-tolerant Plant-growth-promoting Endophytic Bacteria for Biosorption Potential, Isolated from Roots of Pb Excluders Grown in Different Habitats

Jiraporn Yongpisanphop[1*] and Sandhya Babel[2]

[1]*Department of Agro-Industrial, Food and Environmental Technology, Faculty of Applied Science, King Mongkut's University of Technology North Bangkok, Bangkok 10800, Thailand*
[2]*School of Bio-Chemical Engineering and Technology, Sirindhorn International Institute of Technology, Thammasat University-Rangsit Campus, Pathum Thani 12120, Thailand*

ARTICLE INFO

Received: 16 Jan 2020
Received in revised: 16 Mar 2020
Accepted: 20 Mar 2020
Published online: 2 Jun 2020
DOI: 10.32526/ennrj.18.3.2020.25

Keywords:
Pb biosorption/ Endophytic bacteria/ Plant-growth-promoting traits/ Phytostabilizer

*** Corresponding author:**
E-mail:
jiraporn.y@sci.kmutnb.ac.th

ABSTRACT

Bioremediation using metal-tolerant plant-growth-promoting endophytic bacteria has been studied. The biosorption potential of endophytic bacteria isolated from roots of non-metalliferous Pb excluders (*Acacia mangium* and *Eucalyptus camaldulensis*), and a metalliferous Pb excluder (*Pityrogramma calomelanos*) was evaluated. Five isolates were selected and designated as "Pc", "Pe", "Ai", "Aj", and "El". Phylogenetic reconstruction suggested that strain Ai was closely related to *Serratia proteamaculans*, Aj to *Pseudomonas* sp., El to *Bacillus cereus*, Pc to *Pseudomonas psychrophila*, and Pe to *Pseudomonas veronii*. They could equally tolerate Pb. Most of them had the capacity to produce siderophores and solubilize phosphate, except *B. cereus*. However, *B. cereus* showed high capacity of Pb uptake (4.54±0.38 mg/g) and removal (8.36±0.70%) with no significant difference ($p>0.05$) from the other strains, except *P. psychrophila* (1.36±0.23 mg/g of Pb uptake, and 2.60±0.44% Pb removal). The results suggest that biosorption capacity may not involve the habitat of a plant host. Plant-growth-promoting traits were not the only factor for biosorption by endophytic bacteria. *S. proteamaculans*, *B. cereus*, and *P. veronii* showed the same Pb biosorption. Strains closely related to *P. veronii* could be promoted as candidates for the removal of Pb in polluted environments.

1. INTRODUCTION

Lead (Pb) toxicity can occur to all organisms living in the world (Bano et al., 2018). However, it is valuable for many industries, and it is also necessary for modern life (Sharma and Dubey, 2005; Gillani et al., 2017; Tseveendorj et al., 2017). Pb is used continuously, and the environment has Pb contamination unavoidably. Effective alternative methods for Pb removal are needed. Conventional methods are used to remediate and stabilize metals (including Pb) in the environment. These methods are precipitation, reverse osmosis, ion exchange, filtration, electrochemical treatment, membrane technologies, solvent extraction, adsorption, etc. (Gillani et al., 2017; Tseveendorj et al., 2017). However, these methods have their own disadvantage in application such as being too expensive or inefficient, and they release toxic waste (Tseveendorj et al., 2017).

Bioremediation strategies using microorganisms (e.g., bacteria, yeast, algae, and fungi) to remediate Pb are becoming more attractive in contrast to the conventional methods. Bioremediation methods are eco-friendly and less expensive (Bhatnagar and Kumari, 2013; Govarthanan et al., 2016; Kumar and Fulekar, 2018). Although microorganisms cannot degrade and destroy heavy metals, they can transform them to less toxic substance to reduce their toxicity (Gupta et al., 2016). Biosorption using living and dead microorganisms as biosorbents can be used to remove heavy metals via a passive adsorption mechanism (Coelho et al.,

Citation: Yongpisanphop J, Babel S. Characterization of Pb-tolerant plant-growth-promoting endophytic bacteria for biosorption potential, isolated from roots of Pb excluders grown in different habitats. Environ. Nat. Resour. J. 2020;18(3):268-274. DOI: 10.32526/ennrj.18.3.2020.25

2015). It is fast, occurring in a few minutes, and reversible. Biosorption occurs under normal conditions (e.g., pressure and temperature) (Aslam et al., 2010; Coelho et al., 2015). In addition, there are many factors (i.e. pH, ionic strength, temperature, biosorbent concentration, and other ions in the solution) that influence the biosorption of metals (Coelho et al., 2015). Among microrganisms, bacteria are important candidates that are largely studied for their bioremediation potential (Gupta et al., 2016).

Currently, the biosorption of heavy metals by metal-tolerant endophytic bacteria (MTEB) with plant-growth-promoting traits (PGPT) is of great interest (Govarthanan et al., 2016; Ma et al., 2016). Bacteria colonizing in the healthy plant's tissues with little negative effects on the host are known as endophytic bacteria (EB). They are widely found in many plant species (Govarthanan et al., 2016). Endophytic bacteria (used for Pb removal) can transform Pb via various mechanisms (e.g., methylation, demethylation, and redox reactions). The bacterial cell surface contains many functional groups (e.g., carbonyl, carboxyl, hydroxyl, sulfhydryl, and phosphodiester groups), and they have key roles in the biosorption mechanism (Abdia and Kazemi, 2015). Pb-tolerant EB can be found in plants that accumulate a high Pb content in their tissues. Normally, they can be isolated from hyperaccumulators (e.g., *Pteris vittata* L. and *Pteris multifida* Poir.). Endophytic bacteria extracted from these hyperaccumulator ferns had PGPT leading to significant metal remediation (Zhu et al., 2014). However, biosorption by Pb-tolerant EB, especially when isolated from the roots of a Pb-excluder grown in diverse environmental habitats (between normal and contaminated sites), are not much investigated. The bacterial endophyte of phytostabilizer growing in the soil contaminated with high concentration of Pb and accumulating high levels of Pb in the root tissues, can tolerate a high amount of Pb due to the stabilizing ability of its host. It is considered as a novel biosorbent for Pb. Naturally, Pb polluted soil is rare, so the non-metalliferous Pb phytostabilizer is an alternative plant host to discover Pb-tolerant endophytic bacteria with plant-growth-promoting traits for the removal of Pb.

The criterion used to select phytostabilizer plants in this study was their ability to accumulate high Pb concentration in root tissue. Plants reported as Pb phytostabilizers with a bioconcentration factor greater than 1 and translocation factor less than 1 were: *Pityrogramma calomelanos* (L.) Link, grown in a Pb contaminated site; and *Acacia mangium* Willd. and *Eucalyptus camaldulensis* Dehnh., grown in non-contaminated sites (Soongsombat et al., 2009; Meeinkuirt et al., 2012; Yongpisanphop et al., 2019). *P. calomelanos* (L.) Link belongs to the Pteridaceae family, and it is widely grown in various parts of Thailand. *P. calomelanos* is an arsenic hyperaccumulator (Francesconi et al., 2002), and Pb phytostabilizer (Soongsombat et al., 2009). *A. mangium* belongs to the Fabaceae family, while *E. camaldulensis* belongs to the Myrtaceae family. They are fast-growing trees, and have phytoremediation potential for Pb remediation (Yongpisanphop et al., 2017). For Pb contaminated areas, *P. calomelanos* was selected based on having the highest Pb concentration in root tissue amongst the plants collected. For plants grown in non-contaminated area, *A. mangium* and *E. camaldulensis* were selected based on the highest Pb concentration in root tissue according to hydroponic experiments.

This study screened Pb tolerant EB from *Acacia mangium*, *Eucalyptus camaldulensis*, and *Pityrogramma calomelanos*, and evaluated the Pb biosorption potential of isolates under *in vitro* conditions.

2. METHODOLOGY

2.1 Screen of Pb-tolerant EB

Six healthy *P. calomelanos* plants were collected from Pb contaminated soil, while those of *A. mangium* and *E. calmaldulensis* were obtained from the Chatuchak market, Bangkok, Thailand. The roots were cleaned using a surface disinfection technique. The roots were cleaned with 70% ethanol for 40 seconds, followed by 2.5% sodium hypochlorite plus a droplet of polyoxyethylene 80, with gentle shaking for 15 min for surface disinfection before extraction (Luo et al., 2011). The endophytic bacteria were isolated, characterized, and identified according to Yongpisanphop et al. (2019). The obtained sequences were aligned by the BLAST tool on the NCBI website. The phylogenetic tree of partial 16S rRNA gene sequences was reconstructed by the Neighbor-Joining method (Saitou and Nei, 1987) based on 1,000 bootstrap replicates (Felsenstein, 1985), and implemented by MEGA7 (Kumar et al., 2016). Kimura 2-parameter model (Kimura, 1980) was used to estimate the evolutionary distances of the tree.

2.2 Pb biosorption

The biosorption experiment was set to investigate the bioremediation potential of the EB isolates. This experiment was carried out under the optimum conditions reported for the maximum Pb biosorption by living bacterial cells: 10 min, pH ranging from 5 to 6, 100 mg/L of initial concentration (Wierzba and Latala, 2010). Pre-culture of each EB isolate was prepared by transferring a loop of each (pure) fresh colony into LB broth, and incubated on a shaker under optimal conditions (100 rpm, 30±2°C, and 48 h). Pre-culture (100 µL) was added to LB medium broth (30 mL), and incubated on a rotary shaker (150 rpm, 30±2°C, and 16 h). Cultured medium was centrifuged (20 min, 3500 rcf, and 4°C) to collect the EB cells, and suspended in 30 mL sterile 0.85% NaCl. The biomass in the cell suspensions was harvested using an Eppendorf tube and determined as the fresh weight of living bacterial cells. Living bacterial cells (50 mg) were re-suspended in a 125 mL Erlenmeyer flask containing 30 mL of 100 mg/L of Pb solution as $Pb(CH_3COO)_2{\cdot}3H_2O$, pH about 5. Non-inoculated Pb solution was used as the control. All flasks were incubated on a rotary incubator (150 rpm, 30±2°C, and 10 min). The solution (10 mL) was filtered through a 0.2-µm Millipore filter, and Pb concentrations were determined using AAS (SpectrAA 553, Varian). The biosorption efficiency (Tseveendorj et al., 2017) and specific metal uptake (Wierzba and Latala, 2010) were calculated as in Equations (1) and (2), respectively.

$$\text{Biosorption efficiency (\%)} = [(Cini - Cfin)/Cini] \times 100 \quad (1)$$
$$\text{Specific metal uptake (mg/g)} = [(Cini - Cfin)/M] \times V \quad (2)$$

Where; Cini and Cfin are the initial and final concentrations of Pb in the solution (mg/L), respectively, V is the volume of the metal solution (L), and m is the fresh weight (g).

2.3 Statistical analysis

All data were expressed as the mean and standard deviation (mean±S.D.) of the three replicates. The data were analyzed by one-way analysis of variance (ANOVA). The means were compared using the LSD with a significant difference at $p \leq 0.05$. All the statistical analyses were carried out using the SPSS trial version for Windows.

3. RESULTS AND DISCUSSION

3.1 Screen of Pb-tolerant endophytic bacteria

In the present study, five EB isolates were discovered. Isolates were designated as “Pc” and “Pe” (isolated from *P. calomelanos*), “Ai” and “Aj” (isolated from *A. mangium*), and “El” (isolated from *E. camaldulensis*). The strains of these EB were indicated via the results of the phylogenetic tree (Figure 1). Isolate Ai was identified as a strain closely related to *S. proteamaculans* (Gram-negative bacteria), belonging to Yersiniaceae. Isolate Aj was identified as a strain closely related to *Pseudomonas* sp. (Gram-negative bacteria), belonging to Pseudomonaceae. Isolate El was identified as a strain closely related to *B. cereus* (Gram-positive bacteria), belonging to Bacillaceae. Isolates Pc and Pe were identified as strains closely related to *P. psychrophila* and *P. veronii*, respectively.

As expected, bacterial endophytes found in this study were members of γ-Proteobacteria (*Pseudomonas* and *Serratia*) and Firmicutes (*Bacillus*), which are a common class of EB. All genera in this study are also cultivable EB (Liotti et al., 2018). Our EB were both Gram-positive and negative corresponding with the variation of EB, which span a significant range of Gram- positive and negative bacteria (Lodewyckx et al., 2002). Moreover, *Pseudomonas* sp. was found in plants with different habitants. This is consistent with Li et al. (2012) who reported that EB with the same genus can be isolated from metal-polluted and non-metal-polluted plants.

The Pb-tolerance and PGPT are shown in Table 1. The ability to tolerate heavy metals plays a significant role in heavy metal contaminated environments for bioremediation (Paul and Sinha, 2015). Our results found that Pb phytostabilizers grown in Pb-contaminated and non-contaminated soils could harbor Pb-tolerant EB. Pb-tolerance is a common ability of endophytic bacteria living in plants grown in Pb contaminated soil. Many studies showed that *Pseudomonas*, *Bacillus*, and *Serratia* can tolerate heavy metals, including Pb (Li et al. , 2012; Alzubaidy, 2012; El Aafi et al., 2012). Li et al. (2012) reported that the same genus of EB extracted from different host species grown in different habitats (metal or non-metal contaminated soil) showed no difference in metal resistance as *Pseudomonas* sp. from this study.

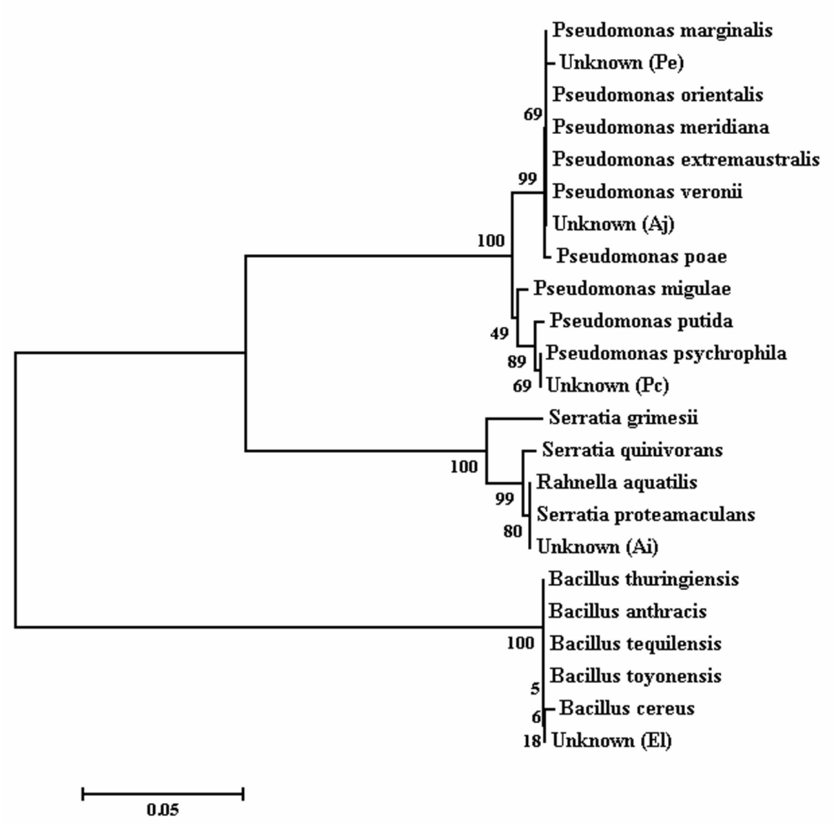

Figure 1. Phylogenetic tree, regenerated by the Neighbor-Joining method implemented in MEGA 7.

The results of our bacterial endophyte's PGPT (isolated from the plant grown in a non-contaminated soil) are in agreement with previous studies. Some bacterial endophytic isolates (RM and RM3) isolated from the roots of *Tridax procumbens* L. grown in non-contaminated soil could produce siderophores and solubilize phosphate like the Aj isolate. However, some isolates (RM1 and RM4) do not have both properties (Govarthanan et al., 2016). Endophytic bacteria, *Microbacterium trichothecenolyticum* and *Agrococcus terreus*, isolated from the roots of wild *Dodonaea viscosa* (L.) could produce siderophores but could not solubilize phosphate. *Pseudomonas geniculata* and *Pseudomonas taiwanensis* could produce siderophores and solubilize phosphate like Aj (*Pseudomonas extremaustralis*) (Afzal et al., 2017). In this study, *Pseudomonas* sp. isolated from the roots of a plant grown in Pb contaminated soil and *Pseudomonas chlororaphis* isolated from the root of *Robinia pseudoacacia* L. grown in a Pb-Zn mining area showed the same PGPT (siderophore production and phosphate solubilization) (Fan et al., 2018).

3.2 Pb biosorption

The results for biosorption capacity are shown in Table 2. The efficacy of this method of using living cells of Pb-tolerant EB (with and without plant growth-promoting traits) as biosorbents was compared in terms of the Pb uptake and removal. *P. psychrophila* showed the lowest biosorption capacity. The Pb biosorption efficacy of *S. proteamaculans*, *B. cereus*, and *P. veronii* showed no significant difference ($p>0.05$). Their efficiency of Pb uptake and Pb removal was higher by 3.57-fold, and 3.12-fold, respectively, compared to *P. psychrophila*. The Pb-biosorption capacity from this study cannot be compared with other studies due to the different conditions that were used.

Table 1. Pb-tolerance and plant-growth-promoting traits (PGPT) of the isolates

Traits	Endophytic bacteria				
	Ai	Aj	El	Pc	Pe
MIC Value (mg/L)			1,875		
Siderophore production	+	+	–	+	+
Phosphate solubilization	–	+	–	+	+

(+) indicates a positive result, having PGPT.
(-) indicates a negative result, lacking PGPT.

Table 2. Biosorption capacity of Pb-tolerant endophytic bacteria

Strains	Biosorption capacity	
	Pb uptake (mg/g)	Pb removal (%)
Serratia proteamaculans (Gram-negative)	4.68±0.54^{bc}	8.37±0.91^{b}
Pseudomonas sp. (Gram-negative)	3.41±1.35^{b}	6.57±1.91^{b}
Bacillus cereus (Gram-positive)	4.54±0.38^{bc}	8.36±0.70^{b}
Pseudomonas psychrophila	1.36±0.23^{a}	2.60±0.44^{a}
Pseudomonas veronii	5.35±0.61^{c}	7.61±0.74^{b}

Values are the mean±S.D. of triplicates. Mean values with a different letter within each column have a significant difference (p≤0.05), according to the LSD test.

Our study showed that endophytic bacteria (*S. proteamaculans*, *B. cereus*, and *P. veronii*) in different plants and grown in different habitats had the same biosorption capacity. This could be because they can use different mechanisms to remove Pb. Generally, bacterial cells use various mechanisms (e.g., complexation, coordination, physical adsorption, chelation, ion exchange, and precipitation) alone and/or combinations of them to remove heave metals (Abdel-Ghani and El-Chaghaby, 2014). *B. cereus* without PGPT uses its cell wall to trap Pb (physical absorption), making its cell wall an important structure playing a key role in the Pb biosorption. On bacterial cell walls, there are many components that respond to metal biosorption, depending on the type of bacteria. In Gram-positive bacteria, cell walls composed of about 90% peptidoglycan component (together with teichoic and teichuronic acids) are responsible for Pb binding. In contrast, Gram-negative bacterial cell walls contain 20% of peptidoglycan (Shamim, 2018). This property can compensate for a lack of PGPT.

S. proteamaculans and *P. veronii* use siderophores to bind with Pb in solution (chelation). Siderophores as low-molecular-mass iron chelators can form stable complexes with metals including Pb (Li et al., 2012). Microbial siderophores can solubilize large amounts of Cr and Pb in soil. This molecule reduces Pb phytotoxicity via enhancing iron uptake by plants (Shin et al., 2012). Phosphate solubilization is not a major role in Pb-biosorption since Gram-negative endophytic bacteria with and without this property showed the same Pb biosorption. Similarly, *S. proteamaculans* cannot convert insoluble inorganic tricalcium phosphate to soluble forms (Sgroy et al., 2009; Ngamau et al., 2012). Many *Pseudomonas* strains express this trait (Ahemad, 2015). However, solubilizing-phosphate bacteria can chelate Pb via secreting organic acids to solubilize it (Paul and Sinha, 2015). Moreover, many studies have shown that phosphate-solubilizing EB can enhance the bioavailability of heavy metals, leading to increased plant uptake (Jeong et al., 2012).

To utilize in a contaminated site, the strain closely related to *P. veronii* could be an appropriate choice based on high Pb-tolerance, uptake, and removal including PGPT. To survive in the harsh Pb contaminated soil, this strain, as a Gram-negative bacteria, may adsorb Pb at phosphate functional groups of lipopolysaccharide as the binding site on the cell wall (Nalik and Dubey, 2013). Moreover, *Pseudomonas* sp. uses exopolysaccharides to bind with Pb (Jarosławiecka and Piotrowska-Seget, 2014). These mechanisms can protect the cellular component of the bacterial cell. Once Pb enters the cell, this strain may precipitate Pb (Jarosławiecka and Piotrowska- Seget, 2014), and accumulate Pb via binding with metallothionein protein to protect metabolisms of bacteria (Nalik and Dubey, 2013). If the Pb concentration in a cell is high, bacteria need to release Pb from the cell. This process may use efflux system via transmembrane transporters (P-type ATPase) to keep Pb homeostasis, leading to high Pb-tolerance (Jarosławiecka and Piotrowska-Seget, 2014). The strain closely related to *P. veronii* from this study can be used to remediate Pb by bioaugmentation and phytoremediation. Normally, Pb has the lowest bioavailability in soil, making it difficult to remove (Ali et al., 2013). Using this bacterium as a bio-inoculant can increase Pb bioavailability and promote sustainable technology for removal. Alternatively, this bacterium can be used to assist a plant for phytoremediation. Generally, EB increase phytoremediative ability using various processes (e.g., promoting plant growth, reducing phytotoxicity, distributing heavy metal in plants, increasing metal bioavailability in soil, and enhancing plant uptake) (Weyens et al., 2009; Rajkumar et al., 2010; Li et al., 2012, Ma et al., 2016). There are many *Pseudomonas* sp. that were tested for Pb removal, especially *Pseudomona aeruginosa*. However, *P. aeruginosa* is a pathogen in plants, animals, and humans (Wu et al., 2015). Therefore, *P. veronii* may be a better choice for Pb removal as it is non-pathogenic bacteria (Montes et al., 2016).

4. CONCLUSION

In this study, Pb-tolerant EB was isolated from roots of Pb phytostabilizers grown in Pb-contaminated and non-contaminated soils. The highest Pb removal capacities by living biomass of isolates Ai, El, and Pe were 4.68, 4.54 and 5.35 mg/g, respectively. Considering PGPT, only isolate Pe could produce siderophore and solubilize phoshate and it was identified as the strain closely related to *P. veronii* which is a non-pathogenic bacteria. These traits in the strain closely related to *P. veronii* could be used as inoculant for assisting phytoremediation and as sorbent media for bioaugmentation of Pb contaminated soil. Moreover, to the best of our knowledge, this is the first research paper reporting that the strain closely related to *P. veronii* can remove Pb. Besides, the results suggest that Pb-tolerant EB could reside in plants growing in various habitats. The potential source of Pb-tolerant EB with PGPT could be metalliferous plants grown in specific habitat as metalliferous soil. However, the optimum conditions influencing the sorption ability and the kinetic modeling of this strain should be studied further.

ACKNOWLEDGEMENTS

This work was supported by the Royal Golden Jubilee (RGJ) Ph.D. program of the Thailand Research Fund (Grant No. PHD/0214/2556).

REFERENCES

Abdel-Ghani NT, El-Chaghaby GA. Biosorption for metal ions removal from aqueous solutions: A review of recent studies. International Journal of Latest Research in Science and Technology 2014;3(1):24-42.

Abdia O, Kazemi M. A review study of biosorption of heavy metals and comparison between different biosorbents. Journal of Materials and Environmental Science 2015;6(5):1386-99.

Afzal I, Iqrar I, Shinwari ZK, Yasmin A. Plant growth-promoting potential of endophytic bacteria isolated from roots of wild *Dodonaea viscosa* L. Plant Growth Regulation 2017;81:399-408.

Ahemad M. Phosphate-solubilizing bacteria-assisted phyto-remediation of metalliferous soils: A review. Biotechnology 2015;5:111-21.

Ali H, Khan E, Sajad MA. Phytoremediation of heavy metals-concepts and applications. Chemosphere 2013;91:869-81.

Alzubaidy SK. The resistance of locally isolated *Serratia marcescens* to heavy metals chlorides and optimization of some environmental factors. Journal of Environmental and Occupational Science 2012;1(1):37-42.

Aslam MZ, Ramzan N, Naveed S, Feroze N. Ni(II) removal by biosorption using *Ficus religiosa* (peepal) leaves. Journal of the Chilean Chemical Society 2010;55(1):81-4.

Bano A, Hussain J, Akbar A, Mehmood K, Anwar M, Hasni MS, Ullah S, Sajid S, Ali I. Biosorption of heavy metals by obligate halophilic fungi. Chemosphere 2018;199:218-22.

Bhatnagar S, Kumari R. Bioremediation: A sustainable tool for environmental management: A review. Annual Research and Review in Biology 2013;3(4):974-93.

Coelho LM, Rezende HC, Coelho LM, de Sousa PAR, Melo DFO, Coelho NMM. Bioremediation of polluted waters using microorganisms [Internet]. 2015 [cited 2019 Sep 13]. Available from: https://www.intechopen.com/books/advances-in-bioremediation-of-wastewater-and-polluted-soil/bioremediation-of-polluted-waters-using-microorganisms.

El Aafi N, Brhada F, Dary M, Maltouf AF, Pajuelo E. Rhizostabilization of metals in soils using *Lupinus luteus* inoculated with the metal resistant rhizobacterium *Serratia* sp. MSMC541. International Journal of Phytoremediation 2012;14(3):261-74.

Fan M, Liu Z, Nan L, Wang E, Chen W, Lin Y, Wei G. Isolation, characterization, and selection of heavy metal-resistant and plant growth-promoting endophytic bacteria from root nodules of *Robinia pseudoacacia* in a Pb/Zn mining area. Microbiological Research 2018;217:51-9.

Felsenstein J. Confidence limits on phylogenies: An approach using the bootstrap. Evolution 1985;39:783-91.

Francesconi K, Visoottiviseth P, Sridokchan W, Goessler W. Arsenic species in an arsenic hyperaccumulating fern, *Pityrogramma calomelanos*: A potential phytoremediator of arsenic-contaminated soils. Science of the Total Environment 2002;284:27-35.

Gillani RA, Shenaz N, Matloob S, Haq F, Ngah WSW, Nasim W, Munis MFH, Rehman A, Chaudhary HJ. Biosorption of Cr(III) and Pb(II) by endophytic *Agrobacterium tumefaciens* 12b3: Equilibrium and kinetic studies. Desalination and Water Treatment 2017;67:206-14.

Govarthanan M, Mythili R, Selvankumar T, Kamala-Kannan S, Rajasekar A, Chang Y-C. Bioremediation of heavy metals using an endophytic bacterium *Paenibacillus* sp. RM isolated from the roots of *Tridax procumbens*. 3 Biotech 2016;6:242.

Gupta A, Joia J, Sood A, Sood R, Sidhu C, Kaur G. Microbes as potential tool for remediation of heavy metals: A review. Journal of Microbial and Biochemical Technology 2016;8(4):364-72.

Jarosławiecka A, Piotrowska-Seget Z. Lead resistance in microorganisms. Microbiology 2014;160:12-25.

Jeong S, Moon HS, Nama K, Kim JY, Kim TS. Application of phosphate-solubilizing bacteria for enhancing bioavailability and phytoextraction of cadmium (Cd) from polluted soil. Chemosphere 2012;88:204-10.

Kimura M. A simple method for estimating evolutionary rate of base substitutions through comparative studies of nucleotide sequences. Journal of Molecular Evolution 1980;16:111-20.

Kumar S, Stecher G, Tamura K. MEGA7: Molecular evolutionary genetics analysis version 7.0 for bigger datasets. Molecular Biology and Evolution 2016;33:1870-4.

Kumar P, Fulekar MH. Rhizosphere bioremediation of heavy metals (Copper and Lead) by *Cenchrus ciliaris*. Research Journal of Environmental Sciences 2018;12(4):166-76.

Li H-Y, Wei D-Q, Shen M, Zhou Z-P. Endophytes and their role in phytoremediation. Fungal Diversity 2012;54:11-8.

Liotti RG, da Silva Figueiredoa MI, da Silvac GF, de Mendonçad EAF, Soaresa MA. Diversity of cultivable bacterial endophytes in *Paullinia cupana* and their potential for plant growth promotion and phytopathogen control. Microbiological Research 2018;207:8-18.

Lodewyckx C, Vangronsveld J, Porteous F, Moore ERB, Taghavi S, Mezgeay M, der Lelie DV. Endophytic bacteria and their potential applications. Critical Reviews in Plant Sciences 2002;21:583-606.

Luo SL, Chen L, Chen JL, Xiao X, Xu TY, Wan Y, Rao C, Liu CB. Analysis and characterization of cultivable heavy metal-resistant bacterial endophytes isolated from Cd-hyperaccumulator *Solanum nigrum* L. and their potential use for phytoremediation. Chemosphere 2011;85(7):1130-8.

Ma Y, Rajkumar M, Zhang C, Freitas H. Beneficial role of bacterial endophytes in heavy metal phytoremediation. Journal of Environmental Management 2016;174:14-25.

Meeinkuirt W, Pokethitiyook P, Kruatrachue M, Tanhan P, Chaiyarat R. Phytostabilization of a Pb-contaminated mine tailing by various tree species in pot and field trial experiments. International Journal of Phytoremediation 2012;14:925-38.

Montes C, Altimira F, Canchignia H, Castro Á, Sánchez E, Miccono M, et al. A draft genome sequence of *Pseudomonas veronii* R4: A grapevine (*Vitis vinifera* L.) root-associated strain with high biocontrol potential. Standards in Genomic Sciences 2016;11:76.

Nalik MM, Dubey SK. Lead resistant bacteria: Lead resistance mechanisms, their applications in lead bioremediation and biomonitoring. Ecotoxicology and Environmental Safety 2013;98:1-7.

Ngamau CN, Matiru VN, Tani A, Muthuri CW. Isolation and identification of endophytic bacteria of bananas (*Musa* spp.) in Kenya and their potential as biofertilizers for sustainable banana production. African Journal of Microbiology Research 2012;6(34):6414-22.

Paul D, Sinha SN. Isolation and characterization of a phosphate solubilizing heavy metal tolerant bacterium from River Ganga, West Bengal, India. Songklanakarin Journal of Science and Technology 2015;37(6):651-7.

Rajkumar M, Ae N, Prasad MNV, Freitas H. Potential of siderophore-producing bacteria for improving heavy metal phytoextraction. Trends in Biotechnology 2010;28(3):142-9.

Saitou N, Nei M. The neighbor-joining method: A new method for reconstructing phylogenetic trees. Molecular Biology and Evolution 1987;4:406-25.

Sgroy V, Cassán F, Masciarelli O, del Papa FM, Lagares A, Luna V. Isolation and characterization of endophytic plant growth-promoting (PGPB) or stress homeostasis-regulating (PSHB) bacteria associated to the halophyte *Prosopis strombulifera*. Applied Microbiology and Biotechnology 2009;85(2):371-81.

Shamim S. Biosorption of heavy metals [Internet]. 2018 [cited 2019 Sep 13]. Available from: https://www.intechopen.com/books/biosorption/biosorption-of-heavy-metals.

Sharma P, Dubey RS. Pb toxicity in plants. Brazilian Journal of Plant Physiology 2005;17:35-52.

Shin MN, Shim J, You Y, Myung H, Bang KS, Cho M, et al. Characterization of lead resistant endophytic *Bacillus sp*. MN3-4 and its potential for promoting lead accumulation in metal hyperaccumulator *Alnus firma*. Journal of Hazardous Materials 2012;199-200:314-20.

Soongsombat P, Kruatrachue M, Chaiyarat R, Pokethitiyook P, Ngernsansaruay C. Lead tolerance and accumulation in *Pteris vittata* and *Pityrogramma calomelanos*, and their potential for phytoremediation of lead-contaminated soil. International Journal of Phytoremediation 2009;11(4):396-412.

Tseveendorj E, Enkhdul T, Lin S, Dorj D, Oyungerel SH, Soyol-Erdene TO. Biosorption of lead (II) from an aqueous solution using biosorbents prepared from water plants. Mongolian Journal of Chemistry 2017;18(44):52-61.

Yongpisanphop J, Babel S, Kruatrachue M, Pokethitiyook P. Phytoremediation potential of plants growing on the Pb-contaminated soil at the Song Tho Pb Mine, Thailand. Soil Sediment Contamination: An International Journal 2017; 26(4):426-37.

Yongpisanphop J, Babel S, Kurisu F, Kruatrachue M, Pokethitiyook P. Isolation and characterization of Pb-resistant plant growth promoting endophytic bacteria and their role in Pb accumulation by fast-growing trees. Environmental Technology 2019;e1615933.

Weyens N, van der Lelie D, Taghavi S, Vangronsveld J. Phytoremediation: plant-endophyte partnerships take the challenge. Current Opinion in Biotechnology 2009;20:248-54.

Wierzba S, Latala A. Biosorption lead(II) and nickel(II) from an aqueous solution by bacterial biomass. Polish Journal of Chemical Technology 2010;12(3):72-8.

Wu W, Jin Y, Bai F, Jin S. *Pseudomonas aeruginosa*. In: Tang Y-W, Sussman M, Liu D, Poxton I, Schwartzman J, editors. Molecular Medical Microbiology. 2nd ed. USA: Academic Press; 2015.

Zhu L-J, Guan D-X, Luo J, Rathinasabapathi B, Ma LQ. Characterization of arsenic-resistant endophytic bacteria from hyperaccumulators *Pteris vittata* and *Pteris multifida*. Chemosphere 2014;113:9-16.

Spatial Relationship of Drug Smuggling in Northern Thailand Using GIS-based Knowledge Discovery

Sumethat Niamkaeo and Ornprapa Robert*

Department of Environmental Science, Faculty of Science, Silpakorn University, Nakornpathom 73000, Thailand

ARTICLE INFO

Received: 30 Aug 2019
Received in revised: 6 Mar 2020
Accepted: 23 Mar 2020
Published online: 20 Apr 2020
DOI: 10.32526/ennrj.18.3.2020.26

Keywords:
Drug smuggling/ GIS knowledge discovery/ Spatial relationship/ Decision tree/ Prediction

*** Corresponding author:**
E-mail: robert_o@silpakorn.edu

ABSTRACT

The number of drug users has been growing, likely caused by oppressive social conditions. The drug situation in Thailand has changed so that it is no longer a production source. However, Thailand is one of the transit sites for narcotics smuggling. Drug smuggling occurs most recurrently along the border of Northern Thailand by topographic roads. Chiang Mai and Chiang Rai Provinces have been shown to have the highest statistics in terms of drug trafficking. In this investigation, eight districts adjacent to neighboring countries were chosen as the areas of study. These areas are Mae Chan, Mae Fa Luang, and Mae Sai located in Chiang Rai Province, as well as Fang, Chiang Dao, Mae Ai, Chai Prakan, and Wiang Haeng situated in Chiang Mai Province. This research studied the spatial relationship of factors related to narcotic smuggling using a data mining-based decision tree technique. The geographic locations of drug trafficking arrests were transferred into a data-mining process in order to assess the spatial relationships among types of exhibited drugs, season, land use, distance from checkpoint and smuggling routes. Drug smuggling risk areas were further predicted using decision tree modeling. The results revealed that the geographic locations of drug trafficking arrests in Mae Chan, Mae Sai, Mae Ai, and Fang Districts were related to the season factor. The distance from checkpoint showed a spatial relationship with drug smuggling arrests in the Chai Prakan District. Narcotic trafficking arrests in Mae Fa Luang were mostly related to land use and type of drug exhibited. Geo-locations of drug smuggling illustrated an independent relationship with smuggling routes. The results retrieved from the prediction-based decision tree method indicated that Chai Prakan, Mae Chan, Mae Sai, Mae Fa Luang, Mae Ai, Fang, Wiang Haeng and Chiang Dao Districts were high-risk drug smuggling areas. The precision value of prediction was found to be 0.652. These results could support spatial decision making for national drug smuggling monitoring and surveillance.

1. INTRODUCTION

According to the United Nations Office on Drug and Crime (UNODC, 2018), there were 275 million drug users worldwide in 2016, a number expected to reach 346 million drug users in 2019. It was observed that the demand of drug users was enhanced, which affected the increasing amount of drug suppliers. Narcotics production also showed an impact on the environment. The cultivation of substances used in production causes deforestation as well as ecological changes (UNODC, 1995). The study of Medel et al. (2015) examined marijuana and opium smuggling in Mexico. Physical, socio-demographic, and drug violence factors were considered and included in smuggling cost estimation using the cost surface principle to predict the trafficking routes for marijuana and opium. Robert et al. (2018) applied the Analytic Hierarchy Process to determine the importance of drug smuggling factors including physical, narcotic and social demographic aspects prior to performing potential surface analysis. The results showed spatial risk areas for drug smuggling in northern Thailand. Ours and Williams (2012) studied the physical and health impact of

Citation: Niamkaeo S, Robert O. Spatial relationship of drug smuggling in northern Thailand using GIS-based knowledge discovery. Environ. Nat. Resour. J. 2020;18(3):275-282. DOI: 10.32526/ennrj.18.3.2020.26

cannabis use. They explained that cannabis use reduced the mental and physical well-being of men and women. The number of drug addicts in Thailand has increased, with approximately two million users discovered (ONCB, 2017). The ONCB (2017) also reported that drug smuggling was found mainly along the border of northern Thailand, originating from the 'Golden Triangle', which includes Mae Chan, Mae Fa Luang, and Mae Sai Districts in Chiang Rai Province, as well as Fang, Chiang Dao, Mae Ai, Chai Prakan, and Wiang Haeng Districts in Chiang Mai Province. In this research, the study areas covered these districts.

Knowledge Discovery from Database (KDD) is a multi-step process involving data warehousing, pattern searching or data mining, knowledge evaluation, and refinement with repetition after modification in order to extract useful information or knowledge retrieved from a collection of data or a set of factors (Fayyad et al., 1996; Harvey and Jiawei, 2009). KDD was used to study the relationship between suicide and temperature change in Mexico (Fernández-Arteaga et al., 2016). Warehousing of suicide using hanging means from 2005 to 2012 was prepared in order to investigate association rules-based data mining. The results illustrated that the highest number of suicides among Mexican men was found mainly on dry days from 30 ºC to 40 ºC. KDD was also applied to study airline passenger management in Taiwan (Wong and Chung, 2007). In this paper, we to applied Geographic Information System (GIS) KDD to discover the spatial relationship of factors related to drug smuggling in northern Thailand. This approach made it different from the study of Fernández-Arteaga et al. (2016). GIS KDD could provide data concerning the geo-specific relationship in knowledge or a set of factors. Moreover, the importance of drug smuggling factors was excluded, which was different from the study of Robert et al. (2018). To the extent of our knowledge, GIS KDD has not previously been applied in drug trafficking investigation.

As mentioned earlier, data mining is one of the GIS KDD multi-step processes. The data mining technique is a process used to analyze key data, identify data relationships, and eventually predict the probability of an expected incident. Data mining is divided into two methods, including unsupervised and supervised learning techniques (Hand et al., 2001). The unsupervised technique comprises clustering and association rule. Thomas et al. (2018) applied clustering means to monitor the chemical process in the Eastman chemical industry. Clustering means could be also applied in environmental study, as seen in the study of Ge et al. (2019), who used clustering in an unsupervised learning technique to extract soil structure information. Calçada et al. (2019) studied the relationship of parameters in fertilizer using the association rule to discover the appropriate parameters of decomposition. Xu et al. (2018) employed the association rule to investigate the relationship for factors affecting traffic congestion. On the other hand, the supervised learning technique in data mining is composed of two methods, which are regression and classification. Data mining-based regression is often applied in environmental studies. Oliveira et al. (2017) predicted sea mussel populations using the data mining-based regression method. Weather conditions, phytotoxin episodes, stock-biomass indicators per species, tourism levels, and surveyed mussel populations were considered in multiple linear regressions. The second method for the supervised learning technique is classification. Kesavaraj and Sukumaran (2013) explained that the supervised learning-based classification technique is a method used to categorize data (a set of factors) for discovering data relationships and prediction. The supervised learning-based classification technique is comprised of Bayesian network, decision tree, K-nearest neighbor (KNN), and neural network algorithms. These classification means are referred to as the prediction technique. Nguyen et al. (2017) used the KNN data mining technique to predict the volume and water retention in soil. Peter et al. (2018) applied the supervised learning-based classification technique in an epidemiology study. Bayesian network was applied to predict the risk areas for malaria in northern Thailand. Zhao et al. (2016) used the decision tree method to explain the relationship in the change of underground water level, rainfall and reservoir level as well as predict landslides in Shaxi city, China. In this study, the aim was to discover the relationship of factors related to drug smuggling in northern Thailand using the data mining-based decision tree method, as well as to predict the geographical risk areas for drug smuggling using the classification-based decision tree technique.

2. METHODOLOGY

The methodology of GIS KDD for investigating the spatial relationship of drug smuggling factors and predicting drug smuggling risk areas comprises three sections, which are (2.1) the collection and manipulation of drug trafficking arrest data, (2.2) finding the spatial relationship for factors related to drug smuggling-based data mining, and (2.3) the prediction of drug smuggling risk areas. The conceptual framework of the study is illustrated in Figure 1 and explained below.

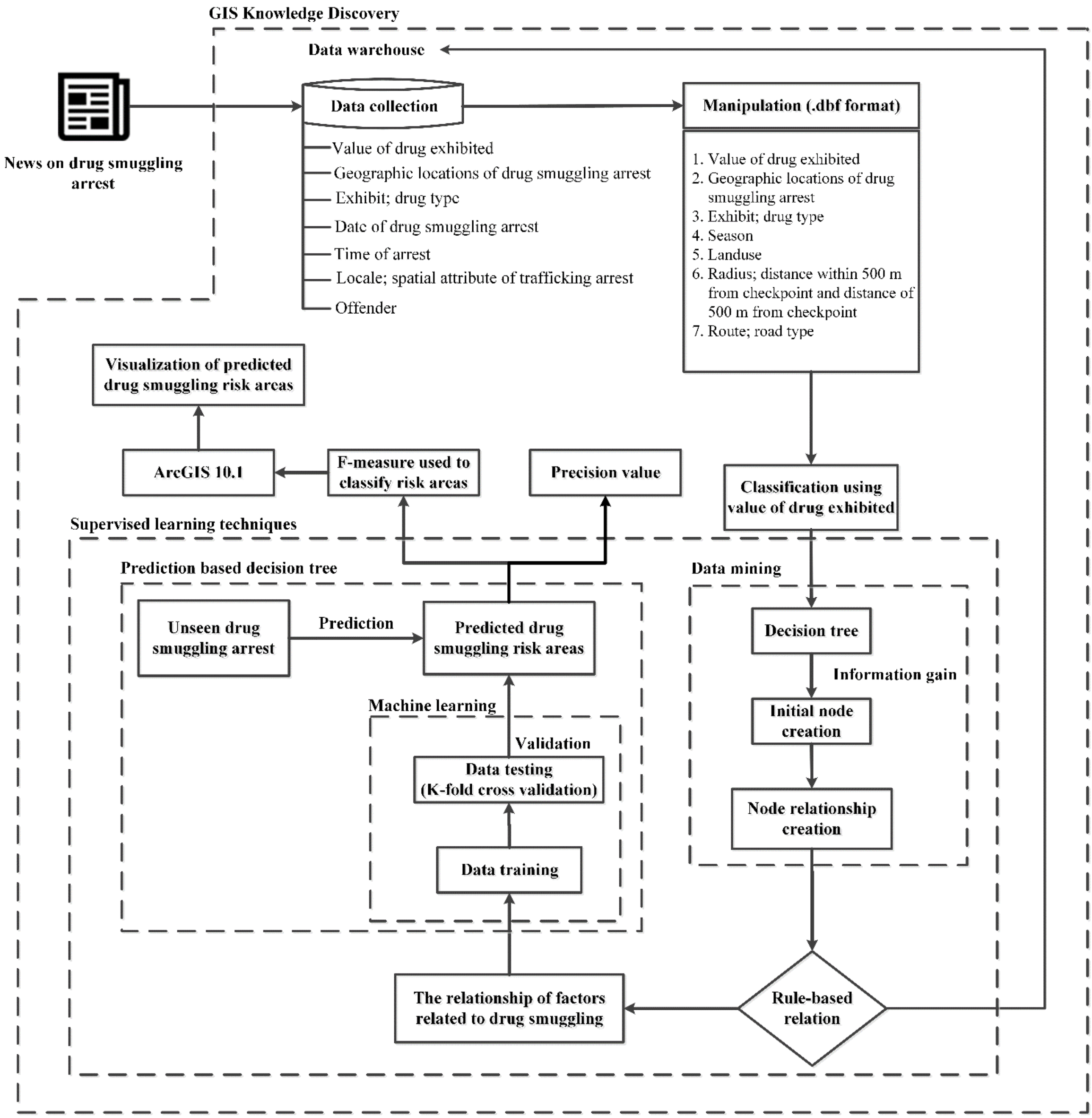

Figure 1. The conceptual framework of the study

2.1 Collection and manipulation of drug trafficking arrest data

Table 1 displays an example of the narcotic trafficking arrest data transformed into a database file (.dbf format) containing X and Y, composed of geographic locations for drug smuggling arrest based datum WGS 1984 Universal Transverse Mercator, date of drug smuggling arrest, time of arrest, Locale; spatial attribute of trafficking arrest, offender, exhibit; drug type and value of drug exhibited in United Stated Dollar (USD). The collected data shown in Table 1 was manipulated and transformed into seven factors prior to transfer into the data mining process. This data manipulation can be elaborated as follows: (1) Value of drug exhibited factor was categorized into five ranges including 0.033 USD to 33,000 USD, 33,001 USD to 330,000 USD, 330,001 USD to 3,300,000 USD, 3,300,001 USD to 33,000,000 USD and above 33,000,000 USD; (2) Location factor (L1-L5) referred to the spatial sites for drug smuggling arrests, which were divided by five district boundaries including Mae Chan and Mae Sai District (L1), Chiang Dao and Wiang Haeng District (L2), Chai Prakan District (L3), Mae Ai and Fang District (L4), and Mae Fa Luang District (L5); (3) Exhibit factor referred to different smuggled drug types, which comprised Amphetamine or Ya-Ba (D1), Crystalline methamphetamine or ICE (D2), *Papaver somniferum* L. (D3), *Mitragyna speciosa* K. (D4), Heroine (D5), Substances (D6), and Exhibit more than one type (D7); (4) Season factor was categorized into three seasons including summer (Feb-May), rainy (Jun-Oct) and winter (Nov-Jan); (5) Land use data was retrieved from the Thailand Land Department and classified into 5 categories including agriculture (A), residence (R), forest (F), water (W) and miscellaneous (M); (6) Radius factor means the distance within 500 meters from checkpoint (T) and the distance more than 500 meters from checkpoint (F), where drug smuggling occurred, and (7) Route factor referred to the road type where drug smuggling occurred. Route characteristics were divided into main or highway (M), sub-route (S) and topographic types (T). The seven factors mentioned above were transferred into the data mining process to discover the spatial relationships among them.

Table 1. Collected data for narcotics trafficking arrests

Value of drug smuggling exhibited	X	Y	Exhibit	Date of arrest	Time	Locale	Offender
500,000	510238.00	2186339.00	20,000 tablets of Amphetamine	02052011	12.00	Lychee garden[1]	Name A Age 36
52,008	514246.00	2172072.00	1,970 tablets of Amphetamine	25082011	13.00	Phahong checkpoint[2]	Name B Age 23
37,880	592503.00	2253528.00	3.5 kg of Heroine	20022011	13.00	Sub-route[3]	Name C Age 30

[1]Located in Mae Ngon sub-district, Fang District, Chiang Mai; [2]Located in Sridongyen sub-district, Chai Prakan District, Chiang Mai; [3]Located in Pong Pha sub-district, Mae Sai District, Chiang Rai

2.2 Finding the spatial relationship in factors related to drug smuggling-based data mining

Data mining using decision tree-based classification is one of the supervised learning techniques. It is implemented to find out the spatial relationship in factors related to drug smuggling. Data mining using decision tree-based classification comprises two steps, which are node creation and ruling spatial relationship of mined data or factors transferred from step 2.1. In the node creation process, factors are transformed into nodes prior to investigation of the spatial relationship. Data training with information gain is employed to specify the initial node describing the most important factors and the non-initial nodes of the study. In the second step of data mining, the designated initial node was investigated for spatial relationship associated with the remaining nodes or factors. In this research, Rapid miner data mining software (Kotu and Deshpande, 2015) was applied. Drug trafficking data was discrete. Hence, the C4.5 principle was used in this investigation. The results of the spatial relationship in factors related to drug smuggling are illustrated as a hierarchy or decision tree structure (Figure 3).

2.3 Prediction of drug smuggling risk areas

The spatial relationship of factors related to drug smuggling retrieved from a previous step was transferred into prediction modeling based on the decision tree approach to reveal the geographic risk areas for drug smuggling. The prediction approach comprised three steps including (1) machine learning for training data related to spatial relationship in drug smuggling, (2) data testing-based K-fold cross validation, and (3) the prediction of drug smuggling risk areas. Firstly, machine learning was applied to investigate the accuracy of spatial relationship for factors related to drug smuggling. Secondly, the data related to spatial relationship of drug smuggling was divided into four categories using K-fold cross validation. One quarter of the data was tested with the remaining data to study the accuracy of data training. Thirdly, unseen drug smuggling arrest data in 2018 was used to validate the predicted drug smuggling risk areas. The prediction value explains the accuracy of predicted drug smuggling areas, which is between 0.0 and 1.0. A precision value close to 1.0 shows higher accuracy. GIS classification technique in ArcGIS 10.1 software was applied to prepare the drug smuggling risk map. Drug smuggling risk was classified into 4 classes using the F-measure value retrieved from validation analysis as a classifier (Figure 4).

3. RESULTS AND DISCUSSION

3.1 Drug smuggling data warehouse

A drug smuggling data warehouse was prepared by capturing news of drug smuggling arrests in northern Thailand. There were 564 news articles collected related to drug smuggling arrests from 2011 to 2017. These articles were manipulated and transformed into GIS format, as seen in Figure 2. It shows the geographic locations of drug smuggling arrests in northern Thailand overlaid with land use, route, checkpoints, and distance from checkpoints layers. The study area covers eight districts of Chiang Mai and Chiang Rai Provinces. The population of these two provinces is approximately 505,403 people (The Bureau of Registration Administration, 2019). The majority of the local population is related to agriculture. This area is a central point connecting to neighboring countries, and the pathway for the Belt and Road Initiative. Hence, this area attracts international investors. The spatial attribute of drug smuggling arrests in the study area was also included in order to investigate the geo-spatial relationship of factors related to narcotics smuggling. Prior to delivering these factors into the Rapid miner data mining software, determining the factors or nodes was carried out. There were seven nodes, as explained in section 2.1. The factor of drug value exhibited was designated to use in the data classification process prior to implementing data mining, as shown in the results in section 3.2.

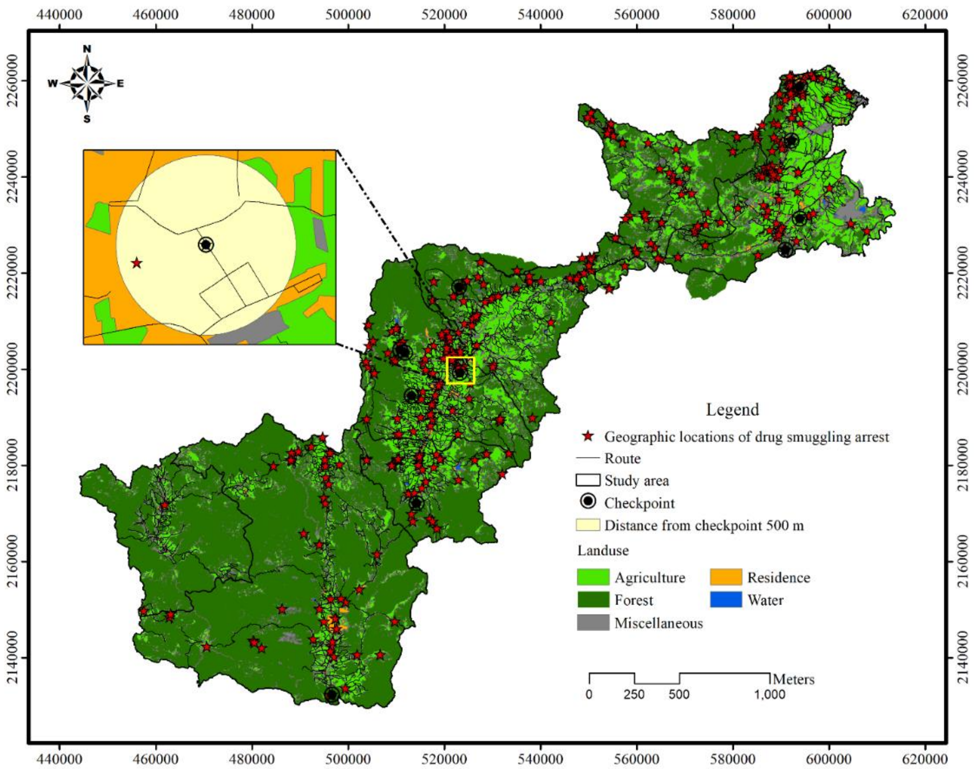

Figure 2. Geographic locations of drug smuggling arrests in northern Thailand

3.2 Spatial relationship of drug smuggling factors

From node creation using data training method, the information gain for factors including geographic location of drug smuggling arrest, type of exhibited drug, land use, season, distance from checkpoint and smuggling route was studied. The information gain for the factors was found to be 0.518, 0.348, 0.194, 0.179, 0.135, and 0.060, respectively. The most influential factor to be specified as an initial node was the geographic locations (L1-L5) of drug smuggling arrests, as shown in Figure 3. It can be further explained that the narcotics smuggling incidents found in Mae Chan and Mae Sai Districts (L1) and Mae Ai and Fang Districts (L4) were related to seasons. The peak season for illegal drug trafficking-based value of drug exhibited (in 330,001-33,000,000 USD range) was discovered in the rainy season. The amount of trafficked drugs per time in the rainy season was generally higher than the quantity of smuggled drugs per time that occurred in the summer and winter. This was to minimize the risk of damage to drugs while smuggling. Drug trafficking incidents in Chiang Dao and Wiang Haeng Districts (L2) displayed the highest value of drug exhibited (More than 33,000,000 USD) and no spatial relationship with other factors. The drug trafficking information in Chiang Dao and Wiang Haeng District was unclassified during relationship creation, showing less of a relationship in drug trafficking information. This was because the entropy of drug trafficking information in Chiang Dao and Wiang Haeng Districts was too high. Regarding the factor of radius from checkpoint, the results illustrated that the distance within 500 meters from checkpoint (T) and the distance more than 500 meters from checkpoint (F) explained the spatial relationship in Chai Prakan District (L3). The comparison between the drug value exhibited within 500 meters from a checkpoint and the distance of 500 meters from a checkpoint described that the value of drugs exhibited within the distance 500 meters from a checkpoint was less than the drugs exhibited from the distance more than 500 meters from a checkpoint. Smugglers aimed to be less suspicious while passing a checkpoint. Narcotics trafficking incidents in Mae Fa Luang District (L5) were related spatially to land use and drug type. The value of drugs exhibited in 0.033-330,000 USD range was shown in the residential area of Mae Fa Luang District. In the agricultural area of this district, the higher value of drugs exhibited was displayed as 3,300,001-33,000,000 USD and the most prevalent drug type for those arrested was heroine. In accordance with the news for illegal drug trafficking arrests in Mae Fah Luang District, the percentage of amphetamine and heroin smuggling in agricultural area was found at 55 and 31, respectively. While heroin trafficking illustrated a lower percentage of arrest information than amphetamine smuggling, the cost of heroin production and exhibited values were higher than for amphetamine. Additionally, the factor of smuggling route was shown to have an independent relationship with other factors. According to the study of Medel et al. (2015), the transportation type could reduce the cost of drug trafficking. In this investigation, it was found that drug smuggling incidents occurred at sub-routes and topographic routes at percentages of 85 and 15, respectively. This was because the drug trafficking data displayed in public news was related to an intercepting and blockade search strategy.

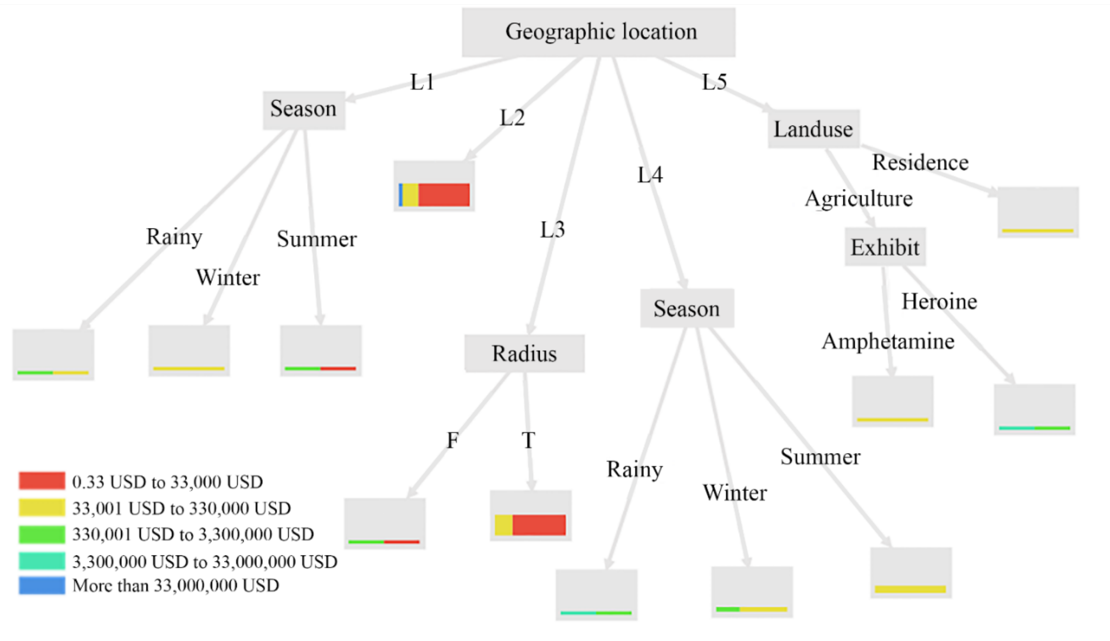

Note: L1 = Mae Chan and Mae Sai district; L2 = Chiang Dao and Wiang Haeng district; L3 = Chai Prakan district; L4 = Mae Ai and Fang district; L5 = Mae Fa Luang district; F = the distance of 500 meter from checkpoint; T = the distance within 500 meters from checkpoint

Figure 3. The decision tree structure of spatial relationship for drug smuggling factors

3.3 Predicted drug smuggling risk areas

The results of the narcotics smuggling prediction-based decision tree approach are as follows. The machine learning technique presented the accuracy of spatial relationship for factors related to drug smuggling at a percentage of 63.5. K-fold cross validation was applied to test the data used in the machine learning process and explained the validation accuracy at a percentage of 57.1. Increasing the amount of data transferred into the prediction approach is possible to enhance the validation accuracy. The predicted geographic risk of drug smuggling was classified into high, medium, low and very low risk level, as illustrated in Figure 4. The drug smuggling risk area for each level was Chai Prakan (F-measure at 0.676), Mae Chan, Mae Sai (F-measure at 0.412), Mae Fa Luang (F-measure at 0.222), Mae Ai, Fang, Chiang Dao, and Wiang Haeng District (F-measure at 0.000). The precision value of prediction was discovered at 0.652, describing moderate accuracy for predicted drug smuggling areas. In order to improve the accuracy, other factors should be considered including drug production site, transit site, and ambush and blockade location. These factors are not publicly available due to data confidentiality issues; hence, it is a limitation of this study.

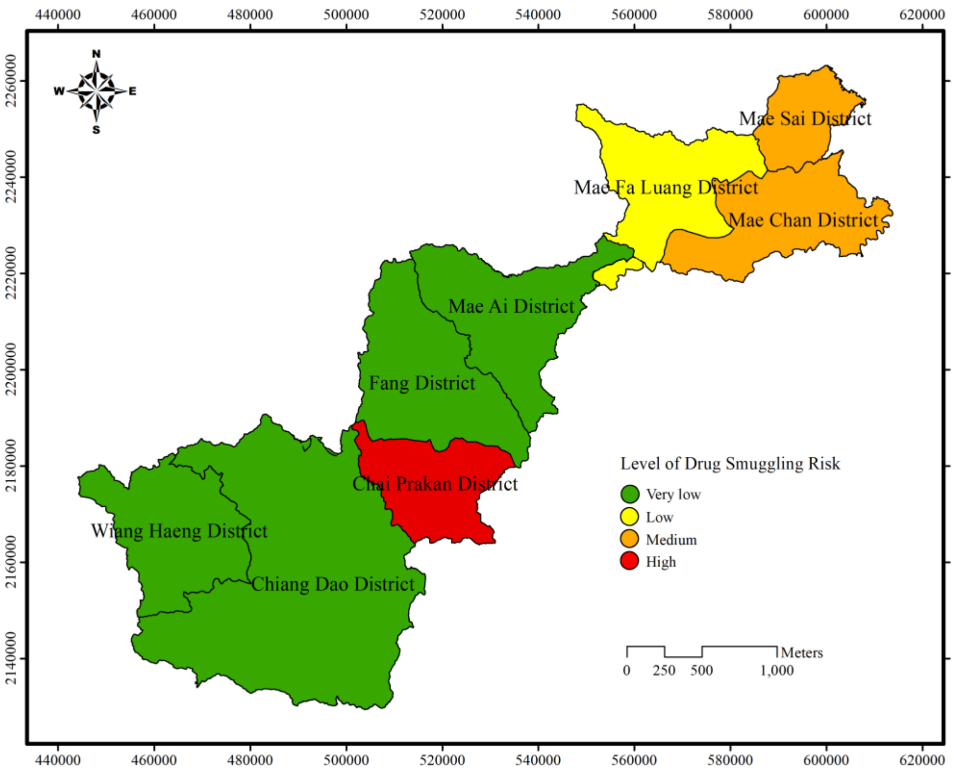

Figure 4. Predicted Drug Smuggling Risk Areas

4. CONCLUSION

To the best of our knowledge, we demonstrated that the GIS KDD method was able to search for patterns and extract key information related to drug smuggling. Data mining-based decision tree made it possible to identify spatial relationships for narcotic smuggling in northern Thailand. The results of spatial relationship for narcotic smuggling are illustrated in graphic format. This approach is less complex and easier to manage since the amount of data is limited. Drug smuggling risk areas were predicted by using a supervised learning-based decision tree classification technique. The precision value for predicted drug risk areas was discovered at 0.652, which was moderately acceptable. The precision of prediction relies on the entropy of data as well as the amount of input data or factors.

ACKNOWLEDGEMENTS

This research was partially supported by the Department of Environmental Science, Faculty of Science, Silpakorn University, Thailand and the geo-database project for military and defense. The authors would like to thank the Office of the Narcotics Control

Board for its assistance and comments, which greatly improved the manuscript.

REFERENCES

Calçada DB, Rezende SO, Teodoro MS. Analysis of green manure decomposition parameters in northeast Brazil using association rule networks. Computers and Electronics in Agriculture 2019;159:34-41.

Fayyad U, Piatetsky-Shapiro G, Smyth P. From data mining to knowledge discovery: An overview. In: Fayyad U, Piatetsky-Shapiro G, Smyth P, Ulthurusamy R, editors. Advances in Knowledge Discovery and Data Mining. Cambridge, United States: MIT Press; 1996. p. 1-34.

Fernández-Arteaga V, Tovilla-Zárate CA, Fresán A, González-Castro TB, Juárez-Rojop IE, López-Narváez L. Association between completed suicide and environmental temperature in a Mexican population, using the Knowledge Discovery in Database approach. Computer Methods and Programs in Biomedicine 2016;135:219-24.

Ge Q, Xiong F, Xie L, Chen J, Yu M. Dynamic interaction of soil-structure cluster. Soil Dynamics and Earthquake Engineering 2019;123:16-30.

Hand D, Mannila H, Smyth P. Principles of Data Mining. Cambridge, United States: MIT Press; 2001.

Harvey JM, Jiawei H. Geographic Data Mining and Knowledge Discovery. Boca Raton, United States: Taylor and Francis Group; 2009.

Kesavaraj G, Sukumaran S. A study on classification techniques in data mining. Proceedings of the Fourth International Conference on Computing, Communications and Networking Technologies (ICCCNT); 2013 Jul 4-6; Tiruchengode: India; 2013.

Kotu V, Deshpande B. Predictive Analytics and Data Mining: Concepts and Practice with Rapidminer. Waltham, United States: Elsevier; 2015.

Medel M, Lu Y, Chow E. Mexico's drug networks: Modeling the smuggling routes towards the United States. Applied Geography 2015;60:240-7.

Nguyen PM, Haghverdi A, Pue J, Botula YD, Le KV, Waegeman W. Comparison of statistical regression and data-mining techniques in estimating soil water retention of tropical delta soils. Biosystems Engineering 2017;153:12-27.

Office of the Narcotics Control Board. Drug situation in the northern region January 2017 [Internet]. 2017 [cited 2018 Aug 6]. Available from: https://www.oncb.go.th.

Oliveira MM, Camanho AS, Walden JB, Miguéis VL, Ferreira NB, Gaspar MB. Forecasting bivalve landings with multiple regression and data mining techniques: The case of the Portuguese artisanal dredge fleet. Marine Policy 2017;84:110-8.

Ours JV, Williams J. The effects of cannabis use on physical and mental health. Journal of Health Economics 2012;31:564-77.

Peter H, Hasan I, Kasantikul R, Lawpoolsri S, Sa-angchai P, Kaewkungwal J. Spatiotemporal bayesian networks for malaria prediction. Journal of Artificial Intelligence in Medicine 2018;84:127-38.

Robert O, Kumsap C, Janpengpen A. Simulation of counter drugs operations based on geospatial technology for use in a military training simulator. International Journal of Simulation and Process Modeling 2018;13:402-15.

The Bureau of Registration Administration. Official statistics registration systems [Internet]. 2019 [cited 2020 Feb 26]. Available from: http://stat.bora.dopa.go.th.

Thomas MC, Zhu W, Romagnoli JA. Data mining and clustering in chemical process databases for monitoring and knowledge discovery. Journal of Process Control 2018;67:160-75.

United Nations Office on Drugs and Crime. World drug report 2018 [Internet]. 2018 [cited 2019 Jun 16]. Available from: https://www.unodc.org/wdr2018.

United Nations Office on Drugs and Crime. The social impact of drug abuse [Internet]. 1995 [cited 2019 Oct 13]. Available from: https://www.unodc.org/pdf/technical_series_1995-03-01_1.pdf.

Wong JY, Chung PH. Managing valuable Taiwanese airline passengers using knowledge discovery in database techniques. Journal of Air Transport Management 2007;13:362-70.

Xu C, Bao J, Wang C, Liu P. Association rule analysis of factors contributing to extraordinarily severe traffic crashes in China. Journal of Safety Research 2018;67:65-75.

Zhao Y, Li Y, Zhang L, Wang Q. Groundwater level prediction of landslide based on classification and regression tree. Geodesy and Geodynamics 2016;7:348-55.

Preparation and Characterization of Biochar from Rice Straw and Its Application in Soil Remediation

Adel S. El-Hassanin[1], Magdy R. Samak[1], Soliman R. Radwan[2], and Ghadir A. El-Chaghaby[2*]

[1]*Department of Natural Resources, Faculty of African Postgraduate Studies, Cairo University, Egypt*
[2]*Regional Center for Food and Feed, Agricultural Research Center, Giza, Egypt*

ARTICLE INFO

Received: 24 Jan 2020
Received in revised: 17 Apr 2020
Accepted: 1 May 2020
Published online: 26 May 2020
DOI: 10.32526/ennrj.18.3.2020.27

Keywords:
Biochar/ Cadmium/ Heavy metals/ Lead/ Rice straw/ Soil

*** Corresponding author:**
E-mail: ghadiraly@yahoo.com

ABSTRACT

In many developing countries, there is a large quantity of agricultural wastes that cause severe pollution problems. Also, the agricultural soils are polluted with heavy metals and there is a need to find an environmentally friendly approach for both getting rid of agro-wastes and helping in having more available soil for agriculture. In the present study, rice straw was used for the production of biochar for application in soil remediation. The biochar prepared by rice straw pyrolysis at 450 °C was characterized by different tools such as X-ray diffraction, Fourier-transformation infrared and scanning electron microscopy. The characterization results indicated that rice straw biochar (RSB) has amorphous porous structure with several functional groups and mainly composed of silicates. RSB was then investigated as soil remediating material for a silty clay soil. In this context, a synthetic polluted soil was prepared to contain 10 and 500 mg/kg of cadmium and lead, respectively. Rice straw biochar (RSB) was applied to the soil at the following (w/w) rates: 0% (control), 1.25% (T1), 2.50% (T2), 5.00% (T3) and 10.00% (T4). After 30 days of incubation, the soil samples were analyzed. The results showed that biochar addition resulted in a significant increase in soil pH, EC, CEC, total organic matter, total carbon and moisture. Application of biochar slightly increased the available N, P and K. The concentrations of plant available Pb and Cd in all biochar treatments were significantly lower than those of the control treatment. It can be concluded that biochar prepared from agricultural wastes is of both economic and environmental interest, especially in developing countries. Rice straw biochar could be further explored for remediating other types of soil pollutants with continuous monitoring of soil properties.

1. INTRODUCTION

Agricultural wastes represent a major environmental problem and re-using these wastes by turning them into valuable materials is an increasing challenge. About 25% of crop straws are burned during harvest season to remove crop residues, which is detrimental to air quality and human health (Xu et al., 2016). Rice straw is a major agricultural residue, accounting for 731 million Tons annually in the world (Park et al., 2014). In Egypt, processing of rice in the river Nile Delta yields large amounts of rice straw as residue; this residue is usually burned causing air pollution and formation of "black cloud" (El-Adly et al., 2015). It is thus imperative to find safe and beneficial ways of getting rid of rice straw instead of burning it and thus, transforming agricultural wastes to biochar may be a good solution. Biochar is a carbon-rich product prepared by combusting biomass (such as agricultural wastes), at temperatures between 350 °C and 700 °C in a closed chamber with insufficient air or no air (Liu et al., 2015). Biochar has several proven applications including its application for soil remediation. The properties and characteristics of biochar depend mainly on the starting material used for its preparation and also on its preparation conditions.

Biochar as soil amendment is of appealing global interest owing to its many benefits, including

Citation: El-Hassanin AS, Samak MR, Radwan SR, El-Chaghaby GA. Preparation and characterization of biochar from rice straw and its application in soil remediation. Environ. Nat. Resour. J. 2020;18(3):283-289. DOI: 10.32526/ennrj.18.3.2020.27

sequestration of carbon, decrease of greenhouse gases, enhancement of soil fertility and crop growth (Zhang et al., 2017). The application of biochar to agriculture soils has many positive effects such as decreasing the phytotoxicity of heavy metals, and increasing cation exchange capacity, water-use efficiency and holding plant nutrients, along with enhancing the nutrient uptake and growth of plants (Sahin et al., 2017). Also, soil amendments have been commonly utilized for in situ remediation of metal polluted soil. Several types of organic and inorganic materials were employed to immobilize heavy metals in soil by converting them into less available forms (Lu et al., 2017). It is thus a challenging issue to find environmental friendly ways to overcome soil pollution. So, the aim of the present study is to use an agricultural waste (rice straw) to prepare biochar and to investigate the effect of applying this biochar for soil remediation and heavy metals immobilization.

2. METHODOLOGY

2.1 Biochar preparation

Rice straw was collected during the harvesting season of rice in Egypt. The collected straw was washed with tap water to remove any adherent dust. The biochar was prepared according to the method described by Cao et al. (2011). Rice straw was oven dried oven-dried for 12 h at 80 ºC and grinded. The dried rice straw material was then placed in tightly covered containers to create an oxygen-limited condition during biochar production and moved to a pyrolysis furnace which was heated by 5 ºC/min to 450 ºC under anaerobic conditions and then maintained for 4 h until no further smoke exhaust. The resulting biochar was then ground and sieved through a 0.25-mm mesh before further application. The resulting biochar was abbreviated RSB.

2.2 Biochar characterization

The produced biochar was characterized by different tools including Fourier transformation infrared spectroscopy (FTIR) using Perkin-Elmer FT-IR 1650 spectrophotometer with a working wave number range (200-4,000 cm^{-1}), X-ray diffraction (XRD) using PanlyticalX'pert Pro X-ray diffractometer and Scanning electron microscopy (SEM) using a JSM-6390LV (JEOL Ltd, Japan).

2.3 Application of biochar for soil remediation

Agricultural soil was obtained from Agricultural Research Center (ARC), Giza, EGYPT. Physical, chemical and mechanical properties of soil were determined in the "Soil, Water and Environmental Research Institute" at the Agricultural Research Center, Giza, Egypt. These properties included: soil texture, EC and pH, CEC, moisture, macro and micronutrients and some heavy metals. All tests were done according to the standard methods given by Estefan et al. (2013). In order to assess the effect of RSB application on soil properties and heavy metals immobilization; a synthetic polluted soil was prepared by adding 500 mg/kg lead in the form of lead nitrate and 10 mg/kg cadmium in the form of cadmium nitrate. The effectiveness of biochar in remediating synthetic polluted soil was tested using the procedure of Abdelhafez et al. (2014). Four levels of biochar were used: 1.25% w/w (T1), 2.5% w/w (T2), 5.0% w/w (T3), 10% w/w (T4) and a control without biochar was also used. At the beginning of the experiment 200 g of soil were thoroughly mixed (on weight basis) with rice straw biochar (RSB) at the suggested rates in plastic pots and the samples were moisturized with deionized water. Soil samples were then incubated at room temperature for 30 days without direct exposure to sunlight with continuous moistening (3 pots /treatment). At the end of incubation, soil samples were collected, dried, sieved and kept for analysis.

Soil samples before and after biochar treatments were analyzed for available macro-nutrients as well as available lead and cadmium concentrations by extracting 20 g of air dried soil in 0.5 M solution of ammonium acetate and 0.02 M EDTA (Lakanen and Erviö, 1971). The element concentrations were then determined using inductively coupled plasma (ICP Ms/Ms QQQ8800 Agilent) (Hartley et al., 2013).

2.4 Statistical analysis

Complete Randomized design was employed to analyze the data (Snedecor and Cochran, 1980) and the significant differences between means were obtained by Duncan's multiple range test (Duncan, 1955) at 5% probability.

3. RESULTS AND DISCUSSION

3.1 Soil properties before biochar application

The results of soil analysis before the addition of biochar are summarized in Table 1.

Table 1. Soil characteristics

Measured property	Result
Fine sand (%)	11.20
Coarse sand (%)	2.50
Silt (%)	44.70
Clay (%)	41.60
Soil texture	Silty Clay
$CaCO_3$ (%)	7.70
Total organic matter (TOM) (%)	7.92
Total organic carbon (TOC) (%)	4.60
Moisture (%)	2.24
pH	8.20
Electrical conductivity (EC; dS/m)	0.818
Cationic exchange capacity CEC (meq/100g)	15.30
Macro-elements (%)	
N	0.1100
P	0.0068
K	0.0586
Ca	0.8295
Na	0.0877
Mg	0.0958
Micro-elements (mg/kg)	
Al	49.48
Cr	0.358
Mn	360.33
Fe	42.33
Cu	15.86
Zn	30.44
Heavy metals (mg/kg)	
*Cd	N.D.
*Pb	N.D.

Remark: 1) N.D. not detected and 2) *detection limit for Cd = 0.012 ppb and for Pb = 0.009 ppb (Sakai, 2015)

3.2 Fourier Transformation Infrared Spectroscopy (FTIR) characterization of rice straw biochar

The surface properties of biochar have a strong effect on its capability of removing metal ions from soil and the FTIR spectroscopy gives a great tool to observe this surface composition. Figure 1 shows the FTIR spectrum of rice straw biochar (RSB) and Table 2 summarizes the main bands and their assignments. The results indicate the presence of many surface functional groups that could be involved in heavy metals adsorption from soil.

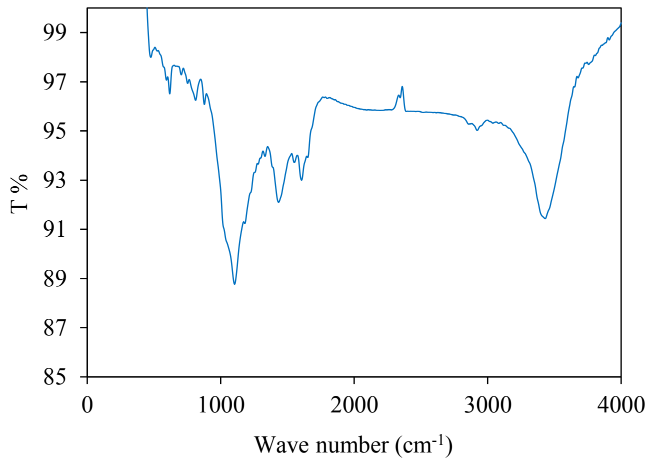

Figure 1. FTIR of rice straw biochar

Table 2. FTIR band assignments

Band	Assignment	Reference
3430.74 cm^{-1}	OH group	(Akhtar et al., 2010)
1605 cm^{-1}	oleifinic C-C and carbonyl C=O stretching	(Akhtar et al., 2010)
1430 and 1020 cm^{-1}	cyclic structures, such as cellulose or lignin	(Velazquez-jimenez et al., 2013)
811.88 and 1104.05 cm^{-1}	SiO_2	(Jindo et al., 2014)
618 cm^{-1}	aliphatic CH_2 deformation	(Han et al., 2013)

3.3 X-ray diffraction (XRD) analysis of rice straw biochar

Another characterization tool that was employed in this work was the XRD. In Figure 2, the XRD pattern of rice straw biochar is given. The results were comparable to previously reported XRD patterns for rice straw based biochars. The figure showed a characteristic peak of Silica (SiO_2) at 2 Theta position ~28°.

The XRD pattern also reveals the presence of potassium as potassium chloride, known to be found as an impurity. Compared with other materials, rice straw is low in lignin and high in Si and K, which gives rise to a high content of SiO_2 and KCl in rice straw biochars (Wu et al., 2012). Rice straw loses its crystalinity at 400 °C, it is thus agreed that in the present work the XRD pattern of RSB is indicative of an amorphous, poorly crystalline and carbon-rich material.

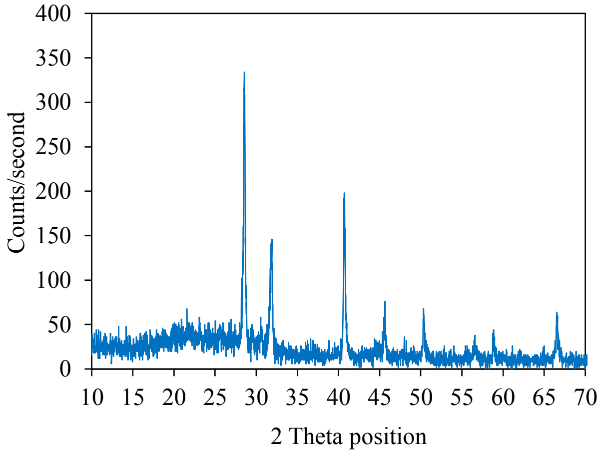

Figure 2. X-ray diffraction pattern of RSB

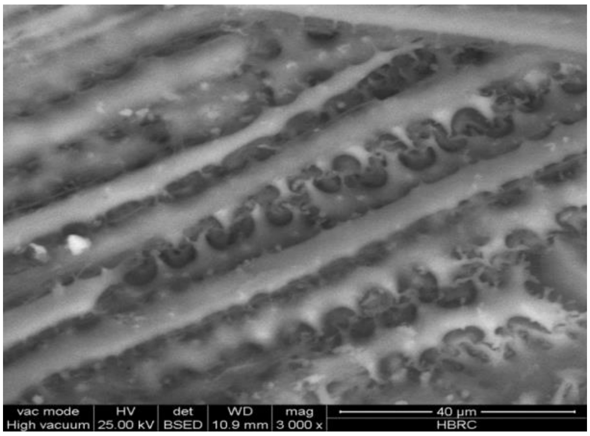

Figure 3. SEM of rice straw biochar (x3000)

3.4 Scanning electron microscopic analysis of RSB

In order to get more characterization about the surface structure of rice straw biochar, the biochar surface was scanned by scanning electron microscope (SEM) and the results are shown in Figure 3.

Figure 3 shows the surface features of rice straw biochar as obtained by SEM at magnification of 3,000. The micrograph shows that RSB consists of non-regular plates with porous structure and a large, accessible surface area which offers effective adsorption sites (Jiang et al., 2012).

3.5 Effect of RSB application on soil properties

The effect of biochar modifications on soil pH, electrical conductivity (EC), ash, humidity, total organic matter (TOM), total carbon (TC), N, P and K is shown in Table 3.

Table 3. Effect of biochar on soil properties

	Control	T1	T2	T3	T4
pH	8.20 ^{b}	8.30 ^{b}	8.30 ^{b}	8.95 ^{a}	9.15^{a}
EC (dS/m)	0.818^{e}	1.859^{d}	2.016^{c}	3.170^{b}	4.900^{a}
CEC meq/100g	15.30 ^{d}	15.90 ^{c}	16.00 ^{c}	16.40 ^{b}	17.10 ^{a}
Ash %	87.47^{a}	87.25^{b}	87.43^{a}	87.02^{c}	86.28^{d}
Moisture %	4.61^{c}	4.49^{d}	4.31^{e}	4.67^{b}	4.72^{a}
TOM %	7.92^{d}	8.25^{c}	8.25^{c}	8.31^{b}	8.98^{a}
TC (g/kg)	46.0^{d}	48.0^{c}	48.0^{c}	48.3^{b}	52.2^{a}
N %	0.11^{c}	0.11^{c}	0.11^{c}	0.12^{b}	0.13^{a}
P %	0.0068^{e}	0.0078^{d}	0.0084^{c}	0.0095^{b}	0.0113^{a}
K%	0.0586^{e}	0.1226^{d}	0.1967^{c}	0.3151^{b}	0.6248^{a}

Remark: Different superscripts of a, b, c, d and e illustrated the significant difference ($p<0.05$) of values in the same row

The data in Table 3 revealed a significant ($p<0.05$) increase in pH, EC and CEC values due to addition of biochar. The highest mean values of pH, EC and CEC were observed in the soil treated with 10% biochar (T4), while the lowest values were recorded at the control. A rise in soil pH will support the adsorption and precipitation of heavy metals, and thus decrease their bioavailability. This could be important for the reduction of plant concentrations of Cd and Pb, metal adsorption to biochar may be one of the routes of metals immobilization (Lu et al., 2014). The CEC is an essential sign of soil fertility and the increase in soil CEC was demonstrated to be effective in the immobilization of metal cations mainly through metal precipitation and surface complexation (Yin et al., 2017).

Biochar addition to soil significantly resulted in greater soil total C content compared to the control soil. The biochar treatment at the level of 10% (52.20 g C/kg) increased soil C by 13.4% compared to 'control' (46.00 g C/kg). These results are consistent with numerous biochar studies where researchers recorded soil C storage (Gao et al., 2016). The organic matter of the soil significantly increased ($p<0.05$) following the application of biochar. The results showed that the total organic matter increased by increasing the biochar amendment level meaning that organic matter is conserved more competently and keeping the activity of the microorganisms accountable for soil organic matter biodegradation (Méndez et al., 2012). Biochar addition significantly increased moisture content of soil indicating increasing soil water holding which is ascribed to the porous structure of biochar (Al-Wabel et al., 2015).

It is generally agreed that biochar application usually increases the essential nutrients in soil, including nitrogen (N), phosphorus (P) and potassium (K), which facilitates plant growth (Agegnehu et al., 2017). In the present work, the application of RSB up to 10% slightly increased the N contents of the treated soils as compared to control. Also, available phosphorus increased after adding the biochar to the soil and increased by increasing the biochar level. The application of biochar at a level of 10% led to a significant ($p<0.05$) increase of available P compared to the control and other treated groups. The concentration of potassium in biochar amended soils significantly ($p<0.05$) increased by increasing the amount of biochar application rates. The increased nutrients' retention of biochar modified soil could be attributed to the biochar surface area, making it easier for nutrients to interact with surface function groups on the biochar (Randolph et al., 2017).

3.6. Effect of biochar on lead and cadmium levels in soil

Heavy metals in soil extracted with EDTA are considered to be plant available (Lu et al., 2017). Regarding the effect of biochar application on available heavy metals in soil, Figures 4 and 5 show the plant availability of lead and cadmium in soils after biochar application. The available concentrations of plant Pb and Cd were considerably ($p<0.05$) lower than those in the control treatment in all biochar treatments. The results showed that lead and cadmium available concentration significantly decreased ($p<0.05$) with increased rates of application of rice straw biochar.

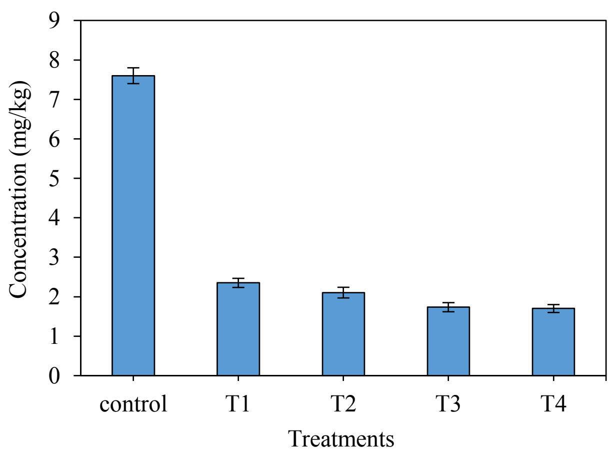

Figure 4. Effect of Rice straw biochar on Cd availability

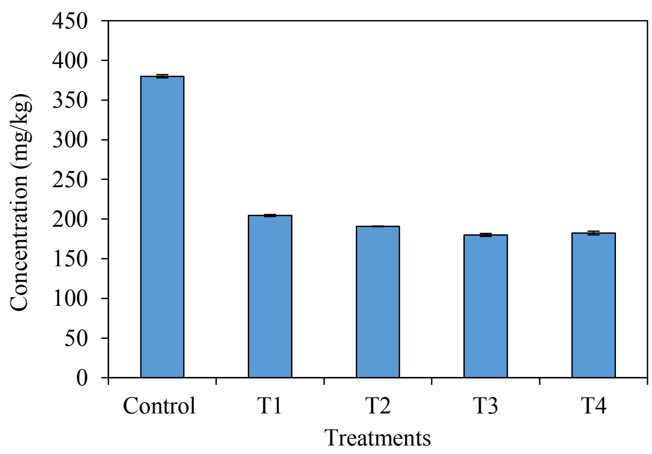

Figure 5. Effect of Rice straw biochar on Pb availability

The results also revealed that the soil amended with rice straw biochar at levels of either 5% (T3) or 10% (T4) possessed significantly lower Cd and Pb concentrations compared to all other treatments. Further results showed that the soil adjusted with rice straw biochar had significantly lower concentrations of Cd and Pb compared to all other treatments at levels of either 5% (T3) or 10% (T4). It was also conspicuous that there were no significant differences ($p>0.05$) in Cd and Pb concentrations of the soil treated with rice straw biochar at levels of either 5% or 10%.

Previous studies supported this finding, suggesting that the relatively high efficiencies of rice straw biochar in immobilizing Cd and Pb may result from the precipitation of Cd and Pb as hydroxides and phosphates (Ahmad et al., 2014; Ok et al., 2010). It is interesting to note that RSB was found to contain a high amount of SiO_2; in this respect, Li et al. (2012) found the addition of silicon to soil contaminated by lead reduced the exchangable fraction of Pb in soil. This reduction in metals availability corresponds to a reduction in metal uptake by plants.

Also in the present study, rice straw biochar had a high pH, Si and P concentrations; this can explain the increased solubility reduction of Cd and Pb with its application because of a metal restriction effect of biochar. This finding was previously verified by several authors (Beesley et al., 2010; Fellet et al., 2011; Lu et al., 2014; Méndez et al., 2012).

The high pH of rice straw biochar could be the reason for the reduction in Pb solubility with its use (Li et al., 2017). The use of biochar increases the pH of soil, therewith increasing complexation and adsorption of metal cations on biochar and lowering their mobility (Ahmad et al., 2014; Beesley and Marmiroli, 2011). The effect of Biochar on soil metal immobilization is influenced by the starting material used, pyrolysis considerations and levels of application. The fact that, most biochars have large microporous structure surfaces, high pHs and some soluble salts make them reduce the solubility of heavy metals in soil through adsorption and precipitation (Chan and Xu, 2009; Yuan et al., 2011; Zhang et al., 2013). The applications of rice straw biochar have also been reported by Jiang and Xu (2013) to increase the proportion of organic materials and immobilizing heavy metals in soil.

4. CONCLUSIONS

Biochar was effectively produced from rice straw and was applied as a soil amendment. The results of this study showed that rice straw biochar can effectively immobilize and reduce the availability of lead and cadmium in soil. Biochar application improved soil properties and increased the availability of macro nutrient elements. Thus, instead of burning agricultural wastes, they can be turned into valuable materials such as biochar that can be used to reduce metal availability of contaminated soils as well as to improve some soil properties. Moreover, caution must be considered due to the possible occurrence of a trace amounts of some heavy metals accumulation for long term application of biochar. This issue should be continuously followed up.

REFERENCES

Abdelhafez AA, Li J, Abbas MHH. Feasibility of biochar manufactured from organic wastes on the stabilization of heavy metals in a metal smelter contaminated soil. Chemosphere 2014;117(1):66-71.

Agegnehu G, Srivastava AK, Bird MI. The role of biochar and biochar-compost in improving soil quality and crop performance: A review. Applied Soil Ecology 2017;119:156-70.

Ahmad M, Rajapaksha AU, Lim JE, Zhang M, Bolan N, Mohan D, Vithanagef M, Lee SS, Ok YS. Biochar as a sorbent for contaminant management in soil and water: A review. Chemosphere 2014;99:19-33.

Akhtar M, Iqbal S, Kausar A, Bhanger MI, Shaheen MA. An economically viable method for the removal of selected divalent metal ions from aqueous solutions using activated rice husk. Colloids and Surfaces B: Biointerfaces 2010;75(1):149-55.

Al-Wabel MI, Usman ARA, El-Naggar AH, Aly AA, Ibrahim HM, Elmaghraby S, Al-Omran A. Conocarpus biochar as a soil amendment for reducing heavy metal availability and uptake by maize plants. Saudi Journal of Biological Sciences 2015;22(4):503-11.

Beesley L, Marmiroli M. The immobilisation and retention of soluble arsenic, cadmium and zinc by biochar. Environmental Pollution 2011;159(2):474-80.

Beesley L, Moreno-Jiménez E, Gomez-Eyles JL. Effects of biochar and greenwaste compost amendments on mobility, bioavailability and toxicity of inorganic and organic contaminants in a multi-element polluted soil. Environmental Pollution 2010;158(6):2282-7.

Cao X, Ma L, Liang Y, Gao B, Harris W. Simultaneous immobilization of lead and atrazine in contaminated soils using dairy-manure biochar. Environmental Science and Technology 2011;45(11):4884-9.

Chan KY, Xu Z. Biochar: Nutrient properties and their enhancement. In: Lehmann J, Joseph S, editors. Biochar for Environmental Management. Science and Technology; 2009. p. 67-81.

Duncan DB. Multiple range and multiple f-test. Biometrics 1955;11:1-5.

El-Adly RA, Yossef MA, Modather FH, Ismail EA, Abbas DM. Biogrease based on biochar from rice straw and waste cooking oil. International Journal of Advances in Pharmacy, Biology and Chemistry 2015;4(1):91-7.

Estefan G, Sommer R, Ryan J. Methods of Soil, Plant, and Water Analysis: A Manual for the West Asia and North Africa Region. 3rd ed. Beirut, Lebanon: West Asia and North Africa Region; 2013.

Fellet G, Marchiol L, Delle Vedove G, Peressotti A. Application of biochar on mine tailings: Effects and perspectives for land reclamation. Chemosphere 2011;83(9):1262-7.

Gao S, Hoffman-Krull K, Bidwell AL, DeLuca TH. Locally produced wood biochar increases nutrient retention and availability in agricultural soils of the San Juan Islands, USA. Agriculture, Ecosystems and Environment 2016;233:43-54.

Han X, Liang C, Li T, Wang K, Huang H, Yang X. Simultaneous removal of cadmium and sulfamethoxazole from aqueous solution by rice straw biochar. Journal of Zhejiang University Science B 2013;14(7):640-9.

Hartley TN, Macdonald AJ, McGrath SP, Zhao F-J. Historical arsenic contamination of soil due to long-term phosphate fertiliser applications. Environmental Pollution 2013;180: 259-64.

Jiang J, Xu R. Application of crop straw derived biochars to Cu (II) contaminated Ultisol: Evaluating role of alkali and organic functional groups in Cu(II) immobilization. Bioresource Technology 2013;133:537-45.

Jiang J, Xu R, Jiang TY, Li Z. Immobilization of Cu(II), Pb(II) and Cd(II) by the addition of rice straw derived biochar to a simulated polluted Ultisol. Journal of Hazardous Materials 2012;229-230:145-50.

Jindo K, Mizumoto H, Sawada Y, Sanchez-Monedero MA, Sonoki T. Physical and chemical characterization of biochars derived from different agricultural residues. Biogeosciences 2014;11(23):6613-21.

Lakanen E, Erviö R. A comparison of eight extractans for the determination of plant available micronutrients in soils. Acta Agriculturae Fenniae 1971;123:223-32.

Li H, Dong X, Silva ED, Oliveira LD, Chen Y, Ma LQ. Mechanisms of metal sorption by biochars: Biochar characteristics and modifications. Chemosphere 2017; 178:466-78.

Li L, Zheng C, Fu Y, Wu D, Yang X, Shen H. Silicate-mediated alleviation of Pb toxicity in banana grown in Pb-contaminated soil. Biological Trace Element Research 2012;145(1):101-8.

Liu N, Charrua AB, Weng CH, Yuan X, Ding F. Characterization of biochars derived from agriculture wastes and their adsorptive removal of atrazine from aqueous solution: A comparative study. Bioresource Technology 2015;198:55-62.

Lu K, Yang X, Gielen G, Bolan N, Ok YS, Niazi NK, Wang H. Effect of bamboo and rice straw biochars on the mobility and redistribution of heavy metals (Cd, Cu, Pb and Zn) in contaminated soil. Journal of Environmental Management 2017;186(5):285-92.

Lu K, Yang X, Shen J, Robinson B, Huang H, Liu D, Wang H. Effect of bamboo and rice straw biochars on the bioavailability of Cd, Cu, Pb and Zn to Sedum plumbizincicola. Agriculture, Ecosystems and Environment 2014;191:124-32.

Méndez A, Gómez A, Paz-Ferreiro J, Gascó G. Effects of sewage sludge biochar on plant metal availability after application to a Mediterranean soil. Chemosphere 2012;89(11):1354-9.

Ok YS, Oh SE, Ahmad M, Hyun S, Kim KR, Moon DH, Yang JE. Effects of natural and calcined oyster shells on Cd and Pb immobilization in contaminated soils. Environmental Earth Sciences 2010;61(6):1301-8.

Park J, Lee Y, Ryu C, Park YK. Slow pyrolysis of rice straw: Analysis of products properties, carbon and energy yields. Bioresource Technology 2014;155(3):63-70.

Randolph P, Bansode RR, Hassan OA, Rehrah D, Ravella R, Reddy MR, Watts DW, Novak JM, Ahmedna M. Effect of biochars produced from solid organic municipal waste on soil quality parameters. Journal of Environmental Management 2017;192:271-80.

Sahin O, Taskin MB, Kaya EC, Atakol O, Emir E, Inal A, Gunes A. Effect of acid modification of biochar on nutrient availability and maize growth in a calcareous soil. Soil Use and Management 2017;33(3):447-56.

Sakai K. Routine soil analysis using an Agilent 8800 ICP-QQQ. Application Note 2015:1-10.

Snedecor GW, Cochran WG. Statistical Methods. 7th ed. Iowa, USA: Iowa State University Press; 1980.

Velazquez-jimenez LH, Pavlick A, Rangel-mendez JR. Chemical characterization of raw and treated agave bagasse and its potential as adsorbent of metal cations from water. Industrial Crops and Products 2013;43:200-6.

Wu W, Yang M, Feng Q, McGrouther K, Wang H, Lu H, Chen Y. Chemical characterization of rice straw-derived biochar for soil amendment. Biomass and Bioenergy 2012;47:268-76.

Xu P, Sun CX, Ye XZ, Xiao WD, Zhang Q, Wang Q. The effect of biochar and crop straws on heavy metal bioavailability and plant accumulation in a Cd and Pb polluted soil. Ecotoxicology and Environmental Safety 2016;132:94-100.

Yin D, Wang X, Peng B, Tan C, Ma LQ. Effect of biochar and Fe-biochar on Cd and As mobility and transfer in soil-rice system. Chemosphere 2017;186:928-37.

Yuan J-H, Xu R-K, Zhang H. The forms of alkalis in the biochar produced from crop residues at different temperatures. Bioresource Technology 2011;102(3):3488-97.

Zhang RH, Li ZG, Liu XD, Wang B, Zhou GL, Huang XX, Brooks M. Immobilization and bioavailability of heavy metals in greenhouse soils amended with rice straw-derived biochar. Ecological Engineering 2017;98:183-8.

Zhang X, Wang H, He L, Lu K, Sarmah A, Li J, Huang H. Using biochar for remediation of soils contaminated with heavy metals and organic pollutants. Environmental Science and Pollution Research International 2013;20(12):8472-83.

Biochemical Responses and DNA Damage of *Chlorella pyrenoidosa* H. Chick upon Exposure to Combined Cu and Cd at Environmentally Realistic Levels

Andhika P. Nugroho*, Niken S.N. Handayani, Sari Darmasiwi, Wildan G. Zulfikar, and Ahmad A. Rizki

Faculty of Biology, Universitas Gadjah Mada, Yogyakarta, Indonesia

ARTICLE INFO

Received: 19 Jan 2020
Received in revised: 29 Apr 2020
Accepted: 13 May 2020
Published online: 29 May 2020
DOI: 10.32526/ennrj.18.3.2020.28

Keywords:
Biomarker/ Copper/ Cadmium/ DNA damage

*** Corresponding author:**
E-mail: andhika_pn@ugm.ac.id

ABSTRACT

Monitoring aquatic ecosystems is necessary to prevent or reduce the impact of metal pollutants on ecosystems and human health. Biological responses, or biomarkers, can provide quick and direct evidence of exposure to environmental stressors. This study evaluated the sensitivity of biomarkers of *Chlorella pyrenoidosa* after short-term exposure to combined copper and cadmium at environmentally realistic concentrations with the following biological endpoints: growth; alkaline phosphatase activity; chlorophylls, pheophytin-a, carbohydrate, and protein content; and DNA damage. *C. pyrenoidosa* was exposed to three combinations of copper and cadmium for 120 min, or for 48 h to assess its DNA damage. To assess the sensitivity of the biological responses to the combined metals, integrated biomarker response (IBR) analysis was also performed. The results demonstrated that exposure to combined Cu and Cd caused an inhibition of growth and activity of alkaline phosphatase, a decrease of chlorophyll-a and -b and protein, and an increase of pheophytin-a and tail factors DNA. The IBR analysis affirmed that the inhibition of alkaline phosphatase activity and the decrease of protein level were responsive biomarkers for exposure to the combined metals.

1. INTRODUCTION

Copper (Cu) and cadmium (Cd) represent metals that generally pollute aquatic ecosystems and can cause toxic effects on aquatic organisms. Copper is an essential metal for organisms at low concentrations and is needed, for example, to stabilize protein structures and catalyze enzymatic reactions (Torres et al., 2008). Increased concentrations of copper in aquatic ecosystems mainly come from anthropogenic activities, such as copper mine drainage and copper-based pesticides (Qian et al., 2009). On the other hand, cadmium is a non-essential metal for organisms and is toxic at low concentrations. The main sources of increased cadmium concentrations in aquatic ecosystems include electroplating, smelting, alloy manufacturing, and batteries (Cheng et al., 2016). Aquatic organisms can absorb metals, which will be transferred through food chains, leading to biomagnification. These metals can cause toxic effects on aquatic organisms, which in turn can disrupt the balance of the ecosystem. Ultimately, these metals can threaten human health (Lecoeur et al., 2004; Qian et al., 2009; Cheng et al., 2016). The toxic effects of metal combinations in organisms can be stronger than the effects of the individual metals (Zeb et al., 2016; Nugroho et al., 2017).

Monitoring aquatic ecosystems is necessary to prevent or reduce the impact of metal pollutants on ecosystems and on human health. Biological markers or biomarkers, which are biological responses at lower levels of biological organization, can provide quick and direct evidence of exposure to environmental stressors (short-term response) (Adams et al., 2001). Biomarkers also integrate the effects of chemical mixtures on organisms in

Citation: Nugroho AP, Handayani NSN, Darmasiwi S, Zulfikar WG, Rizki AA. Biochemical responses and DNA damage of *Chlorella pyrenoidosa* H. Chick upon exposure to combined Cu and Cd at environmentally realistic levels. Environ. Nat. Resour. J. 2020;18(3):290-303. DOI: 10.32526/ennrj.18.3.2020.28

ecosystems (Bartell, 2006). In the development of biomarkers for environmental monitoring, it is important to evaluate the effectiveness of their responses in quantifying the environmental condition. The sensitivity of the responses to environmental stressors is a critical component of the evaluation process. The response should be sensitive to an environmental stressor at lower concentrations and should occur within a short time period after an exposure (Bartell, 2006).

Microalgae, primary producers in the food chains of aquatic ecosystems, are known to have high sensitivity to the presence and concentrations of metals. The use of microalgal growth as a parameter of metal presence is considered more useful and consistent than biomass and total cell count (Campanella et al., 2000; Lin et al., 2005; Jiang et al., 2016). The toxicity of metals in microalgae can also be studied by measuring inhibition of enzyme activities in the microalgae. Inhibition of alkaline phosphatase enzyme activity is often used as a parameter to determine the presence and concentration of metals in aquatic ecosystems. Alkaline phosphatase resides on the microalgal cell wall, so metals will readily interact with the enzyme (Awasthi, 2012; Jiang et al., 2016). Microalgal interaction with Cu and Cd may also interfere with protein and carbohydrate metabolism, inhibit the biosynthesis of chlorophylls, and increase the concentration of pheophytin-a (Campanella et al., 2000; Tripathi and Gaur, 2006; Perales-Vela et al., 2007; Arunakumara and Xuecheng, 2008; Ngo et al., 2009; Nugroho and Frank, 2011; Miazek et al., 2015).

Cu and Cd play a role in increased reactive oxygen species (ROS) production (Qian et al., 2009). These species cause DNA damage through the oxidation process. Genotoxicity of DNA damage can be analyzed with a comet assay by determining the number of denatured DNA fragments that migrate out of the cell nucleus during electrophoresis. The test has high sensitivity to detect DNA damage in single cells (Erbes et al., 1997; Desai et al., 2006; Cadet and Wagner, 2013).

Previous research has generally considered the biological responses of microalgae to a single metal, and only rarely have the combined effects of two or more been assessed. This study evaluated the sensitivity of biological responses of *Chlorella pyrenoidosa* to short-term exposure to combinations of copper and cadmium at environmentally realistic levels with biological endpoints: growth, alkaline phosphatase activity, DNA damage, and chlorophylls, carbohydrate, and protein content. The rapid and sensitive responses of the endpoints were assessed by integrated biomarker response analysis. The results identify promising biomarkers for biomonitoring of aquatic metal pollution.

2. METHODOLOGY

2.1 Chemical materials and glassware

Chemicals were of analytical grade (Merck, Jakarta, Indonesia). Walne's medium (Walne, 1970) was used as a microalga growth medium and was sterilized before use. To test the effects of combined Cu and Cd, stock solutions were prepared by dissolving 0.01 g $CuSO_4{\cdot}5H_2O$ and 0.01 g of $CdCl_2$ separately with bidistilled water in a 100 mL volumetric flask, resulting in Cu and Cd concentrations of 0.40 and 0.55 mmol/L.

All glassware was washed twice with 50% HNO_3 solution (65%, 225 g/L), aquadest, and bidistilled water, and then sterilized in an autoclave at 121 ^{o}C for 15 min.

2.2 Test organism and culture conditions

Chlorella pyrenoidosa was obtained from the Research Centre for Brackish Water Aquaculture (Jepara, Indonesia). In the laboratory, the culture was maintained in Walne's medium in 1-L Erlenmeyer (Pyrex) flasks following the method of Nugroho and Frank (2011). Cultures in the exponential phase were used for all tests, and the initial density for each test was 5-6 × 10^6 cells/mL.

2.3 Experimental design

For testing the combined effects of Cu and Cd, into each of three flasks containing 600 mL *C. pyrenoidosa* culture (5-6 × 10^6 cells/mL) was added Cu and Cd from a stock solution to establish different concentrations of Cu and Cd, respectively, i.e., 0.3 and 0.09, 1.5 and 0.9, and 15 and 9 µmol/L. Three flasks containing 600 mL of microalgal culture were used as controls. The concentrations of metals represent the range which might typically be found in aquatic ecosystems that receive effluent from industry and agricultural land use. The range was from the water quality standard (0.3 µmol/L Cu and 0.09 µmol/L Cd) to 15 µmol/L Cu and 9 µmol/L Cd (Rajaganapathy et al., 2011; Tjahjono and Suwarno, 2018; Elfidasari et al., 2019).

At 0, 15, 30, 60, 90, and 120 min after the addition of Cu and Cd, 2-mL aliquots were transferred into 2-mL microtubes to calculate the growth of microalgae. Furthermore, 2-mL aliquots were taken from each Erlenmeyer flask and transferred into 15-mL polypropylene (PP)_tubes (Biologix, Jakarta, Indonesia) for the analysis of alkaline phosphatase activity. At the same sampling times, a 90-mL aliquot was divided into two 50-mL PP tubes of known weights. The first tube was used for protein and carbohydrate analyses, and the second for chlorophyll analysis. For DNA damage analysis, 2 mL was transferred from each Erlenmeyer flask into 2-mL microtubes at 2, 12, 24, and 48 h after addition of the metals.

2.4 Growth

Microalgal growth was followed by calculating cell density using a hemocytometer (Grigoryev, 2014). Specific growth rate was calculated according to Gani et al. (2016):

$$\mu = \frac{\ln N_2 - \ln N_1}{T_2 - T_1}$$

Where; μ = specific growth rate
N_2 and N_1 = cell density at time t_2 and t_1

The growth inhibition of microalgae was expressed as an inhibition percentage (PI) as PI (%) = (1-(N/N_o) × 100), where N and N_o are cell density (cells per mL) in the culture with a combination treatment of metals and in the control culture, respectively (Qian et al., 2009).

2.5 Determining chlorophyll-a, chlorophyll-b, and pheophytin-a

An aliquot (45 mL) of culture was centrifuged at 6,000 g at 4 °C for 10 min; the supernatant was removed, and 30 mL of distilled water was added and the suspension centrifuged again at 6,000 g at 4 °C for 10 min. The supernatant was again removed, and the pellet was weighed to obtain the wet weight. The pellet was used for chlorophyll and pheophytin analyses.

Chlorophyll-a and chlorophyll-b were determined using the method of Warren (2008). The pellet in a 2-mL microtube (Eppendorf) was ground with a pestle and then mixed with 1 mL of methanol and centrifuged at 16,873 g at 4 °C for 2 min. The supernatant was transferred to another microtube and the pellet was re-extracted by adding 1 mL of methanol, and again centrifuged at 16,873 g at 4 °C for 2 min. The supernatant obtained was mixed with the previous supernatant, and 200 µL was put into a microplate (Iwaki, Jakarta, Indonesia), and absorbance values were recorded using a microplate reader (SH-1000 Corona Electric, Jakarta, Indonesia) at wavelengths of 652 and 665 nm. The absorbance value reading was converted to 1-cm pathlength microplate using the following formula:

$$A_{652,\ 1\ cm} = (A_{652,\ microplate} - \text{blank})/\text{pathlength}$$

$$A_{665,\ 1\ cm} = (A_{665,\ microplate} - \text{blank})/\text{pathlength}$$

The analysis was completed by calculating the concentration of chlorophylls through the following formula:

$$\text{Chlorophyll-a } (\mu g/mL) = -8.0962\ A_{652,\ 1\ cm} + 16.5169\ A_{665,\ 1\ cm}$$

$$\text{Chlorophyll-b } (\mu g/mL) = 27.4405\ A_{652,\ 1\ cm} - 12.1688\ A_{665,\ 1\ cm}$$

Pheophytin-a content was determined using samples whose absorbance value had been read through the chlorophyll analysis. The samples were mixed with 10 µL 0.1 M HCl, allowed to stand for 90 sec, and their absorbance value was read using a microplate reader at a wavelength of 665 nm. Pheophytin-a concentration was calculated with the formula of Lorenzen in Sartory (1982):

$$\text{Pheophytin-a } (mg/L) = (A_{665b} - 3.0\ (A_{665b} - A_{665a}))12.5 \times 1.5 \times 0.973$$

Where; A_{665b} = absorbance value before acid is added
A_{665a} = absorbance value after acid is added

Chlorophyll and pheophytin-a contents were expressed as µg/g wet weight (ww).

2.6 Determining proteins and carbohydrates

Forty-five mL of culture in a 50-mL PP tube of known weight was centrifuged at 6,000 g at 4 °C for 10 min. The supernatant was discarded, and the pellet was washed with 40 mL phosphate-buffered saline (PBS) and 40 mL bidistilled water through resuspension and centrifugation. The wet weight of the pellet was calculated by subtracting the weight of the PP tube from the weight of the tube containing the algae. For analysis of protein and carbohydrate, 40 mL liquid nitrogen was transferred into the tube, and then the pellet was ground using a pestle to break the cells. The addition of liquid nitrogen and grinding were conducted twice, and 2 mL of protease inhibitor cocktail was then immediately added to the tube. The sample was then centrifuged at 6,000 g at 4 ºC for 10 min. The supernatant was transferred to a 2-mL microtube.

Protein content was determined with a dye-binding assay (Kruger, 1994), using a bovine serum albumin standard curve, and expressed as µg/g ww. Carbohydrate was measured using the phenol-sulfuric acid assay (Masuko et al., 2005). The carbohydrate content was determined using a glycogen standard curve and expressed as µg/g ww.

2.7 Determining alkaline phosphatase activity

An aliquot of 2 mL culture in a 15-mL PP tube was mixed with 1 mL 0.5 M Tris-HCl buffer pH 8 and 2 mL 0.3 mM p-nitrophenyl phosphate, incubated for 4 h at 37 ºC and then mixed with 0.1 mL 0.1 M NaOH. Subsequently, the sample was filtered with Whatman paper number 42 (Whatman, Jakarta, Indonesia) of known weight and used for alkaline phosphatase activity analysis following the modified method of Ihlenfeldt and Gibson (1975) and Yuan et al. (2017), with a 4-nitrophenol standard curve. Activity was expressed as nmol/min/g ww.

2.8 Analysis of DNA damage

DNA damage was measured with an alkaline comet assay following the method of Hazlina et al. (2019). Tail factors were used to assess the extent of DNA damage, by measuring the comet's tail length (tail factor) of about 100 cells using TriTek Comet Index 2.0 under a fluorescence microscope. Tail factors were calculated according to Ivancsits et al. (2002).

2.9 Data analysis

The variability of alkaline phosphatase, chlorophylls, pheophytin-a, proteins, and carbohydrates was tested with one-way analysis of variance (ANOVA) with exposure time as an independent variable, followed by Dunnett's test ($p<0.05$) if a significant difference was obtained.

To assess the stress of combined Cu and Cd on the microalgae, all biomarkers except DNA damage were combined into a stress index termed the integrated biomarker response (IBR). The IBR index was determined following Bertrand et al. (2016) and Iturburu et al. (2018) for each combined concentration. The IBR index was calculated based on the S values of all biomarkers. The S value shows the gradient value of a biomarker on combined metal exposure, in which the highest S value follows the highest biological effect. The IBR analysis is presented in a star plot.

3. RESULTS AND DISCUSSION

3.1 Growth

During exposure to combined Cu and Cd, growth was decreased, especially in the first 15 min (Figure 1). However, the decrease compared to the 0 min value was significant only at the two highest concentrations of combined Cu and Cd ($p<0.05$). The specific growth rate (µ) showed negative values and tended to decrease with increasing combined Cu and Cd concentrations (Table 1). At the end of the exposure, the growth inhibition value (PI) increased with increasing combined Cu and Cd concentrations, i.e., 16% (0.3 µmol/L Cu+0.09 µmol/L Cd), 32% (1.5 µmol/L Cu+0.9 µmol/L Cd), and 37% (15 µmol/L Cu+9 µmol/L Cd).

The results indicated that the inhibitory metals' effect on microalgal growth depends on metal concentrations (Zulfikar, 2018). This growth inhibition could reflect the physiological and biochemical status of the microalgae. The inhibited growth may be caused by the effect of the metals on photosynthesis by blocking electron transport in photosystem II (PSII) or inhibition of chlorophyll biosynthesis, resulting in reduced cell mitotic rate and affecting microalgal growth (Cid et al., 1995; Pawlik-Skowrońska and Skowroński, 2001; Tripathi and Gaur, 2006; Arunakumara and Xuecheng, 2008). Qian et al. (2009) demonstrated that upon individual exposures to Cu (1.5 µmol/L) and Cd (1.0 µmol/L) in *C. vulgaris* for 48 h, the PI was 16% and about 8%, respectively. When *C. vulgaris* was exposed to combined Cu and Cd at the same concentrations for 48 h, the PI increased to 60%, reflecting synergistic growth inhibition (Qian et al., 2009). The current study also demonstrated a synergistic effect since exposure to 1.5 µmol/L Cu+0.9 µmol/L Cd for 120 min, the PI was 32%.

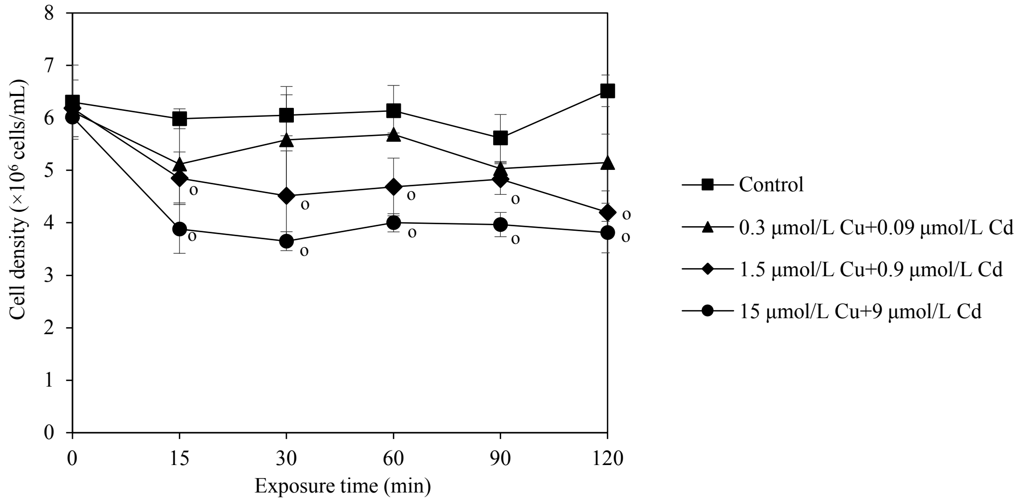

Figure 1. Growth of *C. pyrenoidosa* during exposure to Cu and Cd in combination. Data are expressed as mean ± standard deviation (n=3). A significant difference in comparison to control in each exposure is indicated by ^{o}.

Table 1. Specific growth rates of *C. pyrenoidosa* during exposure to combinations of Cu and Cd

Combination concentration of Cu and Cd (μmol/L)	Specific growth (rate/h)
0	0.02^{a} ± 0.01
0.3+0.09	-0.09^{b} ± 0.02
1.5+0.9	-0.19^{c} ± 0.01
15+9	-0.23^{c} ± 0.02

Data are expressed as mean ± standard deviation (n=3). Identical letters indicate no significant difference (p>0.05).

3.2 Chlorophyll-a, chlorophyll-b, and pheophytin-a

Administration of combined Cu and Cd to the microalgae caused a decrease in chlorophyll-a and chlorophyll-b (Figures 2 and 3). For chlorophyll-a, a significant decrease occurred at 120 min for the combination of 0.3 μmol/L Cu+0.09 μmol/L Cd (Figure 2(b)), and at 60 min for the combinations of 1.5 μmol/L Cu+0.9 μmol/L Cd (Figure 2(c)) and 15 μmol/L Cu+9 μmol/L Cd (Figure 2(d)). At the end of the exposure, the decrease in chlorophyll-a in all three combinations ranged from 20% to 30%. For chlorophyll-b, the combination of the lowest Cu and Cd concentration resulted in a significant decrease of chlorophyll-b at 15 min (Figure 3(b)). On the other hand, in the combinations of 1.5 μmol/L Cu+0.9 μmol/L Cd and 15 μmol/L Cu+9 μmol/L Cd, a significant decrease began at the 60 min (Figure 3(c) and (d)). The decrease in chlorophyll-b continued until the end of the exposure, eventually ranging from 20% to 25%.

These findings indicated that the effects were associated with increased concentrations of Cu and Cd and the duration of exposure (Zulfikar, 2018). Qian et al. (2009) also reported effects of Cu and Cd on the chlorophyll-a and chlorophyll-b of *C. vulgaris* at a similar concentration as used in this study, namely 1.5 μmol/L Cu and 1.0 μmol/L Cd, for 48 h. Upon individual exposures to Cu and Cd, the chlorophyll-a decreased by about 27 and 16%, and the chlorophyll-b also decreased by about 20 and 10%, respectively. Exposure to the combined Cu and Cd decreased the chlorophyll-a and chlorophyll-b by about 77 and 50%, indicating a strong synergistic effect. Combined Cu and Cd inhibited the expression of psbA, the gene that encodes the D1 protein of PSII. The inhibition decreased in PSII activity and the rate of electron transfer, thereby reducing the content of chlorophylls (Qian et al., 2009). Such a combination (1.5 μmol/L Cu+1.0 μmol/L Cd) also synergistically enhanced the induction of reactive oxygen species (ROS) formation in *C. vulgaris*, which caused damage to the photosynthetic apparatus, resulting in the decrease of chlorophyll content and producing a synergistic inhibition of algal growth (Qian et al., 2009). In comparison with the study of Qian et al. (2009), the results of this study did not lead to synergistic effects.

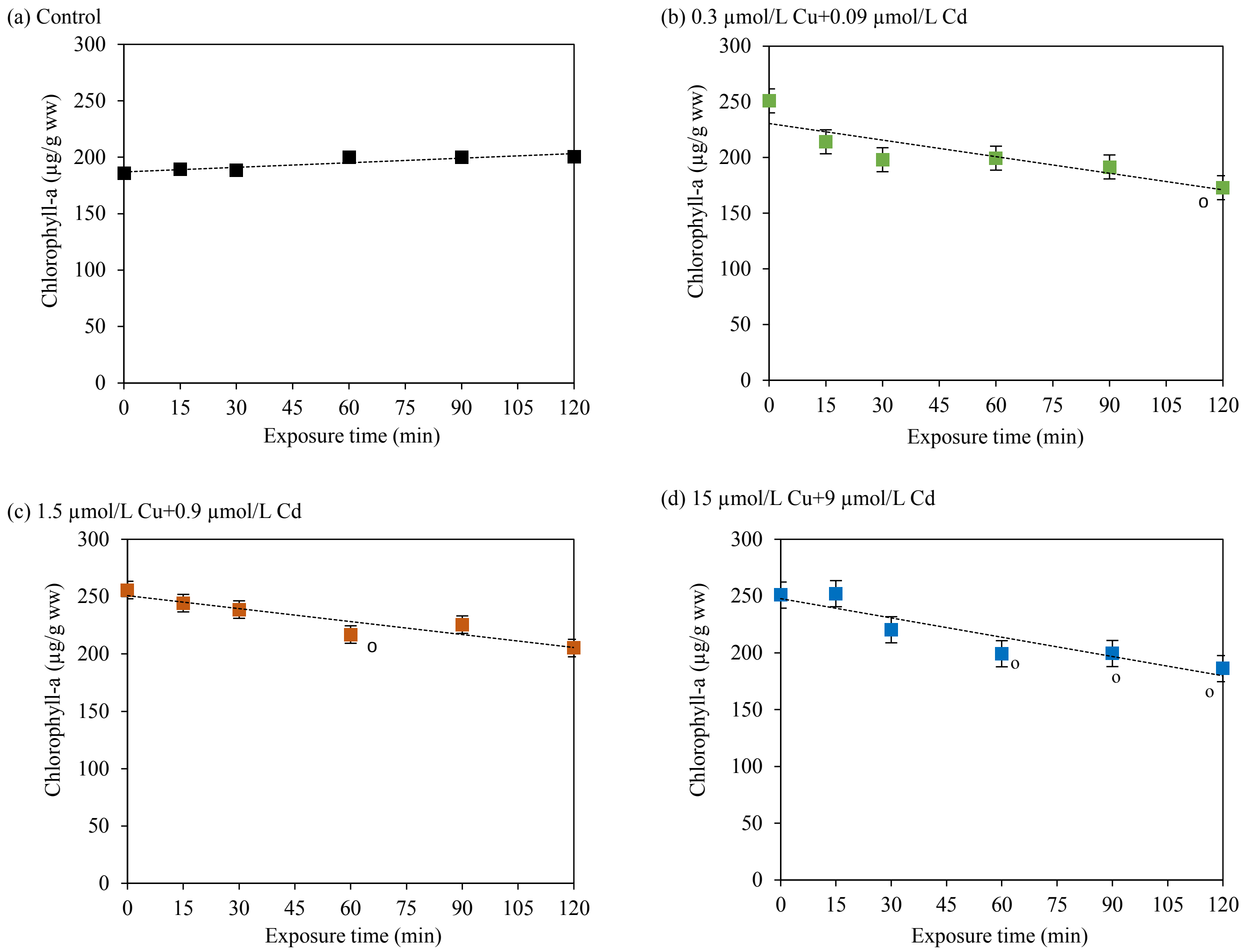

Figure 2. Chlorophyll-a content (µg/g ww) in *C. pyrenoidosa* after exposure to the combinations of (a) 0 µmol/L Cu+0 µmol/L Cd (control), (b) 0.3 µmol/L Cu+0.09 µmol/L Cd, (c) 1.5 µmol/L Cu+0.9 µmol/L Cd, and (d) 15 µmol/L Cu+9 µmol/L Cd. Data are expressed as mean ± standard deviation (n=3). A significant difference in comparison to control is indicated by º.

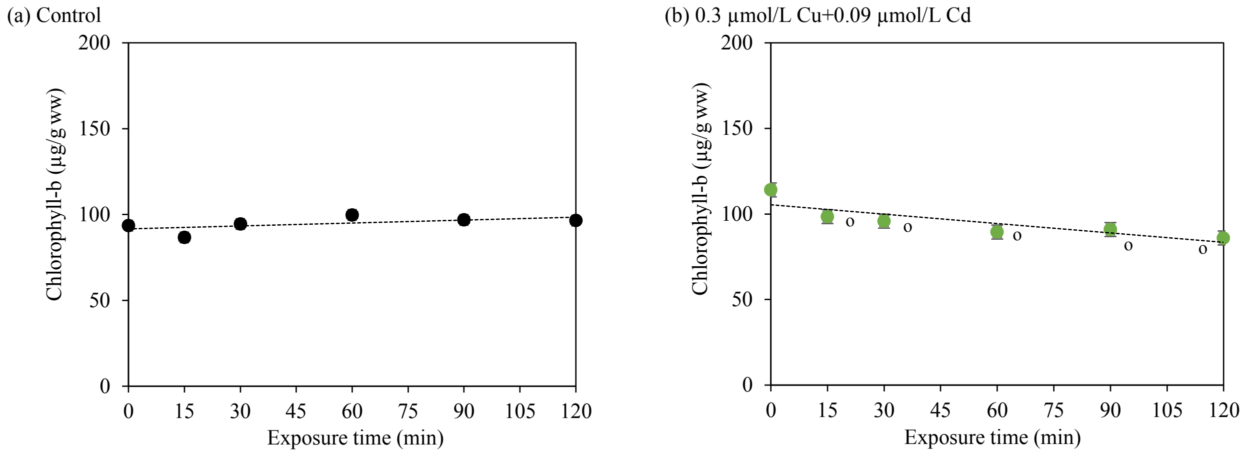

Figure 3. Chlorophyll-b content (µg/g ww) in *C. pyrenoidosa* after exposure to the combinations of (a) 0 µmol/L Cu+0 µmol/L Cd (control), (b) 0.3 µmol/L Cu+0.09 µmol/L Cd, (c) 1.5 µmol/L Cu+0.9 µmol/L Cd, and (d) 15 µmol/L Cu+9 µmol/L Cd. Data are expressed as mean ± standard deviation (n=3). A significant difference in comparison to control is indicated by º.

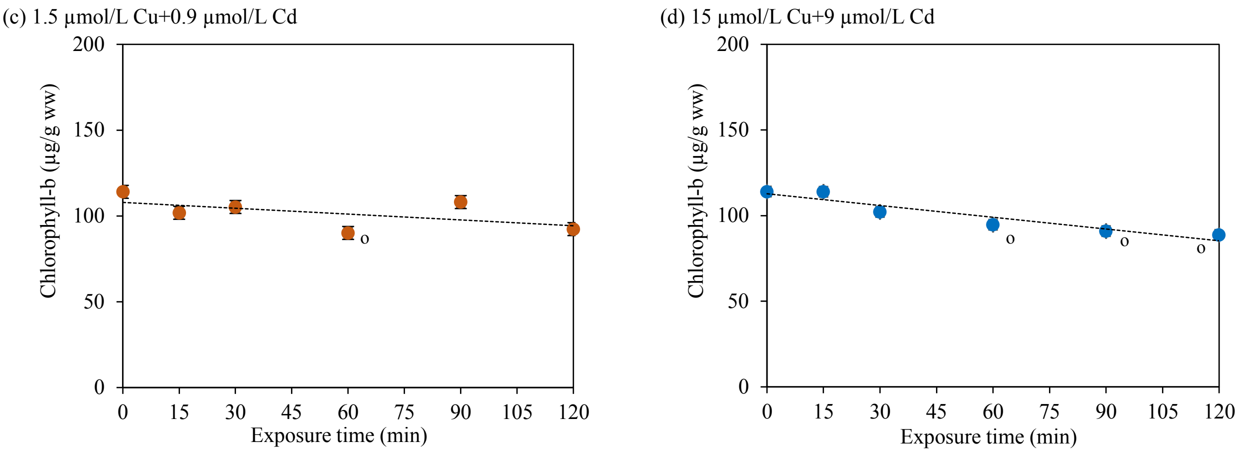

Figure 3. Chlorophyll-b content (µg/g ww) in *C. pyrenoidosa* after exposure to the combinations of (a) 0 µmol/L Cu+0 µmol/L Cd (control), (b) 0.3 µmol/L Cu+0.09 µmol/L Cd, (c) 1.5 µmol/L Cu+0.9 µmol/L Cd, and (d) 15 µmol/L Cu+9 µmol/L Cd. Data are expressed as mean ± standard deviation (n=3). A significant difference in comparison to control is indicated by º (cont.).

Pheophytin-a content tended to increase during the exposure (Figure 4). For all metal combinations, these elevations were significant at 15 min after the exposure (Zulfikar, 2018). At the end of the exposure, the content of pheophytin-a at the combinations of 0.3 µmol/L Cu+0.09 µmol/L Cd (Figure 4(b)), 1.5 µmol/L Cu+0.9 µmol/L Cd (Figure 4(c)), and 15 µmol/L Cu+9 µmol/L Cd (Figure 4(d)) increased by 28%, 53%, and 45%, respectively, compared to the content of pheophytin-a at 0 min.

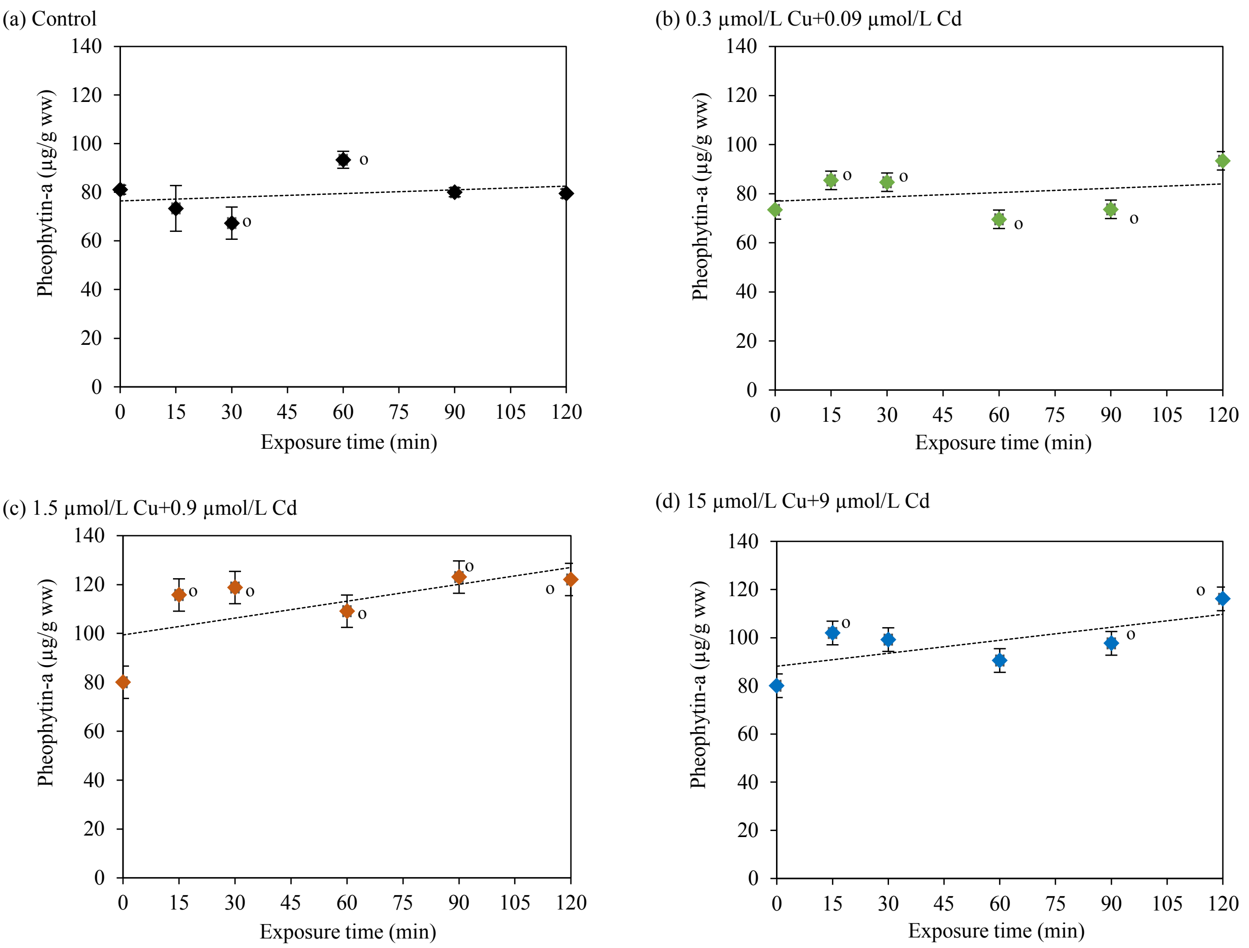

Figure 4. Pheophytin-a content (µg/g ww) in *C. pyrenoidosa* after exposure to the combinations of (a) 0 µmol/L Cu+0 µmol/L Cd (control), (b) 0.3 µmol/L Cu+0.09 µmol/L Cd, (c) 1.5 µmol/L Cu+0.9 µmol/L Cd, and (d) 15 µmol/L Cu+9 µmol/L Cd. Data are expressed as mean ± standard deviation (n=3). A significant difference in comparison to control is indicated by º.

In this study, the decrease of chlorophyll-a content was accompanied by a significant increase of pheophytin-a content starting from the lowest combination of Cu and Cd concentration at 15 min after the exposure (Figure 4(b), (c), and (d)). The increased pheophytin-a level is due to the degradation of chlorophyll-a by the replacement of Mg on the porphyrin ring with free metal (Küpper et al., 1998). In *Parachlorella kessleri*, administration of Cu alone (5.9 µmol/L) increased the content of pheophytin-a (44%, p<0.05) at 96 h after the exposure (Nugroho and Frank, 2011). For Cd, the concentration of 0.07 µmol/L administered to *P. kessleri* for 120 h significantly increased the pheophytin-a content (50%) (Ngo et al., 2009). Shehata et al. (1999) reported that exposure of a mixture of metals, including Cu (1.6 µmol/L) and Cd (0.4 µmol/L), to natural phytoplankton assemblages (*Oscillatoria mougeotii* and *Scenedesmus quadricauda*) for 10 days resulted in an inverse relationship between chlorophyll-a and pheophytin-a. This current study also showed a similar pattern, but the decreased chlorophyll-a and increased pheophytin-a occurred at a shorter exposure period. The reverse relationship was also confirmed by the ratio of chlorophyll-a and pheophytin-a. From control to the highest combined concentration, the ratio tended to decrease, i.e., 2.5, 1.9, 1.7, and 1.6. This ratio reportedly serves as a good indicator of the physiological state of microalgae (Bačkor and Váczi, 2002).

3.3 Carbohydrates and proteins

After combined metal exposure, carbohydrate content in all combinations of Cu and Cd tended to decrease (Figure 5(b), (c), and (d)), but the carbohydrate levels were not significantly different from that at 0 min (p>0.05). At the end of the exposure, the carbohydrate decrease ranged from 12% to 22%, and the highest decrease occurred at the highest combined concentration (Zulfikar, 2018).

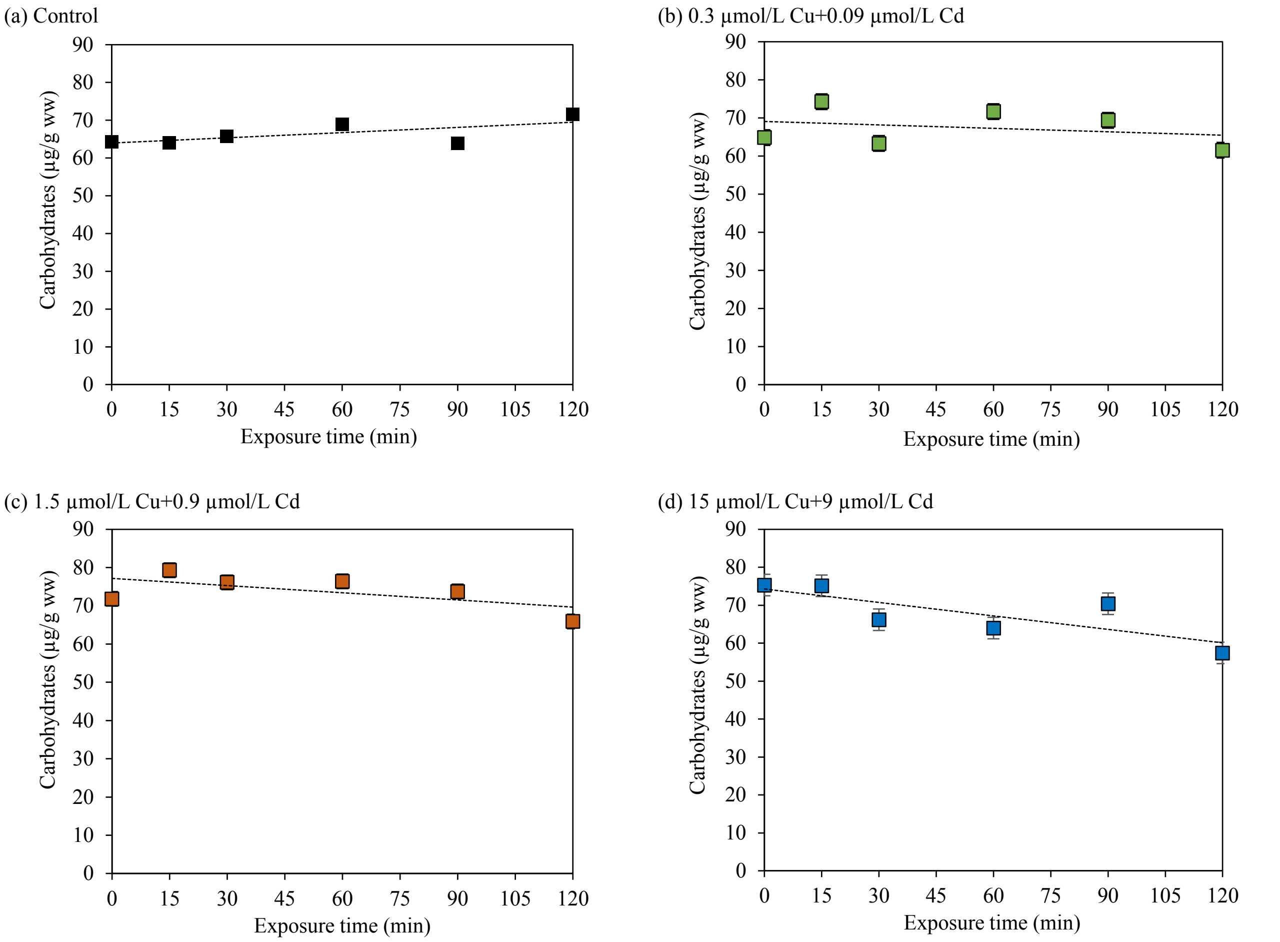

Figure 5. Carbohydrate content (µg/g ww) in *C. pyrenoidosa* after exposure to the combinations of (a) 0 µmol/L Cu+0 µmol/L Cd (control), (b) 0.3 µmol/L Cu+0.09 µmol/L Cd, (c) 1.5 µmol/L Cu+0.9 µmol/L Cd, and (d) 15 µmol/L Cu+9 µmol/L Cd. Data are expressed as mean ± standard deviation (n=3).

The same pattern also occurred with protein content for all combinations of Cu and Cd (Figure 6(b), (c), and (d)). A significant difference was found at the highest combined concentration of Cu and Cd, i.e. between 0 and 120 min ($p<0.05$). The decrease of protein content correlated with increasing concentration of Cu and Cd (Zulfikar, 2018). At the end of the exposure, the protein content was between 8% and 13% lower than at 0 min.

In *P. kessleri*, Cu concentrations greater than 6 µmol/L decreased protein and carbohydrate content (Nugroho and Frank, 2011). For Cd, the metal concentration of 0.07 µmol/L reduced the protein content but increased the carbohydrate content of *P. kessleri* (Ngo et al., 2009). In the present study, at the lowest combined concentration, the tested concentrations of Cu and Cd were similar to those used in studies of *P. kessleri* (Ngo et al., 2009; Nugroho and Frank, 2011). However, the results showed no significant differences, indicating that exposure to the combined metals at the lowest concentration did not result in synergistic effects. Decreased carbohydrate and protein may be associated with increased ROS, since this species can oxidize macromolecules including carbohydrates, proteins, and DNA (Leonard et al., 2004; Nikookar et al., 2005; Valko et al., 2005; Bajguz, 2011; Cadet and Wagner, 2013). As reported by Qian et al. (2009), almost the same concentration combination as the middle one used in this study (1.5 µmol/L Cu and 1.0 µmol/L Cd) increased ROS formation. This species damaged the photosynthetic apparatus, reducing the chlorophyll content and the rate of photosynthesis (Bajguz, 2011), which ultimately decreased the carbohydrate content. ROS also caused peptide chain breakage and increased susceptibility to proteolysis by proteases, leading to protein degradation (Rezayian et al., 2019).

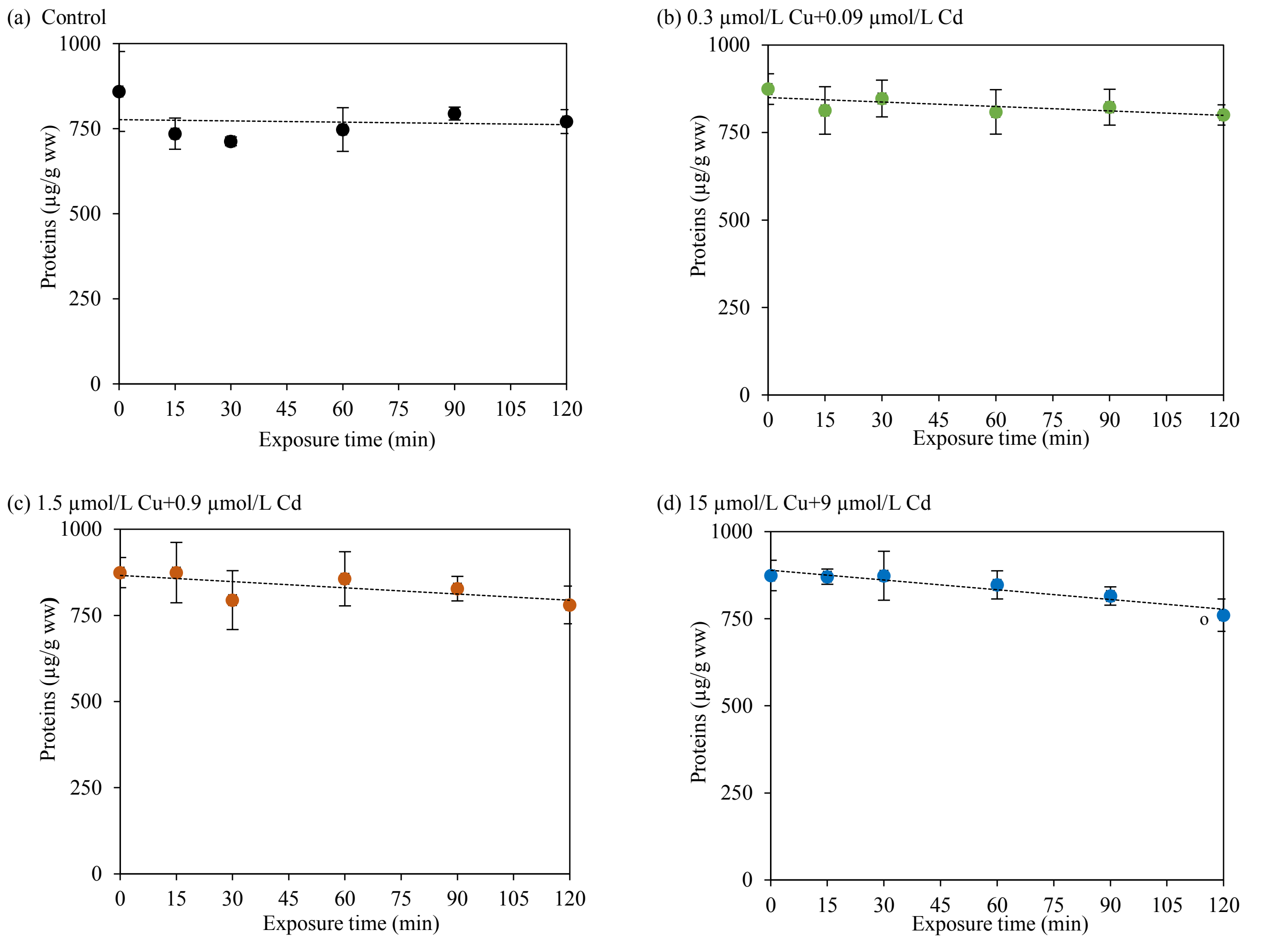

Figure 6. Protein content (µg/g ww) in *C. pyrenoidosa* after exposure to the combinations of (a) 0 µmol/L Cu+0 µmol/L Cd (control), (b) 0.3 µmol/L Cu+0.09 µmol/L Cd, (c) 1.5 µmol/L Cu+0.9 µmol/L Cd, and (d) 15 µmol/L Cu+9 µmol/L Cd. Data are expressed as mean ± standard deviation (n=3). A significant difference in comparison to control is indicated by º.

3.4 Alkaline phosphatase activity

The activity of the enzyme decreased drastically in the first 30 min after exposure ($p<0.05$), by 50% (0.3 µmol/L Cu+0.09 µmol/L Cd) (Figure 7(b)), 62% (1.5 µmol/L Cu+0.9 µmol/L Cd) (Figure 7(c)), and 62% (15 µmol/L Cu+9 µmol/L Cd) (Figure 7(d)). At the end of the exposure (120 min), the decrease of enzyme activity ranged from 54% to 68%. The results also showed that increased inhibition of the enzyme activity accompanied increased combined Cu and Cd concentrations (Zulfikar, 2018).

The studies of Awasthi (2012) and Jiang et al. (2016) showed inhibition of this enzyme activity by several metals including Cu and Cd: the higher the concentrations of the metals, the lower the activity of alkaline phosphatase. These metals may displace essential metal cofactors from the central and functional part of alkaline phosphatase, reducing the activity of the enzyme (Awasthi, 2012). Jiang et al. (2016) reported that in *Chlamydomonas reinhardtii*, the enzyme activity decreased by 50% after exposure to Cu and Cd individually (8.18 and 0.27 µmol/L) for 5 h. Another study on the effect of combined Cu and Cd at lower concentration on the activity of alkaline phosphatase of *C. vulgaris* has also been conducted by Ferro and Durrieu (2012), who demonstrated that the activity of the enzyme decreased by about 50% after exposure to Cu (0.05–0.15 µmol/L) and Cd (0.01 µmol/L) for 48 h. In this study, at a similar combined concentration, the decrease of enzyme activity by about 50% occurred in a shorter time period (30 min).

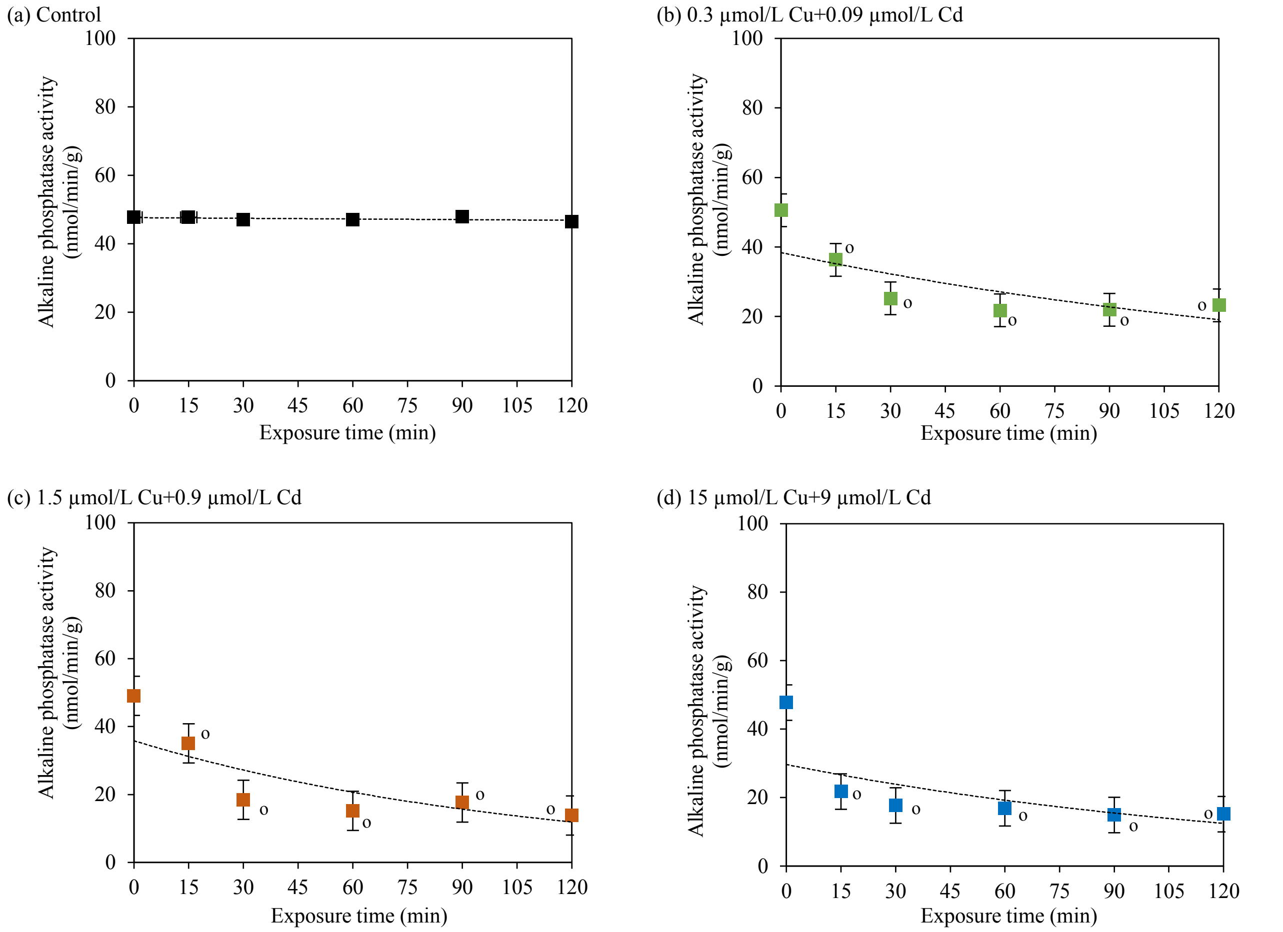

Figure 7. Alkaline phosphatase activity (nmol/min/g) in *C. pyrenoidosa* after exposure to the combinations of (a) 0 µmol/L Cu+0 µmol/L Cd (control), (b) 0.3 µmol/L Cu+0.09 µmol/L Cd, (c) 1.5 µmol/L Cu+0.9 µmol/L Cd, and (d) 15 µmol/L Cu+9 µmol/L Cd. Data are expressed as mean ± standard deviation (n = 3). A significant difference in comparison to control is indicated by ^{o}.

3.5 DNA damage

Under the combined metal administration, at the beginning of exposure (2 h), the percentages of tail comets DNA were about 6- to 11-fold higher (Figure 8(b), (c), and (d)) than in the control (Figure 8(a)) and tended to increase until the end of the exposure. Higher Cu and Cd concentrations in combination led to a stronger effect on the integrity of DNA, and the duration of the exposure also affected the level of damage (Rizki, 2019).

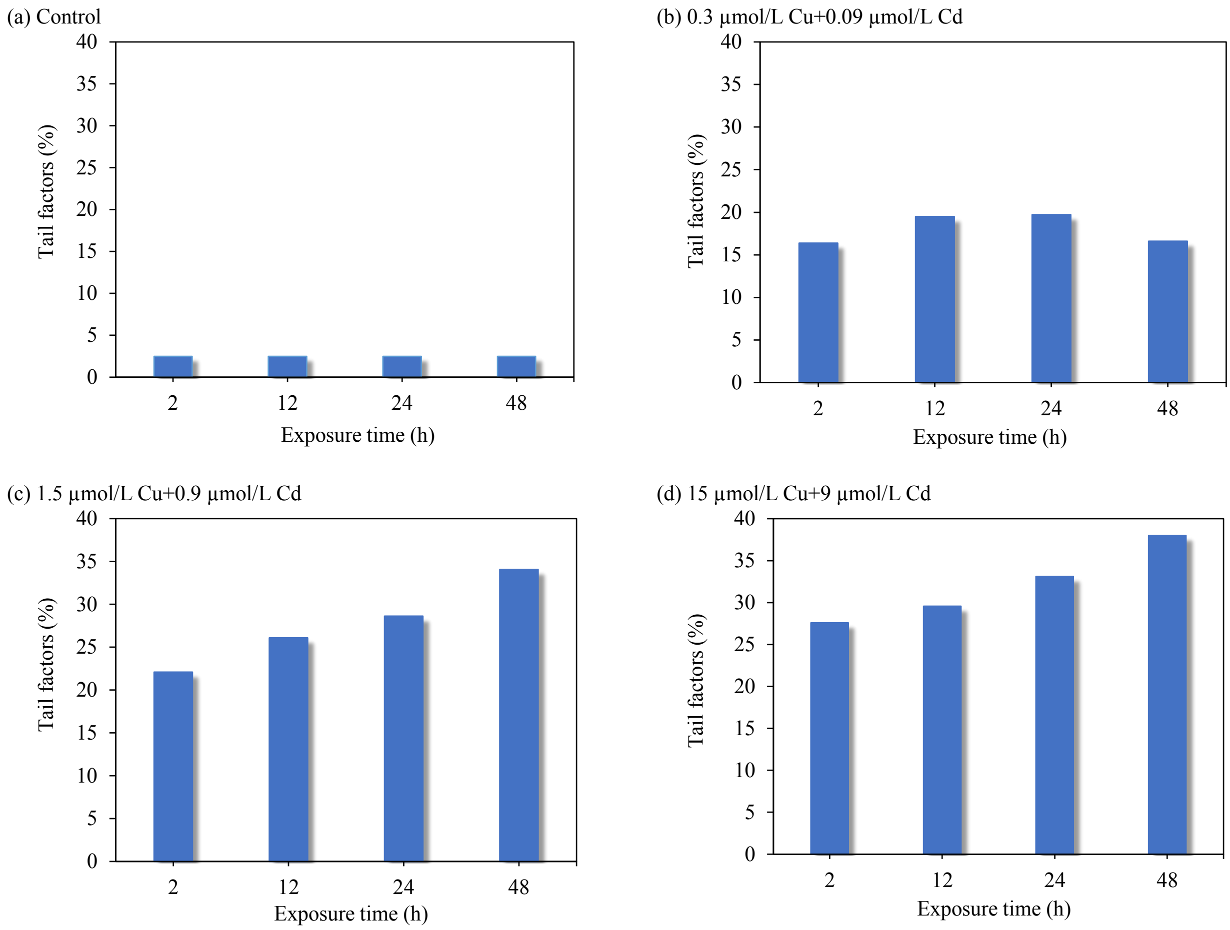

Figure 8. Tail factors of comet-nuclei of *C. pyrenoidosa* after exposure to the combinations of (a) 0 µmol/L Cu+0 µmol/L Cd (control), (b) 0.3 µmol/L Cu+0.09 µmol/L Cd, (c) 1.5 µmol/L Cu+0.9 µmol/L Cd, and (d) 15 µmol/L Cu+9 µmol/L Cd.

Qian et al. (2009) reported that exposure to combined 1.5 µmol/L Cu+1.0 µmol/L Cd for 48 h resulted in overproduction of ROS in *C. vulgaris*, which is one possible mechanism of oxidative stress in microalgae, inducing DNA damage (Pinto et al., 2003). Oxidative attack on DNA causes strand breakage, deoxyribose oxidation, and removal of nucleotides (Cadet and Wagner, 2013). Desai et al. (2006) reported that exposure of Cd to *Chaetoceros tenuissimus* at 0.09 mmol/L for 2 days caused DNA damage in up to 15% of observed cells. Prado et al. (2015) found similar results: the percentage of comet-nuclei of *C. moewusii* and *C. vulgaris* under copper administration at concentrations of 0, 0.02, 0.08, 0.16, 0.31, and 0.47 mmol/L for 3 h ranged from 15.2-95.1% and 15.1-49.2%, respectively. In comparison with the studies of Desai et al. (2006) and Prado et al. (2015), our results indicate that a short-term exposure (2 h) at lower combined metal concentrations (in µmol/L) may lead to synergistic effects.

3.6 Integrated biomarker response

In the IBR star plots, among the selected parameters, alkaline phosphatase activity had the highest S value at all combined metal concentrations: the values ranged from 1.5 to 1.6 (Figure 9(a), (b), and (c)), indicating that this biomarker was the most responsive parameter to the presence of metals in the environment. The high S value of proteins also showed that this parameter was affected strongly by exposure to the combined metals. This demonstrates that the two biomarkers are the most important weights on the IBR index.

Based on the IBR index, the combined concentration of 1.5 µmol/L Cu+0.9 µmol/L Cd resulted in greater stress on the microalgae (Figure 9(b), IBR index=5.8) than the highest combined concentration (Figure 9(c), IBR index = 4.8). These results suggest the occurrence of metal detoxification mechanisms in the microalgae, such as sequestration and compartmentalization, due to excess metals at the highest combined concentration. Metal detoxification would decrease the concentration of soluble metals, reducing their effects on biochemical parameters (Arunakumara and Xuecheng, 2008; Levy et al., 2008). This would have implications for the S values of the observed parameters.

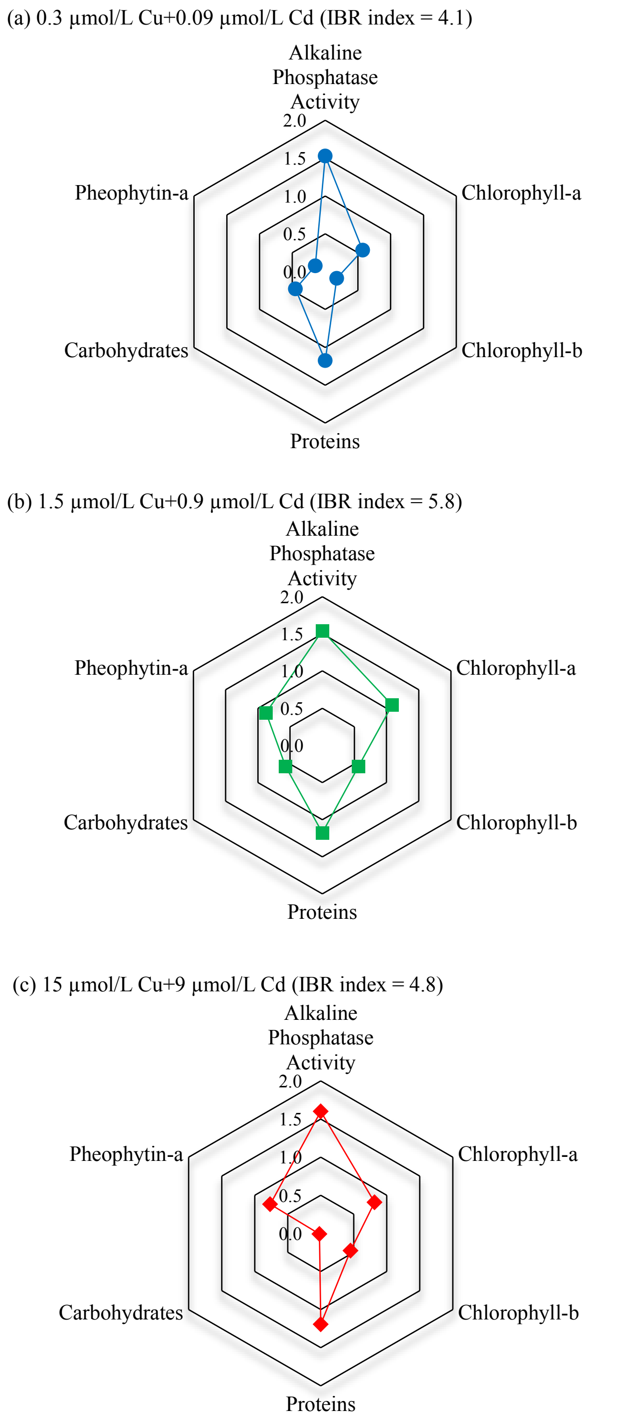

Figure 9. Star plots (IBR) for biomarker responses in *C. pyrenoidosa* exposed to the combinations of (a) 0.3 µmol/L Cu+0.09 µmol/L Cd, (b) 1.5 µmol/L Cu+0.9 µmol/L Cd, and (c) 15 µmol/L Cu+9 µmol/L Cd.

4. CONCLUSION

Short-term exposure to combined Cu and Cd at environmentally realistic levels or lower concentrations can lead to inhibition of growth and activity of alkaline phosphatase, a decrease of chlorophyll-a, chlorophyll-b, and protein content,, an increase of pheophytin-a content, and an increase of tail factors DNA. IBR analysis affirmed that inhibition of alkaline phosphatase activity and a decrease of protein level are responsive biomarkers to exposure to combinations of metals; therefore, these are promising biomarkers for biomonitoring of aquatic metal pollution.

ACKNOWLEDGMENTS

This work was financially supported by the Ministry of Research, Technology, and Higher Education of the Republic of Indonesia (grant number 20/UN1/DITLIT/DIT-LIT/LT/2018).

REFERENCES

Adams SM, Giesy JP, Tremblay LA, Eason CT. The use of biomarkers in ecological risk assessment: recommendations from the Christchurch Conference on biomarkers in ecotoxicology. Biomarkers 2001;6:1-6.

Arunakumara KKIU, Xuecheng Z. Heavy metal bioaccumulation and toxicity with special reference to microalgae. Journal of Ocean University of China 2008;7(1):60-4.

Awasthi M. Relevance of alkaline phosphatase activity of immobilized green algae and cyanobacteria for heavy metal toxicity monitoring. Journal of Materials and Environmental Science 2012;3(3):446-51.

Bačkor M, Váczi P. Copper tolerance in the lichen photobiont *Trebouxia erici* (Chlorophyta). Environmental and Experimental Botany 2002;48:11-20.

Bajguz A. Suppression of *Chlorella vulgaris* growth by cadmium, lead, and copper stress and its restoration by endogenous brassinolide. Archives of Environmental Contamination and Toxicology 2011;60:406-16.

Bartell SM. Biomarkers, bioindicators, and ecological risk assessment: A brief review and evaluation. Environmental Bioindicator 2006;1:60-73.

Bertrand L, Monferrán MV, Mouneyrac C, Bonansea RI, Asis R, Amé MV. Sensitive biomarker responses of the shrimp *Palaemonetes argentinus* exposed to chlorpyrifos at environmental concentrations: Roles of alpha-tocopherol and metallothioneins. Aquatic Toxicology 2016;179:72-81.

Cadet J, Wagner JR. DNA base damage by reactive oxygen species, oxidizing agents, and UV radiation. Cold Spring Harbor Perpectives in Biology 2013;5(2):1-18.

Campanella F, Cubadda F, Sammartino MP, Saoncella A. An algal biosensor for the monitoring of water toxicity in estuarine environments. Water Research 2000;35(1):69-76.

Cheng J, Qiu H, Chang Z, Jiang Z, Yin W. The effect of cadmium on the growth and antioxidant response for freshwater algae *Chlorella vulgaris*. Springerplus 2016;5(1)1290:1-8.

Cid A, Herrero C, Torres E, Abalde J. Copper toxicity on the marine microalga *Phaeodactylum tricornutum*: Effects on photosynthesis and related parameters. Aquatic Toxicology 1995;31:165-74.

Desai SR, Verlecar XN, Nagarajappa, Goswami U. Genotoxicity of cadmium in marine diatom *Chaetoceros tenuissimus* using the alkaline comet assay. Ecotoxicology 2006;15(4):359-63.

Elfidasari D, Ismi LN, Sugoro I. Heavy metal contamination of Ciliwung River, Indonesia. Ecology and Safety 2019;13:106-11.

Erbes M, Weβler A, Obst U, Wild A. Detection of primary DNA damage in *Chlamydomonas reinhardtii* by means of modified microgel electrophoresis. Environmental and Molecular Mutagenesis 1997;30:448-58.

Ferro Y, Durrieu C. Development of an algal biosensor for toxicity assessment of urban wet weather effluents. Proceedings of the SIDISA 2012 Sustainable Technology for Environmental Protection; 2012 Jun 26-29; Politecnico di Milano, Milan: Italy; 2012.

Grigoryev Y. Cell counting with a hemocytometer: easy as 1, 2, 3 [Internet]. 2014 [Cited 2020 Jan 18]. Available from: http://bitesizebio.com/13687/cell-counting-with-a-hemocytometer-easy-as-1-2-3/.

Gani P, Sunar NM, Matias-Peralta H, Latiff AAA, Razak ARA. Influence of initial cell concentrations on the growth rate and biomass productivity of microalgae in domestic wastewater. Applied Ecology and Environmental Research 2016; 14(2):399-409.

Hazlina AZ, Devanthiran L, Fatimah H. Morphological changes and DNA damage in *Chlorella vulgaris* (UMT-M1) induced by Hg^{2+}. Malaysian Applied Biology 2019;48(1):27-33.

Ihlenfeldt MJA, Gibson J. Phosphate utilization and alkaline phosphatase activity in *Anacystis nidulans* (*Synechococcus*). Archives of Microbiology 1975;102:23-8.

Iturburu FG, Bertrand L, Mendieta JR, Amé MV, Menone ML. An integrated biomarker response study explains more than the sum of the parts: Oxidative stress in the fish *Australoheros facetus* exposed to imidacloprid. Ecological Indicators 2018;93:351-7.

Ivancsits S, Diem E, Pilger A, Rudiger HW, Jahn O. Induction of DNA strand breaks by intermittent exposure to extremely low frequency electromagnetic fields in human diploid fibroblasts. Mutation Research 2002;519:1-13.

Jiang H, Islam MdS, Sazawa K, Hata N, Taguchi S, Nakamura S, Sugawara K, Kuramitz H. Development of an electrochemical bioassay based on the alkaline phosphatase activity of *Chlamydomonas reinhardtii* to assess the toxicity of heavy metals. International Journal of Electrochemical Science 2016;11:5090-102.

Kruger NJ. The Bradford method for protein quantitation. In: Walker JM, editor. Methods in Molecular Biology: Basic Protein and Peptide Protocols Vol. 32. New Jersey: Humana Press, Inc.; 1994. p. 9-15.

Küpper H, Küpper F, Spiller M. In situ detection of heavy metal substituted chlorophylls in water plants. Photosynthesis Research 1998;58:123-33.

Lecoeur S, Videmann B, Berny PH. Evaluation of metallothionein as a biomarker of single and combined Cd/Cu exposure in *Dreissena polymorpha*. Environmental Research 2004; 94:184-91.

Leonard SS, Harris GK, Shi X. Metal-induced oxidative stress and signal transduction. Free Radical Biology and Medicine 2004;37:1921-42.

Levy J, Angel B, Stauber JL, Poon WL, Simpson SL, Cheng S, Jolley DF. Uptake and internalisation of copper by three marine microalgae: comparison of copper-sensitive and copper-tolerant species. Aquatic Toxicology 2008;89:82-93.

Lin J-H, Kao W-C, Tsai K-P, Chen C-Y. A novel algal toxicity testing technique for assessing the toxicity of both metallic and organic toxicants. Water Research 2005;39:1869-77.

Masuko T, Minami A, Iwasaki N, Majima T, Nishimura S, Lee YC. Carbohydrate analysis by a phenol-sulfuric acid method in microplate format. Analytical Biochemistry 2005;339:69-72.

Miazek K, Iwanek W, Remacle C, Richel A, Goffin D. Effect of metals, metalloids and metallic nanoparticles on microalgae growth and industrial product biosynthesis: A review. International Journal of Molecular Sciences 2015;15:23929-69.

Nikookar K, Moradshahi A, Hosseini L. Physiological responses of *Dunaliella salina* and *Dunaliella tertiolecta* to copper toxicity. Biomolecular Engineering 2005;22:141-6.

Ngo HTT, Gerstmann S, Frank H. Toxicity of cadmium to the green alga *Parachlorella kessleri*: Producing Cd-loaded algae for feeding experiments. Toxicological and Environmental Chemistry 2009;91(2):279-88.

Nugroho AP, Handayani NSN, Pramudita IGA. Combined effects of copper and cadmium on *Chlorella pyrenoidosa* H. Chick: subcellular accumulation, distribution, and growth inhibition. Toxicological and Environmental Chemistry 2017;99:1368-77.

Nugroho AP, Frank H. Producing Cu-loaded algae for feeding experiments: effects of copper on *Parachlorella kessleri*. Toxicological and Environmental Chemistry 2011;93(3): 537-48.

Pawlik-Skowrońska B, Skowroński T. Freshwater algae. In: Prasad MNV, editor. Metals in the Environment: Analysis by Diversity. New York: Marcel Dekker, Inc.; 2001. p. 70.

Perales-Vela HG, González-Moreno S, Montes-Horcasitas C, Cañizares-Villanueva RO. Growth, photosynthetic and respiratory responses to sub-lethal copper concentrations in *Scenedesmus incrassatulus* (Chlorophyceae). Chemosphere 2007;67:2274-81.

Pinto E, Sigaud-Kutner TCS, Leitão MAS, Okamoto OK, Morse D, Colepicolo P. Heavy metal-induced oxidative stress in algae. Journal of Phycology 2003;39:1008-18.

Prado R, García R, Rioboo C, Herrero C, Cid Á. Suitability of cytotoxicity endpoints and test microalgal species to disclose the toxic effect of common aquatic pollutants. Ecotoxicology and Environmental Safety 2015;114:117-25.

Qian H, Li J, Sun L, Chen W, Sheng GD, Liu W, Fu Z. Combined effect of copper and cadmium on *Chlorella vulgaris* growth and photosynthesis-related gene transcription. Aquatic Toxicology 2009;94:56-61.

Rajaganapathy V, Xavier F, Sreekumar D, Mandal PK. Heavy metal contamination in soil, water and fodder and their presence in livestock and products: A review. Journal of Environmental Science and Technology 2011;4(3):234-49.

Rezayian M, Niknam V, Ebrahimzadeh H. Oxidative damage and antioxidative system in algae. Toxicology Reports 2019; 6:1309-13.

Rizki AA. Effect of the Mixture of Cu and Cd on the DNA Damage *Chlorella sorokiniana* Shirira et Krauss [undergraduate]. Yogyakarta, Universitas Gadjah Mada; 2019.

Sartory DP. Spectrophotometric Analysis of Chlorophyll *a* in Freshwater Phytoplankton [dissertation]. Bloemfontein, University of Orange Free State; 1982.

Shehata SA, Lasheen MR, Kobbia IA, Ali GH. Toxic effect of certain metals mixture on some physiological and morphological characteristics of freshwater algae. Water, Air, and Soil Pollution 1999;110:119-35.

Tjahjono A, Suwarno D. The spatial distribution of heavy metal lead and cadmium pollution and coliform abundance of waters and surface sediment in Demak. Journal of Ecological Engineering 2018;19(4):43-54.

Torres MA, Barros MP, Campos SCG, Pinto E, Rajamani S, Sayre RT, Colepicolo P. Biochemical biomarkers in algae and marine pollution: A review. Ecotoxicology and Environmental Safety 2008;71:1-15.

Tripathi BN, Gaur JP. Physiological behaviour of *Scenedesmus* sp. during exposure to elevated levels of Cu and Zn and after withdrawal of metal stress. Protoplasma 2006;229:1-9.

Valko M, Morris H, Cronin MTD. Metals, toxicity and oxidative stress. Current Medicinal Chemistry 2005;12:1161-208.

Walne PR. Studies on the food value of nineteen genera of algae to juvenile bivalves of the genera *Ostrea*, *Crassostrea*, *Mercenaria*, and *Mytilus*. Fishery Investigations 1970;26:1-62.

Warren CR. Rapid measurement of chlorophylls with a microplate reader. Journal of Plant Nutrition 2008;31:1321-32.

Yuan Y, Bi Y, Hu Z. Phytoplankton communities determine the spatio-temporal heterogeneity of alkaline phosphatase activity: Evidence from a tributary of the three gorges reservoir. Scientific Reports 2017;7(16404):1-9.

Zeb B, Ping Z, Mahmood Q, Lin Q, Pervez A, Irshad M, Bilal M, Bhatti ZA, Shaheen S. Assessment of combined toxicity of heavy metals from industrial wastewaters on *Photobacterium phosphoreum* T3S. Applied Water Science 2016;7:2043-50.

Zulfikar WG. Combined Effects of Copper (Cu) and Cadmium (Cd) to Protein, Carbohydrate, and Chlorophylls Contents and Alkaline Phosphatase Activity on *Chlorella pyrenoidosa* H. Chick [undergraduate]. Yogyakarta, Universitas Gadjah Mada; 2018.

Factors Related to Coastal Communities' Water-Related Natural Disaster Awareness, Preparedness, Resilience and Recovery in Three Cyclone Nargis Affected Areas in the Ayeyarwaddy Delta Region, Myanmar

Zay Yar Min[1], Kampanad Bhaktikul[1*], Sayam Aroonsrimorakot[1], Saranya Sucharitakul[1], Allan Sriratana Tabucanon[1], and Budi Eko Siswoyo[2]

[1]*Faculty of Environment and Resource Studies, Mahidol University, Nakhon Pathom 73170, Thailand*
[2]*Faculty of Social Sciences and Humanities, Mahidol University, Nakhon Pathom 73170, Thailand*

ARTICLE INFO

Received: 15 Jan 2020
Received in revised: 12 May 2020
Accepted: 26 May 2020
Published online: 12 Jun 2020
DOI: 10.32526/ennrj.18.3.2020.29

Keywords:
Awareness/ Preparedness/ Resilience/ Recovery/ Coastal communities/ Water-related natural disaster

*** Corresponding author:**
E-mail:
kampanad.bha@mahidol.ac.th

ABSTRACT

Natural disasters have a negative impact on the socio-economy of a country. This cross-sectional analytical study determined the factors that influence coastal communities' water-related disaster awareness, preparedness, resilience and recovery in Cyclone Nargis affected areas in Myanmar. A total of 390 respondents from the three townships most affected by Cyclone Nargis in the Ayeyarwaddy Delta Region were purposively selected. Data were analyzed using SPSS Version 22.0. Associations between variables were analyzed by using binary logistic regression with $p<0.05$. Multivariate analysis was performed for the final model and interpreted with adjusted odds ratio and 95% confidence interval. Among respondents, more than 75% were not only aware and prepared before the disaster but had recovered and demonstrated resilience following the disaster. The respondents who had problems recovering on the "financial" index were 0.5 times less likely to exhibit recovery (OR=0.558, 95% CI=0.346-0.899, p=0.016) in binary analysis. The respondents who had problems recovering on the "health" index were 0.3 times less likely to demonstrate recovery (OR=0.387, 95% CI=0.194-0.772, p=0.007) in multivariate analysis. It is recommended that awareness and disaster management education programs that shape behavioral change are initiated which target both rural and urban areas in Myanmar.

1. INTRODUCTION

Natural disasters such as floods, tornadoes and cyclones have negative impacts on human life and the environment as well as economic implications. Globally, an average of 60,000 people die from natural disasters every year (OWID, 2019). Over the past decade, natural disasters have been responsible for 0.1% of deaths across the world (OWID, 2019). According to the UNDP (2014), it is estimated that disasters, mostly cyclones, hurricanes and earthquakes, cost >$ 180 billion (US) per annum and have become key global issues.

Disasters can be caused not only by nature but also by human error. Human societies are often created which lack sufficiently strong infrastructure to withstand natural pressures. This can lead to societies being placed in a vulnerable position. People who live in poorer countries are most vulnerable such that 90% of disaster fatalities occur in developing countries (UNDP, 2014). More generally, the same people are often the most affected by disasters because of poorly planned infrastructure and their inability to access resources. There are several factors that need to be considered to prevent disasters which impact on human environments, and it is essential to apply strategies to reduce the negative outcomes of natural disasters. To address this need, the United Nations Strategy for Disaster Risk Reduction (UNISDR) has

Citation: Min ZY, Bhaktikul K, Aroonsrimorakot S, Sucharitakul S, Tabucanon AS, Siswoyo BE. Factors related to coastal communities' water-related natural disaster awareness, preparedness, resilience and recovery in three cyclone Nargis Affected Areas in the Ayeyarwaddy Delta Region, Myanmar. Environ. Nat. Resour. J. 2020;18(3):304-313. DOI: 10.32526/ennrj.18.3.2020.29

Home

developed a systematic approach called Disaster Risk Reduction (DRR), which mainly focuses on proactive activities to reduce disaster risks, and to strengthen capacities in vulnerable communities with information that supports sustainable development (UNISDR, 2005).

The occurrence of natural hazards which can lead to disasters has become more frequent, and repercussions more widespread due to vulnerability and a lack of resilience. Developing countries such as Myanmar are particularly vulnerable, and the effects of natural hazards can have a negative effect on their progress in achieving the Sustainable Development Goals (SDGs) set by the United Nations. This paper focuses on the Ayeyarwaddy Delta Region which is one of the low-lying disaster-prone areas in Myanmar where flooding frequently occurs as a consequence of storm surges, tropical storms and cyclones.

In May 2008, Myanmar suffered a severe and slow-moving cyclone, Nargis, which crossed the south of the country during a period which lasted over two days. The Ayeyarwaddy Delta Region, and its coastal communities, experienced the worst water- related natural disaster in the history of the region. According to the UN estimate, a total of 2.4 million people were affected (IFRC, 2011; PONJA, 2008). The number of people who died totaled 84,500 while 53,800 people were declared missing (IFRC, 2011). Although Myanmar had experienced disasters before Cyclone Nargis, the lack of public awareness and disaster preparedness exacerbated the effects of the cyclone. Awareness and preparedness were not limited to disaster risk reduction and sustainable resource management (UNEP, 2009), but technically refer to awareness on places to stay, community leaders' instruction, and water and food relocation; while preparedness includes evacuation plans and measures, early warning information sources, and government-supported training/drill exercises.

Stakeholders at the state and local level in Myanmar tend to put more effort into emergency relief and humanitarian assistance than reinforce the concept of "resilience" for sustainable integrated DRR. Disaster resilience is embedded in perspectives of sustainability, capability, and the capacity of individual, communities, organizations, and states to cope in response to a disaster. In this regard, disaster recovery can offer a strategic approach to increase resilience in farming communities to combat future shocks through risk-informed development activities (Parsons et al., 2016). The recovery process tries to ensure "build back better", to reduce pre-disaster risks (UNISDR, 2005) and consider aspects of restoration and reconstruction. A literature search revealed a limited number of natural disaster studies in Myanmar; in fact, no studies were found to have reported on factors related to disaster awareness, preparedness, resilience and recovery at community level in Myanmar. Accordingly, this paper studies the factors influencing disaster awareness, preparedness, resilience and recovery of water-related disaster among coastal communities in the Cyclone Nargis affected Ayeyarwaddy Delta Region of Myanmar.

2. METHODOLOGY

2.1 Study design and study area

This cross-sectional analytical study uses a mixed-methods approach and semi-structured questionnaires to investigate the coastal Ayeyarwaddy Delta Region which was purposively selected due to its long history as a water-related natural disaster-prone region in Myanmar. The paper is written with specific reference to the aftermath of the severe Cyclone Nargis in 2008. Based on The World Bank (2014) data, the three most Cyclone Nargis affected coastal communities, namely the townships of Bogale, Pyapon, and Ngapudaw, (Figure 1), were selected for this present study.

2.2 Sample size, sampling technique and data collection tools

The survey sample size of 390 respondents selected from three townships was calculated using Cochran's formula (Barlett et al., 2001). The survey respondents were selected through a multi-stage sampling process, using a mix of purposive and random sampling methods. Simple random sampling, the lottery method, was adopted to select respondents. This design includes the collection, analysis, and integration of qualitative and quantitative data in a single or multiphase study (Hanson et al., 2005).

A semi-structured questionnaire, adapted from an earlier study on knowledge and perceptions of natural disasters (Cvetković et al., 2015; Ozkazanc and Yuksel, 2015; OECD, 2010), was administered to respondents. The questionnaire, which mostly used Likert scale, consisted of six parts: Socio-demographic characteristics, Knowledge of the history of Cyclone Nargis, Awareness of disaster, Preparedness for disaster, Resilience arising from the 2008 Cyclone Nargis and Recovery from the 2008 Cyclone Nargis (Cvetković et al., 2015).

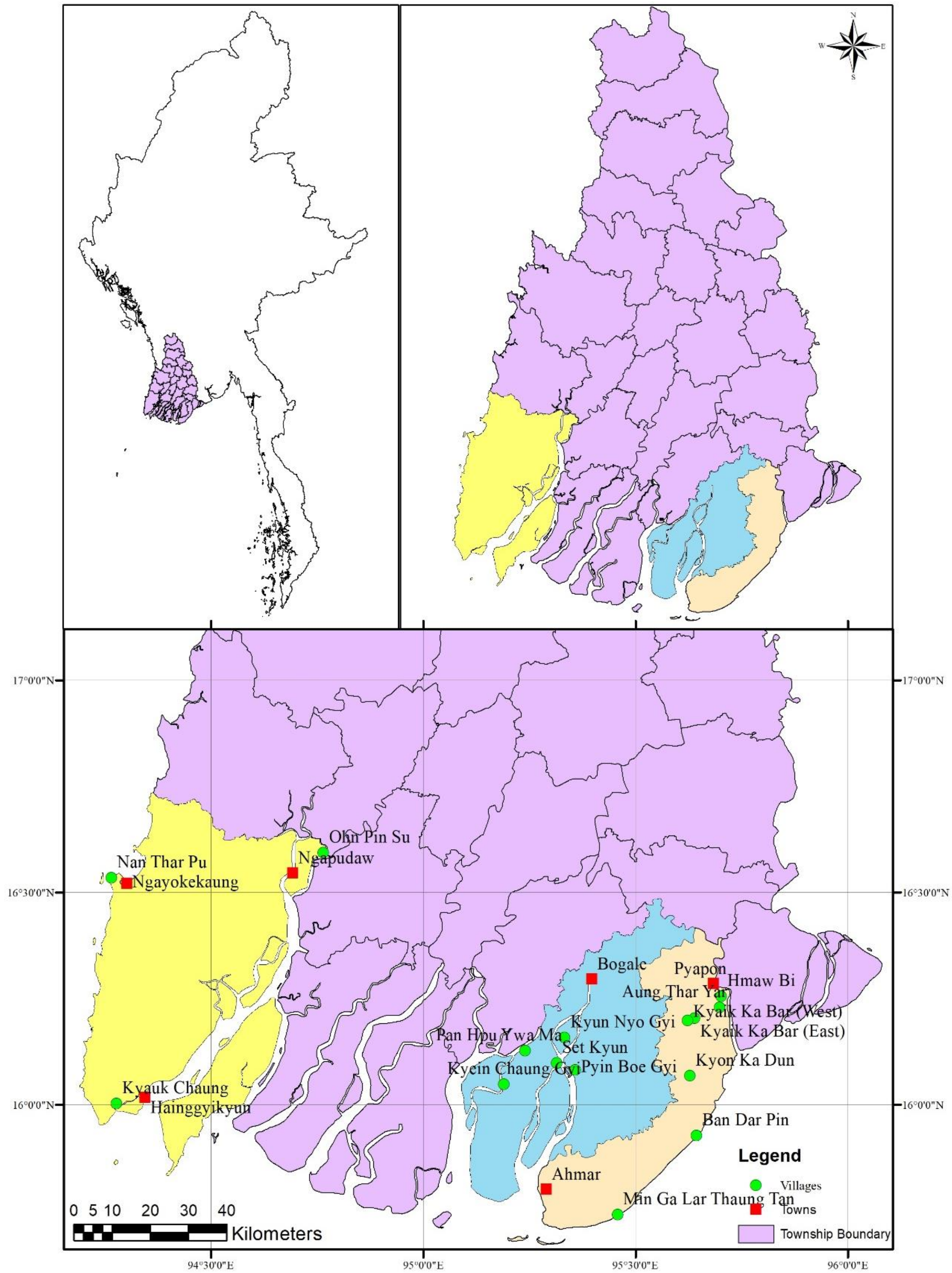

Figure 1. Selected study area in the Ayeyarwady Delta Region, Myanmar Myanmar (MIMU, 2019)

In the Awareness part of the survey, the total score varied from 0 to 7 where "0" represented "poor awareness" and "more than and equal to one" represented "active awareness". This variable consists of indicators related to play to stay, leader of the community, water for drinking, and food for store. In the Preparedness part, the total score varied from 0 to 11 where "0 to 3" represented "poor preparedness" and "more than and equal to 4" represented "active preparedness". This variable consists of indicators related to plans for evacuation, measures to prepare for natural disasters, finding the source of disaster predictions for early warning, and the status of local government in conducting training/drill. The use of the term "Government" which didn't specifically mentioned its level, indicates government at all three levels, national, regional and local.

In the Resilience part of the survey, the total score varied from 0 to 3 where "0" represented "less resilience" and a score of "more than and equal to one" represented "high resilience". This variable consists of indicators related to hours/day closed before being evacuated, status of receiving food and water, and person organized for distribution of food and water. The Recovery question was categorized into "yes" and "no". This variable refers to current recovery of household after ten years from previous disasters.

2.3 Data analysis

Data analysis was performed using the software package Statistical Product and Service Solutions (SPSS) Version 22.0. All categorical variables were measured by frequency and percentage (Table 1). Associations between independent variables (socio-demographic characteristics, knowledge of the past history of Cyclone Nargis 2008) and dependent variables (awareness, preparedness, resilience and recovery) were analyzed using binary logistic regression (Table 2-5). Multivariate analysis was performed using multiple logistic regressions to check for a clear association between independent and dependent variables (Table 2-5). The results were interpreted with adjusted odds ratio (OR) and 95% confidence interval (95% CI). Statistically significant association was determined at a significance level of 0.05.

3. RESULTS AND DISCUSSION

3.1 Descriptive results

3.1.1 Descriptive results of independent variables

Most respondents (53.8%) were aged between 40-60 years, (83.1%) were married, 64.9% were self-employed, and among the 390 respondents, 69.2% were male and 30.8% were female. Regarding their resident township, 34.9% were from Bogale Township, 36.1% from Pyapon Township and 29% were from Ngapudaw Township. Among the respondents, almost all of them (82.6%) were from rural areas and 77.4% of their households were close to the river or coast. With regard to households, 53.3% of respondents had fewer than 4 household family members. In this study, most of the respondents (79.2%) received some storm warning before Nargis hit and among the 390 respondents, 72.2% received information from government, 16.8% from NGO and 11% from community leader respectively. Most of the respondents (83.1%) traveled to an evacuation shelter during Nargis by themselves, 30.5% got medical help from the government and 24.1% from an NGO. Regarding the most affected impact after one year of 2008 Nargis, 30.3% had an impact to their household income, 27.4% to theie livelihood, 22.3% to their health status and 20% to their related-education.

3.1.2 Descriptive results of dependent variables

According to the findings, more than 80% of respondents had an active awareness of water-related disaster. Among the respondents, almost all of them: 77.9% had an active preparedness, 82.7% had high resilience, and 74.4% of the households fully recovered overall. This result was supported by a study conducted in India among postgraduate students in a private dental institute on disaster management (Rajesh et al., 2011) and a study in Nepal on disaster risk reduction knowledge among local people (Tuladhar et al., 2015), which reported that more than 80 % of the respondents had an active awareness. Study on the impact of education and experience of disaster preparedness in the Philippines and Thailand (Hoffmann and Muttarak, 2017) also reported that about 78% of respondents had active disaster preparedness consistent with the disaster preparedness action.

Table 1. Level of awareness, preparedness, resilience and recovery of Ayeyarwaddy Delta Region respondents (n=390)

Variables	Frequency (n)	Percentage (%)
Awareness		
Active	326	83.6
Poor	64	16.4
Preparedness		
Active	304	77.9
Poor	86	22.1
Resilience		
High	343	87.9
Low	47	12.1
Recovery		
Yes	290	74.4
No	100	25.6

3.2 Associations between independent and dependent variables

3.2.1 Final model for the factors associated with awareness

Education level of the household head showed a statistically significant association with disaster awareness in the binary analysis, but the association was not statistically significant in multivariate analysis. These results are consistent with a study in Pakistan of the earthquake-prone city of Quetta on risk perception among households which showed that the higher the education level of a respondent, the more active awareness they had (Ainuddin et al., 2014). Another global project on reducing vulnerability to natural disasters (Muttarak and Lutz, 2014) stated that the promotion of public education would enhance adaptive capacity and reduce vulnerability in natural disasters. The 390 respondents in the Ayeyarwaddy Delta Region study who received "NGO" storm-warning information were found to be 3.6 times more likely to have active awareness than those who received information from their "Government" (OR=3.570, 95% CI=1.059-12.031, p=0.040) in binary analysis, and this association was statistically significant in multivariate analysis (OR=4.087, 95% CI=1.059-15.773, p=0.041). These local results were consistent with findings from a contemporary study on community-based disaster reduction activity in Sri Lanka (Kurita et al., 2007). It seems that "NGO" engagement with the local coastal communities in Myanmar was greater than that of the "Government" due to awareness-raising programs being widely conducted by NGOs after Cyclone Nargis in 2008. Findings of the key informant interviews reported that the community leaders, NGOs, and religious leaders also organized distributions of food, water, and medical assistance. Below, Table 2 shows the final model for the factors associated with awareness.

Table 2. Final model for the factors associated with awareness

Variable	Awareness	
	AOR (95% CI)	p-value
Residence township		
Bogale	1 (ref :)	
Pyapon	3.796 (1.320-10.917)	0.013*
Ngapudaw	2.569 (1.101-5.995)	0.029*
Residence area		
Urban	1 (ref :)	
Rural	2.413 (0.986-5.905)	0.054
In 2008, Received Warning Information from		
Government	1 (ref:)	
Community leader	0.398 (0.147-1.077)	0.070
NGO	4.087 (1.059-15.773)	0.041*
Longer-term support for crops after 2008 Cyclone Nargis (provision of rice seeds, fertilizers etc. for 2 to 8 years)		
No	1 (ref :)	
Yes	16.008 (1.492-171.739)	0.022*
Preparedness		
Poor	1 (ref :)	
Active	2.628 (1.167-5.916)	0.020*

*p-value <0.05, CI=Confidence interval

3.2.2 Final model for the factors associated with preparedness

Binary analysis shows that compared with families where the "father" was the head of household, those headed by "other relatives" were 0.1 times less likely to demonstrate active preparedness (OR=1.138, 95% CI=0.025-0.775, p=0.024). This result was consistent with a recent study in Serbia on the role of gender in preparedness and response behaviors towards flood risk (Cvetković et al., 2018). This consistency could be due to the same cultural context whereby the "father" takes the leading role in the family compared to other relatives in respect of both family affairs and other circumstances. The 390 Ayeyarwaddy Delta Region respondents who received "NGO" storm-warning information, however, were 0.3 times less likely to show active preparedness compared to those who received information from the "Government" (OR=0.256, 95% CI=0.132-0.499, <0.001) in binary analysis and (OR=0.222, 95%

CI=0.106-0.466, p<0.00) in multivariate analysis. This disparity between the effectiveness of "NGO" and "Government" storm-warning information could be due to underestimation of the risk of weather-related disasters by the population of coastal communities, based on their "natural" tendency to think that information-sharing by the "Government" was more accurate than that from other sources (Somers and Svara, 2009). Findings of the key informant interviews also reported that the government department of disaster management not only developed the disaster information and early warning system through TV, FM radio, and social media, but also through the "DAN (Disaster Alert Notification)" as a mobile application platform.

The respondents who received medium- term support (4 months to 2 years) and longer-term support (2 to 8 years) for education were 2.4 and 3.6 times more likely to have active preparedness (OR=2.444, 95% CI=1.033-5.784, p=0.042; OR=3.620, 95% CI=1.575-8.319, p=0.002) than other respondents according to the binary analysis. This result was consistent with another recent study on the importance of education on disasters and emergencies (Torani et al., 2019). These medium- and longer-term programs could be due to support not only for education in general but also for disaster education so that the respondents had active preparedness. The respondents who had "health" problems were 3.2 times more likely to have active preparedness (OR=3.219, 95% CI=1.317-7.870, p=0.010) in binary analysis and (OR=5.674, 95% CI=1.577-20.419, p=0.008) in multivariate analysis. In contrast, medically vulnerable cohorts of the population were less likely to have household disaster preparedness according to a study in the United States on disaster preparedness among medically vulnerable populations (Bethel et al., 2011). However, these medically vulnerable populations were more likely to prepare for their medical supply and this present study in Myanmar did not include detailed and specific questions related to health problems and medications. Below, Table 3 shows the final model for the factors associated with preparedness.

Table 3. Final model for the factors associated with preparedness

Variable	Preparedness	
	AOR (95% CI)	p-value
In 2008, Received Warning Information from		
Government	1 (ref :)	
Community leader	0.299 (0.131-0.682)	0.004*
NGO	0.222 (0.106-0.466)	<0.001**
In 2008, when Nargis hit your village/town, who took you to the evacuation place (Refuge/ Shelter)?		
Family member/myself	1 (ref :)	
Government	0.901 (0.274-2.965)	0.864
Community leader/NGO	0.276 (0.098-0.777)	0.015*
Awareness		
Poor	1 (ref :)	
Active	2.053 (0.969-4.350)	0.060
Longer-term Support for Education after 2008 Cyclone Nargis (from 2 to 8 years)		
No	1 (ref :)	
Yes	2.809 (1.218-6.481)	0.015*
Health problems from which to recover (problems to recover from 2008 Cyclone Nargis)		
No	1 (ref :)	0.008*
Yes	5.674 (1.577-20.419)	

* p-value <0.05, **p<0.001, CI=Confidence interval

3.2.3 Final model for the factors associated with resilience

The respondents who received storm-warning information before 2008 Cyclone Nargis were 2.2 times more likely to have high resilience (OR=2.207, 95% CI=1.140-4.275, p=0.019) according to binary analysis. This analysis pointed out that "receiving storm-warning information" was important in strengthening the resilience of the respondents during natural disasters as they needed to prepare for the disaster and to gain resilience. This result was consistent with another study that encouraged developing integrated and people-centered early warning systems to make progress toward the resilience (Tanner et al., 2009). The respondents who had problems in recovering from "house destroyed and reconstruction constraints" were 3.9 times more likely to have higher resilience than those who did not have reconstruction constraints (OR=3.923, 95% CI=2.058-7.476, p<0.001) in binary analysis. Those two variables also maintained a statistically significant association in multivariate analysis where the value of p<0.001 (OR=3.906, 95% CI=2.037-7.489). Although respondents' houses were destroyed, they showed higher resilience than those whose houses were not destroyed. Their resilience could be due to support from the Government, local authority and NGOs in settling housing issues. Findings of the key informant interviews also reported that there is a Myanmar national action plan and framework for community disaster resilience and it has a short, medium, and long term mitigation strategies and activities plan. The Ministry of Home Affairs was in charge on maintaining law and order during the disaster, while the Department of Meteorology and Hydrology was responsible for disaster warnings. Below, Table 4 shows the final model for factors associated with resilience.

Table 4. Final model for factors associated with resilience

Variable	Resilience	
	AOR (95% CI)	p-value
In 2008 Cyclone Nargis, received storm warning		
No	1 (ref:)	
Yes	2.126 (1.061-4.260)	0.033*
Who organized medical help and assistance for injured people?		
Family member/Myself	1 (ref:)	
Government	0.473 (0.211-1.059)	0.069
Community leader/NGO	0.962 (0.420-2.206)	0.928
Longer-term Support for Education after 2008 Cyclone Nargis (from 2 to 8 years)		
No	1 (ref:)	
Yes	2.043 (0.956-4.365)	0.065
Problems from which to recover (House destroyed and reconstruction constraints) following 2008 Cyclone Nargis		
No	1 (ref:)	
Yes	3.906 (2.037-7.489)	<0.001**

* p-value <0.05, **p<0.001, CI=Confidence Interval

3.2.4 Final model for the factors associated with recovery

In multivariate analysis, respondents who were more than 60 years of age were 0.3 times less likely to recover than those who were below 40 years of age (OR=0.0325, 95% CI=0.148-0.712). The result of this study was consistent with a study on long-term impacts of natural disasters among survivors of a disaster in Azerbaijan which found that older population cohorts made less recovery and were more vulnerable compared to younger population cohorts (Rafiey et al., 2016). Less recovery and more vulnerable conditions could be due to factors associated with age such as chronic health conditions including cognitive ability and sensory awareness in terms of the long- term impacts of natural disaster (Rafiey et al., 2016). Those with a "high school" level of education among Cyclone Nargis survivors was 4.4 times more likely to lead to recovery compared with those who had attended "no school/illiterate" (OR=4.413, 95% CI=1.425-13.668, p= 0.010) in binary analysis and (OR=5.250, 95% CI=1.386-19.888, p=0.015) in multivariate analysis. This result was supported by a study on reducing vulnerability to natural disasters which found that a higher education level led not only to better ability in situations of vulnerability but also a better perception of understanding risks thereby enabling those who participated in the study to act on threats and recover from natural disasters (Muttarak and Lutz, 2014). The respondents who received storm-warning information before Cyclone Nargis in 2008 were 1.7 times more likely to recover (OR=1.739, 95% CI=1.025-2.950, p=0.040) in binary analysis. This finding was consistent with an earlier study which demonstrated that those respondents who received storm-warning information before a disaster showed greater recovery which could have been due to personal responses to disaster management evacuation orders (Paul and Dutt, 2010). The Ayeyarwaddy Delta Region respondents who had problems recovering from "financial" difficulties were 0.5 times less likely to experience recovery than those who did not have home reconstruction constraints

(OR=0.558, 95% CI=0.346-0.899, p=0.016) in binary analysis. The respondents who had problems recovering in terms of their "health" were 0.5 times less likely to have experienced recovery than those who did not have health problems (OR=0.496, 95% CI=0.279-0.885, p=0.017) in binary analysis and (OR=0.387, 95% CI=0.194-0.772, p=0.007) in multivariate analysis. As respondents in these three coastal communities had low incomes, they needed financial support to recover from the disaster because they had suffered negative impacts including financial and health problems. On the other hand, findings of the key informant interviews also reported that the main challenges for the disaster management in Myanmar not only related to community knowledge and participation, but also budget capacity for emergency response, preparedness, and recovery. Below, Table 5 shows the final model for the factors associated with recovery.

Table 5. Final model for the factors associated with recovery

Variable	Recovery	
	AOR (95% CI)	p-value
Age		
<40 years	1 (ref:)	
40-60 years	0.958 (0.495-1.852)	0.898
>60 years	0.325 (0.148-0.712)	0.005*
Residence Township		
Bogale	1 (ref:)	
Pyapon	0.676 (0.306-1.495)	0.333
Ngapudaw	2.087 (0.994-4.379)	0.052
Education level of Household		
No school/Illiterate	1 (ref:)	
Primary school	3.754 (1.111-12.691)	0.033*
Middle school	7.974 (2.241-28.377)	0.001*
High school	5.250 (1.386-19.888)	0.015*
University education	16.869 (2.455-115.917)	0.004*
Number of household members		
<4	1 (ref:)	
>4	1.678 (0.978-2.881)	0.060
Medium-term Support for Crops after 2008 Cyclone Nargis (provision of rice seeds, fertilizers etc. (for_4 months to 2 years)		
No	1 (ref:)	
Yes	4.214 (2.040-8.702)	<0.001**
Medium-term Support for Livelihoods after 2008 Cyclone Nargis (from 4 months to 2 years)		
No	1 (ref:)	
Yes	0.441 (0.244-0.798)	0.007*
Health problems from which to recover (problems requiring recovery from 2008 Cyclone Nargis)		
No	1 (ref:)	
Yes	0.387 (0.194-0.772)	0.007*
Awareness		
Poor	1 (ref:)	
Active	0.465 (0.202-1.069)	0.071

* p-value <0.05, **p<0.001, CI=Confidence interval

3.3 Moving forward

In this present study, socio-economic index factors and health were not the focuses of inquiry, so further studies should be conducted to address these determinants with regard to disaster awareness, preparedness, resilience and recovery. Disaster management planning to strengthen disaster awareness, preparedness, resilience and recovery always requires some form of change in behavior, and change is often difficult to bring about. Government, private-sector organizations, or other social units have many priorities other than disaster planning, and societal and community needs are invariably greater than the resources that are available (Tierney, 1993). On the other hand, disaster introduces greater uncertainty into decision making and this uncertainty calls for an understanding of the social processes that shape behavioral change pre- and post-disaster (Birkmann et al., 2010). Therefore, appropriate risk communication should be emphasized to reach the targeted audiences and induce the desired changes in behavior and perception (Gwee et al., 2011), which can be applied both to coastal communities' water-related disaster awareness, preparedness, resilience and recovery in Ayeyarwaddy Delta Region. Government has developed the disaster information and early warning system through TV, FM radio, social media, and DAN mobile application, however Son et al. (2018) emphasized to consider complex socio-behavioral-technical interaction, situation awareness approach through IT-based systems designed is important for effective situation aware decision making support. The perception of 'community' changes and sustained behavioral change through social media use from a geographic locality to communities of interest and, ideally, disaster resilience communities of learning (Dufty, 2012) can also be considered.

4. CONCLUSION

All the collected data were analyzed and interpreted to determine the factors that influence coastal communities' water-related disaster awareness, preparedness, resilience and recovery. It can be concluded that active awareness and preparedness, high resilience and high recovery were demonstrated by all 390 respondents in the coastal communities of the Ayeyarwaddy Delta Region of Myanmar. However, as more than 80% of the respondents were from rural areas, it can be suggested that future awareness-raising programs and disaster management planning should be focused not only in rural area but also in urban areas. Although Government has a disaster warning system in the Ayeyarwaddy Delta Region, it should be extended to all low-lying disaster-prone areas in Myanmar as well as strengthen public-private partnership (i.e., NGOs and community leader engagement) to emphasize intended sustained behavioral change. There were only a few organizations and activities regarding emergency evacuation and assistance; therefore, the Government should have a plan and trained teams readied for emergency evacuation alongside medical teams with available health professional networks and organizations to strengthen disaster preparedness and management. Furthermore, the Government should conduct monitoring and evaluation visits to disaster-prone areas with the help of NGOs and multi-sectoral involvement to develop specific policies, procedures and practices for disaster management. As the population in this study was affected by Cyclone Nargis in 2008, with 25% of them still needing to recover from a previous cyclone, especially for the informal workers who were self-employed with more than 4 household family members, it is necessary to consider strategies to achieve full recovery in terms of short, medium and long term support of their needs, effectively with available resources. It is recommended that further studies are conducted including qualitative studies to investigate factors relating to the socio-economic index factors and health, and their impacts on disaster awareness, preparedness, resilience and recovery in order to know and solve problems at a variety of scales from households and townships to regions.

ACKNOWLEDGEMENTS

This research was conducted with financial support provided a "Mahidol University-Norway Capacity Building Initiative for ASEAN" scholarship. The authors would like to thank the reviewers for their constructive comments on the earlier version of the paper. Local stakeholders, facilitators and assistance offered by the local administrations in Bogale, Pyapon and Ngapudaw Townships in the Ayeyarwady Delta Region of Myanmar are also gratefully acknowledged for their cooperation and contribution along with field data collection. Our greatest appreciation goes to the participating respondents for their time in answering the questionnaires which provided vital information for this study.

REFERENCES

Ainuddin S, Routray JK, Ainuddin S. People's risk perception in earthquake prone Quetta city of Baluchistan. International Journal of Disaster Risk Reduction 2014;7:1-11.

Barlett JE, Kotrlik JW, Higgins CC. Organizational research: Determining appropriate sample size in survey research. Information Technology, Learning, and Performance Journal 2001;19(1):43-50.

Bethel JW, Foreman AN, Burke SC. Disaster preparedness among medically vulnerable populations. American Journal of Preventive Medicine 2011;40(2):139-43.

Birkmann J, Buckle P, Jaegar J, Pelling M, Setiadi N, Garschagen M, Fernando N, Kropp J. Extreme events and disasters: A window of opportunity for change? analysis of organizational, institutional and political changes, formal and informal responses after mega-disasters. Natural Hazards 2010;55:637-55.

Cvetković V, Ivanov A, Sadiyeh A. Knowledge and perceptions of students of the academy of criminalistic and police studies about natural disasters. International Scientific Conference "Archibald Reiss Days"-Thematic Conference Proceedings of International Significance; 2015 Mar 3-4; Belgrade: Serbia; 2015.

Cvetković VM, Roder G, Ocal A, Tarolli P, Dragicević S. The role of gender in preparedness and response behaviors towards flood risk in Serbia. International Journal of Environmental Research and Public Health 2018;15(2761):1-21.

Dufty N. Using social media to build community disaster resilience. Australian Journal of Emergency Management 2012;27(1):40-5.

Gwee QR, Shaw R, Takeuchi Y. Chapter 2 disaster education policy: Current and future. In: Shaw R, Shiwaku K, Takeuchi Y, editors. Disaster Education. Bingley: Emerald Group Publishing; 2011. p. 23-44.

Hanson WE, Creswell JW, Clark VLP, Petska KS, Creswell JD. Mixed methods research designs in counseling psychology. Journal of Counseling Psychology 2005;52(2):224-35.

Hoffmann R, Muttarak R. Learn from the past, prepare for the future: impacts of education and experience on disaster preparedness in the Philippines and Thailand. World Development 2017;96:1-20.

International Federation of Red Cross and Red Crescent Societies (IFRC). Myanmar: cyclone nargis 2008 facts and figures [Internet]. 2011 [cited 2019 Dec 24]. Available from: https://www.ifrc.org/en/news-and-media/news-stories/asia-pacific/myanmar/myanmar-cyclone-nargis-2008-facts-and-figures/.

Kurita T, Ikeda M, Suzuki K, Colombage SRN. Promotion of community-based disaster reduction activity through hands-on training in Sri Lanka. Journal of Natural Disaster Science 2007;29(2):41-51.

Muttarak R, Lutz W. Is education a key to reducing vulnerability to natural disasters and hence unavoidable climate change? Ecology and Society 2014;19(1):42.

Myanmar Information Management Unit (MIMU). Ayeyarwady region [Internet]. 2019 [cited 2019 Dec 16]. Available from: https://themimu.info/states_regions/ayeyarwady.

Organisation for Economic Co-operation and Development (OECD). Policy Handbook on Natural Hazard Awareness and Disaster Risk Reduction Education. Publishing Paris, 2010.

Our World in Data (OWID). Natural disasters [Internet]. 2019 [cited 2019 Dec 20]. Available from: https://ourworldindata.org/natural-disasters.

Ozkazanc S, Yuksel UD. Evaluation of disaster awareness and sensitivity level of higher education students. Procedia - Social and Behavioral Sciences 2015;197:745-53.

Parsons M, Glavac S, Hastings P, Marshall G, McGregor J, McNeill J, Morley P, Reeve I, Stayner R. Top-down assessment of disaster resilience: A conceptual framework using coping and adaptive capacities. International Journal of Disaster Risk Reduction 2016;19:1-11.

Paul BK, Dutt S. Hazard warnings and responses to evacuation orders: The case of Bangladesh's cyclone SIDR. Geographical Review 2010;100(3):336-55.

Post-Nargis Joint Assessment (PONJA). Post-nargis joint assessment report [Internet]. 2008 [cited 2019 Dec 16]. Available from: https://www.gfdrr.org/sites/default/files/GFDRR_Myanmar_Post-Nargis_Joint_Assessment_2008_EN.pdf.

Rafiey H, Momtaz YA, Alipour F, Khankeh H, Ahmadi S, Khoshnami MS, Haron SA. Are older people more vulnerable to long-term impacts of disasters? Clinical Interventions in Aging 2016;11:1791-5.

Rajesh G, Chhabra KG, Shetty PJ, Prasad KVV, Javali SBJ. Survey on disaster management among postgraduate students in a private dental institution in India. American Journal of Disaster Medicine 2011;6(5):309-18.

Somers S, Svara J. Assessing and managing environmental risk: Connecting local government management with emergency management. Public Administration Review 2009;69(2):181-93.

Son J, Aziz Z, Peña-Mora F. Supporting disaster response and recovery through improved situation awareness. Structural Survey 2008;26(5):411-25.

Tanner T, Mitchell T, Polack E, Guenther B. Urban governance for adaptation: assessing climate change resilience in ten Asian cities. IDS Working Paper 2009;315:1-47.

Tierney KJ. Disaster preparedness and response: research findings and guidance from the social science literature. US-ROC Workshop on Natural Disaster Reducation; 1993 June 24-26; Taipei: Taiwan; 1993.

Torani S, Majd PM, Maroufi SS, Dowlati M, Sheikhi RA. The importance of education on disasters and emergencies: A review article. Journal of Education and Health Promotion 2019;8(85):1-7.

Tuladhar G, Yatabe R, Dahal RK, Bhandary NP. Disaster risk reduction knowledge of local people in Nepal. Geoenvironmental Disasters 2015;2(5):1-12.

United Nations Development Programme (UNDP). Fast facts: disaster risk reduction and recovery [Internet]. 2014 [cited 2019 Dec 16]. Available from: https://www.undp.org/content/dam/undp/library/corporate/fast-facts/english/FF_DRR_11042014.pdf.

United Nations Environment Programme (UNEP). Learning from cyclone nargis: investing in the environment for livelihoods and disaster risk reduction - A case study [Internet]. 2009 [cited 2019 Dec 16]. Available from: http://hdl.handle.net/20.500.11822/14116.

United Nations International Strategy for Disaster Reduction (UNISDR). Hyogo framework for action 2005-2015: building the resilience of nations and communities to disasters [Internet]. 2005 [cited 2019 Dec 16]. Available from: https://www.unisdr.org/we/coordinate/hfa.

World Bank. Another nargis strikes every day post-nargis social impacts monitoring five years on [Internet]. 2014 [cited 2019 Dec 16]. Available from: https://www.gfdrr.org/sites/default/files/publication/Another-Nargis-Strikes-Every-Day.pdf.

The Effectiveness of Nitrogen Fertilization in *Codiaeum variegatum* L. and *Sansevieria trifasciata* L. and the Effects on Pb Accumulation

Mahayu Woro Lestari[1*], Anis Rosyidah[1], and Bulbul Purkait[2]

[1]*Faculty of Agriculture, University of Islam Malang, MT. Haryono Street No. 193, Malang, East Java 65144, Indonesia*
[2]*Department of Biochemistry, Midnapore Medical College, West Bengal, India*

ARTICLE INFO

Received: 2 Feb 2020
Received in revised: 4 May 2020
Accepted: 4 Jun 2020
Published online: 16 Jun 2020
DOI: 10.32526/ennrj.18.3.2020.30

Keywords:
Ammonium fertilizer/ Accumulation/ *Codiaeum*/ Lead/ *Sansevieria*

*** Corresponding author:**
E-mail: mwlestari@unisma.ac.id

ABSTRACT

The use of $(NH_4)_2SO_4$ fertilizer is vital in increasing plant growth and reducing the Pb content in soil. This study determined the ability of *Codiaeum* and *Sansevieria* to accumulate Pb due to $(NH_4)_2SO_4$ fertilization and its effects on their growth rate. The ammonium fertilizer was applied three days after repotting according to these treatment levels: 0, 100, and 200 kg N/ha, denoted as P_0, P_1, and P_2, respectively. The height of *Codiaeum* decreased by 45.04%, 24.67%, and 13.70% in treatment P_0, P_1 and P_2, respectively, one week after repotting. The Pb concentrations in *Codiaeum* decreased with increasing doses of N fertilizer, while in *Sansevieria*, Pb concentrations increased with higher doses of N fertilizer. A reduction in the soil pH was seen with increasing dosage of N fertilization in *Codiaeum*, while the pH of the medium with *Sansevieria* was stable. Therefore, the effect of the different N doses, which causes a decrease in soil pH, was more significant in *Codiaeum* compared with *Sansevieria*. Furthermore, the highest value of TF was found in *Codiaeum* treated with 200 kg N/ha.

1. INTRODUCTION

Lead (Pb) is one of the heavy metal pollutants that is one of the most important worldwide ecological problems. It is heavy metal contaminant in the environment. Pb poisoning is an old and significant public-health problem throughout the world (Flora et al., 2006). Pb contamination in the plant environment has been shown to be highly toxic with affects on some processes such as depression of seed germination (Islam et al., 2007).

Most soil used for the purpose of agriculture obtains its heavy metals from agrochemicals through synthetic fertilizers and pesticides. Parkpian et al. (2003), and Atafar et al. (2010) reported that chemical fertilization increased the presence of heavy metals in soils. Also, Ogunlade (2011) reported that the use of heavy metals such as Cu, Pb, and Hg in various pesticides contribute to the increase in their concentration in soils and plants.

Additionally, soil naturally contains these heavy metals, some of which play vital roles in the physiological processes of plants. Examples include Fe, Cu, Zn, and Ni, but in relatively small amounts. An excess of these metals is generally toxic to the plants. However, Cd and Pb are very poisonous, and, so far, their role is unknown in plant chemistry. According to (Lawlor et al., 2004), both elements are essential chemical contaminants in the environment and highly toxic to plants, animals, and humans. However, strategies implemented to clean up contaminated areas are generally costly (Longhurst et al., 2004), hence, there is a need to develop a cheap and environmentally friendly approach, such as fertilizing nitrogen using Ammonium Sulfate ($(NH_4)_2SO_4$).

In general, $(NH_4)_2SO_4$ is an inorganic salt with several uses, among which is as a soil fertilizer since it contains 21% nitrogen and 24% sulfur. When added to a planting medium, it forms Ammonium $(NH_4)^+$ and Sulfide $(SO_4)^{-2}$. In addition, the sulfide ions could bind with Pb^{+2} to form $PbSO_4$, which plants easily absorb (Gurnita et al., 2017). Additionally, it has been shown through some studies that ammonium sulfate has the capacity to accumulate Pb content in *Brassica pekinensis* and *B. juncea* var. multiceps (Wang et al., 2008b; Xiong and Lu, 2002), and in bicolor sorghum leaves (Zhuang et al., 2009).

Citation: Lestari MW, Rosyidah A, Purkait B. The effectiveness of nitrogen fertilization in *Codiaeum variegatum* L. and *Sansevieria trifasciata* L. and the effects on Pb accumulation. Environ. Nat. Resour. J. 2020;18(3):314-321. DOI: 10.32526/ennrj.18.3.2020.30

Phytoremediation is defined as the use of green plants to remove pollutants from the environment or to render them harmless. Phytoremediation can be applied to both organic and in-organic pollutants, present in solid substrates (e.g., soil), liquid substrates (e.g., water), and the air. One area of phytoremediation is phytoextraction. Salt et al. (1998), and Schmidt (2003) reported that the application of ammonium sulfate fertilizers to plants helps in increasing the efficiency of phytoextraction. According to Garbisu and Alkorta (2001), Quartacci et al. (2006), and Laidlaw et al. (2012), phytoextraction uses green plants to eliminate toxic metals from contaminated soil, making it an environmentally safe, relatively cheap and technically applicable strategy for the improvement of soils contaminated with heavy metals. However, its efficiency in hyperaccumulators is generally considered too slow due to low biomass production, slow growth rates and high metal specificity (Mulligan et al., 2001; Puschenreiter et al., 2001; Lesage et al., 2005).

The process of absorption and accumulation of heavy metals by plants starts with root absorption. Heavy metals must be in the form of a solution so that they can be absorbed by the roots of the plant. Heavy metals can reach the endoderm layer of the roots of the plant and then pass through xylem and phloem to the top of the plant. In this method, the plant attempts to avoid heavy metal contamination from its cells by storing heavy metals in certain organs, such as roots or leaves, so as not to inhibit the metabolism of tissue processes (Tangahu et al., 2011). Two of the plants that can absorb and accumulate heavy metals are *Codiaeum variegatum* and *Sansevieria trifasciata*. Both of these plants have been shown to be effective in removing Pb from polluted soil (Kumar and Saritha, 2014).

Application of inorganic fertilizers containing NH_4^+, on plant mobilization of Pb is greatly increased even at low pH (Tu et al., 2000; Schmidt, 2003). Similarly, the application of nitrogen modifications effectively increased the accumulation of Pb (Lin et al., 2010). However, the influence of $(NH_4)_2SO_4$ on the improvement of Pb uptake was not very prominent.

This project studied the growth rate of *Codiaeum* and *Sansevieria* and their ability to accumulate Pb due to fertilization with $(NH_4)_2SO_4$.

2. METHODOLOGY

2.1 Time and place

This research was conducted in the greenhouse of Agriculture Faculty, University of Islam Malang, East Java, Indonesia from September to November 2018. The altitude is 550 m above sea level, with a temperature of 20-29ºC, at 112º06′-112º07′ east longitude and 7º06′-8º02′ north latitude.

2.2 Materials

The varieties of plants used in this study were *Codiaeum* with Gracepink and *Sansevieria*. The *Codiaeum* was two months old with height ±30 cm and ±40 cm for the *Sansevieria* with the same age range. Both plants were acclimatized to the greenhouse for one month before planting. Also, one week prior to planting, the soil was prepared in a 5 kg plastic bag mixed with $Pb(NO_3)_2$ at a dose of 350 mg/kg of soil. Then the N fertilizer using ammonium sulfate was applied 3 days after repotting according to these treatments -0, 100 kg N/ha (1.19 g $(NH_4)_2SO_4$ /polybag) and 200 kg N/ha (2.38 g $(NH_4)_2SO_4$ /polybag).

2.3 Parameters measured

The growth of *Codiaeum* and *Sansevieria* was evaluated starting one week after planting at intervals once a week, by measuring the plant height and leaf area. Plant height was determined by extending the last collared leaf upright. Plant heights were also measured for each individual plant before harvest. Leaf areas were measured with Leaf Area Meter (LAM). Also, the effect of N fertilizer in the accumulation of Pb was determined using an Atomic Absorption Spectrophotometer. The effects on growth rate were evaluated by measuring the total root length, root dry weight, soil pH, concentration of Pb on soil, crop and root, and the Translocation Factor (TF). According to MacFarlane et al. (2002), TF values are calculated to determine the transfer of accumulated metal from roots to the plant crop. It is calculated as follows:

$$\frac{\text{Pb on shoot}}{\text{Pb on root}}$$

2.4 Experimental design

The data analysis used in this study was the Factorial Random Block Design. The treatment have two factors. The first factor was a dose of nitrogen, consisting of three levels -0, 100, and 200 kg N/ha.(Wati et al., 2019). The second factor were the plants used *Codiaeum* and *Sansevieria*. Then, all the combination treatments were replicated three times, and each treatment consisted of three samples.

2.5 Statistical analysis

The statistical analysis was performed using SPSS V.17 software (SPSS Inc., Chicago, IL, USA). The data were expressed in the form of means±standard error, and the means were statistically compared using the Duncan's multiple range test (DMRT) at the p<0.05% level.

3. RESULTS AND DISCUSSION

3.1 Result

3.1.1 The effect of nitrogen dose to plant growth

The height of the *Codiaeum* decreased by 45.04% in treatment P_0, although not significantly different from P_1 (24.67%) and P_2 (13.70%) in one week after repotting. This decrease was due to falling leaves. It supposedly happens due to the influence of Pb on the media. Then from the second week onwards, *Codiaeum* started forming new leaves. However, *Sansevieria* showed more resistance to Pb, as the different doses of N had no influence on the plant height. Figure 1 shows that there was no significant change in plant height from the first to the seventh week.

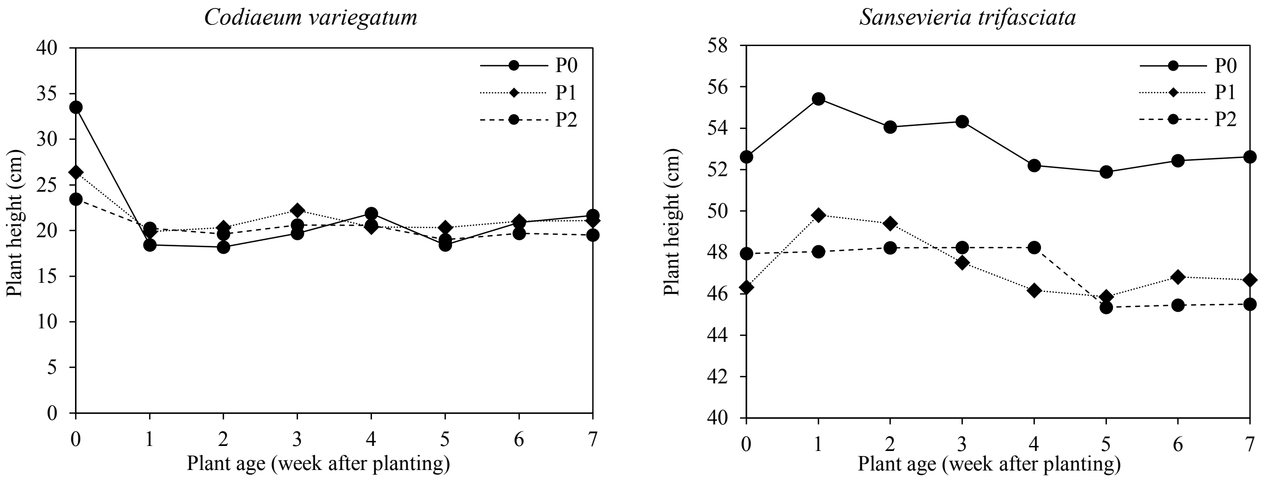

Figure 1. *Codiaeum variegatum* and *Sansevieria trifasciata* plant height development due to N fertilization. (P_0: control; P_1: dose of N 100 kg/ha; P_2: dose of N 200 kg/ha).

The mean of leaf area decreased by 21.19% (P_0), 21.62% (P_1), and 21.40% (P_3), respectively, for the three treatments for *Codiaeum* as shown in Figure 2. This was as a result of leaf loss due to soil exposure to Pb. However in *Sansevieria*, the reduction occurred only in the first week by 13.46% (P_0), 23.08% (P_1), and 17.82% (P_2). The decrease started with contraction at the leaves tips, which eventually dried out. The different doses of nitrogen did not affect the leaf area. The N fertilizer in *Codiaeum* is not able to increase plant height and leaf area. The loss of leaves in the first week is more due to the influence of Pb on media. In *Sansevieria*, N fertilizer and Pb had no significant effect.

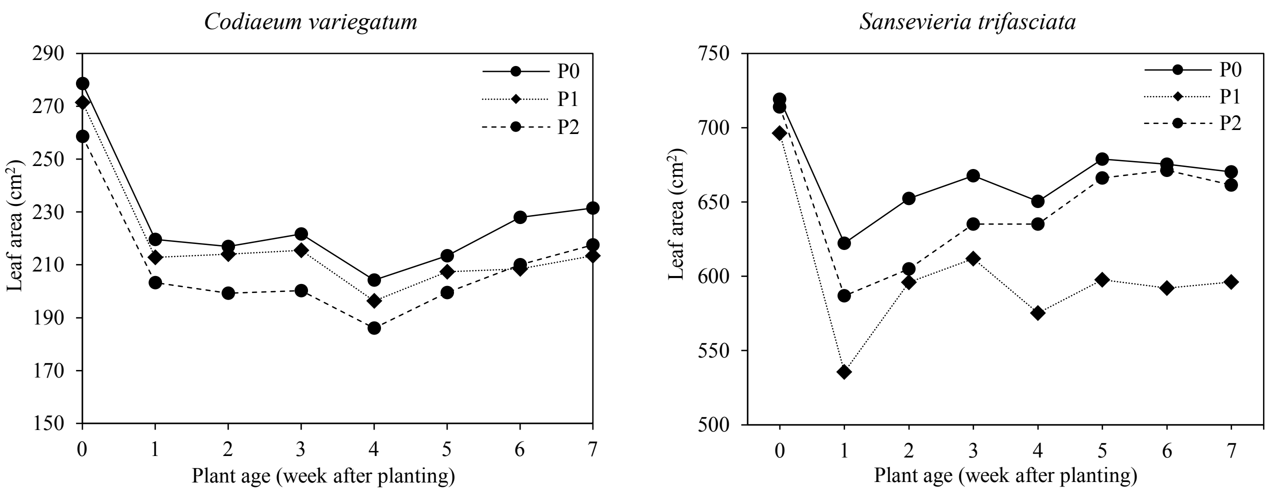

Figure 2. *Codiaeum variegatum and Sansevieria trifasciata* leaf area development due to nitrogen fertilizer (P_0: control; P_1: dose of N 100 kg/ha; P_2: dose of N 200 kg/ha).

3.1.2 The effect of nitrogen dose and concentration of Pb on crop, root and soil

In *Codiaeum*, the concentrations of Pb in the crop, roots, and soil decreased with increasing dose of N fertilizer. However in *Sansevieria*, the concentrations of Pb in the crop increases with an increasing dose of N fertilizer. N fertilizer does not affect Pb uptake in roots and soil. N fertilizer in *Codiaeum* can reduce Pb uptake in crops, roots, and soil, but it is not effective for *Sansevieria* (Figure 3).

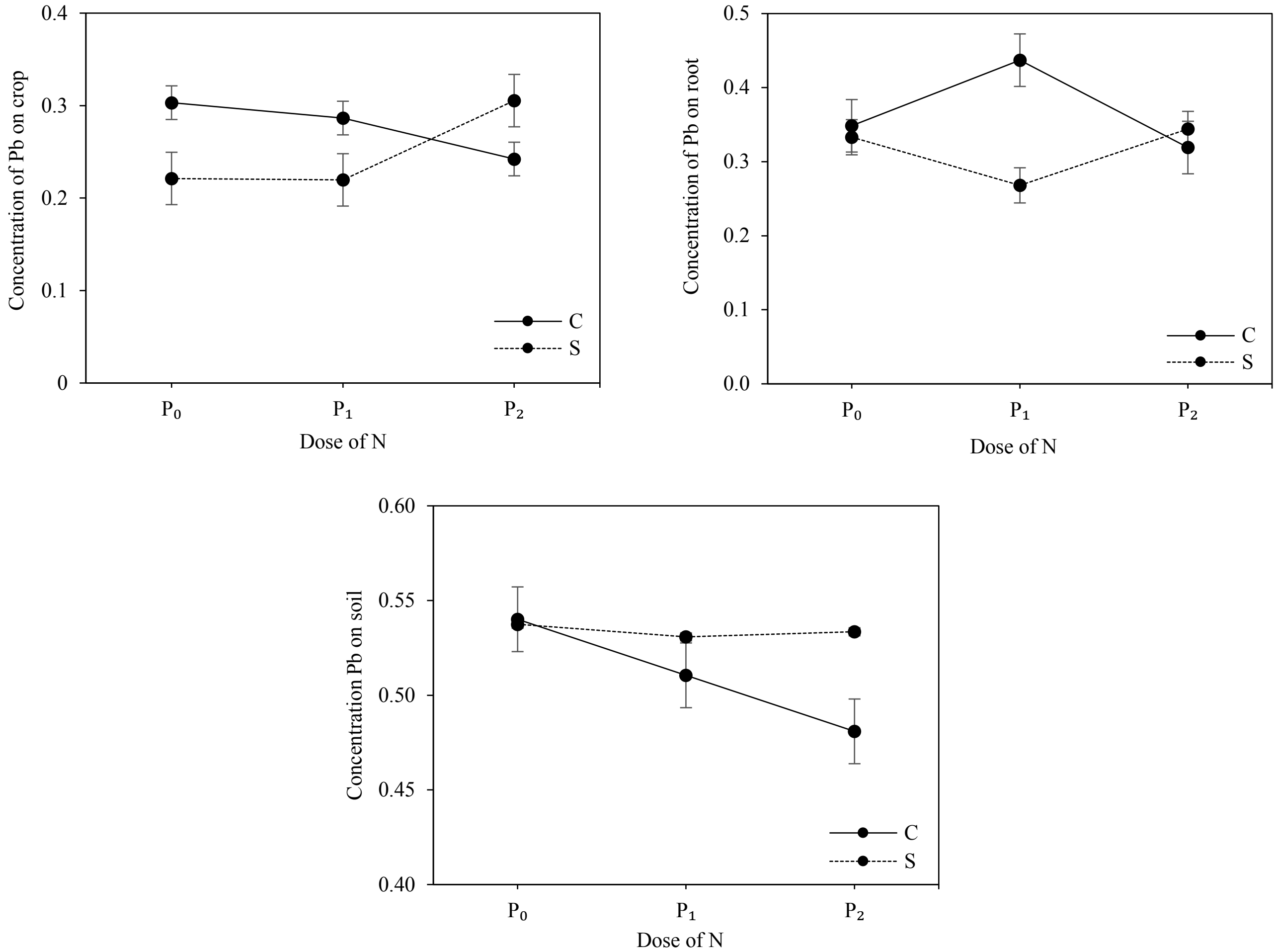

Figure 3. Concentration of Pb on crop, root, and soil due to dose of nitrogen fertilizer (P_0: control; P_1: dose of N 100 kg/ha; P_2: dose of N 200 kg/ha; C: *Codiaeum*; S: *Sansevieria*).

3.1.3 The effect of nitrogen dose with soil pH and tranlocation factor (TF)

The analysis of the *Codiaeum* soil shows that increasing the dose of N fertilization reduces the soil pH but tend to be stable in the medium planted with *Sansevieria* (Figure 4). Hence, the higher the fertilizer dose, the lower the pH value. The effect of N fertilizer doses with respect to decreasing soil pH was more significant in the *Codiaeum* compared with *Sansevieria*. Similarly, the highest TF value was found in *Codiaeum* treated with 200 kg N/ha fertilizer, as shown in Figure 4. This means that *Codiaeum* fertilized with 200 kg of N/ha was better for translating Pb from the root to the plant crop.

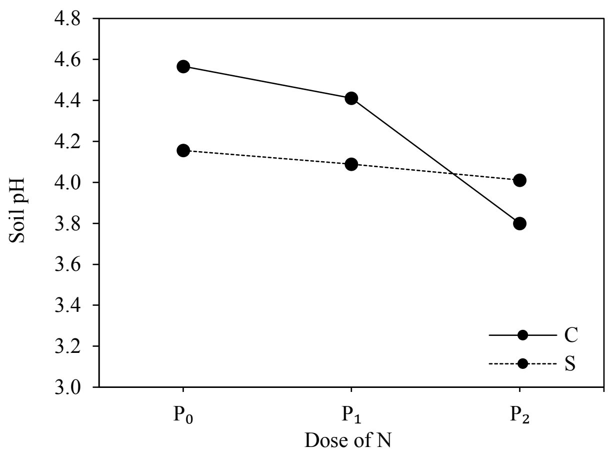

Figure 4a. Soil pH value due to dose of N fertilizer (P_0: control; P_1: dose of N 100 kg/ha; P_2: dose of N 200 kg/ha; C: *Codiaeum*; S: *Sansevieria*).

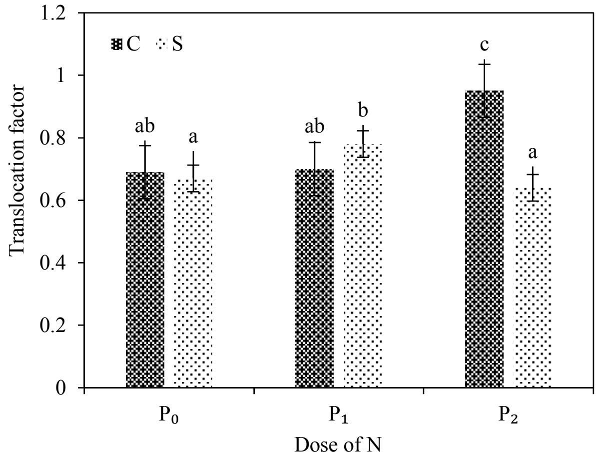

Figure 4b. TF value due to dose of N fertilizer (P_0: control; P_1: dose of N 100 kg/ha; P_2: dose of N 200 kg/ha; C: *Codiaeum*; S: *Sansevieria*) (cont.).

The relationship between the dose of N fertilizer and the absorption of Pb in the root and crop, as shown in Figure 5 tend to follow a quadratic pattern. The higher the dose of N fertilizer at a certain level, the greater the absorption of Pb in the root and crop, and after this level, the absorption of Pb decreases. Also, the optimal dose for *Codiaeum* was between 95-166.7 kg N/ha with root and crop absorption levels of Pb at 0.43875 ppm and 0.32753 ppm respectively. In addition, the optimal dose of *Sansevieria* was between 108.3-116.7 kg N/ha with root and crop absorption levels of Pb at 0.37383 ppm and 0.29292 ppm respectively.

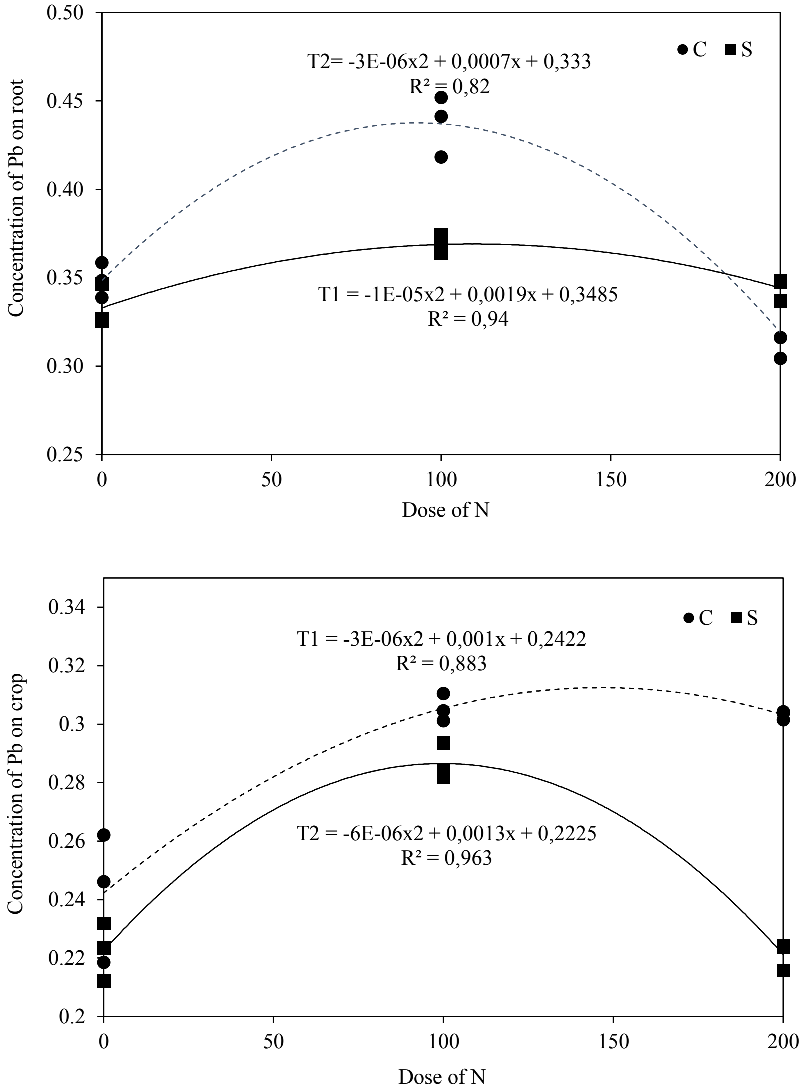

Figure 5. Graph of the relationship between the dose of N fertilizer and the absorption of Pb in roots and crops in *Codiaeum* and *Sansevieria*.

3.2 Discussion

Plants have a huge sensitivity to the presence of heavy metals in the growing media. The response shown by plants is strongly influenced by their species and the growth media, which was soil in this case. The effect of Pb largely depends on its concentration, soil properties, and plant species involved (Patra et al., 2004; Yilmaz et al., 2009). Additionally, there are many reports of toxicity of Pb in plants (Choudhury and Panda, 2005), including mitotic disorders (Jiang and Liu, 2000), inhibition of root and shoot growth (Liu et al., 2009), induction of leaf chlorosis (Pandey et al., 2007), reduction of photosynthesis (Xiao et al., 2008) and inhibition or activation of some enzymatic activities (Verma and Dubey, 2003; Sharma and Dubey, 2005; Liu et al., 2009). All these are mainly obvious in *Codiaeum* plant. However, the leaves of *Sansevieria* showed symptoms of dryness (necrosis) and wrinkles. Also, a study conducted by Sorrentino (2018) shows that the exposure of leaves to heavy metals causes an indirect decrease in its pigment concentration as a result of decrease in the rate at which Fe is transported to the leaves, resulting in the interruption of pigment synthesis.

Pb is absorbed by plants when the soil organic matter content and fertility are low. The soil composition, pH and cation exchange capacity (CEC) also affect the transfer of Pb from soil to plants. The Pb in this situation is separated from the bonding of the earth in the form of ions which move freely and then absorbed by plants through ion exchange. In addition, Pb are absorbed by plant roots when other heavy metals are unable to inhibit their presence. This causes the soil to be dominated by Pb cations, thereby reducing other cations in the root absorption complex. Furthermore, the absorbed Pb^{2+} from the roots into the plant inhibits the formation of enzymes and the process of plant metabolism, which includes the process of respiration which produces ATP used for photosynthesis. Hence, cell division (height, number and biomass) and reproduction are disrupted. According to (Alloway, 1990), the continuous occurrence of this, has a long term effect of reducing the quality of fragrant root plants growth, thereby affecting the general plant growth.

Soil pH is also important to plants and according to Brown et al. (1994), Dijkshoorn et al. (1983), and Zeng et al. (2011), who reported that pH is a key factor influencing the availability of heavy metals for root uptake. Zaccheo et al. (2006) revealed that the administration of $(NH_4)_2SO_4$ and $(NH_4)_2S_2O_3$ reduces soil pH by approximately two units, and the presence of metals increases in soil solution. Also, the higher the pH value, the lower the presence of Pb metal, but high pH affects the precipitation of metal complexes (Wang and Chen, 2006). Fertilizers with high content of NH_4^+ leads to the reduction in the soil pH. Also, the application of $(NH_4)_2SO_4$, being an oxidizing acid fertilizer, has the capacity to reduce the soil pH and increase the availability of heavy metals in the soil. These have been confirmed by many researchers (Eriksson, 1990; Lou, et al., 2005; Wang et al., 2008a). Furthermore, Schmidt (2003) suggested that the use of $(NH_4)_2SO_4$ could be considered a low cost phytoextraction strategy because it is proven that the dissolution of Pb and Cu occurs at lower pH values. Mainly, phytoremediation is a means of reducing heavy metal pollution which saves energy and is cost effective. Also, one of the applications of phytoremediation is phytostabilization. This is usually carried out to reduce contaminants in the soil, thereby reducing the movement levels of metals. Also, during phytostabilization, the concentrations of metals in the crop are lower compared with those in the roots (Ma et al., 2001). Based on calculating the concentrations of metals in the crop and roots, *Sansevieria* is considered a more tolerant plant against heavy metals or as a good candidate for phytostabilization strategies.

Generally, plants actively prevent the movement of metals from the root to the crown by sequestering the metal available in the roots, especially in the vacuole or cell wall (Gupta and Sinha, 2008). Additionally, the root has a system of preventing the transport of metal to the leaves, especially the non-essential metals, thereby leading to its accumulation at the root. According to Yoon et al. (2006), Pb is one of the non-essential metals plants tend to stack in the roots.

4. CONCLUSION

The *Sansevieria* is more responsive to N fertilization, hence, it could be considered as a more tolerant plant against heavy metals or as a good candidate for phytostabilization strategies.

REFERENCES

Alloway BJ. Heavy metals in soils. In: Alloway BJ, editor. Soil Processes and the Behaviour of Metals. United Kingdom: Blackie and Son ltd; 1990. p. 7-28.

Atafar Z, Mesdaghinia A, Nouri J, Homaee M, Yunesian M, Ahmadimoghaddam M, Mahvi AH. Effect of fertilizer application on soil heavy metal concentration. Environmental Monitoring and Assessment 2010;160(1-4):83.

Brown SL, Chaney RL, Angle JS, Baker AJ. Phytoremediation potential of *Thlaspi caerulescens* and bladder campion for zinc-and cadmium-contaminated soil. Journal of Environmental Quality 1994;23(6):1151-7.

Choudhury S, Panda SK. Toxic effects, oxidative stress and ultrastructural changes in moss *Taxithelium nepalense* (Schwaegr.) broth. under chromium and lead phytotoxicity. Water Air and Soil Pollution 2005;167(1-4):73-90.

Dijkshoorn W, Lampe JEM, Van Broekhoven LW. The effect of soil pH and chemical form of nitrogen fertilizer on heavy metal contents in rye grass. Fertilizer Research 1983;4(1):63-74.

Eriksson JE. Effects of nitrogen-containing fertilizers on solubility and plant uptake of cadmium. Water, Air, and Soil Pollution 1990;49(3-4):355-68.

Flora SJ, Flora G, Saxena G. Environmental occurrence, health effects and management of lead poisoning. In: Casas JS, Sordo J, editors. Lead Chemistry, Analytical Aspects, Environmental Impact and Health Effects. Elsevier B.V.; 2006. p. 158-228.

Garbisu C, Alkorta I. Phytoextraction: A cost-effective plant-based technology for the removal of metals from the environment. Bioresource Technology 2001;77(3):229-36.

Gupta AK, Sinha S. Decontamination and/or revegetation of fly ash dykes through naturally growing plants. Journal of Hazardous Materials 2008;153(3):1078-87.

Gurnita, Sondari N, Budiasih R. The effect of ammonium sulfate inducer on growth and content of lead metal (Pb) on *Vetiveria zizanoides* L. grass planted on gold mine tailings. Biosfer: Journal of Biology Education 2017;2(1):26-35.

Islam E, Yang X, Li T, Liu D, Jin X, Meng F. Effect of Pb toxicity on root morphology, physiology and ultrastructure in the two ecotypes of *Elsholtzia argyi*. Journal of Hazardous Materials 2007;147(3):806-16.

Jiang WS, Liu DH. Effects of Pb^{2+}on root growth, cell division, and nucleolus of *Zea mays* L. Bulletin of Environmental Contamination and Toxicology 2000;65(6):786-93.

Kumar GH, Saritha K. Lead uptake and its effects on antioxidant defence system in *Sansevieria roxburghiana* schult & schult. F. International Journal of Current Research in Chemistry and Pharmaceutical Sciences 2014;1(5):33-9.

Laidlaw WS, Arndt SK, Huynh TT, Gregory D, Baker AJ. Phytoextraction of heavy metals by willows growing in biosolids under field conditions. Journal of Environmental Quality 2012;41(1):134-43.

Lawlor DW, Mengel K, Kirkby EA. Principles of plant nutrition. Annals of Botany 2004;4(93):479-80.

Lesage E, Meers E, Vervaeke P, Lamsal S, Hopgood M, Tack FM, Verloo MG. Enhanced phytoextraction: II. Effect of EDTA and citric acid on heavy metal uptake by *Helianthus annuus* from a calcareous soil. International Journal of Phytoremediation 2005;(2):143-52.

Lin C, Zhu T, Liu L, Wang D. Influences of major nutrient elements on Pb accumulation of two crops from a Pb-contaminated soil. Journal of Hazardous Materials 2010;174(1-3):202-8.

Liu D, Zou J, Meng Q, Zou J, Jiang W. Uptake and accumulation and oxidative stress in garlic (*Allium sativumL.*) under lead phytotoxicity. Ecotoxicology 2009;18(1):134-43.

Longhurst RD, Roberts AHC, Waller JE. Concentrations of arsenic, cadmium, copper, lead, and zinc in New Zealand pastoral topsoils and herbage. New Zealand Journal of Agricultural Research 2004;47(1):23-32.

Lou Y, Zhang Y, Lin X. Effects of forms of nitrogen fertilizer on the bioavailability of heavy metals in the soils amended with bio solids and their uptake by corn plant. Journal of Zhejiang University: Agriculture and Life Sciences 2005;31(4):392-8.

Ma LQ, Komar KM, Tu C, Zhang W, Cai Y, Kennelley ED. A fern that hyperaccumulates arsenic. Nature 2001;409:579.

MacFarlane GR. Leaf biochemical parameters in *Avicennia marina* (Forsk.) Vierh as potential biomarkers of heavy metal stress in estuarine ecosystems. Marine Pollution Bulletin 2002;44(3):244-56.

Mulligan CN, Yong RN, Gibbs BF. Remediation technologies for metal contaminated soils and sediments: An evaluation. Engineering Geology 2001;60(1-4):193-207.

Ogunlade MO, Agbeniyi SO. Impact of pesticides use on heavy metal pollution in cocao soil of Cross- River, Nigeria. African Journal of Agriculture Research 2011;6(16):3725-8.

Pandey S, Gupta K, Mukherjee AK. Impact of cadmium and lead on Catharanthusroseus: A phytoremediation study. Journal of Environmental Biology 2007;28(3):655-62.

Parkpian P, Leong ST, Laortanakul P, Thunthaisong N. Regional monitoring of lead and cadmium contamination in a tropical grazing land site, Thailand. Environmental Monitoring and Assessment 2003;85(2):157-73.

Patra M, Bhowmik N, Bandopadhyay B, Sharma A. Comparison of mercury, lead and arsenic with respect to genotoxic effects on plant systems and the development of genetic tolerance. Environmental and Experimental Botany 2004;52(3):199-223.

Puschenreiter M, Stoeger G, Lombi E, Horak O, Wenzel WW. Phytoextraction of heavy metal contaminated soils with *Thlaspi goesingense* and *Amaranthus hybridus*: Rhizosphere manipulation using EDTA and ammonium sulfate. Journal Plant Nutrition Soil Science 2001;164(6):615-21.

Quartacci MF, Argilla A, Baker AJM, Navari-Izzo F. Phytoextraction of metals from a multiply contaminated soil by Indian mustard. Chemosphere 2006;63(6):918-25.

Salt DE, Smith RD, Raskin I. Phytoremediation. Annual Review of Plant Biology 1998;49(1):643-68.

Schmidt U. Enhancing phytoextraction. Journal of Environmental Quality 2003;32(6):1939-54.

Sharma P, Dubey RS. Lead toxicity in plants. Brazilian Journal of Plant Physiology 2005;17:35-52.

Sorrentino MC, Capozzi F, Amitrano C, Giordano S, Arena C, Spagnuolo V. Performance of three cardoon cultivars in an industrial heavy metal-contaminated soil: Effects on morphology, cytology and photosynthesis. Journal of Hazardous Materials 2018;351:131-7.

Tangahu BV, Abdullah S, Rozaimah S, Basri H, Idris M, Anuar N, Mukhlisin M. A review on heavy metals (As, Pb, and Hg) uptake by plants through phytoremediation. International Journal of Chemical Engineering 2011;2011:ID 939161.

Tu C, Zheng CR, Chen HM. Effect of applying chemical fertilizers on forms of lead and cadmium in red soil. Chemosphere 2000;41(1-2):133-8.

Verma S, Dubey RS. Lead toxicity induces lipid peroxidation and alters the activities of antioxidant enzymes in growing rice plants. Plant Science 2003;164(4):645-55.

Wang JL, Chen C. Biosorption of heavy metal by *Saccharomyces cerevisiae*: A review. Biotechnology Advances 2006;24(5): 427-51.

Wang L, Zhou Q, Sun Y. Intensification of *Solanum nigrum* L. remedying cadmium contaminated soils by nitrogen and potassium fertilizers. China Environmental Science 2008a;28(10):915-20.

Wang YH, Ai SY, Li MJ, Yang SH, Yao JW. Effects of using nitrogen fertilizer on distribution of Pb in the soil. Environmental Pollution Control 2008b;30(7):39-42.

Wati DR, Sholihah A, Rosyidah A. Response of *Codiaeum variegatum* L. and *Sansevieria trifasciata* L. due to addition of types of nitrogen fertilizers to polluted soil of lead. Agronisma 2019;7(1):84-90.

Xiao W, Hao H, Liu XQ, Liang C, Chao L, Su MY, Hong FH. Oxidative stress induced by lead in chloroplast of spinach. Biological Trace Element Research 2008;126(1-3):257-68.

Xiong ZT, Lu P. Joint enhancement of lead accumulation in Brassica plants by EDTA and ammonium sulfate in sand culture. Journal of Environmental Sciences 2002;14(2):216-20.

Yilmaz K, Akinci İE, Akinci S. Effect of lead accumulation on growth and mineral composition of eggplant seedlings (*Solarium melongena*). New Zealand Journal of Crop and Horticultural Science 2009;37(3):189-99.

Yoon J, Cao X, Zhou Q, Ma LQ. Accumulation of Pb, Cu, and Zn in native plants growing on a contaminated Florida site. Science of the Total Environment 2006;368(2-3):456-64.

Zaccheo P, Crippa L, Pasta VDM. Ammonium nutrition as a strategy for cadmium mobilisation in the rhizosphere of sunflower. Plant and Soil 2006;283(1-2):43-56.

Zeng F, Ali S, Zhang H, Ouyang Y, Qiu B, Wu F, Zhang G. The influence of pH and organic matter content in paddy soil on heavy metal availability and their uptake by rice plants. Environmental Pollution 2011;159(1):84-91.

Zhuang P, Wensheng SHU, Zhian LI, Bin LIAO, Jintian LI, Jingsong SHAO. Removal of metals by sorghum plants from contaminated land. Journal of Environmental Sciences 2009;21(10):1432-7.

GUIDE FOR AUTHORS

Publication and Peer-reviewing processes of Environment and Natural Resources Journal

Environment and Natural Resources Journal is a peer reviewed and open access journal that is published twice a year (January-June and July-December). Manuscripts should be submitted online at https://www.tci-thaijo.org/index.php/ennrj/ by registering and logging into this website. Submitted manuscripts should not have been published previously, nor be under consideration for publication elsewhere (except conference proceedings papers). A guide for authors and relevant information for the submission of manuscripts are provided in this section and also online at: www.tci-thaijo.org/index.php/ennrj/navigationMenu/view/author. All manuscripts are refereed through a **double-blind peer-review** process.

Submitted manuscripts are reviewed by outside experts or editorial board members of **Environment and Natural Resources Journal**. This journal uses double-blind review, which means that both the reviewer and author identities are concealed from the reviewers, and vice versa, throughout the review process. Steps in the process are as follows:

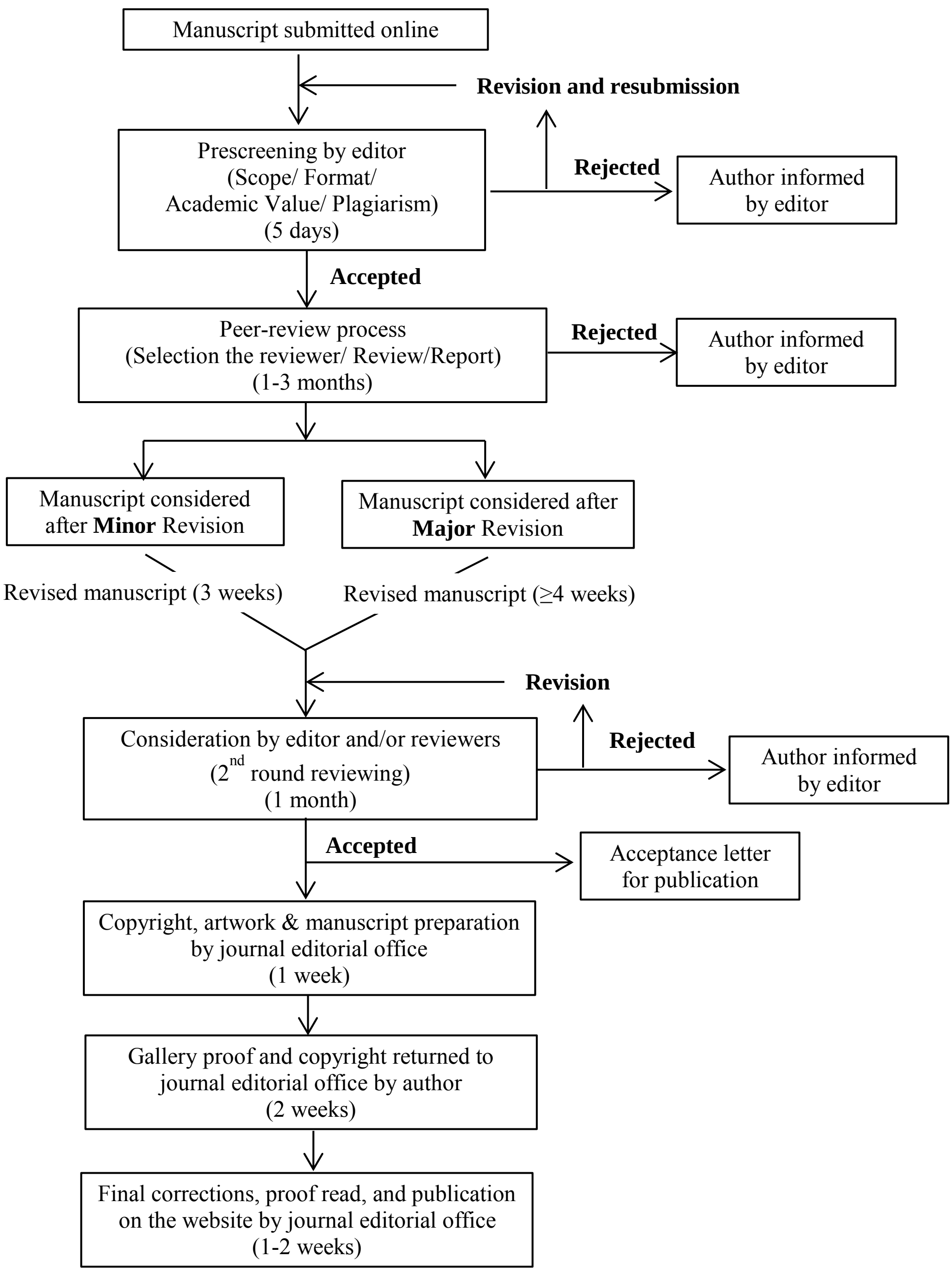

The Environment and Natural Resources Journal (EnNRJ) accepts 2 types of articles for consideration of publication as follows:

- *Original Research Article:* Manuscripts should not exceed 3,500 words (excluding references).
- *Review Article (by invitation):* This type of article focuses on the in-depth critical review of a special aspect in the environment and also provides a synthesis and critical evaluation of the state of the knowledge of the subject. Manuscripts should not exceed 6000 words (excluding references).

Preparation of Manuscripts

Manuscript should be prepared strictly as per guidelines given below. The manuscript (A4 size page) should be submitted in Microsoft Word (.doc or .docx) with Times New Roman 12 point font and a line spacing of 1.5. *The manuscript that is not in the correct format will be returned and the corresponding author may have to resubmit*. The submitted manuscript must have the following parts:

Title should be concise and no longer than necessary. Capitalize first letters of all important words, in Times New Roman 12 point bold.

Author(s) name and affiliation must be given, especially the first and last names of all authors, in Times New Roman 11 point bold.

Affiliation of all author(s) must be given in Times New Roman 11 point italic.

Abstract should indicate the significant findings with data. A good abstract should have only one paragraph and be limited to 200 words. Do not include a table, figure or reference.

Keywords should adequately index the subject matter and up to six keywords are allowed.

Text body normally includes the following sections: 1. Introduction 2. Methodology 3. Results and Discussion 4. Conclusions 5. Acknowledgements 6. References

Reference style must be given in Vancouver style. Please follow the format of the sample references and citations as shown in this Guide below.

Format and Style

Paper Margins must be 2.54 cm on the left and the right. The bottom and the top margin of each page must be 1.9 cm.

Introduction is critically important. It should include precisely the aims of the study. It should be as concise as possible with no sub headings. The significance of problem and the essential background should be given.

Methodology should be sufficiently detailed to enable the experiments to be reproduced. The techniques and methodology adopted should be supported with standard references.

Headings in Methodology section and Results and Discussion section, no more than three levels of headings should be used. Main headings should be typed (in bold letters) and secondary headings (in bold and italic letters). Third level headings should be typed in normal and no bold, for example;

2. Methodology
2.1 Sub-heading
2.1.1 Sub-sub-heading

Results and Discussion can be either combined or separated. This section is simply to present the key points of your findings in figures and tables, and explain additional findings in the text; no interpretation of findings is required. The results section is purely descriptive.

Tables Tables look best if all the cells are not bordered; place horizontal borders only under the legend, the column headings and the bottom.

Figures The journal does not normally use color for figures. Figures should be submitted in black and white; make sure that they are clear and understandable. Photographs converted from color to black and white format usually need to have their contrast adjusted. Regardless of the application used, when your electronic artwork is finalized, please 'save as' or convert the images to TIFF (or JPG) and separately send them to EnNRJ. Do not directly cut and paste them from MS Excel. The images require a resolution of at least 300 dpi (dots per inch). The lettering used in the artwork should be consistent in size and type.

Conclusions should include the summary of the key findings, and key take-home message. This should not be too long or repetitive, but is worth having so that your argument is not left unfinished. Importantly, don’t start any new thoughts in your conclusion.

Acknowledgements should include the names of those who contributed substantially to the work described in the manuscript but do not fulfill the requirements for authorship. It should also include any sponsor or funding agency that supported the work.

References should be cited in the text by the surname of the author(s), and the year. This journal uses the author-date method of citation: the last name of the author and date of publication are inserted in the text in the appropriate place. If there are more than two authors, “et al.” after the first author’ name must be added. Examples: (Frits, 1976; Pandey and Shukla, 2003; Kungsuwas et al., 1996). If the author’s name is part of the sentence, only the date is placed in parentheses: “Frits (1976) argued that . . .”

In the list of references at the end of the manuscript, full and complete references must be given in the following style and punctuation, arranged alphabetically by first author’s surname. Examples of references as listed in the References section are given below.

Book

Tyree MT, Zimmermann MH. Xylem Structure and the Ascent of Sap. Heidelberg, Germany: Springer; 2002.

Chapter in a book

Kungsuwan A, Ittipong B, Chandrkrachang S. Preservative effect of chitosan on fish products. In: Steven WF, Rao MS, Chandrkachang S, editors. Chitin and Chitosan: Environmental and Friendly and Versatile Biomaterials. Bangkok: Asian Institute of Technology; 1996. p. 193-9.

Journal article

Muenmee S, Chiemchaisri W, Chiemchaisri C. Microbial consortium involving biological methane oxidation in relation to the biodegradation of waste plastics in a solid waste disposal open dump site. International Biodeterioration and Biodegradation 2015;102:172-81.

Published in conference proceedings

Wiwattanakantang P, To-im J. Tourist satisfaction on sustainable tourism development, amphawa floating marketSamut songkhram, Thailand. Proceedings of the 1st Environment and Natural Resources International Conference; 2014 Nov 6-7; The Sukosol hotel, Bangkok: Thailand; 2014.

Ph.D. thesis

Shrestha MK. Relative Ungulate Abundance in a Fragmented Landscape: Implications for Tiger Conservation [dissertation]. Saint Paul, University of Minnesota; 2004.

Website

Orzel C. Wind and temperature: why doesn’t windy equal hot? [Internet]. 2010 [cited 2016 Jun 20]. Available from: http://scienceblogs.com/principles/2010/08/17/wind-and-temperature-why-doesn/.

Remark

** Please be note that manuscripts should usually contain at least 15 references and some of them must be up-to-date research articles.*

** Please strictly check all references cited in text, they should be added in the list of references. Our Journal does not publish papers with incomplete citations.*

Copyright transfer

The copyright to the published article is transferred to Environment and Natural Resources Journal (EnNRJ) which is organized by Faculty of Environment and Resource Studies, Mahidol University. The accepted article cannot be published until the Journal Editorial Officer has received the appropriate signed copyright transfer.

Online First Articles

The article will be published online after receipt of the corrected proofs. This is the official first publication citable with the Digital Object Identifier (DOI). After release of the printed version, the paper can also be cited by issue and page numbers. DOI may be used to cite and link to electronic documents. The DOI consists of a unique alpha-numeric character string which is assigned to a document by the publisher upon the initial electronic publication. The assigned DOI never changes.

Mahidol University

Wisdom of the Land

Research and Academic Service Section, Faculty of Environment and Resource Studies, Mahidol University
999 Phutthamonthon 4 Rd, Salaya, Nakhon Pathom 73170, Phone +662 441-5000 ext. 2108 Fax. +662 441 9509-10
E-mail: ennrjournal@gmail.com Website: https://www.tci-thaijo.org/index.php/ennrj

Crossref Google Scholar